

COMPREHENSIVE STUDIES ON DEEP SOIL MIXING AND
LIGHTWEIGHT AGGREGATES APPLICATIONS TO
MITIGATE APPROACH SLAB
SETTLEMENTS

by

EKARUT ARCHEEWA

Presented to the Faculty of the Graduate School of
The University of Texas at Arlington in Partial Fulfillment
of the Requirements
for the Degree of

DOCTOR OF PHILOSOPHY

THE UNIVERSITY OF TEXAS AT ARLINGTON

December 2010

Copyright © by EKARUT ARCHEEWA 2010

All Rights Reserved

I would like to dedicate this research to my parents and teachers.

ACKNOWLEDGEMENTS

I would like to convey my sincere gratitude to Dr. Anand J Puppala, my supervising professor, for his continual guidance and support given to me throughout my study at University of Texas at Arlington. He has given many efforts and encouragement helping me throughout three years of my stay at UTA, this research could not be accomplished without them. In addition, I also believe that with the academic motivation and inspiration that I had learnt from him would help me in being successful for my future career. I am really indebted to him and grateful forever for his help.

I also would like to express my appreciation for the valuable time and suggestions from the members of the supervising committee including Dr. Ali Abolmaali, Dr. Chein-Pai Han, Dr. Laureano R. Hoyos, and Dr. Mohammad Najafi. I also thank them for enhancing my knowledge of soil mechanics, statistics and construction management.

I would like to give my gratitude to Texas Department of Transportation (TxDOT) for the funding of the research, especially Richard Williammee for his kind cooperation. I especially thank the Department of Civil and Environmental Engineering of the University of Texas at Arlington for the financial assistance throughout this study, and also extend my thanks to UTA staffs, Ginny Bowers, Sarah Ridenour, Ava Chapman, and Paul Shover for their assistance during my study.

I own my most appreciation to my friends, Dr. Thammanoon Manosuthikij and Thornchaya Wejrungsikul, who gave me brotherly supports for all kinds during my stay in the US. I also would like to extend my special thanks to my other friends and colleagues Dr. Sireesh Saride, Varagorn Puljan, Guojun Cai, Nagasreenivasu Talluri, Seema Kalla, Dr. Chakkrit Sirivitmaitrei, Raja Veerendra Yenigalla, Rajini Kanth Reddy, Srujan Rao Chikyala, Vijay Ganne,

and Dr Venkata Subrahmanyam Dronamraju for their help during construction of test sections, field monitoring and during laboratory tests. Without their helps and supports, this research would not be possible to be accomplished.

Finally, I would like to thank my parents, Udom and Jareerat Archeewa, and my sister for their wholehearted supports given to me from Thailand.

November 16, 2010

ABSTRACT

COMPREHENSIVE STUDIES ON DEEP SOIL MIXING AND LIGHTWEIGHT AGGREGATES APPLICATIONS TO MITIGATE APPROACH SLAB SETTLEMENTS

Ekarut Archeewa, Ph.D.

The University of Texas at Arlington, 2010

Supervising Professor: Anand J. Puppala

Bridge approach settlement is a common problem to the Transportation Departments nationwide. This uneven transition causes inconvenience to passengers and increases the cost of maintenance and repair of the distressed approach slabs. The Texas Department of Transportation spends millions of dollars annually to mitigate this problem across the state. The potential causes for this problem are numerous and purely site specific. Hence this problem may not have a unique solution.

In this research, two methods were selected to mitigate the approach slab settlements. The first one is an improvement of ground foundation technique by using Deep Soil Mixing (DSM) columns to stabilize soft foundation soil. The second one is an improvement of fill material by using a lightweight fill material, Expanded Clay Shale (ECS), as a backfill in embankment construction. Therefore, this research was performed on two bridge sites - DSM site on IH30 and ECS site on SH360 located in the North and South of Arlington, respectively. In order to study effectiveness of the two mitigation methods, three tasks were carried out including, laboratory studies, instrumentation and field monitoring, and numerical analysis.

Soil samples from two bridge sites from IH30 and SH360 were taken to perform laboratory studies at University of Texas at Arlington. The results reveal that foundation soils from both sites were classified as low plasticity clay. The laboratory investigations were also conducted to study the properties of DSM samples prepared in the laboratory and the ECS. The test results show that the foundation soil gained more strength by the DSM technique and the ECS exhibited its high internal friction property.

Equipment installation was done on the DSM and ECS sites with various types of instrument including vertical inclinometer, horizontal inclinometer, sondex, and rod extensometers. The site investigation with the elevation surveys had been performed in every fortnight to monitor soil movements both in the horizontal and vertical directions. Results from the field observations from two bridge sites showed that both of the DSM and ECS techniques can be used to mitigate the settlement occurred in the embankment. In the DSM study, the settlement was reduced from 85 mm to 49 mm (measured in the control and test sections, respectively). On the ECS site, it is found that to construct embankment with the ECS could bring down the settlement from 85.3 mm occurred in the control section to 36.5 mm in the test section.

The monitored soil movement data from the field studies were also used as a data validation in the numerical analysis to ensure that the numerical model would have a good prediction about soil displacements. After the results from the FEM closely matched with the field data, the models were used further to predict the long-term settlement. The analysis results show that in the long-term, the DSM and ECS methods can decrease the settlement in the embankment from 277 to 66 mm, and from 136 to 50 mm, respectively.

Consequently, a parametric study was conducted to investigate parameters influencing on the amount of the settlement. The interesting parameters in both DSM and ECS studies include slope and height of the embankments, and area-ratio between DSM and foundation soil (only in the DSM study). The FEM results from both studies show that embankment height

mainly affects the amount of the settlement, while the embankment slope does not affect much. Another factor can influence the settlement in the embankment is the area-ratio. From the DSM study, the area-ratio with a range from 0.5-0.7 exhibit greatly influence on the settlement. Finally, from a parametric study, the DSM and ECS design charts could be established in various heights, slopes and area-ratios to facilitate in ECS embankment and DSM columns design.

TABLE OF CONTENTS

ACKNOWLEDGEMENTS	iv
ABSTRACT	vi
LIST OF ILLUSTRATIONS.....	xiv
LIST OF TABLES	xxvi
Chapter	Page
1. INTRODUCTION.....	1
1.1 General.....	1
1.2 Research Objectives	2
1.3 Dissertation Organization.....	3
2. LITERATURE REVIEW	6
2.1 Introduction.....	6
2.2 Definition of the Bump and the Bump tolerance	6
2.2.1 Definition of the Bump.....	6
2.2.2 Bump Tolerances	7
2.3 Mechanisms Causing the Formation of the “Bump”	8
2.3.1 Consolidation Settlement of Foundation Soil	14
2.3.2 Poor Compaction and Consolidation of Backfill Material.....	16
2.3.3 Poor Drainage and Soil Erosion.....	17
2.3.4 Types of Bridge Abutments.....	20
2.3.5 Traffic Volume	25
2.3.6 Age of the Approach Slab	25
2.3.7 Approach Slab Design	26

2.3.8 Skewness of the Bridge	27
2.3.9 Seasonal Temperature Variations	28
2.4 Mitigation Techniques for Approach Settlements of New Bridges	31
2.4.1 Improvement of Embankment Foundation Soil.....	31
2.4.2 New Foundation Technologies	52
2.4.3 Improvement of Approach Embankment/Backfill Material.....	67
2.4.4 Design of Bridge Foundation Systems	83
2.4.5 Design of Approach Slab	94
2.4.6 Effective Drainage and Erosion Control Methods	104
2.5 Maintenance Measures for Distressed Approach Slabs	112
2.5.1 Replacement Method	115
2.5.2 Mud/Slab Jacking.....	115
2.5.3 Grouting.....	117
2.5.4 Other Methods	126
2.5 Summary	129
3. SELECTION OF SETTLEMENT MITIGATION METHODS.....	130
3.1 Introduction and Dissertation Research Objectives	130
3.2 TxDOT Districts' Surveys	131
3.3 Ranking Analysis of Mitigation Techniques	139
3.4 Summary.....	142
4. DESIGN OF DEEP SOIL MIXING (DSM) FOR SETTLEMENT CONTROL.....	143
4.1 Introduction.....	143
4.2 Procedure for Design of DSM Columns.....	143
4.2.1 Theoretical Formulation	143
4.2.2 Design Steps.....	147

4.2.3 Design Specifications of Materials for DSM Treated Test Sections	152
4.3 Summary	155
5. LABORATORY INVESTIGATIONS FOR DSM AND LIGHT WEIGHT FILL STUDIES.....	156
5.1 Introduction.....	156
5.2 Site Selection and Field Soil Sampling	157
5.3 Experimental Program	159
5.3.1 Sample Preparation	160
5.3.2 Atterberg Limit Tests	160
5.3.3 Standard Proctor Compaction Test.....	161
5.3.4 Determination of Linear Shrinkage Strains	162
5.3.5 One-Dimensional Free Swell Tests	163
5.3.6 Unconfined Compression Strength (UCS) Test.....	164
5.3.7 One-dimensional Consolidation Test.....	165
5.3.8 Deep Soil Mixing Related Laboratory Studies	167
5.4 Discussion of Test Results.....	170
5.4.1 Physical Properties of Subgrade Soils.....	170
5.4.2 Engineering Properties of Soils.....	174
5.5 Summary.....	178
6. CONSTRUCTION AND INSTRUMENTATION OF DSM AND ECS SECTIONS.....	179
6.1 Introduction.....	179
6.2 Sites Descriptions	179
6.2.1 DSM Columns, IH 30, Arlington, Texas	179
6.2.2 ECS Backfill Material, SH 360, Arlington, Texas	180
6.2.3 Geopier, SH-6 across US-90 A, Houston, Texas	180

6.3 Design Specifications of Materials and Geometry Details for DSM Treated Test Sections.....	181
6.3.1 Specifications of Binder Materials.....	181
6.3.2 Specifications of Geogrid	182
6.3.3 Specifications of DSM Column Geometry and Arrangement	182
6.4 Construction of DSM Columns.....	183
6.5 Construction of the Embankment with ECS.....	184
6.6 Construction of the Geopiers	185
6.7 Instrumentation.....	188
6.7.1 Inclinometers	190
6.7.2 Sondex Settlement System.....	201
6.7.3 Rod Extensometer System	203
6.8 Summary.....	211
7. ANALYSIS OF FIELD MONITORING DATA	213
7.1 Introduction.....	213
7.2 Performance Evaluation of DSM Stabilization Treated Section.....	213
7.2.1 DSM treated section.....	213
7.2.2 Control Section.....	234
7.2.3 Settlement Comparisons between DSM Treated Section and Untreated Section	238
7.3 Performance Evaluation of Light Weight Expanded Clay Shale or ECS Fill	240
7.3.1 ECS Test Section.....	240
7.3.2 Conventional Fill Section.....	248
7.3.3 Comparisons of Data between ECS Test Section and Control Section	249
7.4 Performance Evaluation based on Geopier Reinforcement	252

7.5 Performance Comparison between DSM and ECS in Mitigating the Settlement	256
7.6 Summary	257
8. NUMERICAL MODELING	259
8.1 Introduction.....	259
8.2 Finite Element Method (FEM)	259
8.3 Modeling of DSM Columns and Control Section, IH30, Arlington, Texas	262
8.3.1 Test Embankment Section	262
8.3.2 Control Embankment Section	273
8.3.3 Comparisons of Vertical Soil Movements Occurred between Treated and Untreated Embankments	281
8.3.4 Analysis of Vertical Soil Movements	282
8.3.5 Prediction of Soil Movements Occurred in the Treated Section with Variations of Embankment and DSM Configurations	285
8.4 Modeling of Light Weight Embankment System	295
8.4.1 ECS Embankment Section.....	295
8.4.2 Control Embankment Section	305
8.4.3 Analysis of Vertical Soil Movements	309
8.4.4 Prediction of Soil Movements Occurred in an ECS Section with Variations of Embankment Configurations	312
8.5 Summary	317
9. SUMMARY AND CONCLUSIONS	320
9.1 General.....	320
9.2 Summary and Conclusions	321
9.3 Limitation and Recommendation.....	325

REFERENCES.....	326
BIOGRAPHICAL INFORMATION	340

LIST OF ILLUSTRATIONS

Figure	Page
2.1 Schematic of Different Origins Lead to Formation of Bump at the End of the Bridge (Briaud et al., 1997)	13
2.2 Cross section of a wingwall and drainage system (Briaud et al., 1997)	18
2.3 Range of Most Erodible Soils (Briaud et al., 1997)	20
2.4 A Simplified Cross Section of an Integral Abutment Bridge (Greimann et al., 1987)	21
2.5 A Simplified Cross Section of a Non-integral Abutment Bridge (Greimann et al., 1987)	22
2.6 Non-integral Abutment Types (TxDOT Bridge Design Manual, 2001).....	23
2.7 Variation of tensile axial stress with front axle distance for skewed and straight approach slabs (Nassif, 2002).....	28
2.8 Thermally Induced IAB Abutment Displacement (Horvath, 2005)	29
2.9 Movement of Bridge Structure (Arsoy et al., 1999).....	29
2.10 Grouping of soils for Dynamic Compaction (after Lukas, 1986)	37
2.11 Configurations of different types of prefabricated vertical drains (after Bergado et al., 1996).....	38
2.12 Preloading with prefabricated vertical drains to reduce consolidation settlements	39
2.13 Schematic arrangement of approach embankment treatment with wick drains and driven piles (after Hsi and Martin, 2005)	40
2.14 Measured and predicted settlements with time (Hsi and Martin, 2005) (a) during construction stages, (b) after construction stages	41
2.15 Construction stages of stone column (Hayward Baker).....	43
2.16 Interfacing of ground improvement techniques beneath embankment approach to piled bridge abutment (after Serridge and Synac, 2007).....	44

2.17 Settlement monitoring results for both surcharge trials on untreated and soil reinforced with stone columns (after Serridge and Synac, 2007)	45
2.18 Sequential operations involved in the construction of compaction piles (after Hausmann, 1990).....	46
2.19 Range of soils suitable for vibro-compaction methods (after Baumann and Bauer, 1974)	46
2.20 Schematic of granular compaction piles with mechanically stabilized earth to support bridge approach embankments (Bergado et al., 1996)	47
2.21 Schematic of bridge approach embankment supported on driven piles (after Hsi, 2007).....	48
2.22 Cross section of embankment with basal geogrid and columns (after Liu et al., 2007)	49
2.23 Geocell foundation mattress supported embankment (Cowland and Wong, 1993)	51
2.24 Typical load/settlement-pore pressure/time profiles for embankment section.....	51
2.25 Geopier construction sequence (after Lien and Fox, 2001).....	53
2.26 Typical geopier system supporting the embankment (after Lien and Fox, 2001)	53
2.27 Comparison of settlement with fill height for both stone column and geopier systems.....	54
2.28 Deep Soil Mixing (DSM) Operation and Extruded DSM Columns	56
2.29 Schematic of DCM columns with varying length to support highway embankment over soft marine clay (Lin and Wong, 1999).....	58
2.30 Instrumentation details of DCM treated embankment.....	59
2.31 Section and plan view of soil-cement pile supported approach embankment (after Shen et al., 2007)	60
2.32 Maintenance cost with differential settlements (Shen et al., 2007).....	61
2.33 Installation of concrete injected columns (after Hsi, 2008)	62
2.34 Bridge approach treatment with concrete injected columns (Sectional and Plan view)	63

2.35 Settlement profiles obtained from settlement plates (after Hsi, 2008)	64
2.36 Construction Procedures for Continuous Auger Piles (O'Neill, 1994)	65
2.37 CFA pile supported railway embankment for Italian railway project (after Brown et al., 2007)	67
2.38 Typical Mechanically Stabilized Abutment (Wahls, 1990)	75
2.39 Schematic Diagram of a GRS Wall and GRS System after Construction (Won and Kim, 2007)	76
2.40 Typical GRS Bridge Abutment with a Segmental Concrete Block Facing.....	78
2.41 A design alternative by using geofoam as a backfill (Horvath, 2000)	80
2.42 Sleeve Port Pipe Installation Plan (Sluz et al., 2003).....	83
2.43 Example of Bridge Foundation using Steel H-Piles	86
2.44 The Down-drag in Piles	88
2.45 Typical Section through Front and Abutment GRS Walls (Abu-Hejleh et al., 2006).....	89
2.46 Simplified cross section of non-integral abutment bridge (Greimann et al., 1987, White et al. 2005).....	91
2.47 Simplified cross section of integral abutment bridge (Greimann et al., 1987, White et al. 2005).....	92
2.48 Movement of bridge structure with temperature (Arsoy et al., 1999)	93
2.49 Bridge approach connected to bridge deck (Missouri DOT 2003).....	95
2.50 Bridge approach connected to abutment (Ohio DOT, 2003)	96
2.51 Test setup for subsoil deformation (Wong and Small, 1994).....	99
2.52 The ribbed slab as an approach slab (Cai et al., 2005)	100
2.53 Schematic of bridge approach slab arrangement adopted by the Fort Worth District of TXDOT, Texas.....	102
2.54 Schematic of an Integral Abutment System with a Sleeper Slab.....	103

2.55 MSE Walls System under Sleeper Slab (Abu-Hejleh et al., 2006)	106
2.56 Drainage Layer of Granular Material and Collector Pipe	107
2.57 Approach Slab Joint Details at Pavement Edge (Briaud et al., 1997)	108
2.58 Riprap used for Erosion Control (Lenke, 2006)	108
2.59 Concrete Slope Protection with Drainage Gutter and Drainage Channel (Lenke, 2006).....	109
2.60 Schematic of Porous Fill Surrounding Subdrain (White et al., 2005).....	110
2.61 Schematic of Granular Backfill Wrapped with Geotextile Filter Material (White et al., 2005).....	110
2.62 Schematic of Geocomposite Vertical Drain Wrapped with Filter Fabric (White et al., 2005)	111
2.63 Simulated approach slab deflection due to washout by UC Davis research team.....	115
2.64 Mud-jacking injection sequences (MoDOT, EPC).....	116
2.65 Location of holes drilled on an approach slab (White et al., 2005)	118
2.66 Schematic of the approach slab with developed void under the bridge at FM 1947 Hill County, Texas	122
2.67 Position of approach slab during and after the Urethane injection process	123
2.68 Hairline crack observed on the approach slab during the urethane injection	123
2.69 The flowable mortar used under a roadway pavement (Smadi, 2001)	125
2.70 The flowable fill used as a base material (Du, 2008)	126
2.71 Pre-cambered Approach Design (Hoppe, 1999).....	127
2.72 Emergency Ramp and High Embankment constructed using the EPS Geofoam at Kaneohe interchange in Oahu, Hawaii.....	128
3.1 Number of districts that encountered bridge approach settlement/ heaving.....	131
3.2 Procedure to identify the problem in the field.....	132

3.3 Number of Districts that conducted any forensic examinations on the distressed approaches to identify potential cause(s) of the problem	133
3.4 Factors attributed to the approach settlement problems.....	134
3.5 Number of Districts that perform a geotechnical investigation on embankment fill and foundation subgrade material	134
3.6 PI value required for embankment material	135
3.7 Number of Districts conducting Quality Assessment (QA) studies on compacted fill material.....	136
3.8 Remedial/maintenance measures taken in responded districts and its performance.....	138
3.9 Methods to control the erosion/slope failure	139
4.1 Schematic of untreated ground depicting layers for settlement prediction	144
4.2 Schematic of composite ground depicting layers for heave prediction.....	147
4.3 Design flow chart for DSM treatment	149
4.4 Design charts for estimating DSM area ratios for $C_{r,soil}$ 0.047 and $C_{r,coil}$ 50-90% of $C_{r,soil}$	151
4.5 Configurations of DSM columns and corresponding equations for column spacing	153
4.6 DSM column spacing details for Square Pattern	154
4.7 DSM column spacing details for Triangular pattern	154
5.1 Details of weak soil and DSM treatment, IH 30 site, Arlington, TX.....	157
5.2 Details of ECS Bridge Site, SH 360, Arlington, TX	158
5.3 Sample preparations by wet analysis for soil classification and determination of Atterberg Limits (a) Soaking stage and (b) Drying stage	161
5.4 Free swell test (a) Schematic Sketch (Das, 2002) and (b) Test Setup.....	163
5.5 UCS tests performed in a triaxial test setup.....	165
5.6 Consolidation test setup.....	166

5.7 Casagrande’s plasticity chart and type of soil samples 171

5.8 Grain size distribution curves of soil samples from site SH360 172

5.9 Standard Proctor curve of selected fill from site IH30..... 173

5.10 Standard Proctor Curve of selected fill from site SH360..... 173

5.11 Free swell test results from studied sites 175

5.12 Consolidation curves of soil specimens from site IH30..... 176

5.13 Consolidation curves of local and ECS soil specimens
from site SH360 176

5.14 Stress-strain curves of soil specimens from unconfined compression tests 177

6.1 Details of weak soil and DSM treatment, IH 30 site, Arlington, TX..... 180

6.2 Details of ECS Bridge Site, SH 360, Arlington, TX 180

6.3 Details of Geopier Bridge Site, SH-6 and US 90A, Houston, TX..... 181

6.4 Sectional details of DSM columns at Site IH30..... 182

6.5 A typical perspective view of DSM treated-geogrid-reinforced
test section..... 183

6.6 Rammed aggregate pier construction process (Sentez Insaat, 2010)..... 188

6.7 Instrumentation details on IH 30, Arlington, Texas 189

6.8 Instrumentation details on SH 360, Arlington, Texas..... 189

6.9 Instrumentation details on SH 6, Houston, Texas..... 190

6.10 Details of inside inclinometer casing and a probe
(Slope Indicator, 2006) 191

6.11 (a) Details of inclinometer casing and (b) Assembling procedure 191

6.12 Details of inclinometer probe (Slope Indicator 2000)
(a) Components and (b) Measurement planes..... 193

6.13 Principle in inclinometers for measuring deformation
(Dunnicliff, 1988)..... 193

6.14 A selected location was bored to install the inclinometer casing 195

6.15 A bottom of the casing was plugged with a bottom cap..... 195

6.16 The casing installation after reaching the required drilling depth..... 196

6.17 The pipe clamping techniques required for casing installation (Slope Indicator, 2009)	196
6.18 The gap between casings and bore was filled with grout mixing	197
6.19 Water was filled into the casing to avoid floating due to buoyancy.....	197
6.20 (a) Schematic of horizontal inclinometer setup and (b) Horizontal probe	199
6.21 A trench was excavated at the selected location	200
6.22 (a) A typical Sondex installation (b) Sondex system components	202
6.23 A corrugated pipe was placed on the vertical casing at a design depth	203
6.24 A corrugated pipe was attached on the casing with (a) mastic tape and (b) rivet.....	203
6.25 Main components of Rod extensometer system	204
6.26 The procedures in rod anchor assembly.....	207
6.27 The procedures in adding rods and protective pipes	208
6.28 The procedures in installing the top part of the rods.....	208
6.29 The components of reference head	209
6.30 The set of assembled rods and reference head were put into the hole	209
6.31 The set of assembled rods and reference head was held up by rope	210
6.32 The VW sensor adapters were screwed into the reference head	210
6.33 The VW sensors were screwed into their adapter	211
7.1 Instrumentation on IH30 DSM site, Arlington, Texas	215
7.2 The closed-end installation of the horizontal inclinometer (Slope Indicator 2004)	215
7.3 The horizontal inclinometer readings scheme (a) 1st Pass (b) 2nd Pass (Slope Indicator 2004).....	216
7.4 The location of the broken casing	217
7.5 Inclinometer data retrieves	217

7.6 The cumulative displacements from 11/8/2008 to 11/14/2009 (compared with a casing profile before the construction of the approach slab finished).....	220
7.7 The cumulative displacements from 11/23/2008 to 4/14/2010 (compared with a casing profile after the construction of the approach slab finished).....	220
7.8 The cumulative displacements from 11/8/2008 to 4/14/2010 (compared with a casing before the construction of the approach slab finished).....	222
7.9 The cumulative displacements from 12/17/2008 to 4/14/2009 (compared with a casing profile after the construction of the approach slab finished).....	222
7.10 The changes in length of the extensometer rods.....	226
7.11 The soil displacement having the bottom rod anchor as a reference	226
7.12 The depth values of the rod head measured by digital gauge	228
7.13 The soil displacement having the bottom rod anchor as a reference	228
7.14 The sondex instrument and the readings.....	229
7.15 The average depth readings in the test embankment at the depth of (a) 10, (b) 20, (c) 40 and (d) 50 ft	231
7.16 The vertical inclinometer reading	233
7.17 Orientation of probe within inclinometer casing (Slope Indicator).....	233
7.18 Lateral soil movements in the test section during 10/19/2008 to 8/4/2010.....	234
7.19 The average depth readings in the untreated embankment at the depth of (a) 10, (b) 20, (c) 40 and (d) 50 ft	236
7.20 Lateral soil movements in the control embankment during 10/19/2008 to 8/4/2010.....	237
7.21 Instrumentations on SH 360, Arlington, Texas	241
7.22 Lateral soil movements during 8/31/2006 to 8/4/2010 in the vertical inclinometers (a) V1, (b) V2	245
7.23 Lateral soil movements during 8/31/2006 to 8/4/2010 in the vertical inclinometers (a) V3, (b) V4	246

7.24 Lateral movement of the platform casing V4	247
7.25 Opening observed between highway pavement and its shoulder	247
7.26 The casing V3 platform close to highway shoulder.....	248
7.27 Opening observed close to abutment of the bridge	248
7.28 Bridge approach in the control embankment was overlaid by Asphalt to mitigate the bump	249
7.29 Instrumentation on SH6, Houston, Texas	253
7.30 Lateral soil movements during 10/27/2008 to 10/23/2009 in the vertical inclinometers (a) V1, (b) V2	254
7.31 Lateral soil movements during 10/27/2008 to 10/23/2009 in the vertical inclinometers (a) V6, (b) V8	255
7.32 Monitored settlement values from DSM and ECS sites	256
8.1 Six-node triangular element (Plaxis Manual)	260
8.2 The results of excess pore pressure as a function of height from Numerical and analytical methods (Plaxis Manual)	261
8.3 Geometry and boundary conditions of the DSM columns model.....	263
8.4 Nodes and elements in the DSM treated section.....	265
8.5 Calculation phase in the settlement calculation	265
8.6 Observation points in the settlement calculation.....	266
8.7 Deformed mesh of the model (scaled up 20 times)	267
8.8 Total displacements in the embankment.....	267
8.9 Horizontal displacements of the model	268
8.10 Vertical displacements of the model	268
8.11 Vertical displacements (a) from horizontal inclinometer (b) from numerical analysis.....	270
8.12 Comparison of vertical displacements in a treated section between data obtained from elevation surveys and results from numerical analysis	271
8.13 Comparison of vertical displacement values between data obtained from Automatic extensometer and results from numerical analysis	272

8.14 Comparison of vertical displacement values between data obtained from Manual extensometer and results from numerical analysis	272
8.15 Lateral soil movements (a) from the vertical inclinometer (b) from results of the numerical analysis at the section of the inclinometer	274
8.16 Geometry and boundary conditions of the untreated section in a model.....	275
8.17 Observation points in the settlement calculation.....	275
8.18 Deformed mesh of the model.....	276
8.19 Total displacements in the embankment	277
8.20 Horizontal displacements of the model	277
8.21 Vertical displacements of the model	278
8.22 Comparison of vertical displacement in a control section values between data obtained from elevation surveys and results from numerical analysis.....	279
8.23 The monitoring location in a control section, IH 30 site, Arlington, TX	279
8.24 Lateral soil movements (a) from the vertical inclinometer (b) from results of the numerical analysis at the section of the inclinometer	281
8.25 Comparison of vertical displacements between data obtained from elevation surveys in a treated section and results from numerical analysis in an untreated section.....	282
8.26 Regression equations from hyperbolic model to predict soil settlement values in both treated (test) and untreated (control) sections	283
8.27 Settlement values from data extrapolation and FEM	285
8.28 Nodes and elements in the DSM treated section with the area-ratio (a_r) of 0.3	286
8.29 Deformed mesh of the DSM treated section with the area-ratio (a_r) of 0.3 (scaled up 20 times)	286
8.30 Vertical soil movements in the DSM treated section with the area-ratio (a_r) of 0.3.....	287
8.31 Horizontal soil movements in the DSM treated section with the area-ratio (a_r) of 0.3.....	287

8.32 Time-settlement in the DSM treated section with various area-ratio (a_r) from 0.3 to 0.8	288
8.33 Settlement with various area-ratios (a_r).....	289
8.34 Geometry of DSM treated section with a slope (V: H) of 1:1	290
8.35 Deformed mesh show total settlements in the embankments with various slopes V:H; a) 1:1, b) 1:2, c) 1:3, d) 1:4, and e) 1:5.....	291
8.36 Geometry of DSM treated section with a height of 7.5 m	292
8.37 Time-settlement in the DSM treated section with various heights of embankment	293
8.38 Design chart for DSM columns with various area-ratios and heights of embankment	294
8.39 Geometry and boundary conditions of the ECS test section	295
8.40 Nodes and elements in the test section	297
8.41 Calculation phase in the settlement analyses.....	298
8.42 Observation points in the settlement calculation.....	298
8.43 Deformed mesh of the test section (displacement scaled up 50 times)	299
8.44 Total displacements in the test section	299
8.45 Horizontal displacements in the test section.....	300
8.46 Vertical displacements in the test section	300
8.47 Comparison of vertical displacements in a test section between data obtained from elevation surveys and results from numerical analysis	301
8.48 Locations of vertical inclinometers installation on ECS embankment, SH 360.....	302
8.49 Comparisons of lateral soil movements between monitored data and numerical results in the vertical inclinometers (a) V1 and (b) V4	304
8.50 Nodes and elements in the control section	305
8.51 Deformed mesh of the control section (displacement scaled up 20 times)	307

8.52 Total displacements in the control section	307
8.53 Horizontal displacements in the control section	308
8.54 Vertical displacements in the control section	308
8.55 Comparison of vertical displacements in a test section between data obtained from elevation surveys and results from numerical analysis	309
8.56 Regression equations from hyperbolic model to predict soil settlement values in both test and control sections	310
8.57 Settlement values from data extrapolation and FEM	311
8.58 Geometry of the test section with a slope (V: H) of 1:1	312
8.59 Deformed mesh showing total settlements in t the embankments with various slopes V:H; a)1:1, b)1:2, c) 1:3, and d) 1:4	314
8.60 Geometry of the test section with a height of 20 ft (6.0 m)	315
8.61 Time-settlement in the DSM treated section with various height of embankment.....	316
8.62 Design chart for ECS embankment.....	317

LIST OF TABLES

Table	Page
2.1 Summary of Ground Improvement Methods Based on Soil Type	32
2.2 Summary of Ground Improvement Techniques based on the Function.....	33
2.3 Embankment Material Specifications (Hoppe, 1999).....	70
2.4 Lift Thickness and Percent Compaction Requirements (Hoppe, 1999).....	71
2.5 CDOT Material Requirements for Flowable fill Backfill	82
2.6 Typical approach slab dimensions used by various DOTs (Hoppe 1999)	97
2.7 Drainage method used by various states (White et al., 2005)	112
2.8 Cost Comparison for Four Slab Faulting Repair Methods	121
3.1 Recommendations for fill material used for embankments.....	138
3.2 Ranking analysis of mitigation techniques for bridge approach settlement.....	141
5.1 Summary of tests performed on natural/artificial soils	159
5.2 Details of Specimen Molds Used	168
5.3 Physical properties of control soils from site IH30	170
5.4 Engineering properties of soil specimens from Sites IH 30 and SH 360.....	178
6.1 Details of the Geogrid.....	182
7.1 Elevation survey data on test section site IH30	224
7.2 Elevation survey data on control section site IH30	235
7.3 Measured vertical displacements in treated and untreated sections	238
7.4 Elevation survey data in treated section and untreated section.....	239

7.5 Depth of sensor rings from Sondex readings in treated and untreated sections	240
7.6 Measured lateral displacements in treated and untreated sections.....	240
7.7 Elevation survey data on Test section site SH360.....	242
7.8 Elevation survey data on the control section site SH 360.....	250
7.9 Comparisons of settlement data on the control and ECS sections on site SH 360	251
8.1 Properties and model type of the materials used in the model analysis.....	264
8.2 Settlement predictions from the Hyperbolic model and the FEM Model	284
8.3 Maximum soil displacement of an embankment with various a_r	288
8.4 The maximum soil displacements with various embankment slopes	290
8.5 Properties and model type of the materials used in the test section model analysis	296
8.6 Properties and model type of the materials used in the control model analysis.....	306
8.7 Settlement predictions from the Hyperbolic and FEM Models for the Test section	311
8.8 Maximum soil displacements with various embankment slopes.....	313

CHAPTER 1

INTRODUCTION

1.1 General

Bridge approach settlement and the formation of the bump are general problems found nationally. This problem usually emanates from soil settlement related problems arising from both embankment fill and subgrade foundation materials. Maintenance of these bridge approach slab settlements cost millions of dollars to repair annually and this mainly absorbs all the maintenance resources. Briaud et al. (1997) reported that 30% of bridges in Texas, i.e., 13,800 out of 46,000 bridges were subjected to the bump problem, while another study cited annual costs for “bump” repairs in Texas is around \$7 million (Seo, 2003). These can signify that the bump is a major if not a premier maintenance problem in Texas.

There have been several researchers studied the bridge approach settlement to determine both the causes of the bump, and the techniques to mitigate the problem. From the literature review, it is found out that the causes of the bump are various and still too complex to identify. However, the primary sources of the problem can be broadly divided into four categories: 1) Material properties of foundation and embankment, 2) Design criteria for bridge foundation, abutment and deck, 3) Construction method, and 4) Maintenance criteria. It should be noted that not all the factors contribute to the formation of the bump or differential settlement concurrently as one factor may be more problematic than the other. Also, one model cannot be developed for capturing the response of settlements underneath the approach slabs.

For the mitigation techniques, it is found that there have already been several methods employed to alleviate the bump problem, which can be summarized based on the groups of treatments as followings; 1) improvement of foundation soil, 2) improvement of backfill material,

3) design of bridge foundation, 4) design of approach slab, and 5) provide effective drainage and erosion control measures.

Two of the major contributors to settlements are weak subgrade conditions and weight of embankments. Hence, any mitigation techniques need to address these conditions. This dissertation research made a comprehensive attempt to address the mitigation techniques using two methods namely Deep Soil Mixing (DSM) columns and Expanded Clay and Shale (ECS). The first method was primarily used for stabilizing weak subsoil conditions and the second method was used as a lightweight embankment fill material. The present dissertation work primarily focused on many aspects of this research including laboratory mix design to field construction and instrumentation, numerical modeling and validation and design method development.

The DSM technique is primarily used to enhance soil strength and its compressibility properties, while the ECS is a lightweight granular material and is used as a backfill material for embankment construction. With its lightweight property, the ECS is expected to decrease the load exerts on the soft foundation, as a consequence, the settlement due to consolidation phenomenon will be decreased.

1.2 Research Objectives

The objectives of this research are to comprehensively evaluate the effectiveness of two different treatment methods, DSM columns for foundation treatment and ECS material for fill construction, in alleviating the differential settlements near a bridge approach slab in the real field conditions. Although these methods have already been utilized in other places, they have not been employed in Texas conditions to serve the purpose related to the bump mitigation problem.

If this study shows that the DSM and ECS techniques can be successful in mitigating the bump occurred at the bridge approach problem, then the results of this study will not only help agencies in lowering their maintenance and repair works of bridge embankments built with

clayey soils, but will also reduce traffic congestion problems arisen due to constant repair works.

1.3 Dissertation Organization

This dissertation consists of nine chapters. The first Chapter is an introduction, which presents the backgrounds, objectives and tasks involved to accomplish this research.

Chapter 2 presents details of the review from available literature addressing the settlement at bridge approach problem. In the chapter, definition of the bump and the causes of the bump are presented first, and followed by viable techniques used to mitigate the settlement at the bridge approach problem, both for new bridge constructions, and for distressed bridge approach mitigation measures.

The means of selecting mitigation methods for studying in this research are presented in Chapter 3. To select practical techniques for this research, two tasks were performed. The first task is a survey questionnaire, which was distributed to all TxDOT Districts. The survey questionnaire was done to understand the bump problems encountered in Texas and to recognize the solutions to minimizing the problem performed by TxDOT. The second task is a ranking analysis of all viable techniques. This analysis was performed by setting up criteria to rank methods feasible for the evaluation study in this research.

Chapter 4 presents the design of DSM technology for settlement mitigation. Since the DSM was selected as one of practical methods to mitigate the bump problem, the procedures used to predict soil settlements occurred in the DSM section is studied and presented in this chapter. The prediction of the settlement is based on the settlement prediction model originally proposed by Rao et al. (1988), which has included overburden pressures, thickness of soil layers and properties of soil in each layer as the primary factors into the settlement calculation. By following the specifications of materials used in both construction and design step, DSM columns and related area ratio values can be determined.

Chapter 5 presents the laboratory results conducted on soil specimens collected from the field for DSM site and ECS site. The laboratory studies were carried out to evaluate the physical engineering properties of the representative soils, which were used further as input data in the numerical analysis. A series of laboratory tests were performed such as the Atterberg Limit test, the consolidation test, the unconfined compression test, and others. It should be noted that all the tests were performed in compliance with the procedures outlined by Texas Department of Transportation (TxDOT) and the American Society of Testing Materials (ASTM) standards, whichever applicable.

Chapter 6 describes the construction practices of each mitigation method along with field instrumentation details used in both fields. In this chapter, the principle mechanisms of each instrument and stepwise procedures of the instrument installation including horizontal inclinometer, vertical inclinometer, rod extensometer and sondex are presented.

Chapter 7 presents the details of data collected from monitoring of field studies. First, the procedures of the data collection are explained and then followed by presenting the values of collected data in the fields. The settlement data analysis performed to consider the efficiency of the mitigation methods by comparing settlement data between both test and control sections. The settlement data obtained in this chapter are not only useful for the aforementioned analysis, but also needed for modeling results evaluation between the observed field values and the numerical modeling analyses results, which are attempted in Chapter 8.

Chapter 8 presents the study results from numerical analysis. The results from the laboratory study in chapter 5 are used as input soil parameters in a finite element numerical model, and thereafter were compared with the monitored data from the field in Chapter 7. The comparisons between the results from the FEM and the field data are performed to validate the numerical model, which are used further to predict the settlements over a long-term condition. Design models and charts are provided on methods to select any of these two for bridge construction practice.

Summary and conclusions from this study, which include the significant findings from field, and numerical analysis studies, and also limitation of this research and the future needs are addressed in Chapter 9.

CHAPTER 2

LITERATURE REVIEW

2.1 Introduction

This chapter presents comprehensive information collected from available literature addressing the problem about the differential settlement at the bridge approach. As a part of this research, the literature review in this chapter was carried out to obtain comprehensive details in five sections. In the first part of this chapter, general information of the definitions of the bump at the end of the bridge and the tolerance of the bump are given. Thereafter, in the second part the mechanisms causing the formation of the bump such as consolidation of foundation soil, poor compaction of the backfill material, poor water drainage and soil erosion closed to the bridge abutments, types of bridge abutments, traffic volume passing over the bridge decks, age of the approach slab, design of the approach slab, skewness of the bridge and seasonal temperature variations are mentioned and reviewed in details. The third part presents the techniques used to mitigate the bump at the end of the bridge for the new bridge. Subsequently, maintenance measures normally employed by highway agencies to alleviate distressed approach slabs are presented. The final section of the chapter is a summary.

2.2 Definition of the Bump and the Bump tolerance

2.2.1 Definition of the Bump

Generally, roadway and embankments are built on subgrade foundation and compacted fill materials respectively, which undergo load induced compression and settlements with time. In contrast, the bridges typically need to rest on deep foundations such as pile, pier or other types of deep foundation systems resting on a firm foundation material such as bedrock. Therefore, by resting on a firm foundation the total settlement of the bridge is usually much

smaller than the total settlement of the roadway or adjacent embankment. As a result, a considerable differential settlement occurs at the area between the bridge and roadway interfaces, and a noticeable bump can develop at the bridge ends.

The “Bump” can affect drivers varying from feeling uncomfortable to being hazardous to their lives (Hopkins, 1969; Ardani, 1987). To eliminate the effects of the bump, the approach slab must be built to provide a smooth grade transition between these two structures (bridge and roadway). Another function of the approach slab is to keep the magnitude of differential settlement within a control limit (Mahmood, 1990; Hoppe, 1999). However, in practice it is found that the approach slabs also exceed differential settlements (Mahmood, 1990, Hoppe, 1999). In such cases, the approach slab moves the differential settlement problem at the end of the bridge to the end of the slab connecting with the roadway. Hence, the “Bump” or “Approach Settlement” can be defined as the differential settlement or heave of the approach slab with reference to the bridge abutment structure.

2.2.2. Bump Tolerances

The differential settlement near the bridge approach is a common problem that plagues several bridges in the state of Texas (Jayawikrama et al, 2005). One of the major maintenance problems is to establish severity levels of the bump that require remedial measures. The differential settlement tolerances need to be established for consideration of when to initiate the repair works.

Walkinshaw (1978) suggested that bridges with a differential settlement of 2.5 in. (63 mm) or greater needs to be repaired. Bozozuk (1978) stated that settlement bumps could be allowed up to 3.9 in. (100 mm) in the vertical direction and 2.0 in. (50 mm) in the horizontal direction. Several researchers define the allowable bumps in terms of gradients as a function of the length of the approach slab. Wahls (1990) and Stark et al. (1995) suggested an allowable settlement gradient as 1/200 of the approach slab length. This critical gradient was also referred by Long et al. (1998), and was used by the Illinois DOT for initiating maintenance operations.

Das et al. (1990) used the International Roughness Index (IRI) to describe the riding quality. The IRI is defined as the accumulations of undulations of a given segment length and is usually reported in m/km or mm/m. The IRI values at the bridge approaches of 3.9 (mm/m) or less indicates a very good riding quality. On the other hand, if the IRI value is equal to 10 or greater, then the approach leading to the bridge is considered as a very poor riding quality. Albajar et al. (2005) established a vertical settlement on the transition zone of 1.6 in. (4 cm) as a threshold value to initiate maintenance procedures on bridge approach areas. In Australia, a differential settlement or change in grade of 0.3% both in the transverse and the longitudinal direction and a residual settlement of 100 mm (for a 40 year design period) are considered as limiting values for bridge approach settlement problems (Hsi and Martin, 2005; Hsi, 2007).

In Texas, the state of practice for repair strategies is different from District to District and these repairs are typically based on visual surveys (Jayawickrama et al., 2005) and International Roughness Index (IRI) values (James et al., 1991). In the study by James et al., (1991), it was indicated that several Districts in Texas have reported bump problems and a few Districts have explored methods such as Urethane injection to moisture control to mitigate settlements. However, these methods have only provided temporary relief as the settlement continues to increase with the service life. As a part of Jayawickrama et al. (2005) study, researchers visited three bridge sites in the Waco, Houston, and San Antonio Districts where Urethane injection was adopted to mitigate approach settlement problems. Their findings are discussed in detail in the subsequent sections of this chapter.

2.3 Mechanisms Causing the Formation of the “Bump”

Bridge approach settlement and the formation of the bump is a common problem that draws significant resources for maintenance, and creates a negative perception of the state agencies in the minds of transportation users. From thorough studies compiled from the existing and on-going research studies on the bridge approach settlement, the causes of the problem can be very variable and are still too complex to identify them easily. However, the primary

sources of the problem can be broadly divided into four categories; material properties of foundation and embankment, design criteria for bridge foundation, abutment and deck, construction supervision of the structures, and maintenance criteria. It should be noted that not all the factors contribute to the formation of the bump concurrently.

There have been many studies employed across the states in the USA to study the causes of the problem and the methodologies to solve it (Hopkins, 1969, 1985; Stewart, 1985; Greimann et al., 1987; Laguros et al, 1990; Kramer and Sajer, 1991; Ha et al, 2002; Jayawikrama et al, 2005; White et al, 2005, 2007).

White et al. (2005) define the term “bridge approach,” not just in terms of the approach slab alone, but in terms of a larger area, covering from the bridge structure (abutment) to a distance of about 100 ft away from the abutment. This definition includes the backfill and embankment areas under and beyond the approach slab as significant contributors to the settlements in the bridge approach region.

Many factors are reported in the literatures that explain the mechanisms causing the formation of bumps on the bridge transition (Hopkins, 1969; Stewart, 1985; Kramer and Sajer, 1991). According to Hopkins (1969), the factors causing differential settlement of the bridge approaches are listed as:

- a. Type and compressibility of the soil or fill material used in the embankment and foundation
- b. Thickness of the compressible foundation soil layer
- c. Height of the embankment and
- d. Type of abutment.

Kramer and Sajer (1991) and Briaud et al. (1997) concurred with these observations later based on extensive surveys of various State DOTs in the USA. Stewart (1985) performed a research study for Caltrans and this study concurred with the finding reported by Hopkins (1969), in particular the observations noting that the original ground and fill materials contribute the

maximum settlement to the approach slab. Based on the results obtained from a field study performed at Nebraska, Tadros and Benak (1989) confirmed that the primary cause of this problem is due to the consolidation of foundation soil but not the consolidation of the compacted embankment fill. The proper compaction of the embankment in accordance with the construction specifications has an important influence on the settlement of embankment fill material. Also, the swell and shrink behaviors of the foundation/ backfill soil and vibration or movements of the backfill soil (in case of granular fill) due to moving traffic loads may significantly impact the development of the approach faults (Hopkins, 1969, 1985).

Ardani (1987), Wahls (1990), and Jayawikrama et al. (2005) also reported that both the time-dependent settlement (primary/secondary consolidation) of foundation soil beneath the embankment and the approach slab embankment as well as the poor compaction of embankment adjacent to the abutment, and erosion of soil at the abutment face and poor drainage system around the abutment are the major contributors to approach settlement problems.

Wahls (1990) stated that the approach-slab design and the type of abutment and foundation can affect the relative settlement of the slab and bridge abutment. Abutments supported by the shallow foundations and when these foundations lay within the approach embankment fill will settle along with the embankment. In addition, Wahls (1990) concluded that the lateral creep of foundation soils and lateral movement of abutments can potentially cause this problem.

Laguros et al. (1990) reported that factors including the age of the approach slab, height of embankment, skewness of the bridge and traffic volume influence the bridge approach settlement. The flexibility of the approach pavements has a considerable influence as well. Laguros et al. (1990) observed greater differential settlement in flexible pavements than rigid pavements during initial stages following construction (short term performance), while both

pavement types performed similarly over the long term. More details are provided in later sections.

Other factors that influence the creation of the bump include the type of bridge abutment and approach slab design (Mahmood, 1990; Wahls, 1990). Design of abutment structures is not unique and varies as per the connection of the slab with the abutment. The abutments are characterized as mainly integral (movable) or non-integral (conventional or stub) type of abutments (Greimann et al., 1987). For an integral abutment, the bridge deck slab is monolithically connected to the abutment, and the abutment is allowed to move laterally along with the bridge deck slab; while for a non-integral one, the bridge deck is independent of the abutment, and the longitudinal movements of the bridge deck are taken care of by roller/pin-bearing plates.

Weather changes also contribute to the differential settlement between the bridge and the approach slab as in the case of integral abutments when seasonal temperature changes from summer to winter (Schaefer and Koch, 1992). Weather changes often lead to soil displacement behind the abutment eventually leading to void development under the approach slab (Schaefer and Koch, 1992; White et al., 2005). This creates water infiltration under the slab, which leads to erosion and loss of backfill material (Jayawikrama et al., 2005).

White et al. (2007) carried a comprehensive field study of 74 bridges in Iowa to characterize problems leading to poor performance of bridge approach pavement systems. White et al. (2007) claimed that subsurface void development caused by water infiltration through unsealed expansion joints, collapse and erosion of the granular backfill, and poor construction practices were found to be the main contributing factors of the approach slab settlements in Iowa.

Other research studies from outside the USA, including Australia and China show that the bump at the end of the bridge is a major concern in highway and freeway constructions. Hsi and Martin (2005) and Hsi (2007) reported that the approach settlement problems were

observed due to very soft estuarine and marine clays in subsoils at the construction of the Yelgun-Chinderah Freeway in New South Wales, Australia. Hsi (2007) reported that rapid construction of deep approach embankments over very soft clay subgrades often experienced the long term settlement of the soft subgrade which has attributed to causing settlements at the approach slabs.

In the following, three studies by Briaud et al. (1997), Seo (2003) and White et al. (2007) listed factors that contribute to bumps. Briaud et al. (1997) summarized various factors that contributed to the formation of bumps/settlements at the approach slabs in Figure 2.1. These factors were grouped and ranked in the following order in which they contribute to the soil movements: fill on compressible foundation; approach slab too short; poor fill material; compressible fill; high deep embankment; poor drainage; soil erosion; and poor joint design and maintenance.

Seo (2003) performed a circular track test involving the approach slab which was repeatedly loaded by a vehicle model. Seo (2003) listed the following observations:

1. Number of cycles of loading over the approach slab is proportional to the increase in the bump
2. Shorter approach slabs result in higher displacements of the slab
3. More highly compacted stiffer soils result in less deflection of the slab
4. The velocity of vehicles has an influence on the increase in magnitude of the bump
5. The weight of vehicles relates to the degree of the settlement.

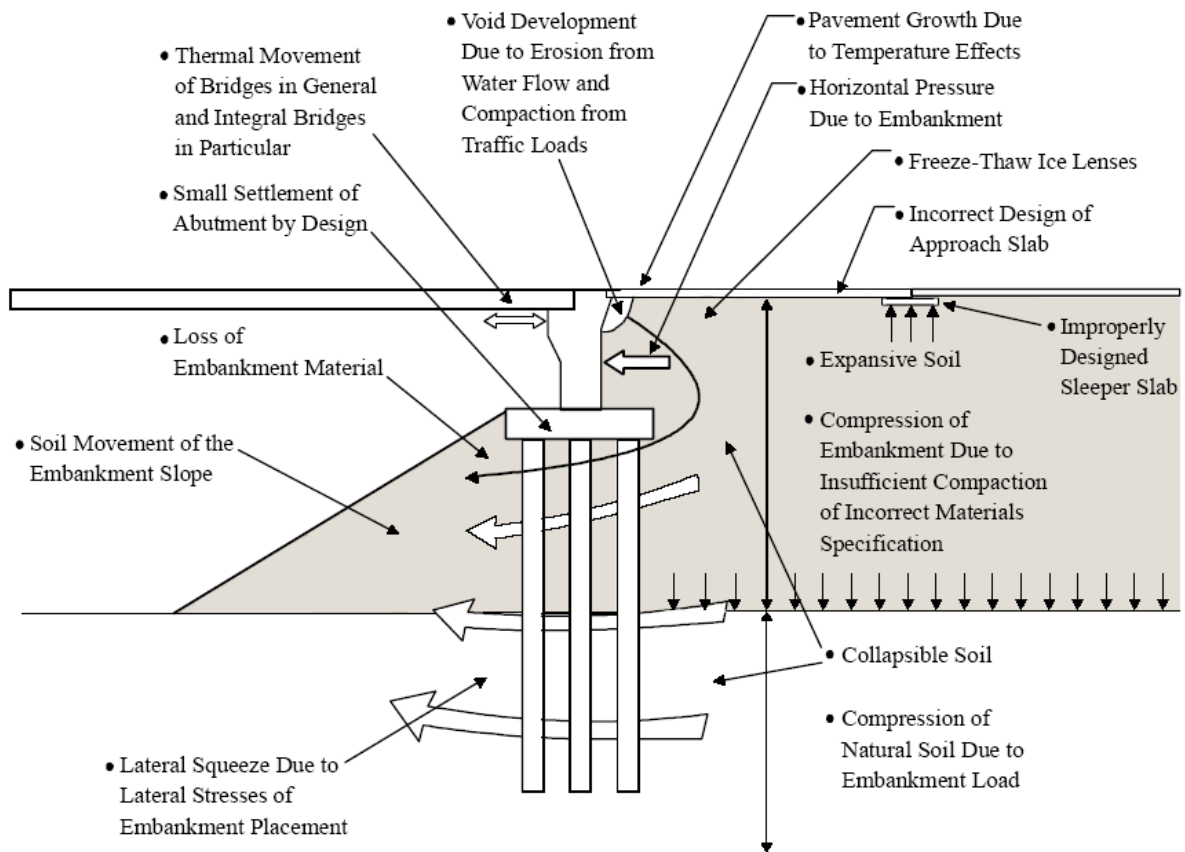


Figure 2.1 Schematic of Different Origins Lead to Formation of Bump at the End of the Bridge (Briaud et al., 1997)

A recent study conducted by White et al. (2007) summarized the following factors as contributors to differential settlements of the approach slab:

1. Backfill materials under poorly performing approach slabs are often loose and under compacted.
2. The foundation soil or embankment fill settles.
3. Many bridge approach elevation profiles have slopes higher than 1/200, which is considered a maximum acceptable gradient for bridge approaches.
4. Voids develop under bridge approaches within one year of construction, indicating insufficiently compacted and erodible backfill material.

5. Inadequate drainage is a major bridge approach problem. Many abutment subdrains are dry with no evidence of water, are blocked with soil and debris, or have collapsed.
6. Many expansion joints are not sufficiently filled, allowing water to flow into the underlying fill materials.

This chapter presents the following major factors that caused approach bumps by summarizing the above studies as well as a review of other investigations that addressed this bump problem:

1. Consolidation settlement of foundation soil
2. Poor compaction and consolidation of backfill material
3. Poor drainage and soil erosion
4. Types of bridge abutments
5. Traffic volume
6. Age of the approach slab
7. Approach slab design
8. Skewness of the bridge
9. Seasonal temperature variations

Salient details of these factors are presented in the following subsections.

2.3.1 Consolidation Settlement of Foundation Soil

Consolidation of foundation soil under an approach embankment is regarded as one of the most important contributing factor to bridge approach settlements (Hopkins, 1969; Wahls, 1990; Dupont and Allen, 2002). It usually occurs because of dynamic traffic loads applied at the embankment surface and static load due to the embankment weight itself (Dupont and Allen, 2002). However, this foundation settlement problem is difficult to address and repair them in-situ, because of the variability in the engineering properties of soils, and the

complexity of accessing the foundation after construction as it is buried deep below the roadway surface (Wahls, 1990).

Foundation problems usually are more severe in cohesive soils than in non-cohesive soils. Since consolidation occurs rapidly in non-cohesive soils, they do not normally represent a serious problem. On the other hand, cohesive soils, such as soft or high plasticity clays, represent a more critical situation, because of their time dependent consolidation behavior. In addition, cohesive soils are more susceptible to lateral or permanent plastic deformation, which can exacerbate the approach settlement problem.

Typically, settlement of soils can be divided in three different phases (Hopkins, 1969); initial, primary and secondary consolidation, which are explained in the following.

2.3.1.1 Initial Consolidation

The initial settlement is the short-term deformation of the foundation when a load is applied to a soil mass. This type of settlement does not contribute to the formation of bumps, because it usually occurs before the construction of the approach structure (Hopkins, 1969). The soil saturation level affects the total contribution of this settlement, and for partially saturated soils, this initial settlement will be generally larger than that of saturated soils.

2.3.1.2 Primary Consolidation

Primary settlement is the main factor that contributes to the total settlement of soils. The gradual escape of water due to the compression of the loaded soil is believed to be the reason for this type of settlement. This primary settlement lasts from a few months for granular soils, to a period of up to ten years for some types of clay (Hopkins, 1973). This significant difference is attributed to the small void ratio and high permeability of granular soils.

2.3.1.3 Secondary Consolidation

This phase occurs as a result of changes in void ratio of the loaded soil after dissipation of excess pore pressure (Hopkins, 1969). In this case particles and water in the soil mass readjust in a plastic way under a constant applied stress. For the case of very soft, highly

plastic or organic clays, secondary consolidation can be as large as the primary consolidation, while in granular soils, it is negligible (Hopkins, 1969).

To mitigate or minimize the settlement, a primary objective of any bridge construction project should include a complete or comprehensive investigation of the foundation soil before the construction of the approach embankment starts (Wahls, 1990). Previous studies have shown that the stresses applied to the foundation subgrades come primarily from the embankment loading rather than the bridge or traffic loads, except for shallow depths (less than 10 ft) (Hopkins, 1969; Wahls, 1990; Dupont and Allen, 2002). Therefore, geotechnical studies have to be carried out with extensive foundation investigations, including laboratory tests to evaluate compression and consolidation potential to better estimate the anticipated post-construction settlements (Dupont and Allen, 2002). It is also important to study the possible shear failures in the foundation that cause lateral deformations and surface settlement problems. This type of failure is more likely to appear in peat and other organic materials.

2.3.2 Poor Compaction and Consolidation of Backfill Material

To minimize construction costs, approach embankments are usually constructed with the most readily available material at or near the site. But when low quality materials (such as locally available soft, cohesive expansive soils and soils sensitive to freeze-thaw) are used, the approach settlements can be induced in terms of bigger “bumps”. In general, cohesive soils are more difficult to compact to their optimum moisture content and density when compared to coarser or granular fill materials (Hopkins, 1973)

Poor compaction control of the embankment material is found to be a factor, resulting in low density and highly deformable embankment mass (Lenke, 2006). Poor compaction can also be attributed to limited access or difficulty in access within the confined working space behind the bridge abutment (Wahls, 1990). Many highway agencies require only granular fills that can be better compacted and are able to reach their maximum consolidation in less time than more cohesive soils (Wahls, 1990; Lenke, 2006). The TxDOT Bridge Design Manual

(2001) notes that either improper backfill materials used for mechanically stabilized earth (MSE) or the inadequate compaction of the backfill materials in the embankment are the contributing factors to the backfill failure.

Compaction type and project schedule are also of great importance (Dupont and Allen, 2002). Field inspectors should ensure that proper compactive effort and compaction levels of the fill material are reached during construction. It is common practice that bridge abutments are constructed before the embankment fill placement and compaction. This practice makes the compaction of the area closest to the bridge more difficult because the equipment access to this critical area becomes limited (Burke, 1987).

In addition to compression of the backfill material, lateral stability and shear strength are of great importance to the overall stability against the approach settlement. For the case of the foundation soil, lateral confining forces are significant, while on embankment fills, the confinement effects are much less pronounced (Wahls, 1990). Hence, slope design, material selection and loads applied to the backfill need to be carefully evaluated to anticipate or minimize the final settlement (Wahls, 1990).

2.3.3 Poor Drainage and Soil Erosion

Several researchers from different state DOTs including Texas DOT, Virginia DOT, Iowa DOT, and Colorado DOT reported the importance of the surface and subsurface drainage and soil erosion near the bridge abutment and embankment interface. Wahls (1990), Jayawikrama et al. (2005), Mekkawy et al. (2005), White et al. (2005), and Abu-Hejleh et al. (2006) identified the drainage system of the abutment and embankment as one of the most important factors that affect approach settlement. The dysfunctional, damaged or blocked drainage systems cause erosion in the abutment and slope, increasing soil erosion and void development. The dysfunctional drainage systems may be caused by either incorrect construction or improper design. Williammee (2008) observed that incorrect placement of the drainage pipes such as outlet flow line higher than inlet flow line in a newly constructed bridge

can impair the drainage system. Briaud et al. (1997) explains how the poor joints between the pavement and the abutment structure as seen in Figure 2.2 can lead to soil erosion of embankment and abutment backfill

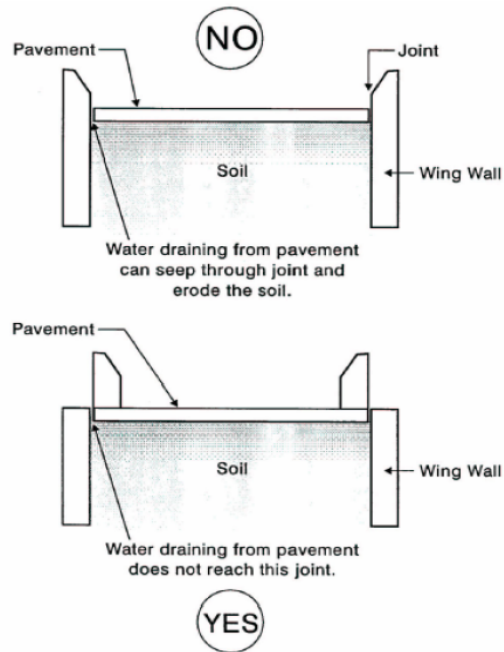


Figure 2.2 Cross section of a wingwall and drainage system (Briaud et al, 1997)

Jayawikrama et al, (2005) noted that the erosion of soil at the abutment face and poor drainage material can induce serious approach settlement problems. This observation was based on the survey responses obtained from various TxDOT District officials. The intrusion of surface water (rain) through weak expansion joints (openings) between the approach slab and bridge abutments can erode backfill material and further amplify the problem of approach slab settlements (Jayawikrama et al, 2005). Based on the detailed study of a few TxDOT bridges, they noted that these joint openings resulted from the poor construction practices such as poor compaction of backfill material near the abutments, poor construction of joint sealants and poor surface and subsurface drainage systems.

In addition, the expansion joints should transfer traffic loads, prevent surface water from entering into the abutment, and allow pavement expansion without damaging the abutment

structure (Wolde-Tinsae et al., 1987). Based on a comprehensive research study performed by White et al. (2005) on many bridges in Iowa most of the expansion joints of the bridges inspected were not sufficiently filled, allowing water to flow into the underlying fill materials. On the other hand, cracks were often encountered next to closed joints in bridge approaches because of the crushing and cracking of neighboring concrete, allowing for leakage of water as well.

Similar observations were made by Mekkawy et al. (2005) which are discussed here. Based on field investigations in different states, Mekkawy et al. (2005) reported that inadequate drainage and subsequent severe soil erosion contributed to settlement problems of 40% of the bridge approach slabs that were surveyed by them. Moisture flow into the backfill coupled with poor drainage conditions can cause failure of embankment, backfill and bridge abutments either by excessive settlement or by soil strength failure. Typically, water can seep into the embankment fill material via faulty joints and cracked concrete pavement sections. The leaked water can soften the embankment fill and can cause internal erosion as the fines typically wash out from the fill material. Without approach slabs, water leakage will immediately induce settlement; with approach slabs, voids beneath the slab will form, amplifying the erosion by compression of the soil.

The erodability of soils is based on their grain size distribution. Some soil gradation guidelines can be found for soils that are erosion resistant and those that are prone to erosion (Briaud et al., 1997; Hoppe, 1999). As indicated in Figure 2.3, a gradation band of material in the sand to silt size materials is a bad choice for embankments and backfill unless additional preventive actions, such as providing appropriate drainage design or erosion control systems, are taken (Briaud et al., 1997).

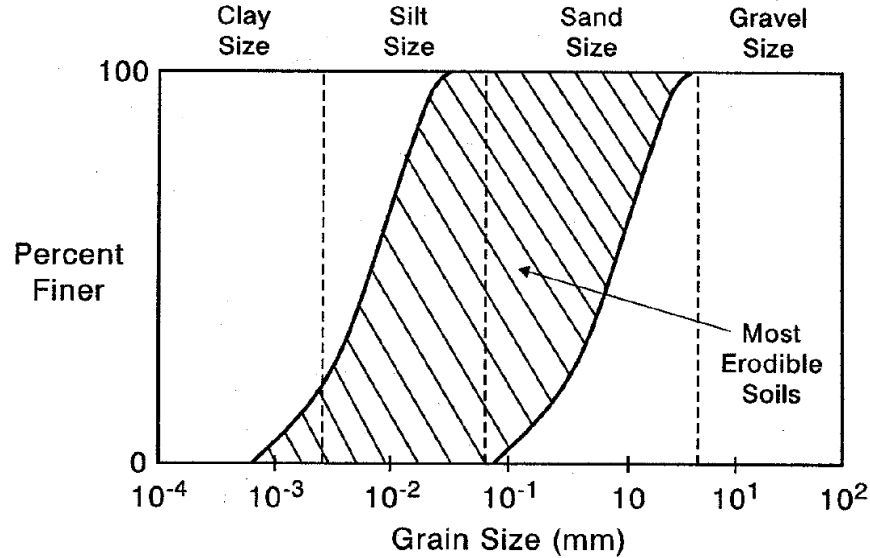


Figure 2.3 Range of Most Erodible Soils (Briaud et al., 1997)

2.3.4 Types of Bridge Abutments

Abutments must be compatible with the bridge approach roadway and they must have backwalls to keep the embankment from covering up the beam ends and to support possible approach slabs (Figure 4). They also usually have wingwalls to keep the side slopes away from the structure and to transition between the guard rail and the bridge rail as shown in Figures 2.4 and 2.5.

Abutments are characterized as integral (movable) or non-integral (conventional or stub) types (Greimann et al., 1987). In the integral type, the bridge deck slab is monolithically connected to the abutment, and the abutment is allowed to move laterally along with the bridge deck slab; while in the non-integral type, the bridge deck is independent of the abutment, and the longitudinal movements of the bridge deck are taken care of by roller/pin-bearing plates (Greimann et al., 1987). The advantages of integral bridge abutments are reduced construction and maintenance costs, minimum number of piles required to support the foundation and enhanced seismic stability (Greimann et al., 1987; Hoppe and Gomez, 1996). To avoid the use of the bearing plates and to reduce potential maintenance problems (such as frequent repair of

bearing plates, expansion joint sealants) associated with non-integral bridge abutments, the use of integral bridge abutments has been increased since 1960's (Horvath, 2000; Kunin and Alampalli, 2000). The following sections describe the advantages and disadvantages of both types of abutments.

2.3.4.1 Integral Abutments

Figure 2.4 shows a simplified cross section of an integral abutment bridge. The approach slab system of an integral bridge consists of the backfill, the approach fill, and the soil foundation. If an approach slab and a sleeper slab are used, they are also considered in the system. Integral abutment bridges are designed to carry the primary loads (dead and live loads) and also the secondary loads coming from creep, shrinkage, thermal gradients and differential settlements. Integral abutments are rigidly connected to the bridge beams and deck with no expansion joint.

Even though integral abutments present structural advantages over non-integral abutments, they also introduce thermal movements in the approach system that can aggravate the bump problem on the approach system (Schaefer and Koch, 1992; White et al., 2005). Hence, special attention has to be paid in this type of abutment to the lateral loads imposed on the foundation piles due to horizontal movements induced by temperature cycles (Wahls, 1990).

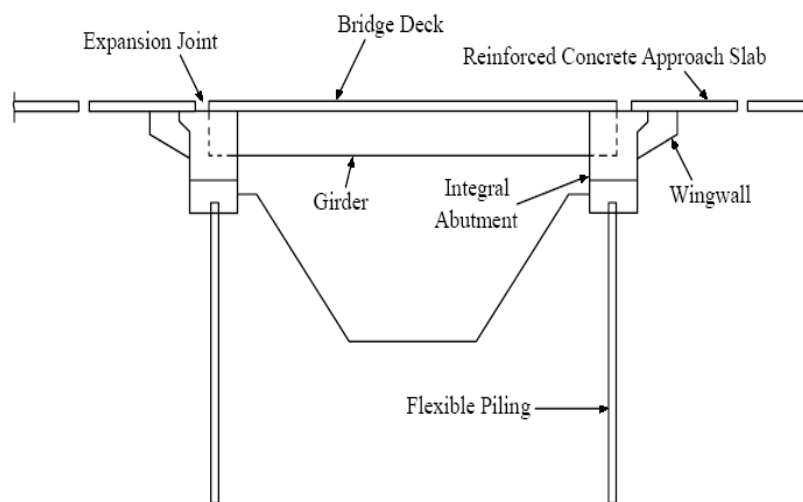


Figure 2.4 A Simplified Cross Section of an Integral Abutment Bridge (Greimann et al., 1987)

2.3.4.2 Non-Integral Abutments

A simplified cross-section of a non-integral abutment is shown in Figure 2.5. In this case, abutments are supported on bearing connections that allow longitudinal movements of the superstructure without transferring lateral loads to the abutment. The non-integral bridge abutment is separated from the bridge beams and deck by a mechanical joint that allows for the thermal expansion and contraction of the bridge (Nassif, 2002).

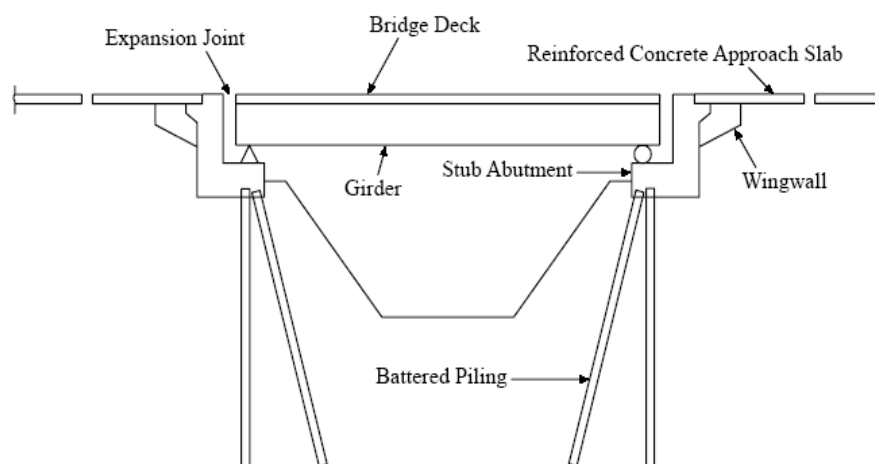


Figure 2.5 A Simplified Cross Section of a Non-integral Abutment Bridge (Greimann et al., 1987)

Three major types of non-integral abutment bridges can be found in the literature. These are: Closed or U-type, Spill-through or Cantilever and Stub or Shelf abutments (Hopkins and Deen, 1970; Timmerman 1976; Wahls 1990; TxDOT Bridge Design Manual, 2001).

2.3.4.3 Closed Abutment or U-type

A simplified cross-section of a closed abutment is shown in Figure 2.6a. The U-type abutments have two side walls and a front wall resting on spread footings below natural ground (TxDOT Bridge Design Manual, 2001). For this type of abutment, the side walls are long enough to keep the embankment from encroaching on the bridge opening. In addition, the taller the abutment is, the longer the sidewalls will be. The compaction of the embankment fill is rather difficult in these abutments, because of confined space near the abutment and due to the

wall which is extended over the whole height of the abutment (TxDOT Bridge Design Manual, 2001). These abutments are also subjected to higher lateral earth pressures than other types.

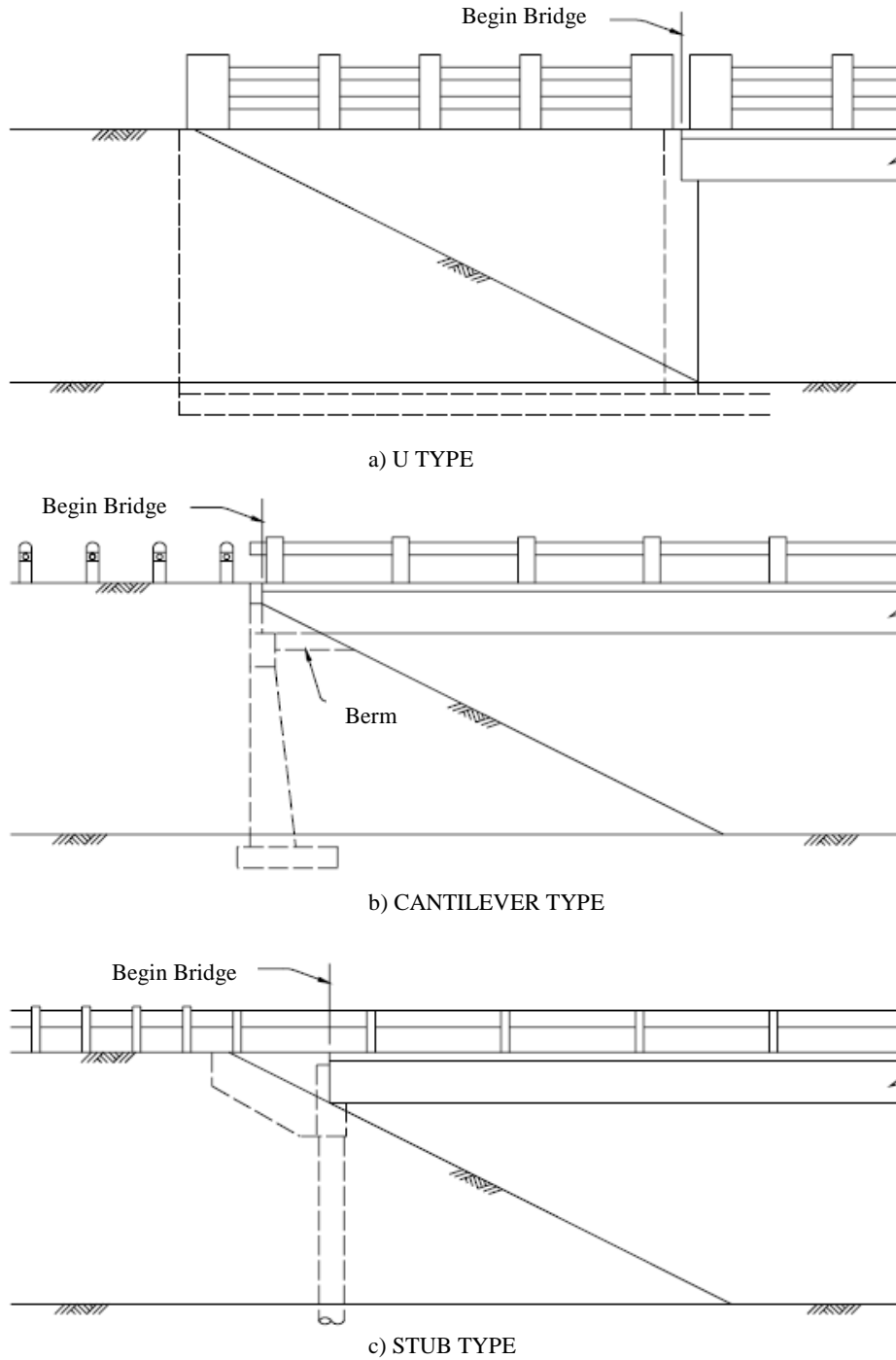


Figure 2.6 Non-integral Abutment Types (TxDOT Bridge Design Manual, 2001)

2.3.4.4 Spill-through or Cantilever Abutment

A simplified cross-section of a spill-through abutment is shown in Figure 2.6b. A spill-through abutment is supported on the columns and hence, the compaction of the backfill material between the columns and near the abutment is very difficult. Cantilever type abutments have variable width rectangular columns supported on spread footings below natural ground (TxDOT Bridge Design Manual, 2001). The fill is built around the columns and allowed to spill through, on a reasonable slope, into the bridge openings. A great number of these types of abutments have been constructed in Texas, and they have performed well in the past (TxDOT Bridge Design Manual, 2001). However, this type of abutment presents detailing and construction problems, as well as high construction costs.

2.3.4.5 Stub or Shelf Abutment

A simplified cross-section of a stub type abutment is shown in Figure 2.6c. A stub abutment is constructed after the embankment, so its height is directly affected by the embankment height. The compaction of the backfill material is relatively easier, compared with the closed type except for the soil behind the abutment (TxDOT Bridge Design Manual, 2001).

Most of the abutments in Texas were of the “stub” or “shelf” type, constructed by driving piling or drilling shafts through the compacted fill and placing a cap backwall and wingwalls on top. The header bank is sloped from the top of the wingwall through the intersection of the cap and backwall into the bridge opening. The bridge must be considerably longer than with U-type abutments but slightly shorter than the cantilever types. The extra length of this abutment is justified on the basis of cost and aesthetics (TxDOT Bridge Design Manual, 2001).

Although more economical, stub abutments have maintenance problems. The “bump at the beginning of the bridge,” caused by fill settlement is particularly noticed on stub type abutments (TxDOT Bridge Design Manual, 2001).

From the past experiences with these non-integral abutment bridges, TxDOT officials attribute the approach settlements to the poor construction practices due to inaccessibility to

compact the backfill/embankment fill near the vicinity of the abutment leading to the aggressive approach settlements (Jayawikrama et al., 2005).

2.3.5 Traffic Volume

Heavy truck traffic has been found in some studies to be a major factor contributing to the severity of this bump along with the age of the bridge and approach, especially for the late 70s or early 80s (Wong and Small, 1994; Lenke, 2006). High-volume traffic has been found as a compelling reason for including approach slabs in the construction of both conventional and integral bridges. Lenke (2006) noted that “the bump” was found to increase with vehicle velocity, vehicle weight, especially heavy truck traffic, and number of cycles of repetitive loading, in terms of Average Daily Traffic (ADT). On the other hand, Bakeer et al., (2005) have concluded that factors such as speed limit and traffic count have no distinguishable impact on the performance of the approach slabs.

2.3.6 Age of the Approach Slab

The age of the approach slab is an important factor in the performance of different elements of bridge structures, especially at the expansion joints next to the approach slab, which could negatively affect the backfill performance in terms of controlling settlements underneath the slab (Laguros et al., 1990; Bakeer et al., 2005). Another factor known as alkali-silica reactivity (ASR) formed under the concrete approach slabs and is known to induce expansion stresses. These stresses can potentially lead to slab expansion and distress in the approach slabs, approach joints, and vertical uplift of the slabs and pavement preceding the slabs (Lenke, 2006).

Bakeer et al. (2005) studied the influence of approach age by investigating a number of approach slabs built in the 1960s, 1970s, 1980s, and 1990s. Based on the condition ratings, the newer pile- and soil-supported approach slabs were generally in better condition than the older ones. The IRI ratings showed that pile-supported approach slabs built in the 1980s

performed better than those built in the 1990s and that the approach slabs built in the 1990s performed better than those built in the 1970s.

Laguros et al. (1990) reported that the flexibility of the approach pavements has a considerable influence as well. They observed greater differential settlement in flexible pavements than rigid pavements during initial stages following construction (short term performance), while both pavement types performed similarly over the long term.

2.3.7 Approach Slab Design

The purpose of the approach slab is to minimize effects of differential settlement between the bridge abutment and the embankment fill, to provide a smooth transition between the pavement and the bridge, to prevent voids that might occur under the slab and to provide a better seal against water percolation and erosion of the backfill material (Burke, 1987). However, a rough transition can occasionally develop with time in bridge approaches due to differential settlements between the abutment and roadway. This can be attributed to the different support systems of the two structures connected by the approach slab. The approach slab and the roadway are typically constructed over an earth embankment or natural soil subgrade, whereas the bridge abutment is usually supported on piles.

Insufficient length of approach slabs can create differential settlements at the bridge end due to high traffic induced excessive destruction in the approach slab (Briaud et al., 1997). Based on an extensive survey performed by Hoppe (1999) in 39 states, approach slabs lengths varied from 10 to 40 ft and thicknesses ranged from 8 to 17 in. Some studies based on the IRI ratings, report that 80 foot-long slabs performed the best, and no significant difference was found when compared to 100 foot-long slabs (Bakeer et al., 2005).

The rigidity of the approach slab is also a major contributing factor. Dunn et al. (1983) compared the performance of various approach slab pavements in Wisconsin and reported that 76% of the flexible approaches rated poor, 56% of the non-reinforced approaches rated fair,

and 93% of the reinforced concrete approaches rated good. All these ratings are based on the performance of the approach slab in controlling the differential settlements.

2.3.8 Skewness of the Bridge

Skew angle also has a significant effect on the formation of approach settlements and the overall bridge performance. Skewed integral bridges tend to rotate under the influence of cyclic changes in earth pressures on the abutment (Hoppe and Gomez, 1996). According to Abendroth et al. (2007) design of skewed integral abutment bridges must account for the transverse horizontal earth pressure applied along the skew. Also, the change in position of the ends of an abutment can be attributed to a combination of two effects: the temperature-dependant volumetric expansion or contraction of concrete in the pile cap and abutment, and the rigid-body translation and rotation of the abutment due to the longitudinal expansion or contraction of the superstructure for a skewed integral abutment bridge. This study also recommended that when skewed integral abutments are used, they should be placed parallel to each other and ideally be of equal height (Abendroth et al. 2007).

Nassif (2002) conducted a finite element study to understand the influence of skewness of bridge approaches and transition slabs on their behavior. It was found that the skew angle of the approach slab resulted in an uneven distribution of the axial load, so that only one side of the axles actually had contact with the approach slab. Figure 2.7 shows that for the same loading conditions, the tensile axial stresses on skewed approach slabs are found to be 20 to 40% higher than the same on straight approach slabs. In addition, the pinned connection at the edge of the approach slabs which connects them with the bridge abutment prevented any displacement taking place along this edge, thus providing more strength to the elements of this region (Nassif, 2002).

Additionally, higher rates of settlements at the bridge exit were considered to be accountable to the effect of the skew angle of the approach slab as well as improper compaction conditions in hard-to-reach soil areas close to the abutments (Nassif, 2002).

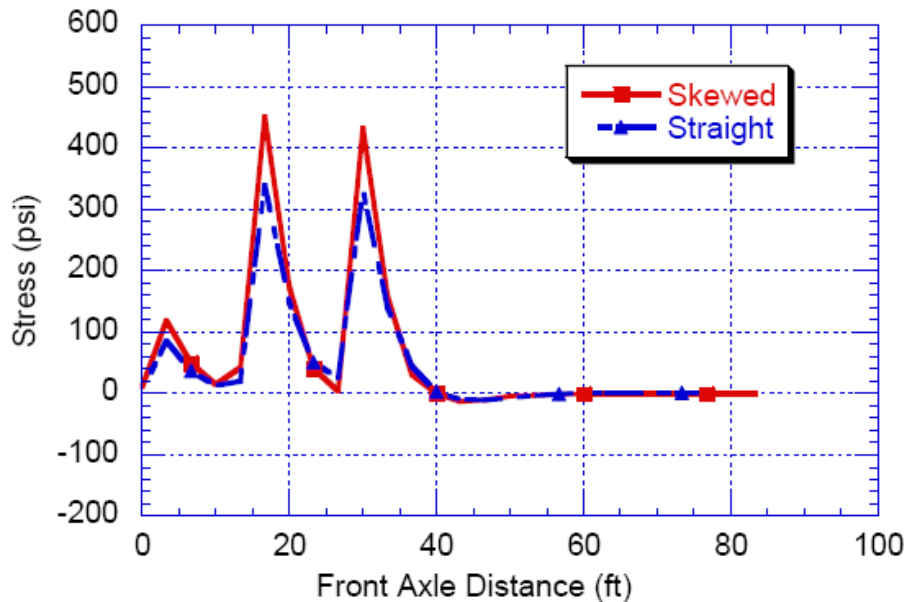


Figure 2.7 Variation of tensile axial stress with front axle distance for skewed and straight approach slabs (Nassif, 2002)

2.3.9 Seasonal Temperature Variations

Some of the factors that contribute to differential settlement between bridge and approach slab, especially for integral abutments, are seasonal temperature changes between summer and winter in the bridge deck (Schaefer and Koch, 1992; Arsoy et al, 1999; Horvath, 2005; White et al., 2005). This temperature change causes cyclical horizontal displacements on the abutment backfill soil, which can create soil displacement behind the abutment, leading to void development under the approach slab (White et al., 2005). As a result, the infiltration of water under the slab and therefore erosion and loss of backfill material may accelerate.

Due to seasonal temperature changes, abutments move inward or outward with respect to the soil that they retain. During winter, the abutments move away (outward) from the retained earth due to contraction of the bridge structure while in summer they move towards (inward) the retained soil due to thermal expansion of the bridge structure (Arsoy et al, 1999; Horvath, 2005) At the end of each thermal cycle, abutments have a net displacement inward and outward from

the soil which is usually retained (see Figure 2.8). This is attributed to the displacement of an 'active soil wedge' which moves downward and towards the abutment during winter but cannot fully recover due to inelastic behavior of the soil during the summer abutment movement. This phenomenon was noted in all types of embankment materials (Horvath, 2005). Besides, these horizontal displacements are observed to be greater at the top of the abutment and hence the problem is aggravated when the superstructure is mainly constructed with concrete (Horvath, 2005). Figure 2.9 shows how the expansion-contraction movements of the bridge with the seasonal temperature change will lead to the creation of voids below the approach slab.

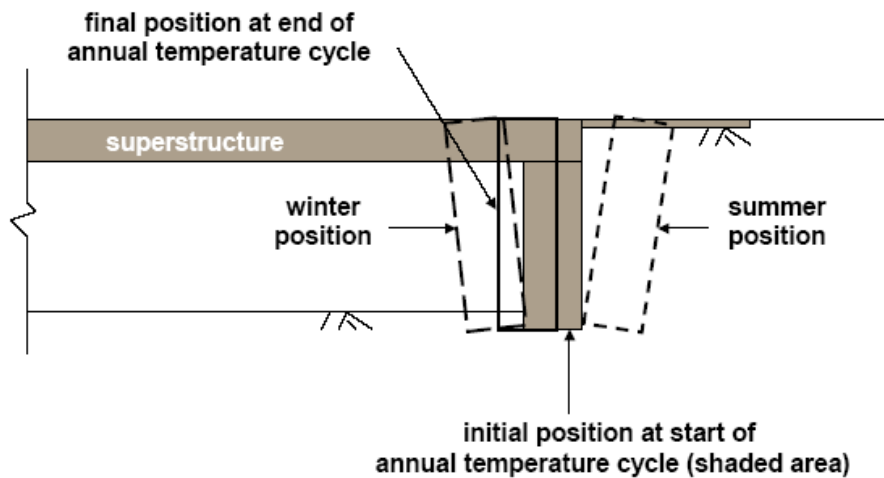


Figure 2.8 Thermally Induced IAB Abutment Displacement (Horvath, 2005)

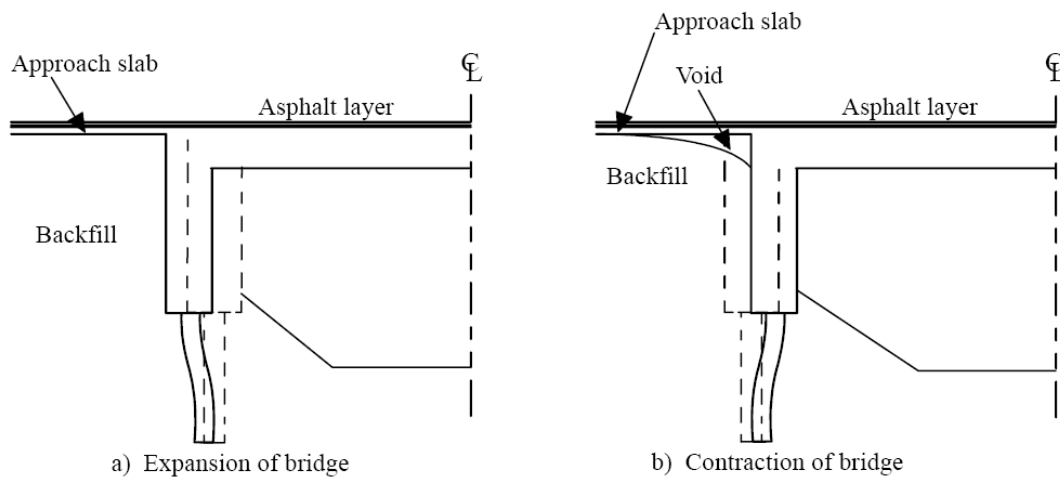


Figure 2.9 Movement of Bridge Structure (Arsoy et al., 1999)

The temperature effect on the bridge-abutment interaction also creates pavement growth due to friction between the pavement and its subbase (Burke, 1993). After the pavement expands, it does not contract to its original length because of this friction. This residual expansion accumulates after repeated temperature cycles, resulting in pavement growth that can be rapid and incremental at pressure relief joints (Burke, 1993). The pressure generated will transmit to the bridge in terms of longitudinal compressive force and therefore, should be considered by engineers when designing the pressure relief joints.

James et al. (1991) documented a case of severe abutment damage for a bridge without pressure relief joints through a numerical study. This numerical stress analysis indicated that the damage was caused by the longitudinal growth of continuous reinforced concrete pavement, causing excessive longitudinal pressures on the abutments.

The cycle of climatic change, especially the temperature change, also can cause certain irreversible damage to the pavement or bridge approach slabs in terms of ice lenses due to frost action. Here ice lenses are derived from freezing and thawing of moisture in a material (in this case soil) and the structure that are in contact with each other (UFC, 2004). The existence of freezing temperature and presence of water on the pavement either from precipitation or from other sources such as ground water movement in liquid or vapor forms under the slabs can cause frost heave in pavements. This phenomenon causes the pavement rising because of ice crystal formation in frost-susceptible subgrade or subbase that can affect the durability of concrete. The frost induced heave is not a serious problem in pavements in dry weather areas like Texas.

As noted by the above sections, bump or differential settlements are induced by several factors either by individual mechanisms or by combination mechanisms. In the following subsections, different treatment or repair techniques adapted for new and existing bridges are detailed.

2.4 Mitigation Techniques for Approach Settlements of New Bridges

This sub-section is a summary of various methods adopted for mitigating potential settlements expected in new bridges. These techniques are listed based on various groups of treatments such as improvement of foundation soil, improvement of backfill material, design of bridge foundation, design of approach slab, and effective drainage and erosion control methods.

2.4.1 Improvement of Embankment Foundation Soil

The behavior of foundation soil beneath the embankment and embankment fill is one of the important factors in the better performance of bridges (Wahls, 1990). Generally, if the foundation soil is a granular material type, such as sand, gravel and rock, which do not undergo long term settlements, then the differential settlement of the bridge structure can be negligible. On the other hand, if the approach embankments are constructed on cohesive soils such as clays, then those soils can undergo large settlements either from primary and/or secondary consolidation settlements. These settlements will subsequently lead to the settlements of embankment structures and thereby formation of the bumps or approach settlement problems leading to poor performance of bridge approaches. Several attempts have been made by many researchers both from the USA and abroad to mitigate these unequal settlements arising from highly compressible embankment fills (Wahls, 1990; Dupont and Allen, 2002; White et al., 2005; Abu-Hejleh et al., 2006; Hsi, 2008).

When the soil/fill underneath the structure is not suitable for construction, the recommended approach is to enhance the properties of the foundation soil such that they undergo less compression due to loading (White et al., 2005). Successful ground improvement methods include preloading the foundation soil (Dupont and Allen, 2002) excavation and replacement of existing soft soil, reinforcement of soil to reduce time-dependent post construction settlements and also lateral squeeze (White et al., 2005). Lightweight embankment materials are also effectively used as embankment fills in order to reduce the embankment loads applied on the foundation soils (Saride et al, 2008).

The selection of ground improvement technique for a particular project is mostly based on the type of soil and partly on the depth of the loose layer, degree of saturation, ground water table location and permeability. If the soil is granular material, then the ground improvement techniques such as surcharge (or) preloading, dynamic compaction, compaction piles, grouting, and gravel columns are preferred (Wahls, 1990; Abu-Hejleh et al., 2006) and if the soil is cohesive in nature, excavation and re-compaction, preloading, installation of wick drains, dynamic compaction, stone columns, lime treatment columns and grouting are proposed (Wahls, 1990; Abu-Hejleh et al., 2006).

Based on the review of literature, the stabilization techniques to improve the embankment foundation soil are grouped as per the soil type. Table 2.1 summarizes these ground improvement techniques adopted, not limited to one, for each foundation soil in a chronological order of their importance and the level of settlement problem.

Table 2.1 Summary of Ground Improvement Methods Based on Soil Type

Technique	Cohesionless soils	Cohesive soils
Excavation and Replacement	✗	✓
Preloading w or w/o Surcharge	✓	✓
Dynamic Compaction	✓	✓
Grouting	✓	✓
Wick Drains	✗	✓
Compaction Piles	✓	✗
Gravel Columns	✓	✗
Lime Treatment	✗	✓
Stone Columns	✗	✓
Soil Reinforcement	✓	✓
Geopier	✓	✓

Most of the techniques in combination are chosen for a particular field situation. For example, preloading with the installation of wick drains will lead to faster consolidation settlement of weak soft foundation soil. These techniques are again divided into three sub categories such as mechanical, hydraulic and reinforcement techniques based on the function of each stabilization technique (Table 2.2).

The following sections describe each ground improvement technique and available literature information with respect to approach settlement problems.

Table 2.2 Summary of Ground Improvement Techniques based on the Function

Embankment Soft Foundation Soil Improvement Techniques		
Mechanical	Hydraulic	Reinforcement
Excavation and replacement	Sand drains	Columns
Preloading and surcharge	Prefabricated drains	Stone and Lime Columns
Dynamic compaction	Surcharge loading	Geopiers
		Concrete Injected Columns
		Deep Soil Mixing Columns
		Deep foundations
		In-situ: Compacted piles
		CFA piles
		Driven piles: Timber and Concrete piles
		Geosynthetics
		Geotextiles/Geogrids
		Geocells

2.4.1.1 Mechanical Modification Techniques

2.4.1.1.1 Excavation and Replacement

In this method, the undesirable top soil is excavated and replaced with a select fill from borrow sites. The removal and replacement concept is one of the options considered when the proposed foundation soils are prone to excessive consolidation (Luna et al., 2004, White et al., 2005, Wahls 1990, Hoppe 1999, Chini et al. 1992). Dupont and Allen (2002) reported that around thirty-two states in the US replace the foundation soil near the bridge approach when they have low bearing stresses. The excavation can be done in the range of 10 ft (3 m) to 30 ft (10 m) from the top soil surface. The selected fill material from the borrow pit must be controlled carefully to avoid pocket entrapments during the compaction process.

Presently the difficulties involved in this excavation and replacement method are due to the difficulty in maintaining uniform replacement and expenses involved in the complete removal and land-filling of undesirable soil. Because of these reasons, this method becomes less favorable. Tadros and Benak (1989) discussed this technique in detail and reported that the excavation and replacement technique may be the most economical solution, only if the compaction areas are underlain by a shallow bedrock or firm ground.

2.4.1.1.2 Preloading/Precompression

One of the effective methods reported in the literature to control foundation settlement is to pre-compress the foundation soil (Dupont and Allen, 2002). According to Bowles (1988), pre-compression is a relatively inexpensive and effective method to improve poor foundation soils. Bowles (1988) noted that this technique is used to accomplish two major goals; one is to eliminate settlements that would otherwise occur after the structure is built and the second is to improve the shear strength of the subsoil by increasing the density, reducing the void ratio, and decreasing the water content.

The pre-compression technique in embankment construction is a process in which the weight of embankment will be considered as a load inducing the consolidation settlement and

completing the process before the beginning of actual pavement or roadway construction. In this method, the construction is delayed, even up to one year in most of the cases, so as to allow embankment settlement prior to roadway construction before the placement of approach pavement (Cotton et al., 1987). Even though this method could be effective in reducing foundation settlement and maintenance costs, many highway agencies do not implement this technique due to lengthy construction periods that could cause significant problems in construction schedules and increase in total project costs (Hsi, 2007). Hence, this technique is often combined with other ground improvement methods such as vertical drains and surcharge loading which will enhance the properties of subsoils from mechanical and hydraulic modifications, resulting in faster enhancements. Design of vertical drains deal with the hydraulic properties of the soil and hence these details are covered in modifications by hydraulic methods.

2.4.1.1.3 Surcharge Loads

A temporary surcharge load might also be applied on top of the embankment to accelerate the consolidation process (Bowles, 1988; Hsi, 2007). In order to achieve this, the applied surcharge load must be greater than the normal load, i.e. the weight of the embankment in this particular case. However, the desired extra load, in terms of extra height of embankment, has to be limited by its slope stability. In order to eliminate this limitation, sometimes a berm is constructed for this purpose. The costs of berm construction, excessive fill placement and its removal will result in an increased overall project cost and duration. These costs have to be weighed against the costs involved in avoiding construction delays (Bowels, 1988).

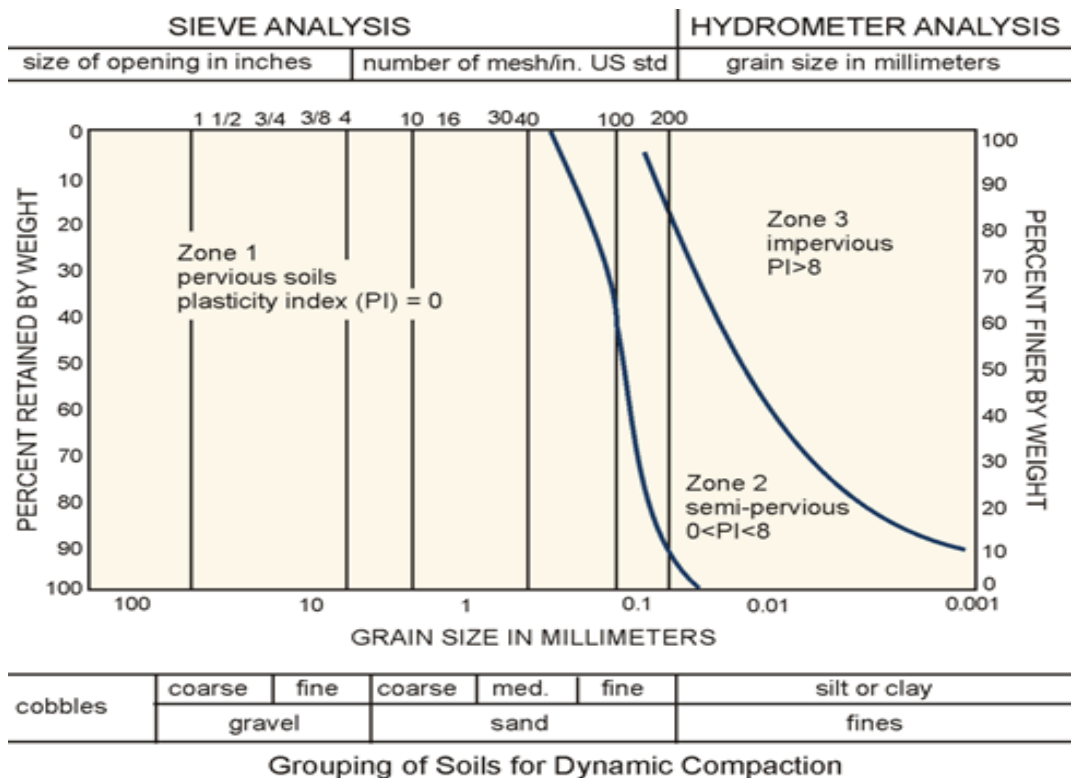
2.4.1.1.4 Dynamic compaction

The dynamic compaction is another alternative to improve the foundation soil. This technique is best suitable for loose granular deposits than medium to soft clays. Heavy tamping and dynamic consolidation are also called dynamic compaction (Hausmann, 1990).

In this technique, a heavy weight is repetitively dropped onto the ground surface from a great height (Lukas, 1986). During this process, densification of a saturated or nearly saturated soil are achieved due to sudden loading, involved shear deformation, temporary high pore pressure generation (possibly liquefaction) and subsequent consolidation (Lukas, 1986; 1996).

Generally the weight of the tamper mass ranges from 6 to 170 tons and the drop height is between 30 and 75 ft (Lukas, 1986). The use of a small mass falling from a lower height, usually 12 tons dropping from 36 ft is typically employed during small scale tamping operations (Hausmann, 1990). The parameters such as degree of saturation, soil classification, permeability and thickness of the clay layer influence the suitability of a particular soil deposit for the dynamic compaction technique. Based on the grain size and the plasticity index (PI) properties of soils, Lukas (1986) characterized and grouped them into three different zones as shown in Figure 2.10.

This figure shows that the zone I (pervious soils) soils are best suited for dynamic compaction. Zone II soils (semi-pervious) require longer duration to dissipate dynamic compaction induced excess pore water pressure to obtain the required level of improvement. Hence, soils in Zone II require multiple phases of dynamic compaction. It can be observed that the soils grouped under Zone III are not suitable for dynamic compaction. The effective depth of dynamic compaction can be as deep as 40 ft (12 m) but usually ineffective for saturated impervious soils, such as peats and clayey soils (Wahls, 1990). Besides, this technique is not feasible when the area of improvement required is smaller such as for highway embankments of confined widths (Hausmann, 1990). The application of this technique in highway related projects is less when compared to the other applications which include compacting sanitary land fills, rocky areas, dams, and air fields (Lukas, 1995). No documented cases where this method was used for mitigating settlements of fills underneath the slabs were found in the literature.



Lukas (1986)

Zone 1: Best

Zone 3: Worst (consider alternate methods)

Zone 2: Must apply multiple phases to allow for pore pressure dissipation

Figure 2.10 Grouping of soils for Dynamic Compaction (after Lukas, 1986)

2.4.1.2 Hydraulic Modification Techniques

2.4.1.2.1 Vertical drains

Vertical drains in the form of sand drains were successfully used to enhance the consolidation process by shortening the drainage path from the vertical to the radial direction (Nicholson and Jardine, 1982). Recently, the usage of sand drains has been replaced by prefabricated vertical drains; also called as wick drains, accounting for their ease in installation and economy. Wick drains basically consist of a plastic core with a longitudinal channel wick functioning as a drain, and a sleeve of paper or fabric material acting as a filter protecting the core. Configurations of different types of prefabricated vertical drains (PVDs)

available in the market are shown by Bergado et al (1996) as shown in the Figure 2.11. Typically PVD's are 100 mm wide and 6-8 mm thick and available in rolls (Rixner et al, 1986). The main purpose of prefabricated vertical drains is to shorten the drainage path and release the excess pore water pressure in the soil and discharge water from deeper depths thereby assisting in a speedy consolidation process of soft soils. Generally vertical drains are installed together with preloading to accelerate the consolidation process (Rixner et al, 1986; Bergado et al., 1996).

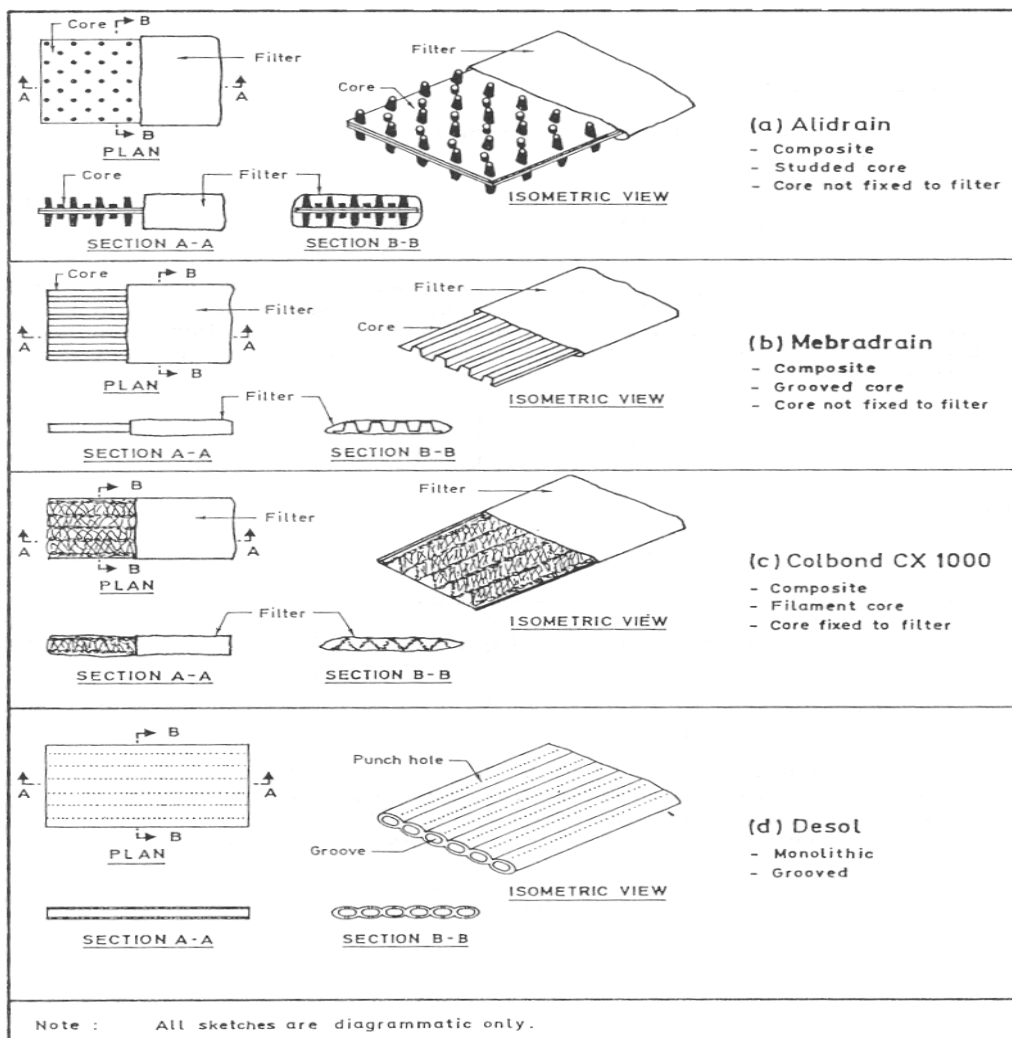


Figure 2.11 Configurations of different types of prefabricated vertical drains (after Bergado et al., 1996)

Based on classic one-dimensional consolidation theory by Terzaghi (1943), Barron (1948) developed a solution to the problem of consolidation of the soil specimen with a central sand drain using two-dimensional consolidation by accounting for radial drainage. Later, Hansbo (1979) modified Barron's equation for prefabricated vertical drain application. The discharge capacity, spacing, depth of installation, and width and thickness of the wick drains are prime factors controlling the consolidation process. These design factors again depend on the in-situ conditions of the project location (Hansbo, 1997). These design procedures are described in detail by Hansbo (1979; 1997; 2001).

The first application of vertical sand drains for settlement control was experimented in California in the early 1930's and the first prototype prefabricated vertical drains were pioneered by Kjellman in Sweden in 1937 (Jamiolkowaski et al., 1983). Several researchers have reported the successful application and functioning of vertical sand and wick drains in highway embankment constructions from all over the world (Atkinson and Eldred, 1981; Bergado et al., 1988; Indraratna et al, 1994; Bergado and Patawaran, 2000). A typical arrangement of vertical drains in a soft soil under embankment with surcharge load is shown in Figure 2.12.

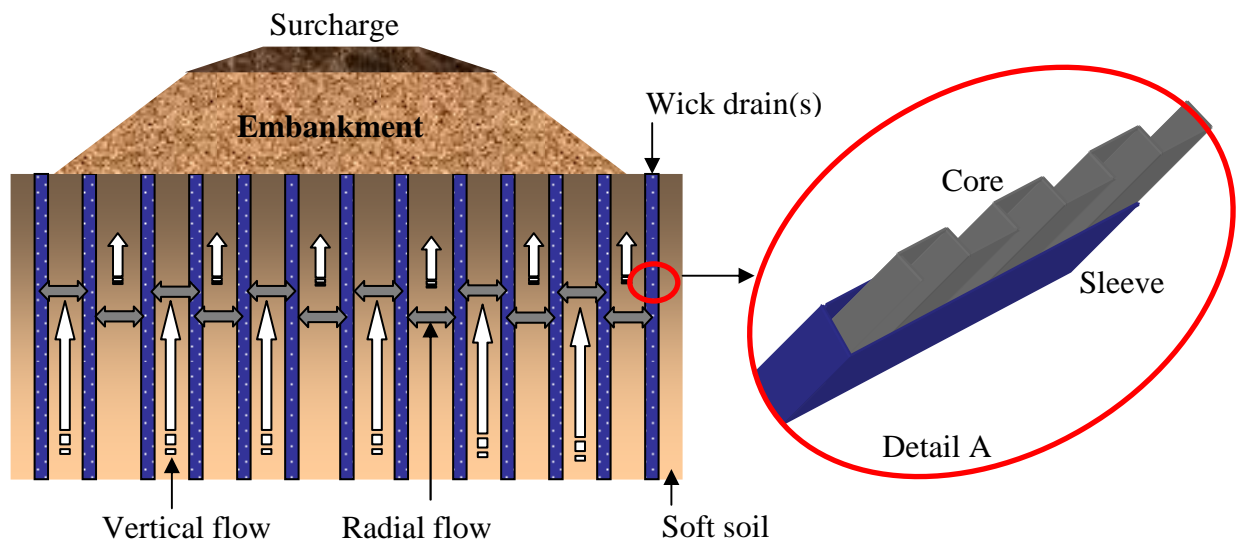


Figure 2.12 Preloading with prefabricated vertical drains to reduce consolidation settlements

Hsi and Martin (2005) and Hsi (2007) described the successful use of wick drains along with reinforcing geotextile layers to mitigate unequal and differential settlements anticipated in highway approach embankments constructed over soft estuarine and marine clays in New South Wales, Australia. The proposed freeway connecting Yelgun and Chindera cities has nine flyovers and thirty-nine freeway bridges over creeks and waterways having most of them located on soft estuarine and marine clays. The involved risks due to the very soft nature of these soils including long-term time dependent consolidation settlements, short-term instability of the embankment, and increase in fill quantity due to excessive settlement of embankment fill lead to the adopting of ground improvement techniques. They reported that installation of wick drains at a spacing of 1-3 m c/c on a grid pattern (Figure 2.13) allowed speedy construction of embankment over these soft soils.

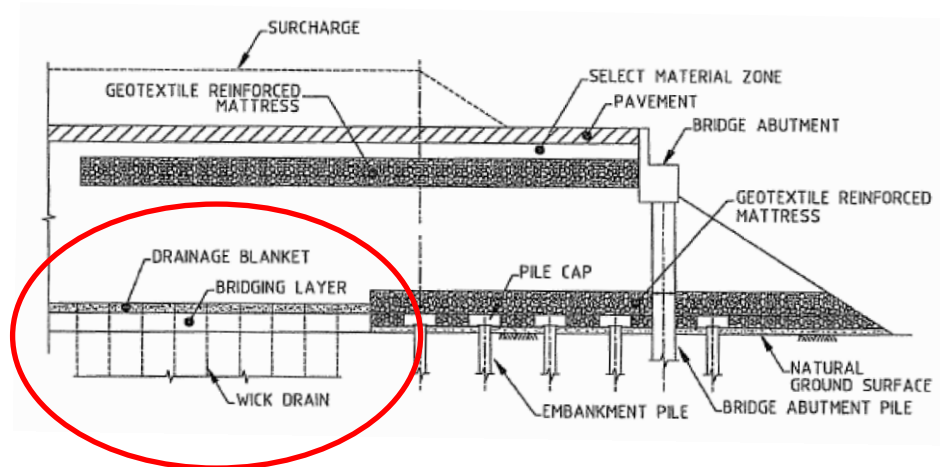


Figure 2.13 Schematic arrangement of approach embankment treatment with wick drains and driven piles (after Hsi and Martin, 2005)

To increase the embankment stability against potential slip failure, which was anticipated due to the speedy construction operations on soft soil, high strength geotextile reinforced mattresses were placed on the surface of the soft ground before placing the embankment (Hsi and Martin, 2005). The embankment near the bridge abutment was supported on timber driven piles to reduce the differential settlements between the approach

embankment and the pile supported bridge abutments. These details about timber driven piles are discussed in the following appropriate section. The embankment section and the soft soil were instrumented with settlement plates to assess the risks during and after the construction.

Figure 2.14 (a, b) presents the measured and predicted settlements in soft foundation soil during and after construction stages. In this figure, the long-term settlements were predicted based on the ratio $(c_a/1+e_0)$ where, c_a is the secondary compression index and e_0 is the initial void ratio. The long-term differential and total settlements are predicted from back-calculated analysis of measured data from settlement plates also presented in the same Figure. From this graph, it can be noted that the reduced rate of long-term creep settlements after the removal of the surcharge and after the completion of construction (Hsi and Martin, 2005).

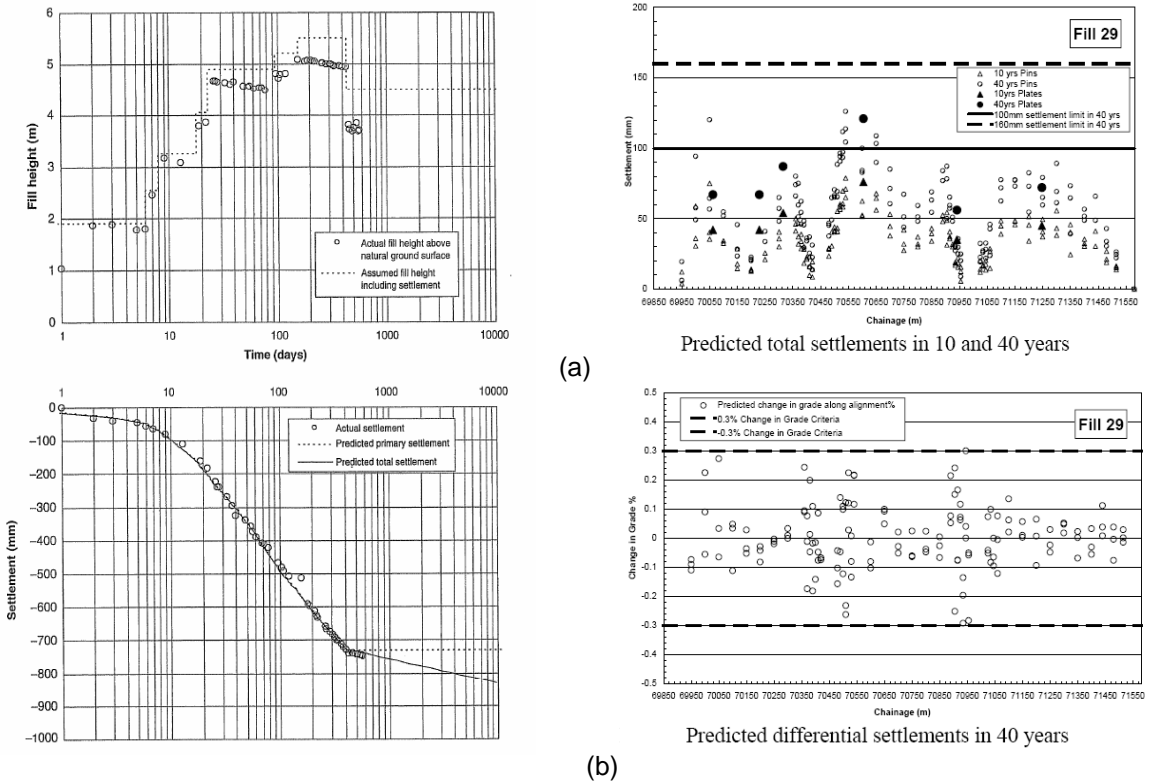


Figure 2.14 Measured and predicted settlements with time (Hsi and Martin, 2005)
 (a) during construction stages, (b) after construction stages

2.4.1.3 Reinforcement Techniques

A wide variety of soil reinforcement techniques are available from which to choose. In all these techniques, good reinforcement elements are inserted to improve the selected property of the native weak soil. These inclusions include stone, concrete or geosynthetics. Based on the type of construction of these methods, they are grouped as column reinforcement, pile reinforcement and geosynthetic reinforcements. The following sections describe each technique in detail with the focus on controlling bridge approach settlements.

2.4.1.3.1 Column reinforcement

a. Stone Columns

The stone columns technique is one of the classic solutions for soft ground improvement. This concept was first used in France in 1830 to improve a native soft soil (Barksdale and Bachus, 1983). The stone columns are a more common method to improve the load carrying capacities of weak foundation soils (Barksdale and Bachus, 1983; Michell and Huber, 1985; Cooper and Rose, 1999; Serridge and Synac, 2007), provide long term stability to the embankments and control settlements beneath the highway embankments (Munoz and Mattox, 1977; Goughnour and Bayuk, 1979; Barksdale and Bachus, 1983; Serridge and Synac, 2007). The secondary function of the stone columns is to provide the shortest drainage path to the excess pore water to escape from highly impermeable soils (Hausmann, 1990). This technique is best suitable for soft to moderately firm cohesive soils and very loose silty sands. In the United States, a majority of the stone column projects are adopted for improving silty sands (Barksdale and Bachus, 1983).

Stone column construction involves the partial replacement of native weak unsuitable soil (usually 15-35%) with a compacted column of stone that usually penetrates the entire depth of the weak strata (Barksdale and Bachus, 1983). Two methods are generally adopted to construct the stone columns including vibro-replacement, a process in which a high

pressure water jet is used by the probe to advance the hole (wet process) and vibro-displacement, a process in which air is used to advance the hole (dry process).

In both the processes, stone is densified using a vibrating probe, also called vibroflot or poker, which is 12 to 18 in. (300 to 460 mm) in diameter. Once the desired depth is reached, stone is fed from the annular space between the probe and the hole to backfill the hole. The column is created in several lifts with each lift ranging from 1 – 4 ft thick. In each lift, the vibrating probe is repenetrated several times to densify the stone and push the stone into the surrounding soil. This procedure is repeated till the column reaches the surface of the native soil. Figure 2.15 shows the construction stages of stone columns.

Successful application of stone columns to improve the stability of highway embankments constructed over soft soils in Clark Fork, Idaho (Munoz and Mattox, 1977) and in Hampton, Virginia (Goughnour and Bayuk, 1979). Stone columns can also be used to support bridge approach fills to provide stability and also to reduce the costly maintenance problem at the joint between the fill and the bridge. Based on an experience report circulated by a vibroflotation foundation company, Barksdale and Bachus (1983) have reported that stone columns were successfully used at Lake Okaoboji, Iowa and Mobridge, South Dakota for a bridge approach and an embankment structure built on soft materials.

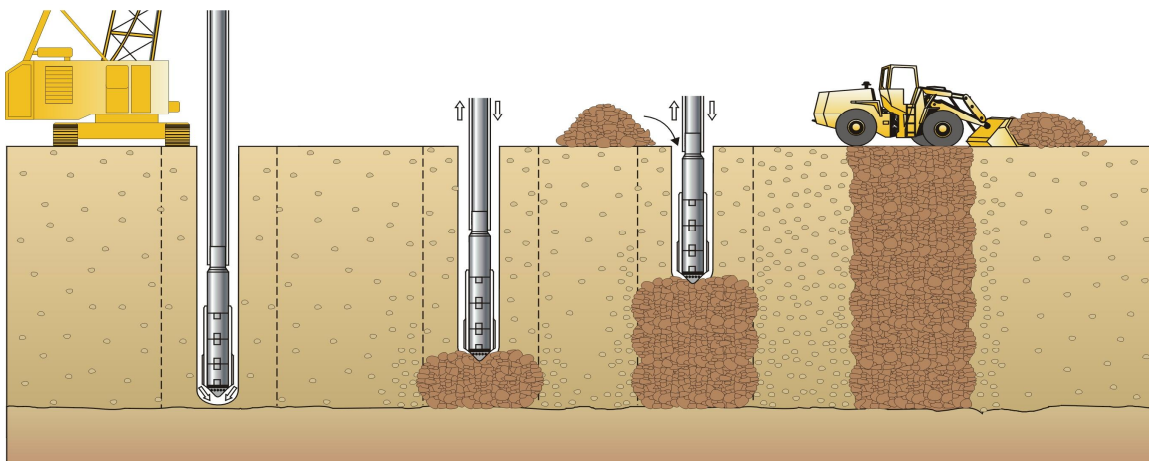


Figure 2.15 Construction stages of stone column
(Hayward Baker; http://www.haywardbaker.com/services/vibro_replacement.htm)

Serridge and Synac (2007) reported the successful use of stone columns along with vibro concrete columns in supporting highway embankment constructed over soft soil in South Manchester, UK. Figure 2.16 shows the schematic of the combination of ground improvement techniques used beneath the highway approach embankment. Prior to the actual construction, trial stone columns were constructed at a relatively low cost to verify the performance of the stone columns. Figure 2.17 depicts the performance of the stone columns in controlling settlements. Results from settlement plates show that the settlements occurring due to actual work were much smaller than the measured settlements in the trial sections.

The application or use of the stone columns technique is widely accepted and adopted in European countries (Barksdale and Bachus, 1983). In addition, McKenna et al., (1975) have reported a neutral performance of stone columns in soft alluvium supporting high embankment. They reported that the columns had no apparent effect on the performance of the embankment based on the comparison of instrumentation results obtained from both the piled and un-piled ground.

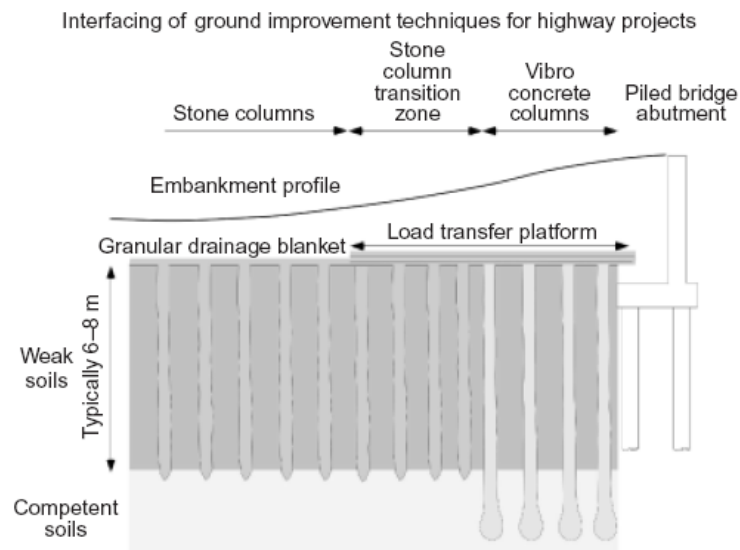


Figure 2.16 Interfacing of ground improvement techniques beneath embankment approach to piled bridge abutment (after Serridge and Synac, 2007)

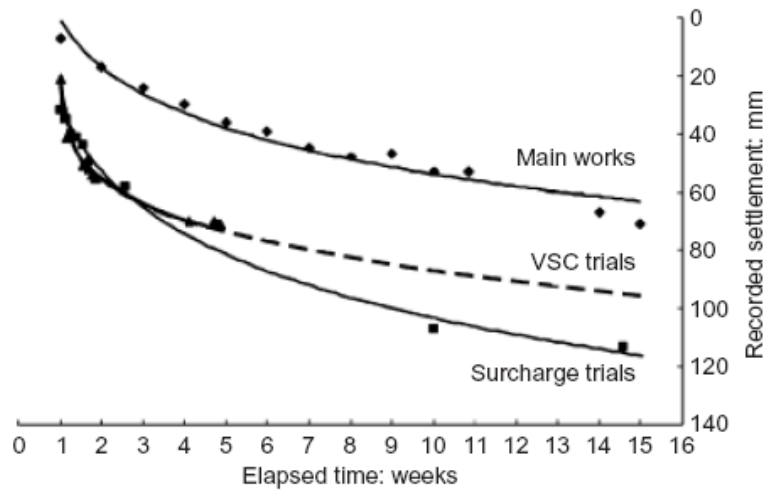


Figure 2.17 Settlement monitoring results for both surcharge trials on untreated and soil reinforced with stone columns (after Serridge and Synac, 2007)

b. Compaction piles

A series of compaction piles are used to improve the foundation soil, only when the deep deposits of loose granular soils such as sand or gravel are present and they can be densified by vibro-compaction or vibro-replacement methods (Hausmann, 1990). In these techniques, a probe is inserted into the soil until it reaches the required treatment depth (Hausmann, 1990). Then, the loosely deposited sands are vibrated in combination with air- or water-jet at a design frequency. Some amount of granular backfill materials are added to compensate for the void spaces resulting from the compaction. Finally, the probe is removed and the compacted granular backfill column is left in-situ. Figure 2.18 (a, b) depicts the sequential operations involved in the construction of compaction piles. Normally, the spacing of compaction piles is between 3 and 10 ft (1 and 3 m) and the depth of improvement can be achieved up to 50 ft (15 m) (Wahls, 1990). However, the vibro-compaction has its own limitation upon the grain size distribution of the granular fill material, which must contain fine material less than 20 percent (Baumann and Bauer, 1974) as shown in Figure 2.19.

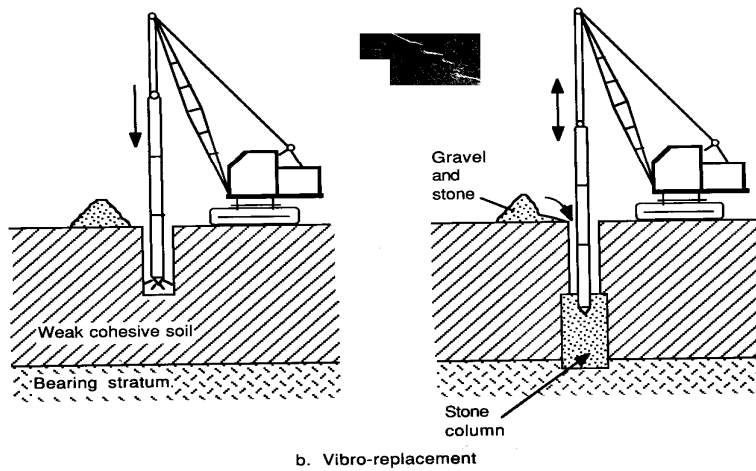
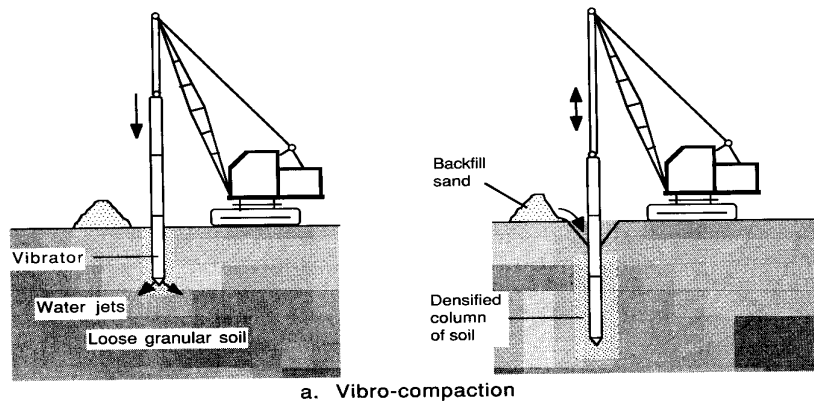


Figure 2.18 (a, b) Sequential operations involved in the construction of compaction piles (after Hausmann, 1990)

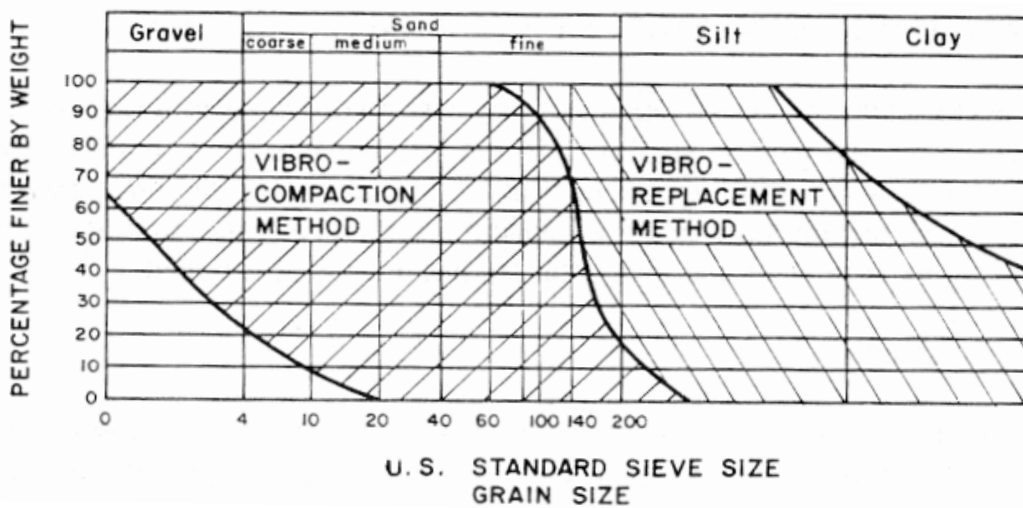


Figure 2.19 Range of soils suitable for vibro-compaction methods (after Baumann and Bauer, 1974)

Application of compaction piles to reduce the bridge approach settlements are not widely reported in the literature except in a few reported in Japan and Thailand. Sand compaction piles were used to support a road test embankment constructed at Ebetsu in Hokkaido, Japan (Aboshi and Suematsu, 1985). A combination of ground improvement techniques chosen in this project includes sand compaction piles, and lime/cement columns. The embankment was constructed using mechanically stabilized earth with grid reinforcement. A schematic of the ground improvement techniques adopted in this study is shown in Figure 2.20. A control embankment was also constructed on native soft soil without any treatment. They reported that the combination of sand and lime/cement columns could support the embankment as high as 8 m, while the control embankment of height 3.5 m was collapsed exhibiting high deformations on the subsoil and heavy cracks in the embankment section.

Similar studies were carried out by Bergado et al (1988; 1990) on soft Bangkok clay and confirmed that the granular compaction piles along with mechanically stabilized earth would be an economical alternative to support bridge approach embankments and viaducts.

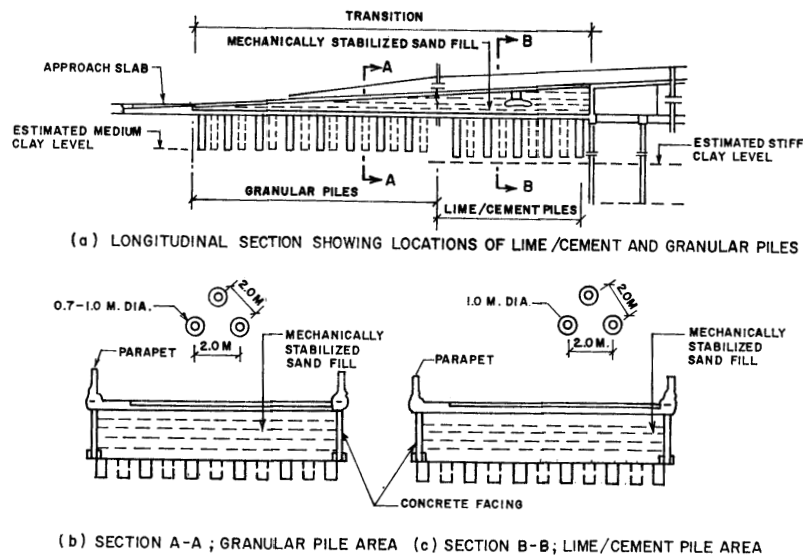


Figure 2.20 Schematic of granular compaction piles with mechanically stabilized earth to support bridge approach embankments (Bergado et al., 1996)

c. Driven piles

To eliminate the impact of embankment settlement on the abutment piles a nest of driven piles consisting of timber piles or precast concrete piles can be installed adjacent to the abutment under the embankment (Hsi, 2007). These driven piles are expected to transfer the embankment loads on to the stiffer layers beneath; as a result, negligible settlements can be expected on the embankment surface.

Hsi (2007) reported the use of timber and concrete piles installed on a 2 m c/c square grid near the pile supported bridge abutment to arrest the differential settlements between the abutment and the embankment constructed along the Yelgun-Chinderah freeway in New South Wales, Australia. A series of pile caps (1 m square each) overlain by a layer of geotextile reinforced rock mattress (0.75 m thick) was also placed over the piles to form an effective bridging layer to transfer the embankment loads on to the piles as shown in Figure 2.21. This method allowed for earlier construction of the abutment piles and hence earlier completion of the bridges to allow haulage and construction traffic through the alignment. The data obtained from the settlement plates and pins installed in the embankment section revealed that the total creep settlements are reduced considerably.

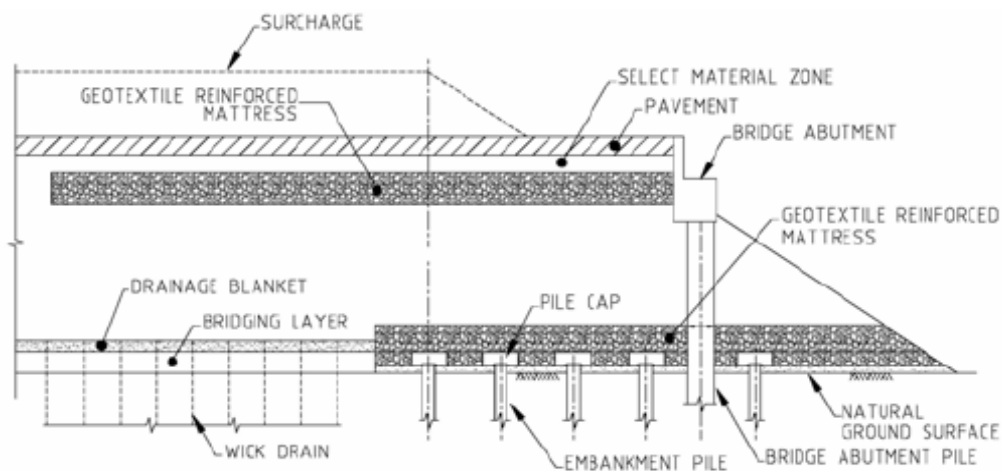


Figure 2.21 Schematic of bridge approach embankment supported on driven piles (after Hsi, 2007)

d. Geosynthetic Reinforcement

Whenever highway embankments are constructed over soft soils, the embankment load is distributed over a large area. These soft soils often exhibit failure due to excessive settlements or due to insufficient bearing capacity (Liu et al, 2007). A variety of techniques are available to increase the stability of these structures as discussed above. The application of geosynthetics in supporting highway embankments is gaining popularity (Magnan, 1994). In conventional piled embankment construction, the spacing is very close between piles, which leads to higher construction costs. However, introducing a layer of geosynthetic reinforcement in the form of geotextile or geogrid at the base of the embankment would not only bring down the cost but also increase the stability of the embankment structure (Liu et al, 2007).

Maddison et al (1996) reported that the combination of a geosynthetic layer at the base of the embankment constructed over highly compressible peats and clays along with a series of vibroconcrete columns has proven to be the most effective method to increase the stability of the embankment structure and reduce long term settlements (Figure 2.22).

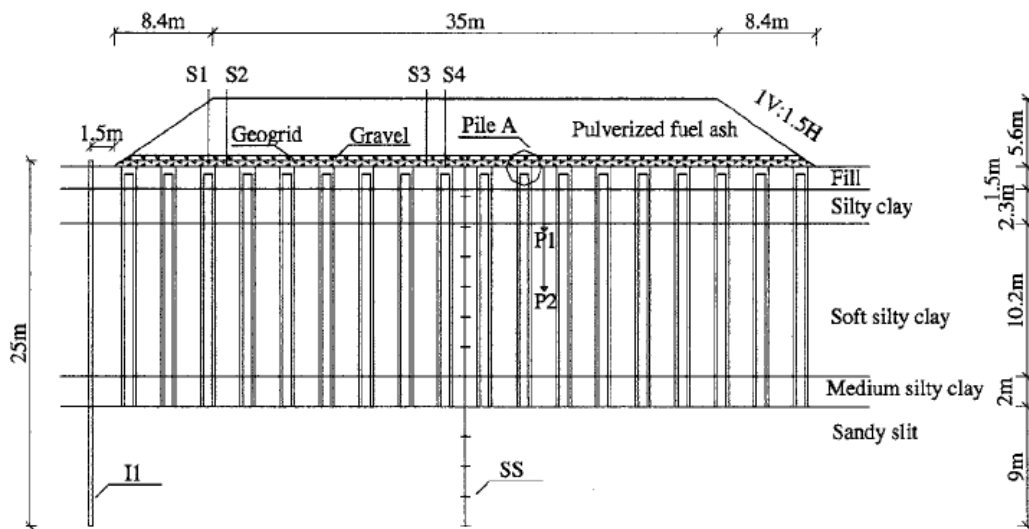


Figure 2.22 Cross section of embankment with basal geogrid and columns (after Liu et al., 2007)

A more recent development in geosynthetic reinforcement is to provide a confinement to the foundation soil using geocells (Bush et al, 1990; Rowe et al, 1995). A geocell is a three dimensional, honey comb-like structure of cells interconnected at joints. These geocells provide lateral confinement to the soil against lateral spreading due to high structural loads and thereby increase the load carrying capacity of the foundation soil (Bush et al, 1990; Rowe et al, 1995; Krishnaswamy et al., 2000). The application of geocells as a foundation mattress for embankments constructed on soft soils has been studied by many researchers (Bush et al., 1990; Cowland and Wong, 1993; Rowe et al, 1995; Lin and Wong, 1999; Krishnaswamy et al., 2000).

Cowland and Wong (1993) reported a case study of the performance of a geocell mattress supported embankment on soft clay. A 10-m high embankment was constructed over soft ground comprised of a lagoon deposit overlain by alluvium supported by geocell foundation in Hong Kong (Figure 2.23). The embankment was extensively instrumented with inclinometers, pneumatic piezometers, hydrostatic profile gauges, settlement plates, surface settlement markers and lateral movement blocks to verify the design assumptions and also to control the speed of the staged construction. Typical instrumentation data is presented in Figure 2.24. Results revealed that the geocell mattress performed very well in most of the instrumented sections. The measured settlement of the embankment was less than 50% of the predicted settlement with geocell foundation mattress. They reported that they measured excessive settlements due to construction on soft lagoon deposits. Overall, they concluded that the geocell foundation mattress behaved as a much stiffer raft foundation supporting the embankment.

Jenner et al. (1988), making use of slip line theory, have proposed a methodology to calculate the increase in bearing capacity due to the provision of a geocell mattress at the base of the embankment resting on soft soil. Krishnaswamy et al. (2000) carried out a series of laboratory model tests on geocell mattress supported earth embankments constructed over

a soft clay bed. Lin and Wong (1999) illustrated the use of mixed soil and cement columns along with geotextile mattress at the base of the embankment in reducing the differential approach settlements. These details are discussed in previous sections. In all these cases, geocell mattress, either backfilled with good granular construction material or locally available mixed soils enhanced the load carrying capacity of the foundation soil and reduction in short term and long term settlements. Hence geocell mattress can be an economical alternative for shallow to moderate soft soil deposits. However, field studies are lacking on this method and its potential in real field conditions.

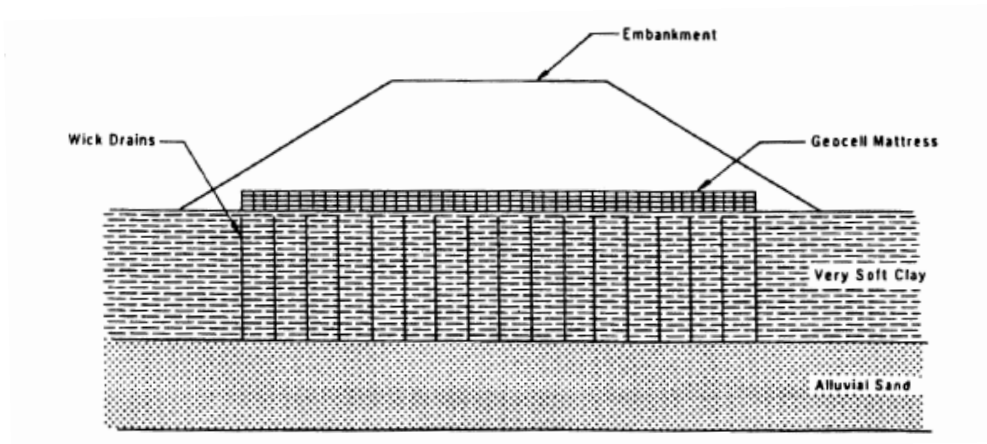


Figure 2.23 Geocell foundation mattress supported embankment (Cowland and Wong, 1993)

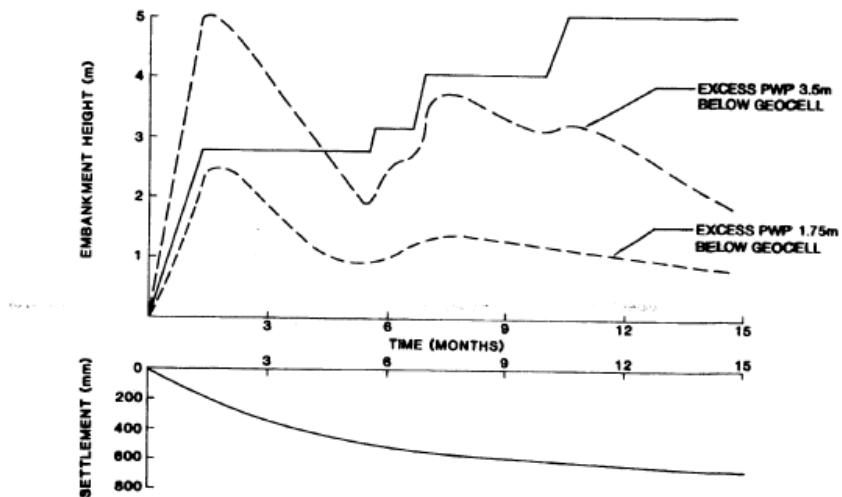


Figure 2.24 Typical load/settlement-pore pressure/time profiles for embankment section

2.4.2 New Foundation Technologies

2.4.2.1 Geopiers

Geopiers, some times, also called as short aggregate piers are constructed by drilling the soft ground and ramming selected aggregate into the cavity, formed due to drilling, in lifts using a beveled tamper (Lien and Fox, 2001). The basic concept in this technique is to push/tamp the aggregate vertically as well as laterally against the soft soil to improve the stiffness against compressibility between the piers. These short piers can also allow radial drainage due to their open graded stone aggregate structure to accelerate the time dependent consolidation process and also to relieve excess pore water pressures generated in the soft soil (Lien and Fox, 2001).

The geopier soil reinforcement system has been adopted in transportation related applications such as roadway embankments and retaining walls to mitigate settlement of these structures (Lien and Fox, 2001; White and Suleiman, 2004). The design and construction details of these short piers are well documented in the literature (Lawton and Fox, 1994; Minks et al, 2001; White and Suleiman, 2004). Figure 2.25 demonstrates the schematic of the geopier construction sequence. Figure 2.26 presents the typical geopier system supporting the highway embankment.

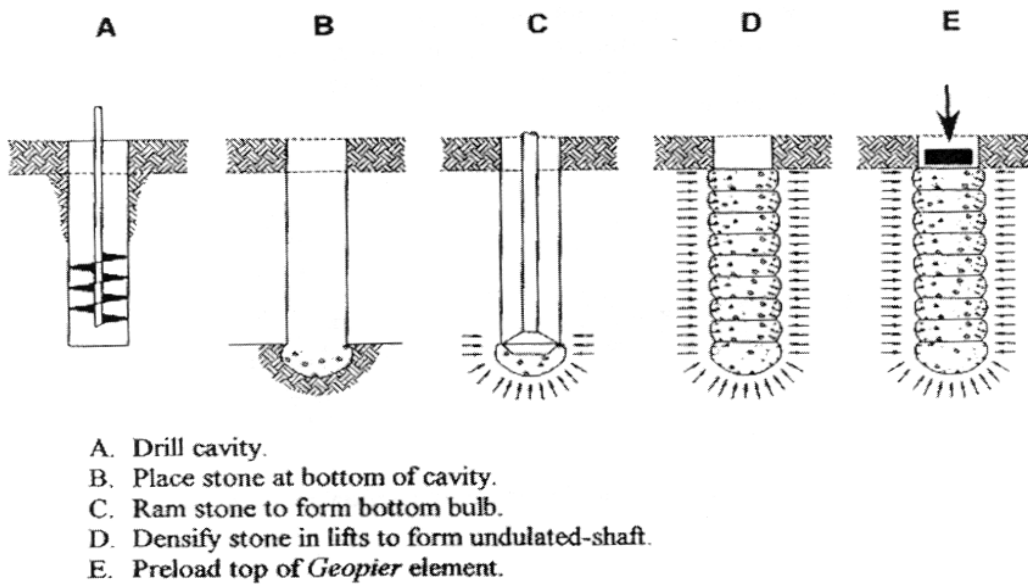


Figure 2.25 Geopier construction sequence (after Lien and Fox, 2001)

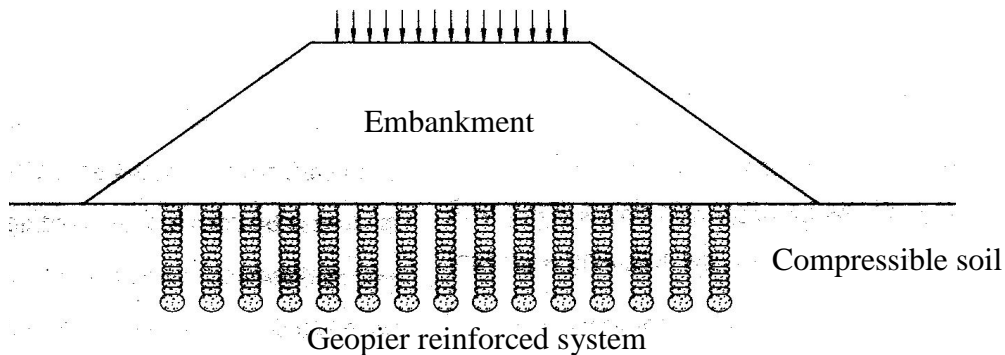


Figure 2.26 Typical geopier system supporting the embankment (after Lien and Fox, 2001)

White et al. (2002) demonstrated the performance of the geopier system over stone columns in supporting highway embankments in Des Moines, Iowa. The purpose of the reinforcement technique was to reduce the magnitude and increase the time rate of consolidation settlements and to facilitate rapid abutment construction. These two sections were instrumented with settlement plates to measure during and post construction settlements. Prior to the embankment construction, geotechnical measurements were made

to characterize both the sections by performing standard penetration tests (SPTs), borehole shear tests (BSTs) and full scale load tests. The SPT tests performed through production columns revealed that the average N-Values of 11 and 17 were obtained for stone columns and geopiers respectively. Figure 2.27 compares the settlement readings with the increase in fill height obtained from settlement plates from both the stone columns section and the geopier system. It can be seen that the settlement of the matrix soil near the stone column is three times higher than the settlements observed in the matrix soil next to the geopier system.

White and Suleiman (2004) demonstrated the design procedures for short aggregate pier systems for a highway embankment construction. They observed two types of failure mechanisms, namely, bulging and plunging of the piers in their study on short aggregate piers. They recommend that the design of piers should be carried out based on the tip resistance to prevent bearing capacity problems.

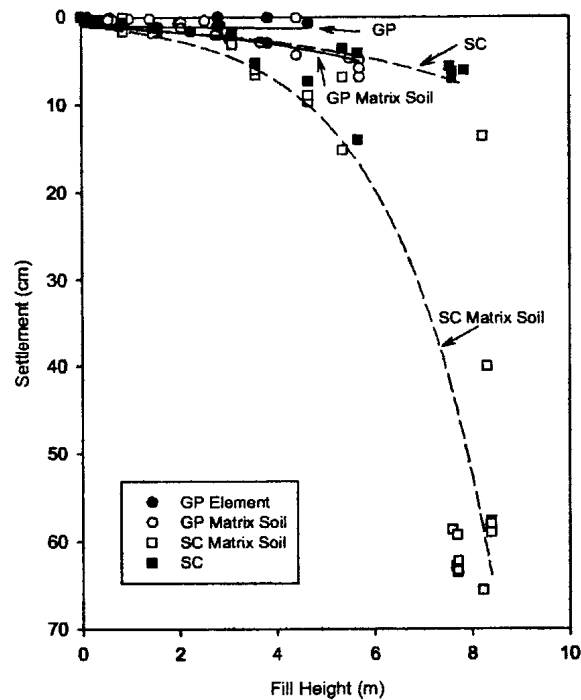


Figure 2.27 Comparison of settlement with fill height for both stone column and geopier systems

2.4.2.2 Deep Soil Mixing (DSM)

Deep Soil Mixing (DSM) technology, was pioneered in Japan in the late 1970's, and has gained popularity in the United States over many years in the field of ground improvement (Barron et al, 2006). DSM is a process to improve soil by injecting grout through augers that mix in with the soil, forming in-place soil-cement columns (Barron et al, 2006). Recently, the cement binder has been replaced with many other cementitious compounds such as lime, flyash or a combination of any two compounds. Hence, in a broader sense, the DSM technique is an in-situ mixing of stabilizers such as quicklime, cement, lime-cement or ashes with soft and/or expansive soils to form deep columns to modify weak subgrade soils (Porbaha, 1998).

Figure 2.28 presents a typical DSM operation and resulting columns in the field. The DSM treated columns provide substantial improvements to soil properties such as strength and compressibility. The DSM columns have been used on several state highways to improve the stability of earth structures, to improve the bearing capacity of soils, to reduce the heave and settlement of embankments and roadways, to provide lateral support during excavations, to improve seismic stability of earthen embankments constructed over soft soils, and to reduce bridge approach settlements. This stabilization technique has been proven effective on soft clays, peats, mixed soils, and loose sandy soils (Rathmayer, 1996; Porbaha, 1998; Lin and Wong, 1999, Porbaha, 2000; Bruce, 2001; Burke, 2001).

The success of DSM-based ground treatment methods has lead to improved processing and novel installation technologies with the use of different additives incorporated as either dry or wet forms to stabilize subsoils. Currently, there are more than eighteen different terminologies used to identify different types of deep soil mixing methods (Porbaha, 1998, 2000). Irrespective of these terminologies, the stabilization mechanisms are similar and their enhancements to soil strength and compressibility properties are considerable. The development of new applications should take advantage of the unique

characteristic of Deep Soil Mixing in which rapid stabilization is possible in a short period of time, which will lead to accelerated construction in the field. Although the initial demand for DSM was to gain higher strength at lower cost, the recent complex construction dilemmas in expansive soils and other problematic soils have led to a greater need of evaluating this technology for expansive soil modification in field settings (Porbaha and Roblee, 2001).

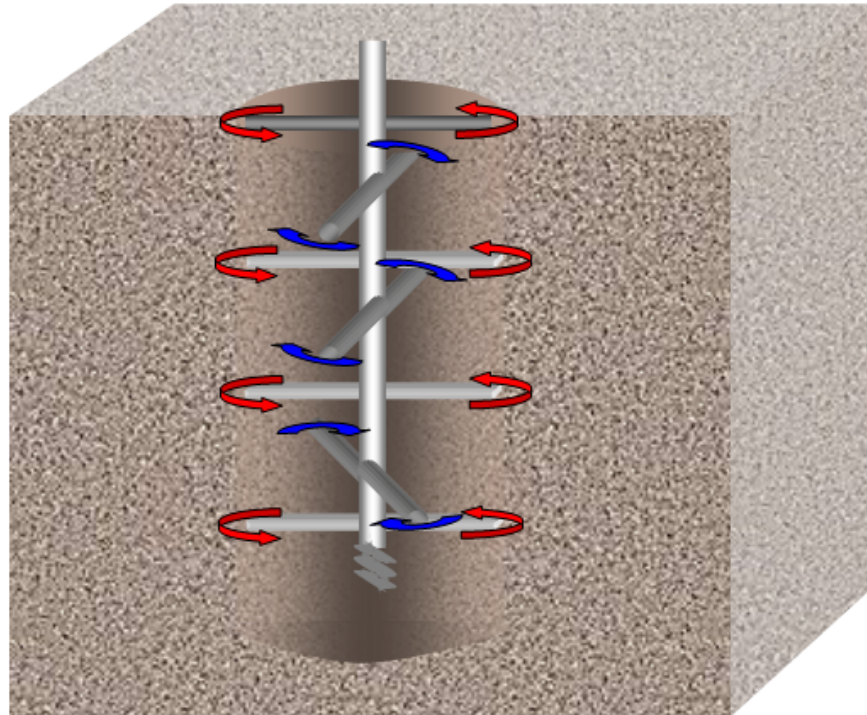


Figure 2.28 Deep Soil Mixing (DSM) Operation and Extruded DSM Columns

This technology has been used by various state highway agencies such as Caltrans, Utah DOT, and Minnesota DOT in cooperation with the National Deep Mixing (NDM) Program, a research collaboration of the FHWA with ten State DOTs. Several other case studies are reported both in and outside the US for the use of DSM columns to reduce embankment settlements. Recently, TxDOT initiated Research Project (0-5179) to evaluate the DSM columns in mitigating the pavement roughness in expansive soils. The results from two instrumented sites demonstrate that the DSM is a promising technique to mitigate the pavement roughness.

Lin and Wong (1999) studied the deep cement mixing (DCM) technique to improve the strength of a 20-m-thick-layer of soft marine clay with high moisture content to reduce the total and differential settlements at bridge embankments constructed along Fu-Xia expressway in the southeast region of China. The bridge abutments were planned to place on deep pile foundations with little to no allowable settlements. The maximum settlement of the embankment fill on the soft marine clays was predicted as 300 mm. To alleviate these differential settlements between pile-supported abutments and embankment fills, soil-cement deep soil mixing columns were selected to reinforce the embankment foundation soil.

Prior to the construction of the actual embankment(s) along the proposed Fu-Xia Expressway, trial embankment sections 2.7 km long were constructed to verify the efficiency of the selected ground improvement techniques such as prefabricated sand drains, plastic band drains, and deep cement mixing columns. They employed varying lengths of DCM columns with the longest columns placed near the bridge abutment and shorter columns away from the abutments as shown in Figure 2.29. This profile of DCM columns was adopted to increase the stiffness of the embankment towards the bridge abutments to result in gradual decrease in the settlements towards the bridge. A combination of band drains with a sand mat adjacent to the DCM treatment was to facilitate faster drainage of the pore water and to

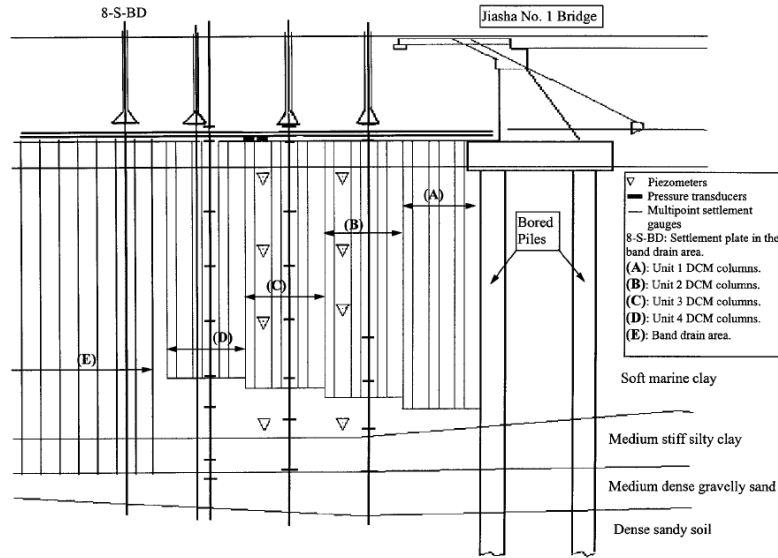


Figure 2.30 Instrumentation details of DCM treated embankment

A similar technique (soil-cement columns) was used as a remediation method by Shen et al. (2007) to mitigate differential settlement of approach embankments along the Saga airport approach road constructed on Ariake clay in Japan. The actual road project was to connect the Saga city with the Saga airport in Japan. After the construction and open for traffic for two and half years, the low embankment adjacent to the bridge abutment settled 0.92 m though the predicted residual settlement due to traffic-load was about 0.2 – 0.4 m over the following 20 years period. Then a detailed geotechnical investigation was carried out which revealed that these road sections were underlain by thick layers of highly sensitive, soft Ariake clay.

Therefore, three remediation techniques were considered such as an asphalt concrete overlay, approach cushion slab method, and column approach (CA) method to mitigate these differential settlements between the approach embankment and the piled abutments. The first two conventional methods were selected based on Japanese pavement design guidelines. Conventional methods were also adopted at two different sections of the road project to compare the cost and performance of the column approach method. In the CA technique, the road approach (transitional zone) was supported by a row of soil-cement

columns with lengths reduced with the increased distance away from the rigid piled abutment structure to smoothen the settlement profile within the transition zone as shown in Figure 2.31.

A connecting slab was used to transfer the embankment loads to the CA system. The details of the design parameters of the CA method such as length of the soil-cement columns, spacing between columns, and details of the connecting slab are clearly described by Shen et al (2007). They reported that the column approach method is proven to be economical and efficient in mitigating the differential settlements though the initial construction costs are higher than the conventional treatment methods discussed. Figure 2.32 shows that the CA method is economical when the differential settlements are more than around 300 mm.

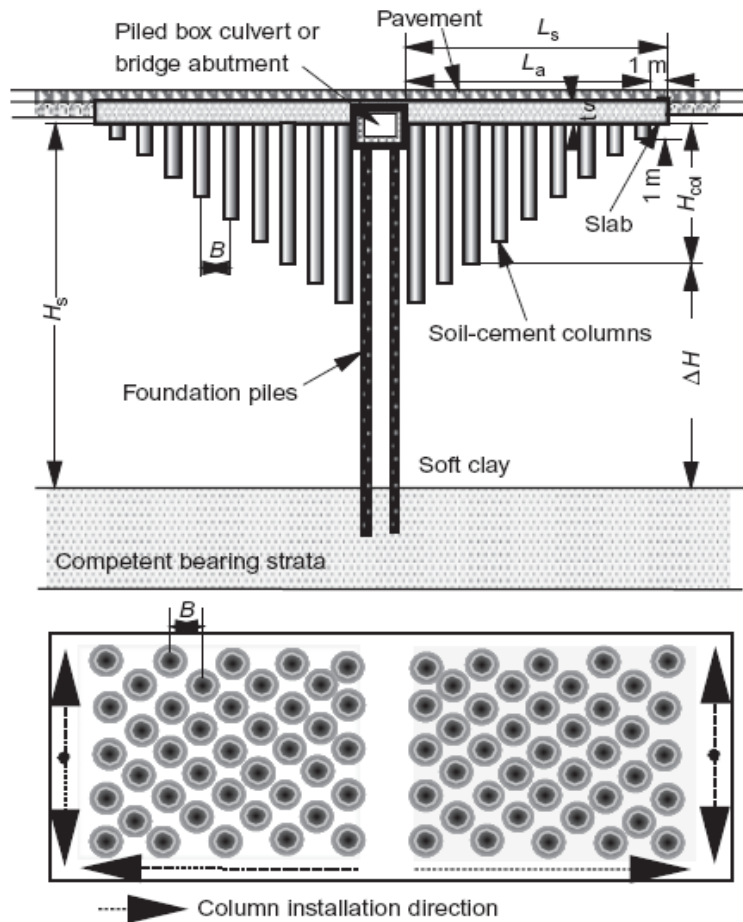


Figure 2.31 Section and plan view of soil-cement pile supported approach embankment (after Shen et al., 2007)

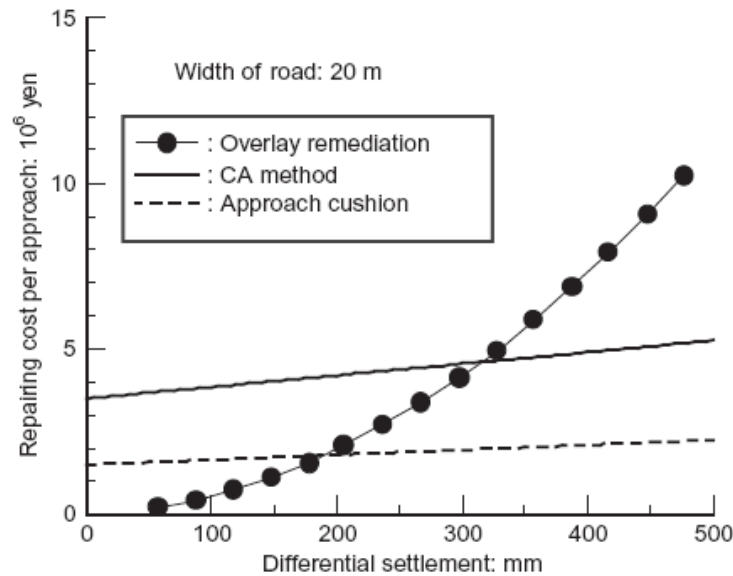


Figure 2.32 Maintenance cost with differential settlements (Shen et al., 2007)

2.4.2.3 Concrete Injected Columns

Concrete injected columns (CICs) are an innovative technique where a soil displacement pile mechanism is used to create in-situ concrete columns without reinforcement (Hsi, 2007; 2008). CICs are installed by inserting a displacement tool (auger) into the soft soil by rotating and pushing the tool. Upon reaching the final level, concrete is pumped through the hollow stem of the tool during extraction of the tool as shown in Figure 2.33. Inserting reinforced casing into the CICs is optional and the depth to which the reinforcement casing can be installed is also limited (Hsi, 2008). Typically these columns are prepared at 500 mm diameter and the length of these columns can be extended to reach a stiff strata or shallow bed rock. This technique is widely used to reinforce the very soft to soft foundation soils (Hsi, 2007). CICs were recently adopted to control the excessive long term settlements of approach embankments constructed on estuarine and marine soft clays along Brunswick Heads – Yelgun upgrade Pacific highway, Australia.

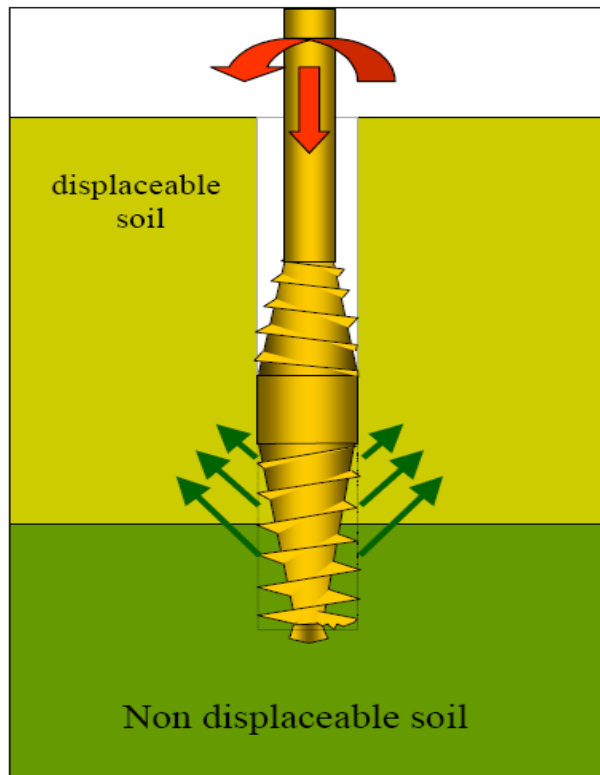


Figure 2.33 Installation of concrete injected columns (after Hsi, 2008)

Two geometric patterns (Zone 1 & 2) of CICs are installed in the soft foundation soil as shown in Figure 2.34. Zone 1 was for the support of the approach embankment and Zone 2 was to eliminate abrupt differential settlement between the closely spaced approach embankment section (Zone 1) and rest of the embankment. The spacing adopted for CICs in Zone 2 is around 2 m c/c and hence provided with a pile cap. These CICs were covered with a pair of geotextile blankets to uniformly distribute the embankment loads to the CICs. This combination of CICs with geotextiles provided a competent base for the embankment.

To assess the performance of CICs, the embankment section was instrumented with inclinometers to measure the lateral movements of the embankment due to construction activity and further, settlement plates to measure the settlement of the embankment. Figure 2.35 presents the data obtained from the settlement plates. The data obtained from this instrumentation imparted that the settlements are well within the allowable limits stipulated for

this project. These limits are that the pavement was required to achieve a maximum of 100 mm residual settlement and a change in grade of 0.3% in any direction over the 40 year design life of the pavement. In addition, this technique allowed constructing the pile foundation for the abutment prior to preloading the embankment which led to a reduction in total project costs.

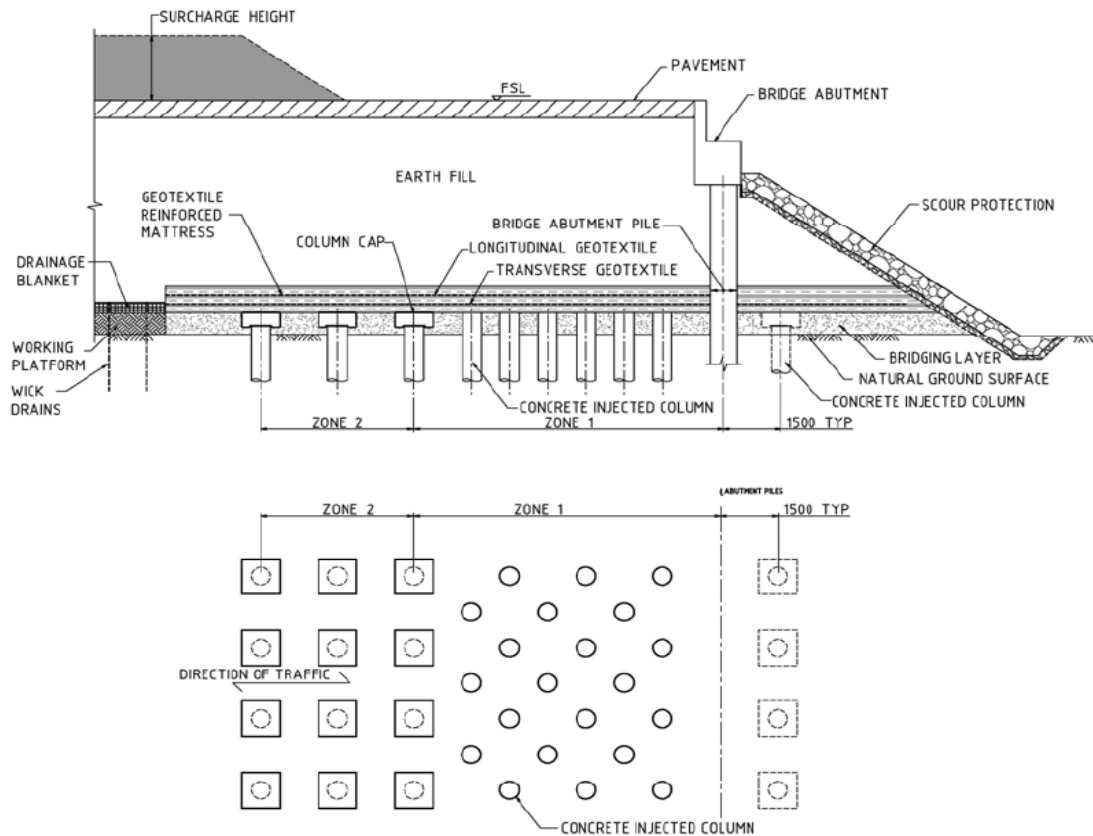


Figure 2.34 Bridge approach treatment with concrete injected columns (Sectional and Plan view)

2.4.2.4 Continuous Flight Auger Cast Piles (CFA)

Continuous Flight Auger Cast Piles (CFA) are installed by rotating a continuous-flight hollow shaft auger into the soil to reach a specified depth. High strength cement grout or sand or concrete is pumped under pressure through the hollow shaft as the auger is slowly withdrawn. If this process uses pressure grouting, these CFA piles are some times termed as

Auger Pressure Grouted (APG) piles. The resulting grout column hardens and forms an auger cast pile (Neely, 1991; Brown et al., 2007). Reinforcing, when required, can be installed while the cement grout is still fluid, or in the case of full length single reinforcing bars, through the hollow shaft of the auger prior to the withdrawal and grouting process (Neely, 1991; Brown et al., 2007).

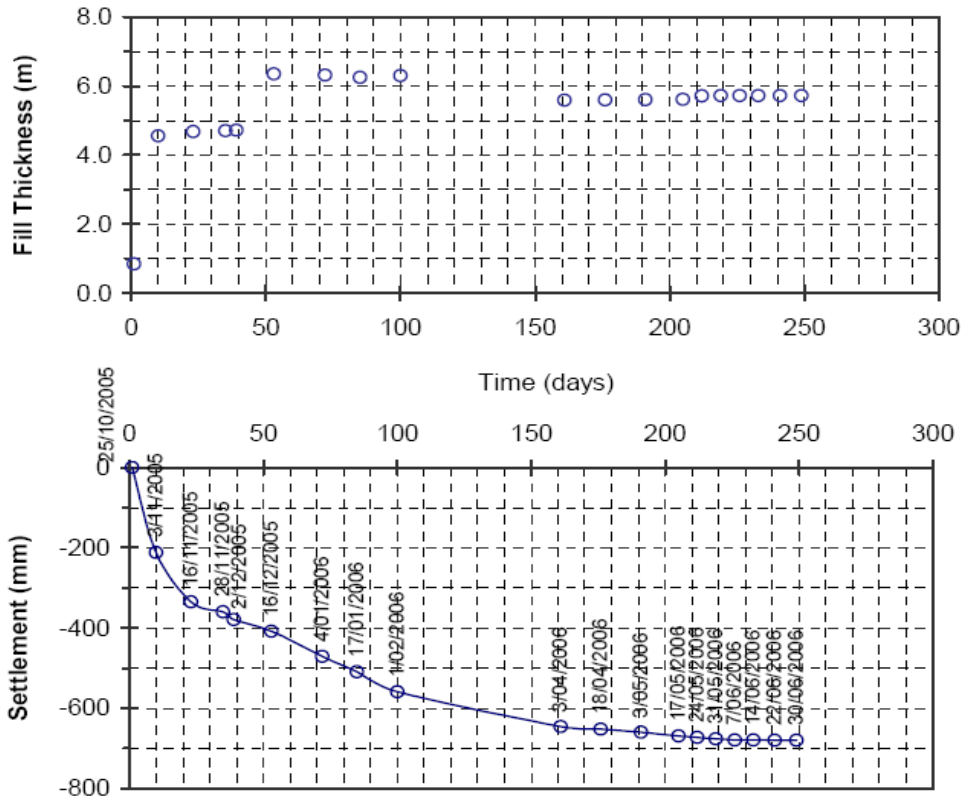


Figure 2.35 Settlement profiles obtained from settlement plates (after Hsi, 2008)

Auger cast piles can be used as friction piles, end-bearing piles, anchor pile; auger cast vertical curtain wall or beam and lagging wall and sheet pile walls (Brown et al., 2007). The advantages of CFA piles over other pile types (driven piles) include less noise, no objectionable vibrations, no casing required, can be installed in limited headroom conditions, and soil samples can be obtained from each borehole (Brown et al., 2007). The typical

dimensions reported are from 12 in. to 18 in. However, auger cast piles with diameters of 24, 30 and 36 in. have been successfully utilized with tests being conducted as high as 350 tons.

O'Neill (1994) and recently Brown et al. (2007) summarized the construction systems of augered piles, and documented different methods available to estimate the axial capacity of CFA piles. Figure 2.36 shows the construction procedures for continuous auger cast piles and screw piles. Brown et al. (2007) summarized the advantages and disadvantages of CFA piles and driven piles. Although several advantages of CFA piles have been stated, the major two disadvantage aspects of these piles must be noted. First, the available QA methods to assess the structural integrity and the pile bearing capacity of these piles are not reliable. Second, the disposal of associated soil spoils when the soils are contaminated. In addition, CFA piles were not considered by public transportation departments in the US prior to 1990's because of the lack of design methods. The use of CFA piles has been increased in the U.S. after recent developments in automated monitoring and recording devices to address quality control and quality assurance issues (EBA Engineering Inc., 1992; Brown et al., 2007).

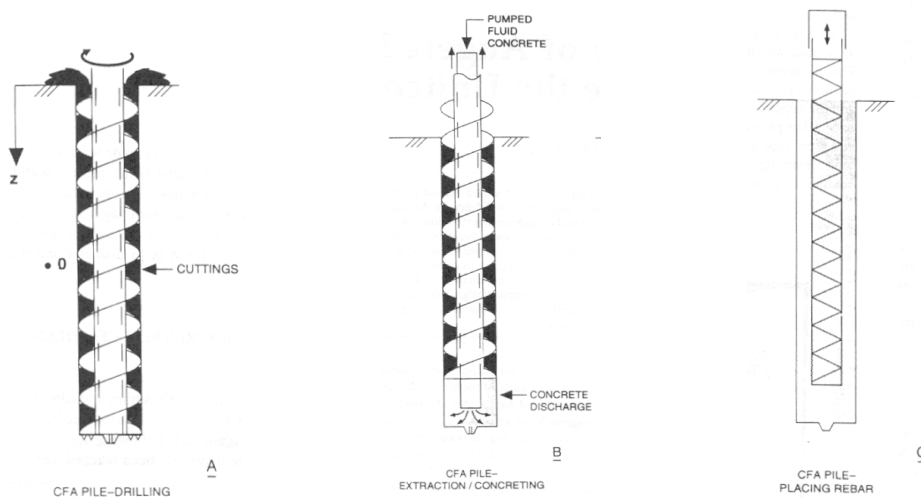


Figure 2.36 Construction Procedures for Continuous Auger Piles (O'Neill, 1994)

Since CFA piles behave somewhere between drilled shafts and driven piles, CFA piles have been designed using both approaches (Zelada and Stephenson, 2000; Brown et al., 2007). McVay et al. (1994) reported the successful use of auger cast piles in

coastal shell-filled sands in Florida. They concluded that the equipment selection, drilling rate, grout's aggregate size, grout pumping, augur removal and grout fluidity significantly affect the quality and the load carrying capacity of the augered piles. They summarized different empirical methods to estimate the capacities of auger cast piles which include, Wright and Reese method, Neely's method and LPC (Laboratoire Des Ponts et Chaussées) method. McVay et al. (1994) compared the measured load-settlement data with predicted capacities from these methods. The Wright and Reese method gave reasonable predictions of capacities at 5 % settlement of the pile diameter. They also concluded that the use of 5% of the pile's diameter for the failure criteria to be acceptable for typical augured cast piles in the 12 in. diameter range.

Vipulanandan et al. (2004) studied the feasibility of CFA piles as a bridge abutment foundation alternative to the driven pile system on a new bridge constructed by the Texas Department of Transportation (TxDOT) near Crosby, Texas. They noticed few construction issues for the installation of the CFA piles including the difficulties involved in reinforcing the entire depth of piles due to excessive grout velocity and/or lack of timely workmanship by the contractor. They also reported that the load carrying mechanism of the CFA piles was entirely due to the mobilization of the side friction resistance of the pile based on the pile load test on the instrumented test piles. They also concluded that the cost involved in installing the CFA pile system was 8% less than that of the driven pile system for the same length of the foundations. In addition, the CFA piles are having a higher factor of safety against axial loading than the other foundations.

CFA piles to support approach embankment are considered only when the foundation soil is highly compressible and the time required for the consolidation settlement is very high, and when minimization of post-construction settlements and construction delays are required (Brown et al, 2007). Only a few studies are available in the literature where the CFA piles were used to support the embankment in order to mitigate settlements. Figure 2.37 shows the

CFA pile supported railway embankment in Italy. Pile support was used to increase the stability of the embankment against excessive settlement anticipated due to extra fill on the existing embankment and load due to increased rail traffic. The CFA piles were capped using concrete filled cylinders and the fill overlain by the pile caps are reinforced with geotextiles. Performance details of these systems for settlement control are not yet documented.

Other details on the CFA piles including construction sequences, materials required, equipment specifications, and performance based design factors of these CFA piles can be found in Brown et al. (2007).

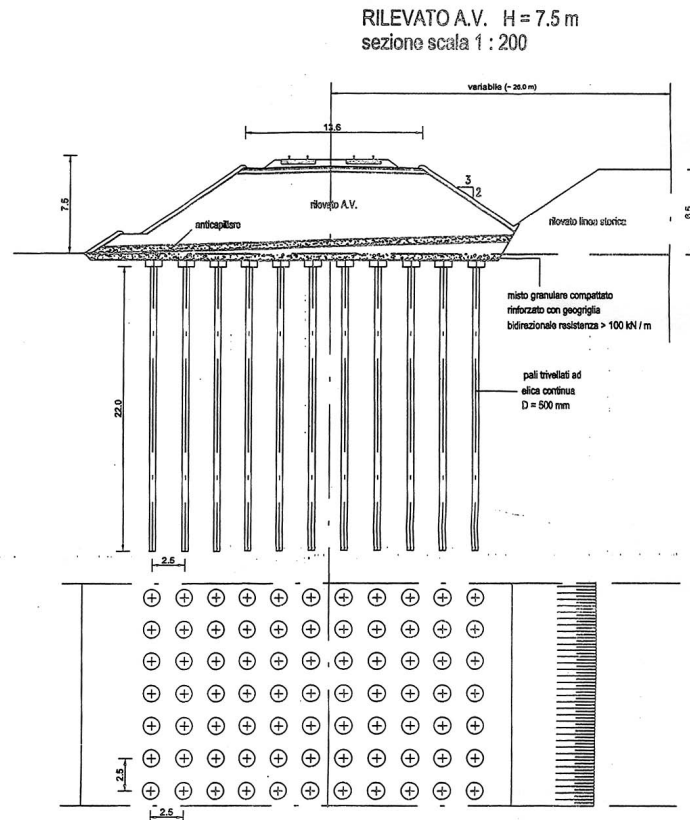


Figure 2.37 CFA pile supported railway embankment for Italian railway project (after Brown et al., 2007)

2.4.3 Improvement of Approach Embankment/Backfill Material

The bridge approach embankment has two functions; first to support the highway pavement system, and second to connect the main road with the bridge deck. Most of the

approach embankments are normally constructed by conventional compaction procedures using materials from nearby roadway excavation or a convenient borrow pit close to the bridge site. This implies that the serviceability of the embankment, in the aspects of slope stability, settlement, consolidation, or bearing capacity issues, depends on the geotechnical properties of the fill materials (Wahls, 1990). In addition, since the embankment must provide a good transition between the roadway and the bridge, the standards for design and construction considerations both in materials quality requirements and compaction specifications must be specified in order to limit the settlement magnitude within a small acceptable degree (Wahls, 1990).

Generally, the materials for embankment construction should have these following properties (White, 2005):

- a. being easily compacted,
- b. not time-dependent,
- c. not sensitive to moisture,
- d. providing good drainage,
- e. erosion resistance and
- f. shear resistance.

Dupont and Allen (2002) cited that the most successful method to construct the approach embankments is to select high quality fill material, with the majority of them being a coarse granular material with high internal frictional characteristics. Several research methods have been attempted to define methods to minimize potential of settlement and lateral movement development in the approach embankments and these studies are discussed in the following.

Hoppe (1999) studied the embankment material specifications from various DOTs. The results from his survey are presented in Tables 2.3 and 2.4. It can be seen from Table 3 that forty-nine (49) percent of the state agencies use more rigorous material specifications for

an approach fill than for a regular highway embankment fill. Furthermore, the study also shows that typical requirements for the backfill materials among the different states varied with one another. One common requirement followed by several states is to limit the percentage of fine particles in the fill material in order to reduce the material plasticity. As an example, the allowable percentage of material passing the No. 200 (75-micron) sieve varies from less than 4% to less than 20%. Another requirement commonly found is to enhance the fill drainage properties by a requisite of pervious granular material.

From the same study by Hoppe (1999), two other conclusions can be further drawn from Table 2.4. First, in many states, a 95% of the standard proctor test compaction condition is generally specified for the compaction of approach fill.

Table 2.3 Embankment Material Specifications (Hoppe, 1999)

State	Same/Different from Regular Embankment	% Passing 75 mm (No.200 sieve)	Miscellaneous
AL	Same		A-1 to A-7
AZ	Different		
CA		<4	Compacted pervious material
CT	Different	<5	Pervious material
DE	Different		Borrow type C
FL	Same		A-1, A-2-4 through A-2-7, A-4, A-5, A-6, A-7 (LL<50)
GA	Same		GA Class I, II or III
ID			A yielding material
IL	Different		Porous, granular
IN	Different	<8	
IO	Different		Granular; can use Geogrid
KS			Can use granular, flowable or light weight
KY		<10	Granular
LA			Granular
ME	Different	<20	Granular borrow
MA	Different	<10	Gravel borrow type B, M1.03.0
MI	Different	<7	Only top 0.9 m (3 ft) are different (granular material Class II)
MN		<10	Fairly clean granular
MO			Approved material
MS	Different		Sandy or loamy, non-plastic
MT	Different	<4	Pervious
NE			Granular
NV	Different		Granular
NH	Same	<12	
NJ	Different	<8	Porous fill (Soil Aggregate I-9)
NM	Same		
NY		<15	<30% Magnesium Sulfate loss
ND	Different		Graded mix of gravel and sand
OH	Same		Can use granular material
OK	Different		Granular just next to backwall
OR	Different		Better material
SC	Same		
SD	Varies		Different for integral; same for conventional
TX	Same		
VT	Same		Granular
VA	Same		Pervious backfill
WA			Gravel borrow
WI	Different	<15	Granular
WY	Different		Fabric reinforced

Table 2.4 Lift Thickness and Percent Compaction Requirements (Hoppe, 1999)

State	Lift Thickness, mm(in.)	% Compaction	Miscellaneous
AL	203(8)	95	
AZ	203(8)	100	
CA	203(8)	95	For top 0.76 m (2.5 ft)
CT	152(6)	100	Compacted lift indicated
DE	203(8)	95	
FL	203(8)	100	
GA		100	
ID	203(8)	95	
IL	203(8)	95	For top, remainder varies with embankment height
IN	203(8)	95	
IO	203(8)	None	One roller pass per inch thickness
KS	203(8)	90	
KY	152(6)	95	Compacted lift indicated; Moisture = +2% or -4% of optimum
LA	305(12)	95	
ME	203(8)		At or near optimum moisture
MD	152(6)	97	For top 0.30 m (1ft), remainder is 92%
MA	152(6)	95	
MI	230(9)	95	
MN	203(8)	95	
MO	203(8)	95	
MS	203(8)		
MT	152(6)	95	At or near optimum moisture
NE		95	
NV		95	
NH	305(12)	98	
NJ	305(12)	95	
NY	152(6)	95	Compacted lift indicated
ND	152(6)		
OH	152(6)		
OK	152(6)	95	
OR	203(8)	95	For top 0.91 m (3ft), remainder is 90%
SC	203(8)	95	
SD	203-305(8-12)	97	0.20 m (8 in.) for embankment, 0.30 m (12 in.) for bridge end backfill
TX	305(12)	None	
VT	203(8)	90	
VA	203(8)	95	+ or – 20% of optimum moisture
WA	102(4)	95	Top 0.61 m (2 ft), remainder is 0.20 m (8 in.)
WI	203(8)	95	Top 1.82 m (6 ft and within 60 m (200 ft) remainder is 90%
WY	305(12)		Use reinforced geotextiles layers

Second, the approach fill material is normally constructed at a lift thickness of 8 in. In Texas, a loose thickness of 12 in. compacted to 8 in. of fill is commonly used and the percent compaction is not always specified. Dupont and Allen (2002) also conducted another survey of 50 state highway agencies in the USA in order to identify the most common type of backfill material used in the embankments near bridge approaches. Their study shows that most of the state agencies, i.e. 38 states use granular material as the backfill; 3 states use sands; 6 states use flowable fill; while 17 states use compacted soil in the abutment area .

A few other research studies were conducted to study the limitations of the percent fine material used in the embankment fill. Wahls (1990) recommended that the fill materials should have a plasticity index (PI) less than 15 with percent fines not more than 5%. The FHWA (2000) recommended backfill materials with less than 15% passing the No. 200 sieve. Another recommendation of the backfill material by Seo (2003) specifies the use of a backfill material with a plasticity index (PI) less than 15, with less than 20 percent passing the No. 200 sieve and with a coefficient of uniformity greater than 3. This fill material is recommended to be used within 100 ft of the abutment.

For the density requirements, Wahls (1990) suggested two required density values; one for roadway embankments and the other for bridge approaches. For embankment material, the recommended compaction density is 90 to 95 percent of maximum dry density from the AASHTO T-99 test method, while the density for the bridge approach fill material is recommended from 95 to 100 percent of maximum dry density from the AASHTO T-99 test method. Wahls (1990) also stated that well-graded materials with less than 5% passing the No. 200 sieve are easy to be compacted and such material can minimize post construction compression of the backfill and can eliminate frost heave problems.

Seo (2003) suggested that the embankment and the backfill materials within the 100 foot-length from the abutment should be compacted to 95% density of the modified proctor test. White et al. (2005) also recommended the same compaction of 95% of the modified

proctor density for the backfill. White et al. (2005) also used a Collapse Index (CI) as a parameter to identify an adequacy of the backfill material in their studies. The CI is an index, which measures the change in soil volume as a function of placement water content. It was found that materials placed at moisture contents in the bulking range from 3% to 7% with a CI value up to 6% meet the Iowa DOT specifications for granular backfills.

In the current TxDOT Bridge Design Manual (2001), the approach slab should be supported by the abutment backwall and the approach backfill. Therefore, the backfill materials become a very important aspect in an approach embankment construction. As a result, the placement of a Cement Stabilized Sand (CSS) “wedge” in the zone behind the abutment is currently practiced by TxDOT. The placement of the CSS “wedge” in the zone behind the abutment is to solve the problems experienced while compacting the fill material right behind the abutment. This placement also provides a resistance to the moisture gain and loss of material, which are commonly experienced under approach slabs. The use of CSS has become standard practice in several Districts and has shown good results according to the TxDOT manual.

Apart from the embankment backfill material and construction specifications, the other alternatives, such as using flowable fills (low strength and flowable concrete mixes) as backfill around the abutment, wrapping layers of backfill material with Geosynthetic or grouting have also been employed to solve the problem of the excessive settlements induced by the embankment. The use of these construction materials and new techniques increases construction costs inevitably. However, the increased costs can be balanced by the benefits obtained by less settlement problems. For example, the use of Geosynthetic can prevent infiltration of backfill into the natural soil, resistance against lateral movements and improves the quality of the embankment (Burke, 1987). Other benefits are explained while describing these new methods in the following sections.

2.4.3.1 Mechanically Stabilized Earth (MSE) Wall

Mechanically Stabilized Earth (MSE) wall has been rapidly developed and widely used since the 1970's (Wahls, 1990). The MSE method is a mitigation technique that involves the mechanical stabilization of soil with the assistance of tied-back walls. As shown in Figure 38, a footing of the bridge is directly supported by backfill; therefore, a reinforcement system in the upper layer of the embankment where the backfill is most affected by the transferred load from the superstructure must be carefully designed (Wahls, 1990). On the contrary, the facing element of the wall does not have to be designed for the loading, since the transferred load from the bridge in the MSE scheme does not act on the MSE wall (Wahls, 1990).

Based on a study conducted by Lenke (2006), the results of this research shows that the MSE walls tend to have lesser approach slab settlements than other types of bridge abutment systems due to these following reasons; first, the MSE walls will have excellent lateral constraints provided by the vertical wall system, second, the tie back straps in the MSE system can provide additional stability to the embankment. These two reasons can minimize lateral loads in the embankment beneath the abutment. Consequently, the potentials of lateral settlements are reduced (Dupont and Allen, 2002).

Other advantages of the use of MSE walls are that it reduces the time-dependent post construction foundation settlements of very soft clay as noted by White et al. (2005). Also, the MSE wall with the use of geosynthetic reinforced backfill and a compressible material between the abutment and the backfill can tolerate a larger recoverable cyclic movement as noted by Wahls (1990) and Horvath (1991).

Regarding construction aspects, the MSE walls have recently become a preferred practice in many state agencies (Wahls, 1990). First, the MSE is considerably an economical alternative to deep foundation or treatment of soft soil foundation. Second, the MSE can be constructed economically and quickly when compared to conventional slopes and reinforced concrete retaining walls. Third, a compacted density in the MSE construction can be achieved

easily by increasing lateral constraint. Finally, the MSE is also practical to build in urban areas, where the right of way and work area are restricted (Wahls, 1990). Abu-Hejleh et al. (2006) cited that the use of an MSE wall for an abutment system should be considered as a viable alternative for all future bridges and it is reported as one of the practical embankment treatment systems to alleviate the bridge bump problem. An example of an MSE wall abutment is shown in Figure 2.38.

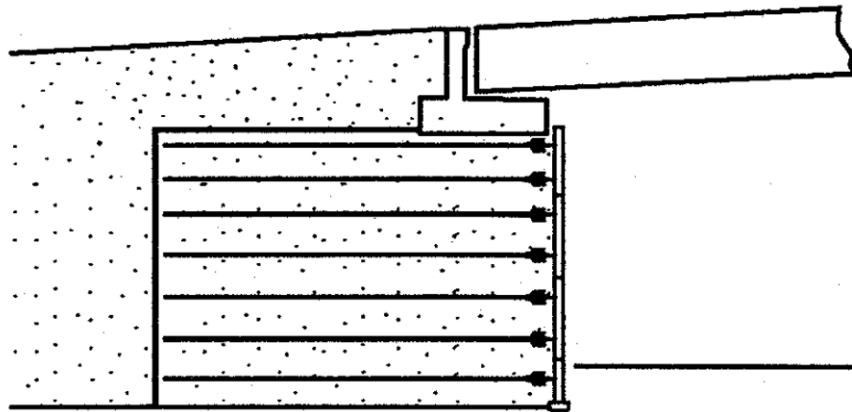


Figure 2.38 Typical Mechanically Stabilized Abutment (Wahls, 1990)

2.4.3.2 Geosynthetic Reinforced Soils (GRS)

Geosynthetic Reinforced Soil (GRS) is recommended as a method to achieve a backfill compaction at the optimal moisture content, especially for a coarse-grained backfill material (Abu-Hejleh et al., 2006). The GRS is a geosynthetic-reinforced soil structure constructed either vertically or horizontally in order to minimize the uneven settlements between the bridge and its approach. Figure 2.39 shows a schematic diagram of a GRS wall structure and a complete typical GRS system after construction. Based on the studies performed by Abu-Hejleh et al. 2006, it was discovered that with the use of GRS, the monitored movements of the bridge structure were smaller than those anticipated in the design or allowed by performance requirements. In addition, they also stated that with the

use of GRS systems, post construction movements can be reduced substantially, thus the bump problem at the bridge transition is minimized.

Another advantage of geosynthetic-reinforced soil is that it increases backfill load carrying capacity and reduces erosion of the backfill material; both can help in the mitigation of approach bumps. Some states have also used layers of geosynthetic reinforcement soil in combination with shallow foundations to support the bridge abutment (Abu-Hejleh et al., 2000).

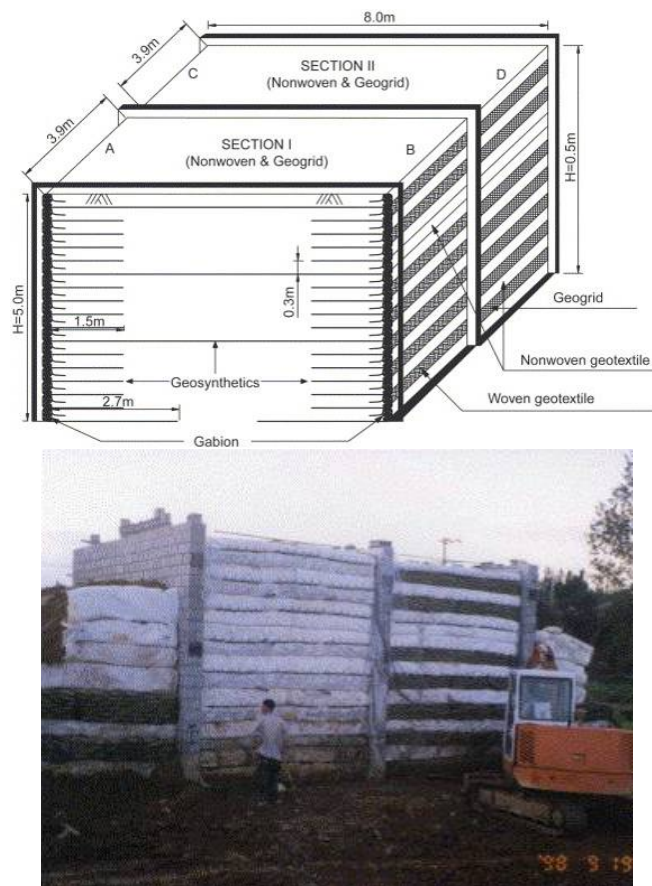


Figure 2.39 Schematic Diagram of a GRS Wall and GRS System after Construction (Won and Kim, 2007)

According to Wu et al. (2003), the GRS system becomes a more viable alternative than other conventional bridge abutments. It provides many advantages, such as being more ductile, more flexible (hence more tolerant to differential settlement), more adaptable to the

use of low quality backfill, easier to construct, more economical, and less over-excavation required. Wu et al. also presented a case study where the GRS was used in a condition in which each footing bears several preloading cycles greater than their design load and sustained for several minutes. It was found that after the first few cycles of preloads, the observed settlement reduced to negligible amounts and subsequent service settlements were less than 0.5 in. The Wyoming Highway Department has used multiple layers of geosynthetic reinforcement within compacted granular material since the 1980s (Monley and Wu, 1993).

Edgar et al. (1989) stated that none of the ninety approach slabs placed on geosynthetic reinforced embankments required maintenance or repair only after 5 years of service. Excellent performance of these systems was also reported by Abu-Hejleh et al. (2006) for both short- and long-term performance of the GRS approaches.

Wu et al. (2006) summarized the advantages of the GRS bridge abutments with flexible or rigid facing over conventional reinforced concrete abutments as follows:

- a. GRS abutment increases tolerance of foundation settlement to seismic loading
- b. GRS abutments are remarkably more stable and have higher ductility
- c. With a proper design and construction, “bumps” can be alleviated
- d. GRS abutments are constructed more rapidly and less expensive
- e. GRS abutments do not require embedment into the foundation soil for stability
- f. The lateral earth pressure behind a GRS abutment wall is much smaller
- g. GRS performs satisfactorily longer under in-service conditions
- h. The load-carrying capacity by GRS is significantly greater

The GRS bridge-supporting structures can be grouped into two types: “rigid” facing and “flexible” facing structures (Wu et al., 2006). Flexibility or rigidity of GRS walls is explained in relation to its deformation capability and its responses to temperature changes during different seasons (Wu et al. 2006). If the construction is done in cold dry seasons (fall/winter), the GRS walls present a rigid response whereas constructions of GRS walls

during warm, wetting, and thawing seasons result in GRS walls with a flexible response, capable of undergoing relatively large deformations.

Rigid facing is typically a continuous reinforced concrete panel, either precast or cast in-place. Rigid facings offers a significant degree of “global” bending resistance along the entire height of the facing panel, thus offering greater resistance to global flexural deformation caused by lateral earth pressure exerted on the facing. A typical cross section of a GRS system with rigid facing is shown in Figure 2.40.

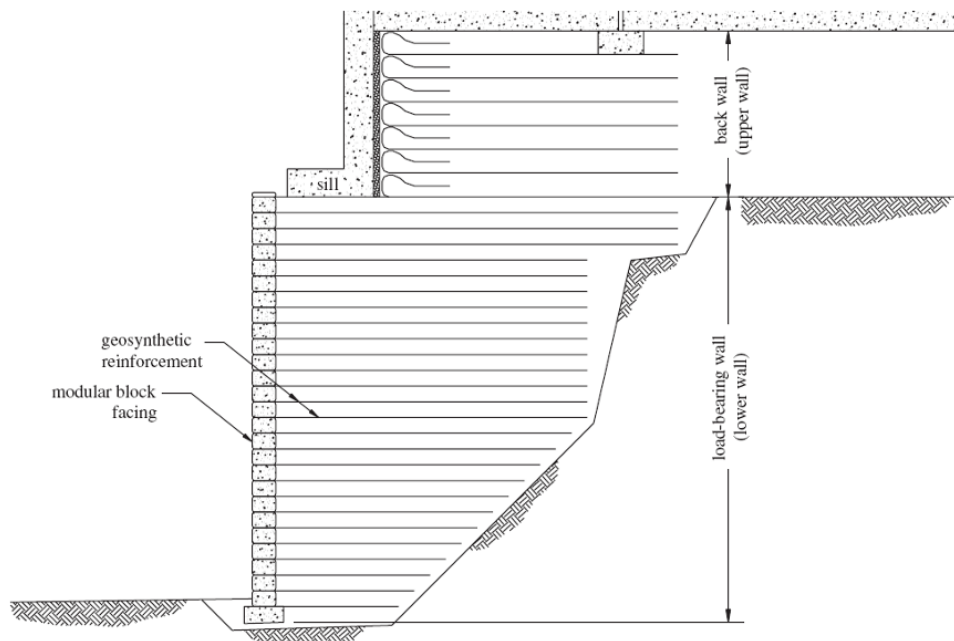


Figure 2.40 Typical GRS Bridge Abutment with a Segmental Concrete Block Facing

Flexible facing is typically a form of wrapped geosynthetic sheets, dry-stacked concrete modular blocks, timbers, natural rocks, or gabions. These wall structures have shown great promise in terms of ductility, flexibility, constructability, and costs. The main advantages of this system over the rigid facing are summarized in the following (Abu-Hejleh et al., 2003, Wu et al., 2006):

- a. Larger mobilization of the shear resistance of the backfill, thus taking more of the lateral earth pressure off the facing and connections

- b. More flexible structure, hence more tolerant to differential settlement
- c. More adaptable to low-quality backfill

Guidelines of GRS walls are provided by the Colorado DOT for designing and constructing GRS bridge abutments (Abu-Hejleh et al., 2000) and a few of the assumptions used in this guideline are presented here:

- a. The foundation soil should be firm enough to limit post construction settlement
- b. The desired settlement of the bridge abutment should be less than 1 in. (25 mm)
- c. The maximum tension line needed in the internal stability analysis should be assumed nonlinear
- d. Ideally construction should be done in the warm and dry season
- e. The backfill behind the abutment wall should be placed before the girders.

Overall, the GRS system walls have been used with success to alleviate approach settlement problems. However, very few state DOTs have implemented this in practice, probably due to the limited amount of familiarity of this method.

2.4.3.3 Lightweight Fill

Another concept to reduce the vertical loading or stress from the embankment as it exerts itself on the foundation subsoil is the use of lightweight material as an embankment fill material. The reduction of embankment weight or load increases the stabilities of the embankment and also reduces the compression on the underlying foundation soil. As a result, the settlement potential of the embankment will be decreased.

The lightweight fills such as lightweight aggregate, expanded polystyrene, lightweight concrete, or others can be used to achieve this benefit (Luna et al., 2004, Dupont and Allen, 2002, Mahmood, 1990). Based on the surveys conducted by Hoppe (1999) approximately 27% of responding DOTs have already experimented with the use of non-soil materials behind bridge abutments.

Horvath (2000) recommended the use of Geofoam as a light weight compressible fill material (Figure 2.41). Other materials could be used as alternative lightweight backfill material; some of these alternative construction materials included shredded tires and expanded polystyrene. However, it must be kept in mind that the suitable fill material must not have only the lightweight property, but it must have other required properties, such as, high strength, high stiffness and low compressibility properties.

Hartlen (1985) listed some satisfactory requirements for the lightweight fill material as follows;

- a. Bulk density less than 63 pcf. (1000 kg/m³)
- b. High modulus of elasticity and high angle of internal friction
- c. Good stability and resistance against crushing and chemical deterioration
- d. Non-frost active
- e. Non-corrosive to concrete and steel
- f. Non-hazardous to the environment

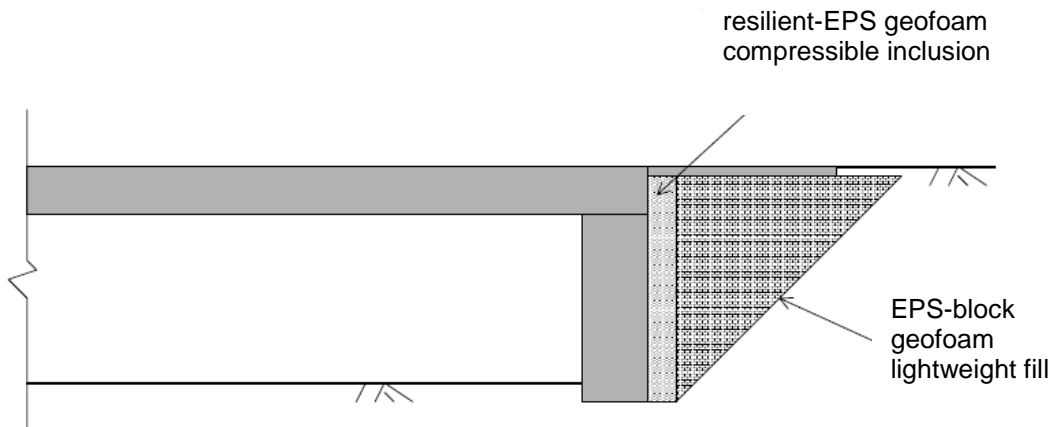


Figure 2.41 A design alternative by using geofoam as a backfill (Horvath, 2000)

2.4.3.4 Flowable fill (Flowfill)

Flowable fill is a low-strength mixing concrete used as a backfill behind the abutment wall to reduce the possibility of approach settlements near the surface, resulting from the compression of the backfill itself (Abu-Hejleh et al., 2006). According to NCHRP (597), the fluidity of flowable fill makes it a rapid and efficient backfilling material. The low-strength mixing concrete works well to prevent erosion of the backfill and to improve constructability/compactability of the fill behind the walls and around corners. The self-leveling ability property allows the flowable fill material to fill voids without the need of any compaction (NCHRP, 597). Although, this method is an expensive construction practice, it is still a practical alternative in certain field and construction scenarios where the use of such practice justifies the higher costs (Abu-Hejleh et al., 2006).

Snethen and Benson (1998) summarized that the use of flowable fill as an embankment material to reduce the potential for developing the bump at the end of the bridge seems to be a simple, reasonably cost effective, and less time-consuming method. This study also concluded that use of the flowable fill as an embankment material has resulted in the reduction of the lateral earth pressure and settlement of the approach embankment.

According to the Colorado DOT specifications, the maximum lift thickness for flowable fill material is 3 ft and a placement of additional layers is not permitted until the flowable fill has lost sufficient moisture to be walked on without indenting more than 2 in.. CDOT specifications do not specify any need for vibration because the vibration may stiffen the flowfill by allowing the setting to occur faster in the field. CDOT specifications for the flowfill backfill are listed in Table 2.5 (Abu-Hejleh et al., 2006).

In a separate section, the use of flowable fills for remediation of approach slab settlements will be discussed.

Table 2.5 CDOT Material Requirements for Flowable fill Backfill

Ingredient	lbs/c.y.
Cement	50
Water	325 (or as needed)
Coarse Aggregate (AASHTO No.57 OR 67)	1700
Fine Aggregate (AASHTO M6)	1845

2.4.3.5 Grouting

Edgar et al. (1989) reported that in a high-speed passageway, ground stabilization methods could be utilized to reduce maintenance requirements. In this study, the use of cement-treated backfill instead of conventional granular backfill material was chosen to reduce the hydro-collapse and increase soil strength. The grouting technique has been also recommended for mitigation of settlement of the embankment in the case of embankments underlain by organic peat layers, which can be easily compressed and consolidated, (Byle 1997 and 2000). It was found that the pressure grouting method was also successful in preventing the loss of materials. However, the main objective of the grouting technique is to restrict the limited mobility displacement (LMD) of the material, as described by Byle (1997 and 2000).

Figure 2.42 shows that the sleeve pipes can be installed in different angles of 50°, 30°, 20° from the horizontal surface (Sluz et al., 2003). The angle at which the sleeve port pipes installed in the soil is important and must be modified by monitoring the amount and the rate of settlement. Details including the settlement after mitigation and the type of grout used were not listed in the report.

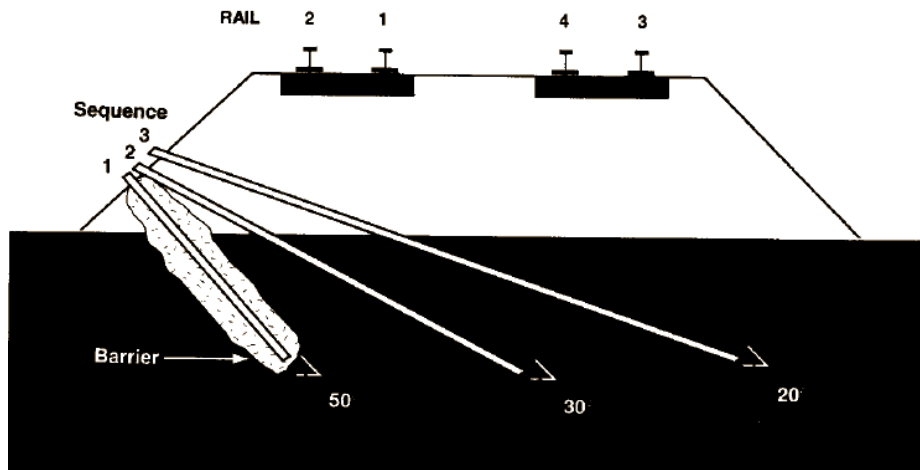


Figure 2.42 Sleeve Port Pipe Installation Plan (Sluz et al., 2003)

2.4.3.6 Other Recommendations

If possible, the slopes of soil embankments should be flattened, which tends to increase the stability and reduce the deformations of the embankment (Luna et al., 2004). Such practice will not be applicable due to high use of ROWs along the embankment sections. If the proposed embankment material is plastic clay with PI greater than 15-20, treatment of the soil or alternate borrow sources should be considered. The select fill also needs to be extended to a certain distance from the abutment, and the distance ranges between 50 and 100 ft and is dependent on the type of embankment and material used as a backfill (Luna et al., 2004).

2.4.4 Design of Bridge Foundation Systems

The bridge foundation is considered as a major factor in bridge structure design. Bridges can be supported either by shallow or deep foundation systems (Wahls, 1990). In both cases, the foundations should be able to carry the loads from the above superstructures and the traffic volumes, but also to limit the horizontal and vertical movement of the abutment to the acceptable levels (Wahls, 1990). The selection of a safe and economical foundation system requires consideration of structural loads, environmental factors, subsurface

conditions, bed rock types and depths, performance criteria, construction methods and economics (ODOT Bridge Foundation Design Practices and Procedures, 2005).

Spread footings, driven piles, and drilled shafts are generally used as a bridge foundation. According to Wahls (1990), the spread footing has its advantage over the deep foundation in aspect of inexpensive cost. However, the uncertainties in the performance prediction and the potential for scouring make the shallow foundation an unattractive choice for a bridge foundation system. Moreover, since the compaction of backfill near the abutment is difficult to achieve, the possibilities of loads from superstructure and traffic volume stressing the poorly compacted backfill and contributing to the settlement of bridge approaches can be high (Wahls 1990).

For those reasons the deep foundations including driven piles or drilled shafts are preferred to support the bridges. The deep pile foundations have been demonstrated to be the most efficient means of transferring heavy loads from superstructures to substructures and bearing materials without significant distress from excessive settlement (Abu-Hejleh et al., 2006). Hopkins (1985) cited that the settlement of the bridge abutment resting on pile foundations is usually negligible. However, due to the fact that the bridges supported by pile foundations do not usually settle as much as the approach embankments, the differential settlement between these two adjacent structures can lead to the bump problems at the bridge approach. Hopkins and Deen (1970) stated that the differential settlement between the abutment and the approach slab is usually high for pile support abutments.

The abutment with embedded pile caps can develop resistance to the movement of the bridge structures as the bridge superstructure expands and contracts with temperature variations, which is also claimed as a cause of high applied stresses on the pile foundations and a reduction of pile axial load capacity (Greimann et al. 1983). Greimann et al. (1986) performed a three dimensional non-linear finite element analysis to study pile stresses and

pile soil structure interaction of integral abutment bridges from thermal fluctuations. They found that the thermal expansion of the bridge reduces the vertical load carrying capacity of the piles. They reported that the vertical load carrying capacity for H piles in very stiff clays is reduced by approximately 50% for 2 in. of lateral displacement and approximately 20% for 1 in. lateral displacement.

Girton et al. (1991) measured the maximum of pile stress at the Boone Bridge and the Maple River Bridge. They found that the maximum pile stresses were only 60% and 70% of the nominal yield stress at both sites, respectively. Lawver et al. (2000) reported that the maximum measured pile stresses were slightly above the nominal yield stress of the pile. Arsoy et al. (2002) investigated the performance of H-piles, pipe piles, and pre-stressed reinforced concrete piles subjected to cyclic lateral displacements. Based on that study, it was concluded that H-piles loaded on the weak axis were the best alternative to support the integral abutments. An example of bridge foundation construction using H-piles is illustrated in Figure 2.43.

The use of precast, pre-stressed concrete (PC) piles in the foundation of bridge piers has been used as a valuable alternative for bridge construction for a long time (Abendroth et al., 2007). However, due to some concerns over pile flexibility at the abutment ends, potential for concrete cracking induced by thermal expansions and seismic movements, and deterioration of the pre-stressing strands due to long-term exposure to moisture, these PC piles in the integral abutment bridges have not been extensively used (Abendroth et al., 2007).



Figure 2.43 Example of Bridge Foundation using Steel H-Piles

According to a survey conducted in several states by Abendroth et al. (2007), the main reasons to avoid PC piles for bridge abutments are attributed to inadequate ductility (48%), insufficient research on the subject matter (52%), limit availability (33%) and high cost of the foundations (24%). In the last ten years, the potential use of PC piles for integral abutments was reported in a few studies (Kamel et al., 1996, PCI, 2001, and Burdette et al., 2004). However, the available literature presents different conclusions regarding the suitability of PC piles for this application (Abendroth et al., 2007).

The precast, pre-stressed concrete piles typically utilize both skin friction and end bearing conditions to carry the vertical loads. The results from the study by Abendroth et al. (2007) showed that with respect to construction costs the usage of PC piles is more economical than

the H-steel pipes in sandy and gravelly soils. Moreover, the study also showed that these precast, pre-stressed concrete piles usually experience less lateral displacement than the H-piles and lower longitudinal movements than the expected range. However, the study also evidenced pile cracking problems after excavation on the abutments. The cracking problems are attributed to moisture penetration, uncoated pre-stressing strands and long-term corrosion problems (Abendroth et al., 2007). For these reasons, periodic inspection of the abutment piles is recommended to detect any additional concrete cracking or deterioration.

When piles are selected for a bridge foundation system, the ability of the foundation piles to carry the vertical loads even when the piles are subjected to temperature-induced displacements must be considered (Arsoy, 1999). The lateral displacements may reduce vertical-load carrying capacities of piles, resulting in pile failure if lateral loads are higher than the elastic buckling load (Greimann and Wolde-Tinsae, 1988). Another important factor is the length of the pile, because it controls the allowable settlement of the structure. Bakeer et al. (2005) indicated that due to loading requirements and to minimize settlement, bridge piers and abutments needed to be supported on relatively long piles or piles with tips driven into stiff soil.

One negative effect that needs to be taken into account for the design of pile foundations is the consideration of negative skin friction or down-drag from compressible soils around the pile lengths. Figure 2.44 presents a schematic of the process that produces down-drag forces on piles. Down-drag is the sum of the negative shaft resistance along the length of the pile where the soil is moving downward relative to the pile and this drag is always treated as a downward acting load (AASHTO, 2004).

Some of the successful methods to mitigate down-drag are listed below (Narsavage, 2007):

- a. Use larger H-pile sections to increase factored structural resistance for piles on rock

- b. Use more piles and reduce the applied load for piles not driven to refusal on rock
- c. Reduce soil settlement that occurs after pile driving by preloading and/or using wick drains
- d. Reduce soil settlement by using lightweight embankment fill material
- e. Use bituminous pile coating

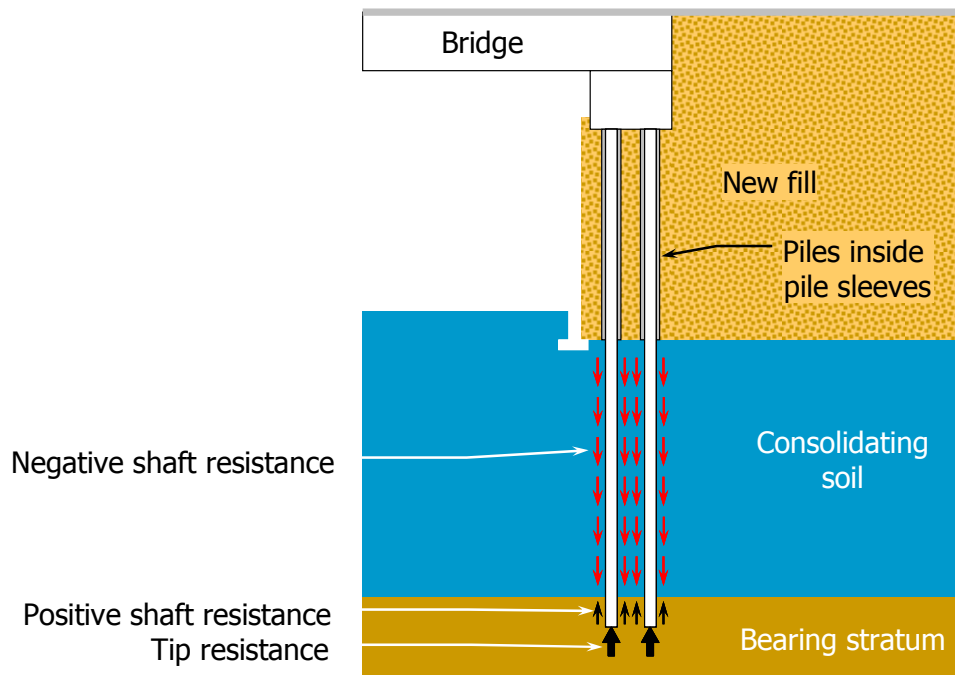


Figure 2.44 The Down-drag in Piles

In order to avoid the downward drag problems, the use of shallow foundations has been suggested (DiMillio, 1982). Generally, the shallow foundations are typically 50% to 60% less expensive and require less construction time than deep foundations (DiMillio, 1982). Some recent studies have demonstrated again the feasibility of implementing shallow foundations for major bridges in the United States (Abu-Hejleh et al., 2003). For example, the Founders/Meadows bridge foundation was built on footings supported directly by a geosynthetic-reinforced soil system, eliminating the use of traditional deep foundations (piles

and caissons) altogether. A typical section of the GRS system of this bridge foundation is detailed in Figure 2.45.

However, the shallow foundations have their own disadvantages. In a study by Grover (1978), he compared the behavior of bridges supported by shallow and pile foundations in Ohio. The result of this study indicated that for the bridge constructed in 1960s, 80% of the abutments supported by shallow spread footings experienced more than 2.5 inches of settlement and 10% of them experienced more than 4 inches of settlement. As a result, Ohio DOT specifications asked for deep pile supported bridge abutments in the place of shallow foundation supported abutments (Grover, 1978).

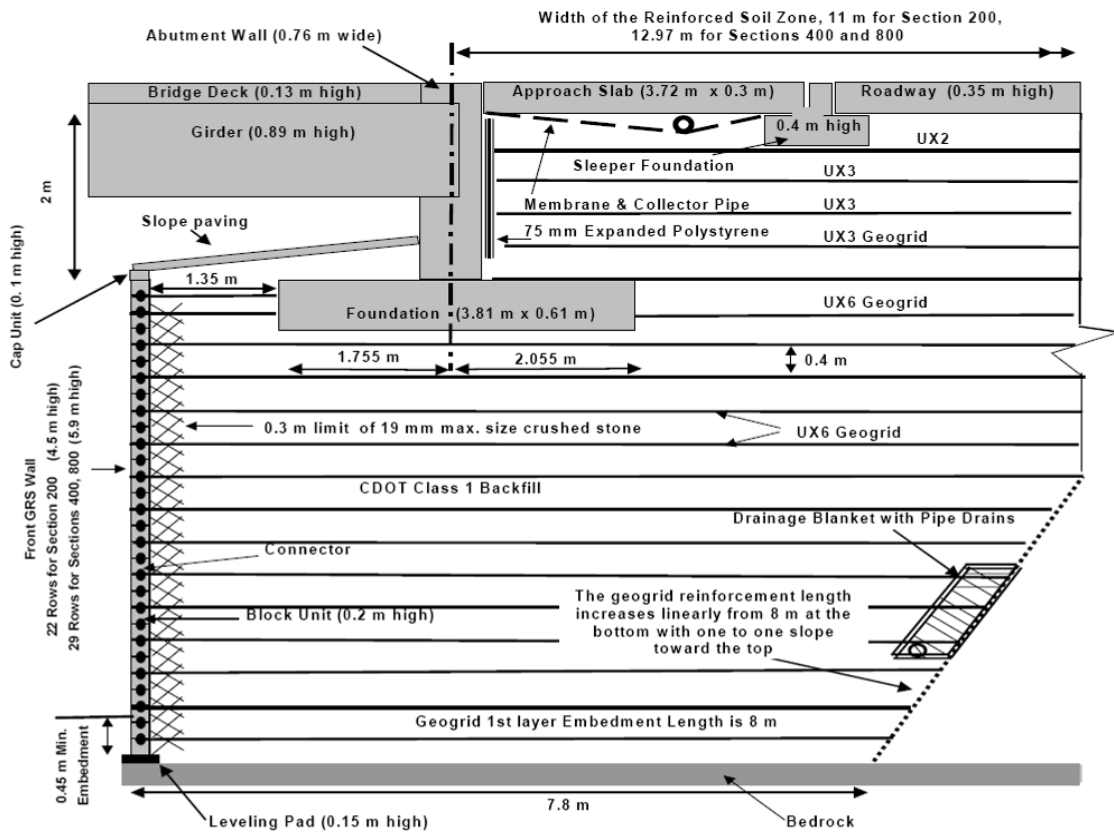


Figure 2.45 Typical Section through Front and Abutment GRS Walls (Abu-Hejleh et al., 2006)

According to the TXDOT Bridge Design Manual (2001), the spread footing was only an alternative used as bridge foundations in Texas in early bridge design, although other options, such as timber and concrete piles were already available. Since the late 1930s, the steel H pile was introduced and then became widely used and a few caissons, pneumatic and open, were used for larger stream crossings. A drilled shaft technology, which was developed in the late 1940s, and pre-stressed concrete pile foundations have now become a dominate foundation in bridge construction in Texas.

2.4.4.1 Design of Bridge Abutments

The type of the bridge abutment plays an important role (Mahmood, 1990). Generally, two types of abutments are used widely in the United States, a Non-Integral (or Conventional) and an Integral type (Greimann et al., 1987).

The Non-integral or Conventional type of bridge abutments (Figure 2.46) have bearing connections and expansion joints to provide the superstructures with a certain amount of lateral movement between the abutment and the bridge deck (Wahls, 1990) The lateral load caused by the lateral movement or the thermal strains in the deck will be lessened by both types of connections (White et al., 2005). However, increased traffic loads and frequent application of de-icing salts during winter could deteriorate the expansion joints and bearing connections, which can lead to costly maintenance problems (Horvath, 2000). These Non-integral abutments are commonly used in many states including Texas.

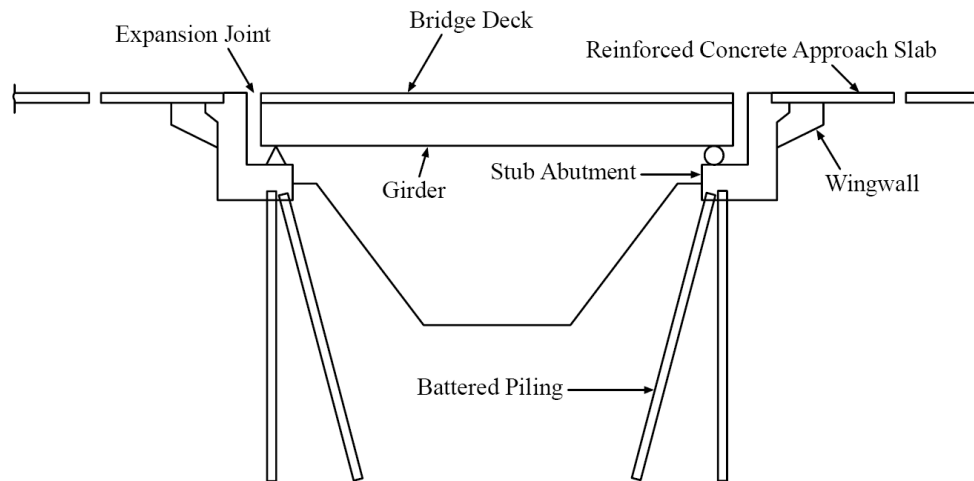


Figure 2.46 Simplified cross section of non-integral abutment bridge (Greimann et al., 1987, White et al. 2005)

The Integral bridge abutment type (Figure 2.47) was developed in order to eliminate the use of bearing plates and to reduce potential maintenance problems (Horvath, 2000). The Integral abutment is a stub abutment connected to the bridge superstructure tightly without any expansion joints (Wahls, 1990). The rigid connections are conventionally included thermal stresses from the bridge deck to the abutment in their design criteria (Wahls, 1990). The advantages of this rigid connection are (Greimman et al., 1987, Hoppe and Gomez, 1996);

- a. simple and reduced construction and maintenance costs
- b. minimum number of piles required to support the foundation
- c. improved seismic stability

The use of Integral bridge abutments has been increased since the 1960's, because it avoids the use of the bearing plates and the potential maintenance problems associated with Non-integral bridge abutments (Wahls, 1990, Horvath, 2000, Kunin and Alampalli, 2000).

Pierce et al., 2001 stated that the bridge approaches with Integral abutments tend to reduce the surface roughness. However, Wahls (1990) reported a problem related to cracking and bulking at the approach pavement due to a lateral cyclic movement of the abutment from

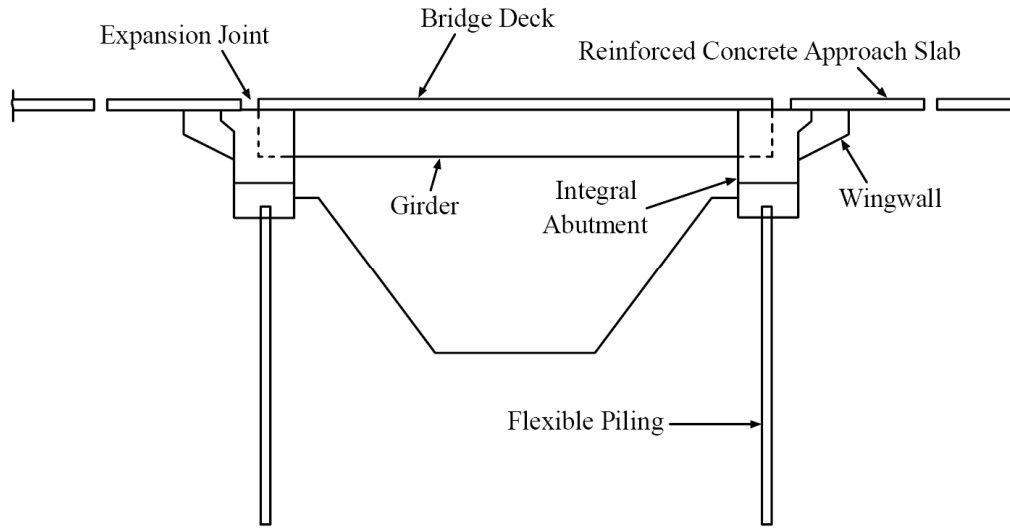


Figure 2.47 Simplified cross section of integral abutment bridge
(Greimann et al., 1987, White et al. 2005)

thermal movement induced stresses at the bridge decks. Schaefer and Koch (1992) and Arsoy et al. (1999) also specified that the same lateral cyclic movements exerted on the backfill soils from daily temperature changes may form voids at the face of the abutment, which contribute to the total approach settlement. The voids are observed within one year of bridge construction, indicating insufficient backfill moisture control/compaction followed by soil collapse upon saturation (White et al, 2005).

Lateral movement is a common occurrence of the Integral bridges (Kunin and Alampalli, 2000; Arsoy et al., 2002, and Arockiasamy et al., 2004). The bridge superstructures will be expanded and contracted by seasonal air temperature fluctuations according to concrete thermal strain characteristics. Because the bridge deck and abutment are integrally connected, both structures will laterally move together. The movement of the structures resulting from the temperature of the bridge deck seasonal changes can cause a cyclic loading subjected toward the approach backfill and the foundation. When the temperature rises, the bridge deck expands and then the superstructure including the bridge abutment moves against the retained embankment soil. The lateral movement induces the stress in the

soil and sometimes can reach the passive pressure limit (Schaefer and Koch, 1992). On the other hand, when the temperature lowers, the superstructure and the abutment move away from the soil and leave voids at the interface between the abutment and the backfill. The size of the voids can become bigger if the weather gets colder. The development of the voids can be a cause of soil erosion that increases the size of the void behind the abutment and below the approach slab as shown in Figure 2.48.

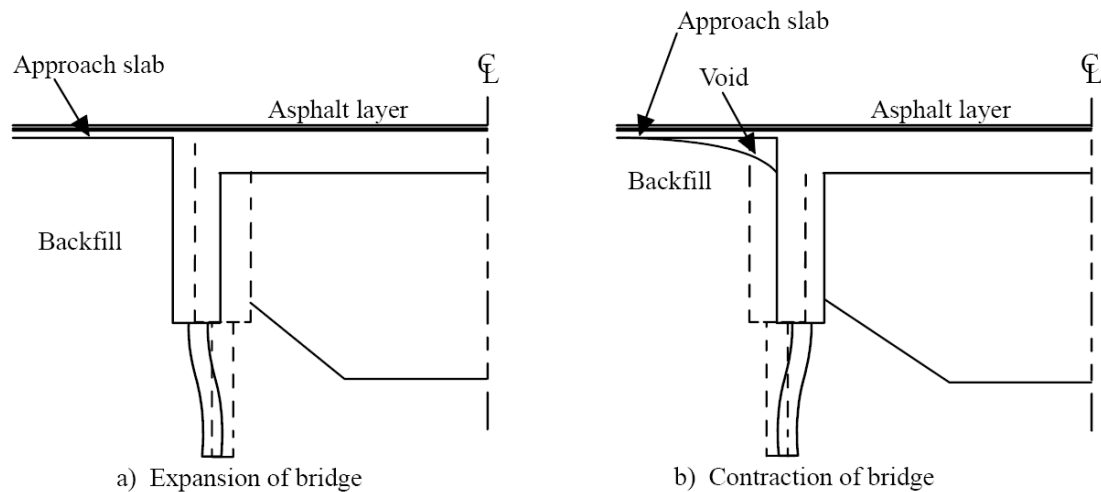


Figure 2.48 Movement of bridge structure with temperature (Arsoy et al., 1999)

Wahls (1990) suggested that the performance of an Integral abutment can be improved by installing compressible elastic materials between the abutment and the backfill. The material should have elastic properties that permit large recoverable cyclic movements and hydraulic properties that provide adequate drainage without erosion of fines from the backfill. Horvath (2000) advocated the use of geofoam as a compressible material. The successful use of compressible and collapsible materials behind the abutment was reported by the North Dakota DOT and Illinois DOT (Wahls, 1990, Kunin and Alampalli, 2000).

According to Mekawy et al. (2005) and White et al. (2005), insufficient drainage is also another problem often found at the bridge abutments. Water that is collected on the bridge pavement can cause severe damage to the bridge approach. If collected water can

flow into the underlying fill materials due to inefficient seals at the joints between the bridge approach slab and the abutments, the water can erode the backfill material, resulting in voids development under the bridge abutments. Therefore, an efficient drainage system should be incorporated in the design of bridge approaches, such as drainage inlets at the end of a bridge deck to collect surface water before getting to the approach slab (Abu-Hejleh et al., 2006).

Furthermore, providing additional surface or internal drainage to keep water off the slopes is recommended for correcting the superficial erosion of embankments (Wahls, 1990). Keeping the water away from the soil is a simple significant factor in reducing the settlement of the soil. Construction costs added to incorporate a good drainage system are not high when compared to the expensive maintenance costs that might be experienced in the service life of a bridge (Dupont and Allen, 2002).

2.4.5 Design of Approach Slab

The bridge approach slab is a part of a bridge that rests on the abutment at one end and on the embankment or a sleeper slab on the other end (Wahls, 1990). The slabs are designed to provide a smooth transition between the bridge deck and the roadway pavement, and to minimize the effect of differential settlements between the bridge abutment and the embankment fill (White et al., 2005). There are two types of approach types used by highway agencies. Some agencies use a bituminous approach pavement, because it can be maintained easily by overlay type rehabilitation. However, the use of bituminous approaches with Portland concrete roadways is still not highly preferred by the DOTs (Wahls, 1990).

Other agencies use a reinforced concrete slab, because they believe the rigid approach slab is successful in preventing the bridge approach settlement (Wahls, 1990). In this case, one end of the slab is connected to the main structure by two ways. In the first alternative (Figure 2.49), the slab is connected directly to the bridge deck by extending the main reinforcement from the bridge deck to the approach slab; while in the second alternative

(Figure 2.50), the approach slab is connected to the abutment by using a dowel/tie bar (White et al., 2005).

Based on a survey on over 131 bridges in Texas by James et al. (1991), they found that the bridges with flexible pavement had a smoother transition than those with rigid pavement. However, Pierce et al. (2001) reported that the approach slab with asphalt overlays tend to increase surface roughness. According to the TxDOT Bridge Manual (2001), the use of approach slabs is only an option, and Districts have had success with and without their use. However, if the approach slab is constructed with the Non-integral bridge system, the use of a dowel/tie bar must be implemented between the slab and the abutment (Hoppe, 1999).

James et al. (1991) stated that the roughness or IRI values of the approach slab are influenced by the longitudinal pavement movements resulting from temperature cycles. They also mentioned that the approach pavement settlement/roughness can be attributed to impact loads due to poor design and constructed expansion joints.

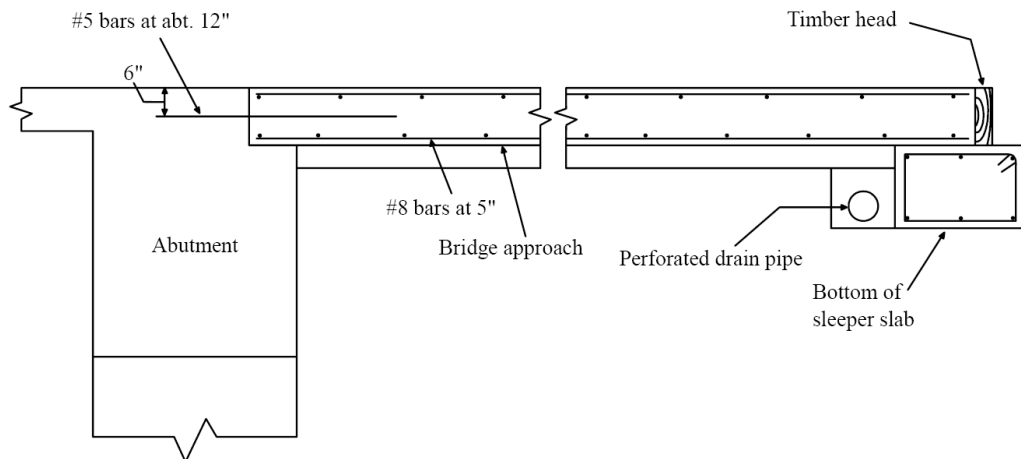


Figure 2.49 Bridge approach connected to bridge deck (Missouri DOT 2003)

White et al., (2005) stated that the performance of the approach slabs depends on these following factors: approach slab dimensions, steel reinforcement, use of a sleeper slab, and type of connection between the approach slab and the bridge.

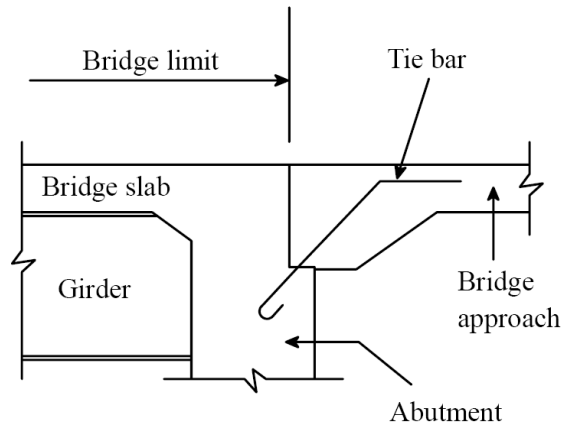


Figure 2.50 Bridge approach connected to abutment (Ohio DOT, 2003)

2.4.5.1 Slab dimensions

Most of the reinforced concrete approach slabs used in the USA have lengths varying from 20 to 40 ft (6 to 16 m) (Wahls, 1990). According to an extensive survey conducted by Hoppe (1999) of different State Agencies, typical approach slab dimensions for the various states surveyed are collected and summarized in Table 2.6. From the Table, it can be seen that most approach slab dimensions vary between 15 - 30 ft (5 - 10 m) in length and 9 - 17 in. (23 - 43 cm) in thickness.

Some states consider the use of a short span slab and this is attributed to causing the bump problem (Lenke, 2006). As a result, some of these states move towards the use of a slab longer than 40 ft (16 m) (LaDOTD, 2002). For example, the Illinois DOT prefers the design of a slab length of 100 ft (30 m), and the Louisiana DOT uses continuous slab lengths from 80 to 120 ft (24 to 36 m) (Wahls, 1990). In both cases, the bridge abutments are pile supported.

Other research summary studies by Briaud et al., 1997, Abu-Hejleh et al., 2006, Lenke, 2006 suggest a criterion to calculate the slab length based on the maximum slope of the approach slab, which is defined as the change in elevation between the beginning of the

Table 2.6 Typical approach slab dimensions used by various DOTs (Hoppe 1999)

State	Length (ft)	Thickness (in)	Width limited to
AL	20	9	Pavement
AZ	15	N/A	N/A
CA	10-30	12	Curb-to-Curb
DE	18-30	N/A	N/A
FL	20	12	Curb-to-Curb
GA	20-30	10	Curb-to-Curb
IA	20	10-12	Pavement
ID	20	12	Length
IL	30	15	Curb-to-Curb
IN	20.5	N/A	N/A
KS	13	10	Curb-to-Curb
KY	25	N/A	Curb-to-Curb
LA	40	16	Curb-to-Curb
ME	15	8	Curb-to-Curb
MA	N/A	10	N/A
MN	20	12	Pavement
MS	20	N/A	Curb-to-Curb
MO	25	12	N/A
NV	24	12	Curb-to-Curb
NH	20	15	N/A
NJ	25	18	N/A
NM	15	N/A	Curb-to-Curb
NY	10-25	12	Curb-to-Curb
ND	20	14	Curb-to-Curb
OH	15-30	12-17	N/A
OK	30	13	Curb-to-Curb
OR	20-30	12-14	Curb-to-Curb
and	Skew	angle	N/A
SD	20	9	N/A
TX	20	10	N/A
VT	20	N/A	N/A
VA	20-28	15	Pavement
WA	25	13	Pavement
WI	21	12	N/A
WY	25	13	Curb-to-Curb

***N/A: Information is not available or not applicable

approach slab (at the sleeper slab) and the bridge abutment divided by the length of the approach slab. The slope of the approach in their studies is defined as:

$$S = \frac{s_f - s_a}{L} \leq \frac{1}{200}$$

where S is the longitudinal slope of the approach slab, L is the length of the approach slab, and s_f and s_a are the settlements of the foundation (embankment and natural soil foundation) and the abutment, respectively. For example, if a settlement analysis indicates a differential settlement between the abutment and the beginning of the approach slab ($s_f - s_a$) equal to 1.5 in., then the length of the approach slab must be greater than 300 in., or 25 ft. From the equation it can be easily understood that when the same settlement happens at both ends of the slab, then a shorter approach slab will be needed.

One way of minimizing “the bump” is to lengthen the approach slab (Lenke, 2006). Seo, 2003 suggested that the approach slabs should have a minimum length of 20 ft and should be designed to support full traffic loading in a free span to account for any unexpected erosion beneath the slab.

Other aspects of approach slabs that are of interest to designers is the acceptable degree of the longitudinal slope. Several research reports recommended a maximum allowable change related slope of 1/200 (Wahls, 1990; Stark et al., 1995; Briaud et al., 1997; and Seo, 2003). Long et al. (1998) also proposed a relative gradient of less than 1/200 to ensure rider comfort and a gradient of between 1/100 and 1/125 as a criterion for initiating remedial measures.

Wong and Small (1994) suggested that the slab with an angle can lessen the bump problem. They studied the effect of orientation of approach slabs on pavement deformation by varying the slopes of the approach slab at 0, 5 and 10 degrees with the horizontal and compared those results with no slab tests in a one-fourth scaled model as shown in the test set-up in Figure 2.51. They concluded that the horizontal slab contributes little to remedy the bump problem. On the contrary, the slab with an angle sloped down beneath the pavement

can alleviate the bump problem better than a horizontal one due to the fact that the deformations at the surface at the pavement above the slab are more gradual and the rate of change of the surface gradient is small.

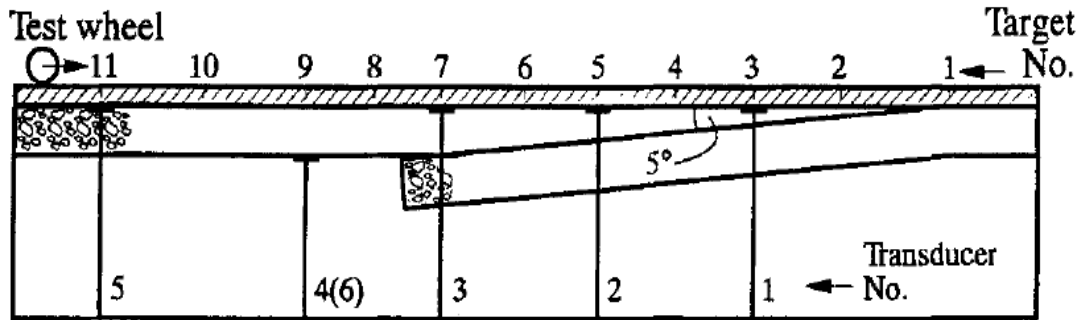


Figure 2.51 Test setup for subsoil deformation (Wong and Small, 1994)

The slab thickness is another factor that needs to be considered for a slab design. Normally, the thickness of the rigid approach slab is uniform. Nassif (2002) conducted a numerical analysis on New Jersey's approach slabs. They concluded that the slab thickness is the most effective parameter in reducing the tensile stresses in the critical elements. From the same study, Nassif (2002) also suggested a constant thickness of the approach slab and embedded beam design to the New Jersey DOT for their use. Overall, the slab thickness can vary depending on the considerations of the length of the slab, other structures and the foundation (Lenke, 2006). The thickness of the slab can be designed as a taper shape in different sections in order to provide more flexibility in areas near the abutment (Wahls, 1990).

Regarding the type of slabs, Cai et al. (2005) studied different types of approach slabs by performing 3D finite element analyses. They recommended the use of a ribbed slab type, as seen in Figure 2.52, over the flat slab type, especially for long approach spans. Since, the internal forces and deformation of the ribbed slab can be lessened due to its slab-on-beam behavior, the thickness of bridge decks or slabs can be reduced when compared with the flat slabs.

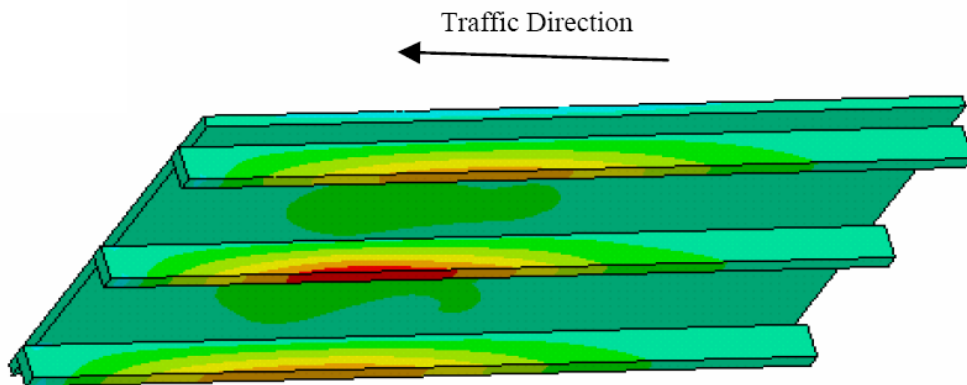


Figure 2.52 The ribbed slab as an approach slab (Cai et al., 2005)

In terms of the width of the approach slab, the curb-to-curb method is the preferred (Briaud et al., 1997). By matching the width of the slab with the width of the bridge decking (between bridge guardrails, or barriers), a few advantages can be realized. These are better erosion control of the underlying embankment soils and effective drainage pouring water away from the bridge structure and approach slab system (White et al., 2005). Since these two factors contribute to the bump problem, use of such widths of approach slabs are often recommended (Briaud et al., 1997, White et al., 2005).

According to the TxDOT Bridge Manual (2001), the use of an approach slab is optional. However, when the use of an approach slab is utilized, the approach slab should have a thickness of 13 in. The slab must also be a lightly reinforced concrete slab, which precedes the abutment at the beginning of the bridge, and follows the abutment at the other end of the bridge.

This manual also cites that TxDOT discourages the use of approach slabs on wingwalls based on previous experience in Texas. Due to the difficulty in compaction of the backfill, and the potential loss of backfill material, the approach slab becomes a slab supported on three sides (i.e. at the two wing walls and the abutment backwall). Without the bearing on the backfill, it leads to the development of a void underneath the slab, and

consequently leads to bumps. For that reason, the standard approach slab and the wing walls designed to carry out the load are not reinforced. Hence, TxDOT suggests that the approach slab should be supported by the abutment backwall and the approach backfill only.

The appropriate backfill material is considered an essential component under the slab. TxDOT is currently supporting the placement of a cement stabilized sand (CSS) “wedge” in the zone behind the abutment (TxDOT Bridge Manual, 2001). The use of CSS can solve the problem of difficult compaction behind the abutment. Furthermore, CSS wedges are resistant to the moisture gain and loss of material, which are common occurring under approach slabs. The use of CSS has become standard practice in several Districts and has shown good results (TxDOT Bridge Manual, 2001). The Fort Worth District in TxDOT uses a cement treated flexible base beneath the approach slab for the same purpose. The 3 ft. deep flex base is prepared by compacting four equal layers (9 in. thick) of Type 1 cement treated (2.4% by weight) base material as shown in Figure 2.53. However, approach slabs with the cement treated flexible base have also experienced the same settlement problems since the heavier flexible base has further consolidated the embankment fill and thus creating a larger “bump” (Williammee, 2008).

An additional component to the approach slab, which is not widely applied, is the use of a sleeper slab. A sleeper slab is a concrete foundation slab placed transversally at the approach slab and opposite to the bridge end (Ha et al., 2002 and Seo et al., 2003). Generally, one end of the rigid approach slab rests on the abutment or connects directly with the bridge deck, while another end sits directly on the embankment or otherwise on a sleeper slab (Wahls, 1990). An example of a sleeper slab for an Integral abutment system is illustrated in Figure 2.54. The sleeper slab is a hidden slab placed under both the approach slab and the roadway pavement.

Dupont and Allen (2002) conducted a survey on the 50 state highways agencies in the USA. Their study shows from 48 states agencies, which use approach slabs that only 31 states

use sleeper slabs. Of the 31 states, 14 states said the sleeper was effective, 2 states said it was not, while 15 states were not sure.

The design purpose of the sleeper slab is to minimize the possibility of the differential settlement by allowing the approach slab to settle with the embankment, thus preventing the bump at the bridge (Dupont and Allen, 2002). However, the improper design of the sleeper slab geometry may lead to settlement problems as well (Lenke, 2006). In addition, when expansion joints are placed on top of the sleeper slabs, cracking and crushing of the approach slab concrete may occur due to the closure of the expansion joints and dragging of the approach slab (Abu-Hejleh et al., 2006).

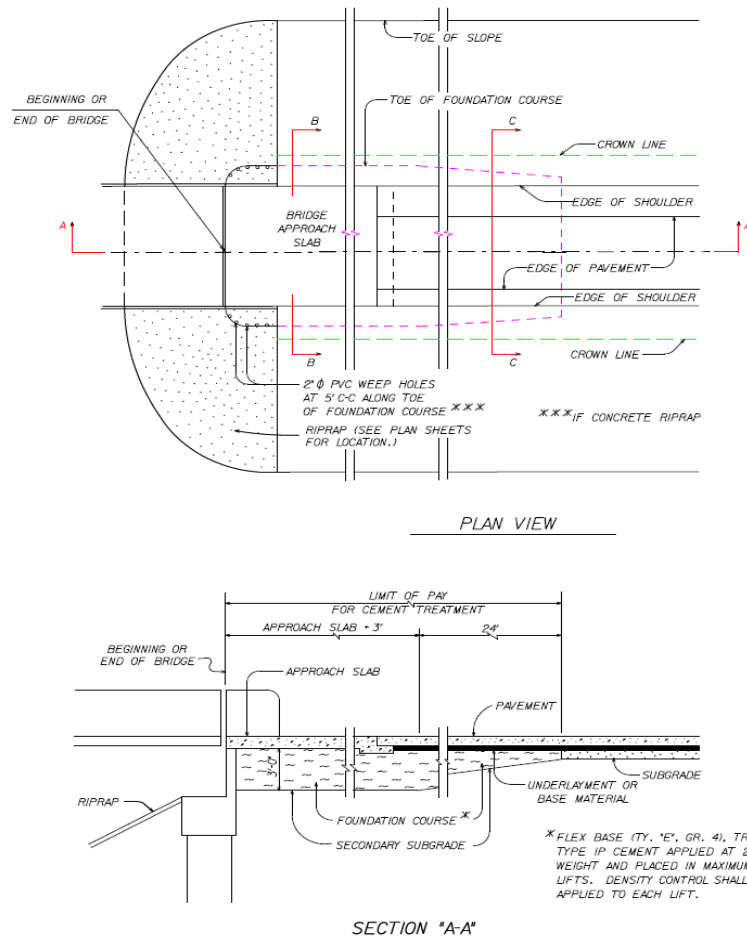


Figure 2.53 Schematic of bridge approach slab arrangement adopted by the Fort Worth District of TXDOT, Texas

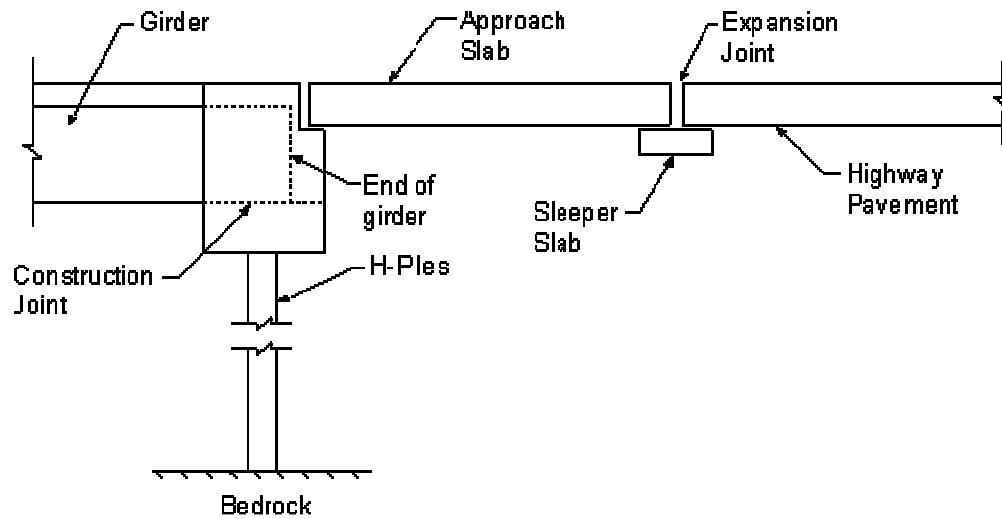


Figure 2.54 Schematic of an Integral Abutment System with a Sleeper Slab

The minimum recommended length of the sleeper slab is 1.5 m. (Seo, 2003). The width of the sleeper slab supporting the approach end of the approach slab should be 5 ft to prevent the bearing failure within the backfill material under the slab (Seo et al., 2002 and Lenke, 2006), while other researchers suggest the use of widths of 3 to 4 ft (Cai et al., 2005, Abu-Hejleh et al., 2006).

Some studies have reported 16 in. thickness sleeper slabs to prevent settlement or the creation of voids beneath the slab (Abu-Hejleh et al., 2000), while other studies recommend the use of thickness of 20 in. (Luna, 2004). Other design considerations of sleeper slabs include placement of drainage material beneath the entire slab and perforated pipes along the sleeper beam to evacuate water infiltrated from expansion joints placed on top of the slab (Luna, 2004, Abu-Hejleh et al., 2006).

Since the sleeper slab is typically supported on the backfill material used in the abutment, similar compaction efforts of the backfill material should be required underneath this slab. Compaction specifications require the maximum density of the fill to be at least 95% of the maximum dry density per AASHTO T-99 (Luna, 2004). Two new supporting systems for the sleeper slab are suggested by Abu-Hejleh et al. (2006). The first system consists of placing higher quality MSE backfill or flowfill under the sleeper slab rather than under the approach

slab. The second supporting system consists of using driven piles to support the sleeper slab and using cheaper backfill material behind the abutments and expansion joint device, typically placed on top of the sleeper slab. In some cases where the settlement problem would be significant and continuous for extended periods, elimination of the approach and sleeper slabs altogether should be considered. As an alternative, full-depth asphalt approach slabs could be used with maintenance overlays as needed (Abu-Hejleh et al., 2006).

2.4.6 Effective Drainage and Erosion Control Methods

According to Mekkawy et al. (2005) and White et al. (2005), insufficient drainage is another problem often attributed to the settlements near the bridge abutments. Water collected on the bridge pavement can flow into the underlying fill materials due to ineffective seals at the joints between the bridge approach slab and the abutments and this infiltrated water can erode the backfill material. The material erosion can cause void development under the bridge abutments, resulting in the eventual settlements of the bridge approach slabs. Hence, the design of bridge approaches has to be incorporated with an efficient drainage system, such as providing drainage inlets at the end of a bridge deck to collect surface water before getting to the approach slab (Abu-Hejleh et al., 2006).

Also, additional surface or internal drainage to keep water off the slopes is also recommended for correcting the superficial erosion of embankments (Wahls, 1990). Keeping the water away from the soil is a simple and a significant factor in reducing the settlement of the soil. Construction costs added to incorporate a good drainage system are not high when compared to the expensive maintenance costs that they might experience during the service life of the bridge (Dupont and Allen, 2002). Hence, all efforts should be made to design the bridges with effective seals and good drainage conditions in and around the bridge structures.

Some of the recommendations reported in the literature to improve drainage conditions include the use of a large diameter surface drain and gutter system in the shoulder of the approach slab and use of a geo-composite vertical drainage system around the embankments,

with both drainage systems having the potential to increase the drainage capacity (White et al., 2005). This study also recommended the use of porous backfill material or limiting the percentage of fine particles in the fill material to reduce material plasticity and enhance drainage properties.

Based on a survey conducted by Hoppe (1999), the allowable percentage of fine material passing the 75-micron (No. 200) sieve in the backfills varied from less than 4% to 20% by different State Agencies. From the same study, it was noted that typical provisions in State Agencies include plastic drainpipes, weep holes in the abutments, and the use of granular, free-draining fill. The use of geosynthetic materials, fabrics and geo-composite drainage panels in the bridge systems was also reported. Other alternatives including the use of a thick layer of tire chips as an elastic zone behind the abutment with a high capacity of drainage was also successfully implemented (White et al., 2005).

Other recommendations including the grading off of the crest to direct runoff away from the back slope and the use of interceptor drains on the back slope are also cited (Wu et al., 2006). It is also recommended to perform periodic maintenance to minimize runoff infiltration and install a combination of granular drain materials, geotextiles or a geo-composite drain along the back and the base of the fill (Wu et al., 2006).

When the MSE structures are used, the drainage systems are recommended to construct in many locations; for example, in the retained soil to intercept any seepage or trapped groundwater, or behind and beneath the wall to interrupt water levels before intersect of the structure (NCHRP, 556). To reduce surface water infiltration into the retained fill and reinforced fill, an impermeable cap and adequate slopes to nearby surface drain pipes or paved ditches with outlets to storm sewers or to natural drains should be provided.

Internal drainage of the reinforced fill can be attained by the use of a free-draining granular material that is free of fines (less than 5% passing the No. 200 sieve). Arrangement should be provided for drainage to the base of the fill to prevent water exiting the wall face and

the embankment (often a granular soil layer) and the foundation soil (usually a cohesive soil layer) (Abu-Hejleh et al., 2006).

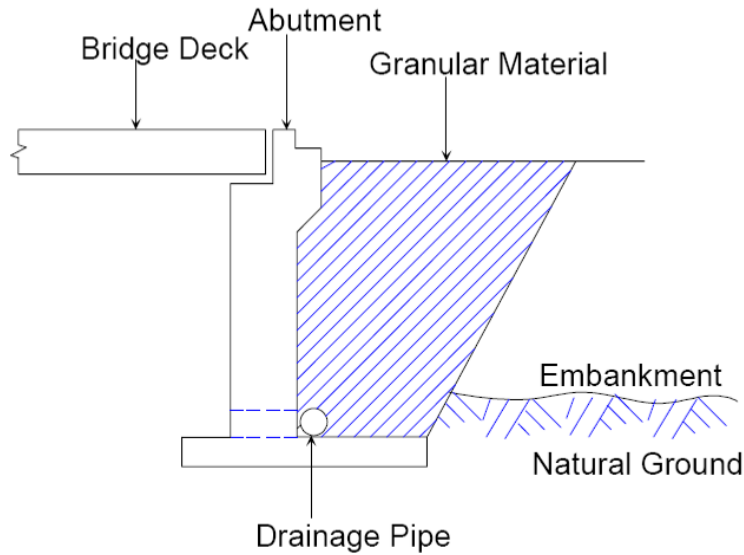


Figure 2.56 Drainage Layer of Granular Material and Collector Pipe

Briaud et al., (1997) encouraged the use of a curb-to-curb design for erosion control and effective drainage of water away from the bridge structure and approach slab system. Figure 2.57a shows a poorly designed approach slab that will allow water into the backfill and embankment materials promoting erosion and weakening of these granular materials. On the contrary, Figure 2.57b shows a system that will prevent infiltration into the soils below the approach slab. Stewart (1985) suggested that the pavement should even be placed as a cantilever system over the wingwall to further mitigate infiltration below the approach slab.

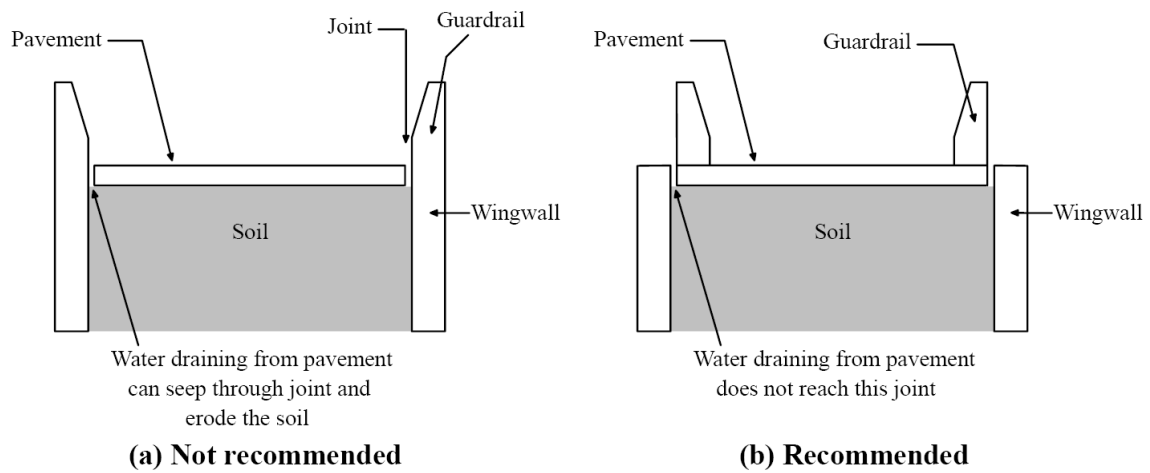


Figure 2.57 Approach Slab Joint Details at Pavement Edge (Briaud et al., 1997)

Figure 2.58 provides an excellent example of good drainage and erosion control on the embankment face underneath the bridge where rip-rap was effectively used to prevent scour on the face which could cause erosion under the approach slab and bridge abutments (Lenke, 2006). In this research, the use of concrete slope protection on the embankment faces and sides and drainage channels were claimed to be successful in mitigating erosion problems and facilitating adequate drainage conditions (see Figure 2.59).



Figure 2.58 Riprap used for Erosion Control (Lenke, 2006)



Figure 2.59 Concrete Slope Protection with Drainage Gutter and Drainage Channel (Lenke, 2006)

White, et al. (2005) performed a review of several drainage designs implemented by various State Agencies to compare different state-of-practices in the United States. The review showed that three main variations of drainage systems were practiced in the US. These are: 1) porous backfill around a perforated drain pipe; 2) geotextiles wrapped around the porous fill; and 3) vertical geo-composite drainage system (Figures 2.60 to 2.62).

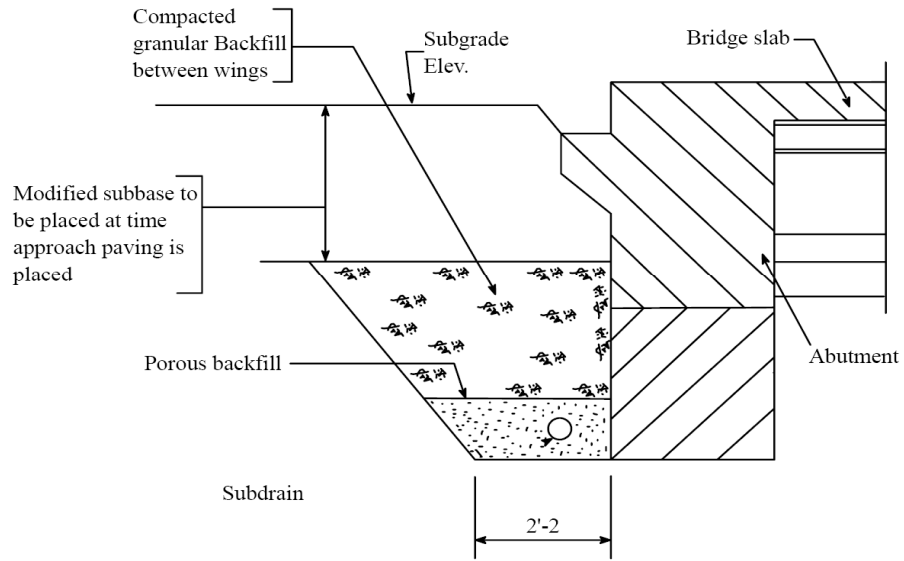


Figure 2.60 Schematic of Porous Fill Surrounding Subdrain (White et al., 2005)

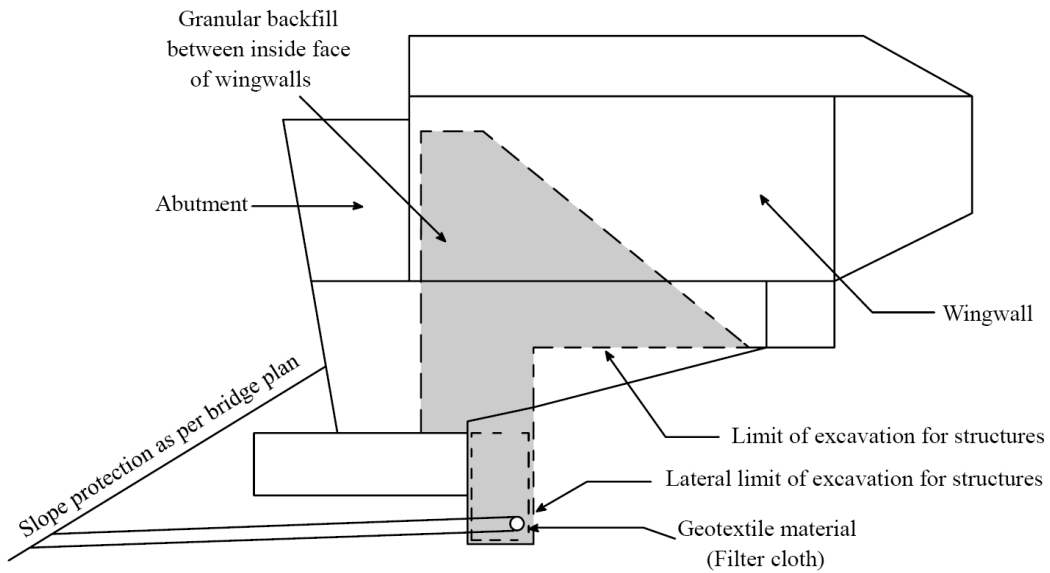


Figure 2.61 Schematic of Granular Backfill Wrapped with Geotextile Filter Material (White et al., 2005)

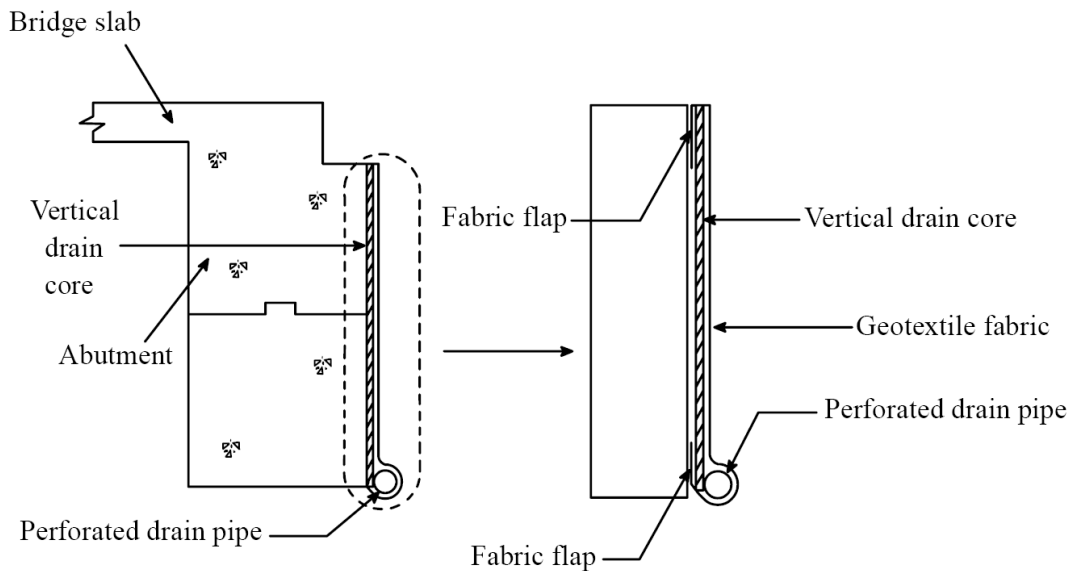


Figure 2.62 Schematic of Geocomposite Vertical drain Wrapped with Filter Fabric (White et al., 2005)

From this study, it was reported that wrapping the porous fill with geotextiles has helped in reducing erosion and fines infiltration. Another interesting observation was from Table 2.7 that reported approximately 14 out of 16 states have used a combination of two or more of these alternatives to increase the drainage efficiency. It was also reported that the Texas practice is predominantly using porous fills and geotextiles as drainage systems (White et al. 2005).

Mekkawy et al. (2005) and White et al. (2005) concluded from a series of large scale laboratory experiments that the porous backfill behind the abutment and/or geocomposite drainage systems would improve the drainage capacity and would reduce the erosion around the abutment, which will mitigate the differential settlements caused by the erosion and void formation of the backfill material.

Table 2.7 Drainage method used by various states (White et al., 2005)

State	Porous Fill	Geotextile	Geocomposite drainage system
Iowa	X	-	-
California	X	X	X
Colorado	-	X	X
Indiana	X	X	-
Louisiana	X	X	X
Missouri	-	X	X
Nebraska	-	X	X
New Jersey	X	X	X
New York	-	-	X
North Carolina	X	X	-
Oklahoma	X	X	-
Oregon	X	X	-
Tennessee	X	X	-
Texas	X	X	-
Washington	X	-	-
Wisconsin	X	X	-

2.5 Maintenance Measures for Distressed Approach Slabs

This subchapter presents several techniques normally used to treat distressed approach slabs. It is estimated that bridge approach maintenance costs are at least \$100 million per year in the United States (Briaud et al, 1997; Nassif et al., 2002). Many states indicate that the best practice to minimize the presence of bridge bumps is to establish up-to-date maintenance activities, by scheduling periodic repair activities in addition to occasional required maintenance (Dupont and Allen, 2002). Depending on the circumstances, maintenance of

distressed approach slabs is comprised of asphalt overlays, slab jacking, and approach slab adjustment or replacement techniques (Dupont and Allen, 2002).

It is also reported that in the case of conventional bridges, much of the cost of maintenance is related to repair of damage at joints, because such joints require periodic cleaning and replacement (Briaud, 1997, Arsoy, 1999). Other times, pavement patching at the ends of the bridge represents most of the maintenance costs. For longer bridges, the pavement patching lengths are longer due to problems experienced by the temperature induced cyclic movements (Hoppe, 1999). However, Arsoy (1999) noted that Integral abutment bridges perform well with fewer maintenance problems than conventional bridges.

Also, a periodic cleanout and maintenance schedule is required for all drainage structures on the bridge and bridge approach system to insure proper removal of water away from the structure and to minimize runoff infiltration into underlying fill layers (Lenke, 2006). Most frequently, maintenance of drainage structures and joints is lacking and must be improved in order to take full advantage of these design features (Lenke, 2006, Wu et al., 2006).

Lenke (2006) presented his study showing many cases of poor maintenance at the expansion joints between the bridge deck, approach slab, and approach pavement, and drainage systems, resulting in many bridge replacement and rehabilitation costs. He suggested that to prevent stress buildup at the expansion joints between the bridge structure, the approach slab and the pavement system, a good maintenance by cleaning and replacement (when necessary) is required. Such stresses can not only cause damage to the deck and the abutment, but can also cause distortions of the approach slab.

Lenke (2006) also identified another maintenance issue resulting from Alkali-Silica Reactivity (ASR) problems. The stresses caused by ASR expansion can lead to severe damage at the joints connecting the bridge deck to the approach slab and the approach slab to the preceding concrete pavement. These ASR expansion stresses can cause spalling and

resultant crack widening, which regularly requires joint filling with bituminous materials work (Lenke, 2006).

White et al. (2005) also conducted a comprehensive study in a case of lack of maintenance of drainage structures, such as clogged or blocked drains, animal interaction, and deterioration of joint fillers, gutters and channels. The study showed that due to the lack of maintenance many problems about maintenance occurred, resulting in numerous and costly repair operations. White et al. (2005) also pointed out some potential causes of bridge approach settlement discovered during the maintenance activities. For example, they mentioned that the loose and not properly compacted backfill materials can cause poorly performing approach slabs. Coring operations revealed that voids are highest near the bridge abutment and decreased with distance with void sizes ranging from 0.5 to 12 in. Snake cameras used at sub-drain outlets demonstrated that most of the investigated subdrains were not functioning properly. The subdrains were either dry with no evidence of water or blocked with soil fines and debris or had collapsed. Some of these problems are attributed to erosion induced movements in the fill material from moisture infiltration. This signifies the need for constant maintenance of joints and drains so that infiltration into the soil layers will be low. Along with the maintenance, reconstruction or rehabilitation of distressed approach slabs are very necessary.

Several soil stabilization techniques were found in the literature to stabilize the fill under the approach slab. These techniques are intended to smooth the approaches by raising the sleeper slab and approaches, especially if application of an asphalt overlay is not feasible (Abu-Hejleh et al., 2006). The most important techniques are pressure grouting under the slab, slab-jacking or mud-jacking technique, the Urethane method, and compaction or high pressure grouting. Most of these techniques are often used as remedial measures after problems are detected. However, the same could be applied even in new bridge constructions. A brief overview of these methods is presented below.

2.5.1 Replacement Method

Highly deteriorated approach slabs due to the formation of a bump are mostly replaced with the new approach slabs. This process is the most expensive and time taking process as the construction process results in frequent closure of lanes, traffic congestion, etc. A new internal research project has been initiated by the California Department of Transportation to examine different replacement alternatives for deteriorated approach slabs. In this project, prefabricated Fiber Reinforced Polymer (FRP) decks as well as FRP gridforms and rebars were investigated as replacement options. Full scale approach slabs were tested under simulated wheel loads. Performance of the approach slabs were also examined under simulated washout conditions. Figure 2.63 shows the test schematic.



Figure 2.63 Simulated approach slab deflection due to washout by UC Davis research team (<http://cee.engr.ucdavis.edu/faculty/chai/Research/ApproachSlab/ApproachSlab.html>)

2.5.2 Mud/Slab Jacking

Mud/Slab jacking is a quick and economical technique of raising a settled slab section to a desired elevation by pressure injecting of cement grout or mud-cement mixtures under the slabs (EM 1110-2-3506, 20 Jan 84). According to EM 1110-2-3506, slab jacking is used to

improve the riding qualities of the surface of the pavement, prevent impact loading over the irregularities by fast-moving traffic, correct faulty drainage, prevent pumping at transverse joints, lift or level other structures, and prevent additional settlement.

In this method, the mud grout is prepared using the topsoil which is free from roots, rocks and debris mixed with cement and enough water to produce a thick grout. This grout is injected to fill the void spaces underneath the approach slab through grout holes made through the approach slabs (Bowders et al, 2002). The injection is performed in a systematic manner to avoid cracks on the approach slab as shown in Figure 2.64. Precautionary measures need to be taken near to side retaining walls and abutment walls (Luna et al., 2004).

Even though this technique has been successfully adopted by several states including Kentucky, Missouri, Minnesota, North Dakota, Oklahoma, Oregon, and Texas for lifting the settled approach slabs, the mud/slab jacking can be quite expensive. Mud jacking may also cause drainage systems next to the abutment to become clogged, and is difficult sometimes to control the placement of the material (Dupont and Allen, 2002). Other difficulties including limited spread of grout into voids, large access holes which must be filled and lack of sufficient procedural process made this technique as uneconomical (Soltesz, 2002). Abu al-Eis and LaBarca, (2007) reported that the cost of this technique was between \$40 and \$60 per one square yard of pavement used based on two test sections constructed in Columbia and Dane counties in Wisconsin.

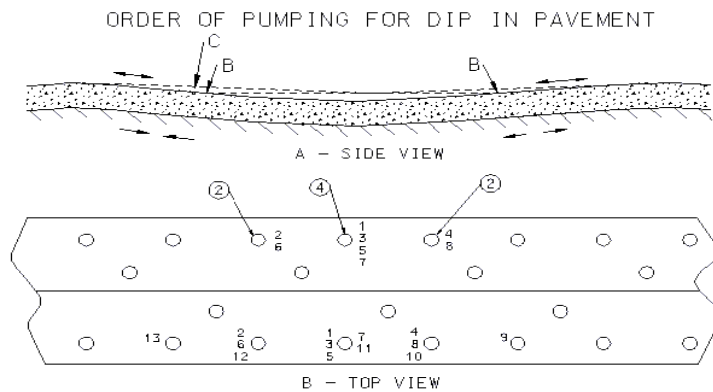


Figure 2.64 Mud-jacking injection sequences (MoDOT, EPC)

2.5.3 Grouting

2.5.3.1 Pressure grouting under the slab

The presence of voids beneath the approach slab can lead to instability, cracking, sinking and pounding problems (Abu-Hejleh et al., 2006). In order to mitigate the problem, pressure grouting is commonly used for bridge approach maintenance practice as a preventive measure (White et al., 2005 and 2007). Pressure grouting under the slab is used to fill the voids beneath the approach slab through injection of flowable grout, without raising the slab (Abu-Hejleh et al., 2006).

According to White et al. (2007), undersealing the approach slab by pressure grouting normally has two operations within the first year after completion of approach pavement construction. The first operation is done within the first 2–6 months, while the second one is employed within 6 months after the first undersealing. The grout mix design consists of Type 1 Portland cement and Class C fly ash at a ratio of 1:3. Water is also added in the grouting material to achieve the specified fluidity (Buss, 1989). Moreover, in order to avoid the lifting of the approach slab, grout injection pressures are kept to less than 35 kPa (White et al., 2007).

Abu-Hejleh et al. (2006) stated that the construction techniques for this method are to drill 1-7/8" holes through the concrete or asphalt approach slabs using a rectangular spacing as shown in Figure 2.65. The depth is determined by the ease of driving the stinger or outlet tube, which is pounded into the hole (Abu-Hejleh et al., 2006). A fence post pounder is used to hammer the stinger and extension pieces into the soil (Abu-Hejleh et al., 2006). As the stinger is pounded down, the operator can determine if the soil is loose or soft and if there are voids under the slab.

Although grouting under the approach slab is commonly used for bridge approach settlement as a mitigation method, White et al. (2007) stated that the grouting is not a long term solution for this problem. The grouting does not prevent further settlement or loss of backfill material due to erosion (White et al., 2005 and 2007).

2.5.3.2 Compaction or High Pressure Grouting

Compaction grouting is a method for improving soil by densifying loose and liquefaction soils and resulting in increasing the soil strength (Miller and Roykroft, 2004). The compaction grouting is a physical process, involving pressure-displacement of soils with stiff, low-mobility sand-cement grout (Strauss et al., 2004).

According to the ASCE Grouting Committee (1980), the grout generally does not enter the soil pores but remains as a homogenous mass that gives controlled displacement to compact loose soils, gives controlled displacement for lifting of structures, or both. The FHWA (1998) also stated that apart from soil densification, the compaction grouting is also employed to lift and level the approach slab and adjacent roadways.

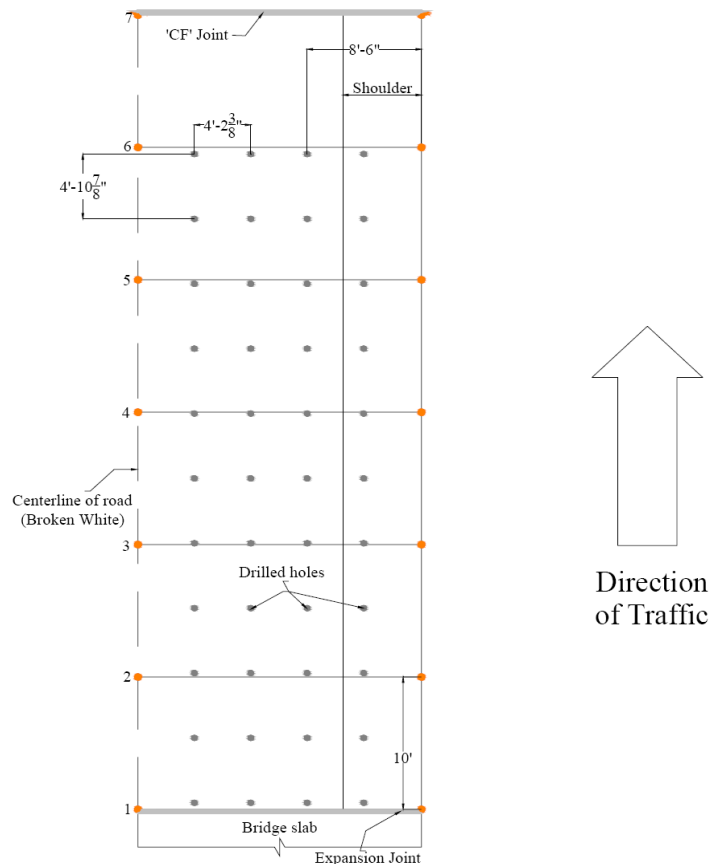


Figure 2.65 Location of holes drilled on an approach slab (White et al., 2005)

The compaction grouting can be used to stabilize both shallow and deep seated soft layers (Abu-Hejleh et al., 2006). Section 211 of the CDOT Standard Specifications describes the grouting must be low slump and a low mobility grout with a high internal friction angle. When the technique is used in weak or loose soils, the grout typically forms a coherent “bulb” at the tip of the injection pipe; thus, the surrounding soil is compacted and/or densified (Miller and Roykroft, 2004). For relatively free draining soils including gravel, sands, and coarse silts the method has proven to be effective (Abu-Hejleh et al., 2006).

2.5.3.3 Urethane Injection Technique

The Urethane injection technique was first developed in 1975 in Finland to lift and under seal concrete pavements and subsequently adopted in several US States in lifting concrete pavements (Abu al-Eis and LaBarca, 2007). In this process, a resin manufactured from high density polyurethane is injected through grout holes (5/8 inch diameter) made through the approach slab to lift, fill the voids and to under seal the slab (Abu al-Eis and LaBarca, 2007). The injected resin will gain 90% of its maximum compressive strength (minimum compressive strength is 40 psi) within 15 minutes. Once the voids are filled, the grout holes are filled with inexpansive grout material. Elevation levels are taken before and after the process to ensure the required lifting is achieved (Abu al-Eis and LaBarca, 2007).

As reported by Abu al-Eis and LaBarca, (2007), the Louisiana Department of Transportation successfully adopted this technique for two different bridge approaches and observed that the international roughness index (IRI) values were reduced by 33% to 57% after monitoring for four years. This method involves the precise liquid injection of high-density polyurethane plastic through small (5/8") holes drilled in the sagging concrete slab (Abu al-Eis and LaBarca, 2007). Once it is applied, the material expands to lift and stabilize the slab, while filling voids in the underlying soil and under sealing the existing concrete (Concrete Stabilize Technology Inc., <http://www.stableconcrete.com/uretek.html>). Based on the manufacturer

provided information, this technology is simple and rapid. It can lead to a permanent solution and also can resist erosion and compression over a time period.

Brewer et al., (1994) first evaluated the Urethane injection technique to raise bridge approach slabs in Oklahoma. They reported that three test slabs out of six were cracked during or after the injection and in one case, the PCC slab broke in half during the injection. The Michigan Department of Transportation reported that this technique provided temporary increase in base stability and improvement in ride quality for one year (Opland and Barnhart, 1995). Soltesz (2002) noticed that the Urethane treatment was successful even after two years where the injection holes are properly sealed. The Oregon Department of Transportation researchers reported that the Urethane material was able to penetrate holes with diameters as small as 1/8 in. and which was added advantage of this technique to fill the minor pores of the subbase and lift the pavement slabs (Soltesz, 2002).

Abu al-Eis and LaBarca, (2007) reported that the cost of this technique was between \$6 to \$7 per pound of foam used which was calculated based on two test sections constructed in Columbia and Dane counties in Wisconsin. They summarized the cost comparison of this technique with other slab lifting methods (as shown in Table 2.8) and concluded that this technique is expensive when compared to other methods if calculated based on direct costs. They also reported that this technique is very fast and can open the lanes for traffic immediately after the treatment. The amount of urethane resin used in each project is also questionable as this quantity is directly used in the cost analysis. Considering this fact, TXDOT amended its Special Specification 3043-001 which requires a Special Provision for determining the quantity of polymer resin used for "Raising and Undersealing Concrete Slabs". Regarding the Special Specification 3043-001, the quantity of the resin utilized will be calculated by one of the following methods:

1. Payment will be made according to the actual quantity of polymer resin used in the work by weighing each holding tank with components by certified scales before and after each day's work.
2. Payment will be made according to the actual quantity of polymer resin used in the work by determining the weight of material placed by measuring the depth of polymer resin in the holding tanks before and after each day's work. A Professional Engineer and a site engineer must approve the calculation method which is based on the certified measured volume of each tank and the unit weight of each component to determine the weight of resins used in the work.

Table 2.8 Cost Comparison for Four Slab Faulting Repair Methods

Location	Method	Total Cost	Cost per yd ²	Days to Complete
I-30 (80 yd ²)	URETEK	\$19,440	\$243	0.75
	Slab Replacement	\$34,000	\$425	3
	HMA Overlay	\$3,630	\$45	1
	Mud-jacking	\$3,000	\$38	1
USH 14 (53.4 yd ²)	URETEK	\$6,260	\$117	0.5
	Slab Replacement	\$22,670	\$425	3
	HMA Overlay	\$3,375	\$63	1
	Mud-jacking	\$3,000	\$56	1

Several Districts in Texas use this method as a remediation method and based on the present research contacts, these methods are deemed effective. Researchers visited two bridge approach slab repair works recently initiated in Hill County, Texas and another completed several years back on several highways in and around Houston, Texas. Both visits were made in late February, 2008.

Figure 2.66 shows the schematic and photographic view of the bridge site with the void developed under the approach slab. The cause of the problem was identified as the erosion of the granular backfill material under the approach slab.

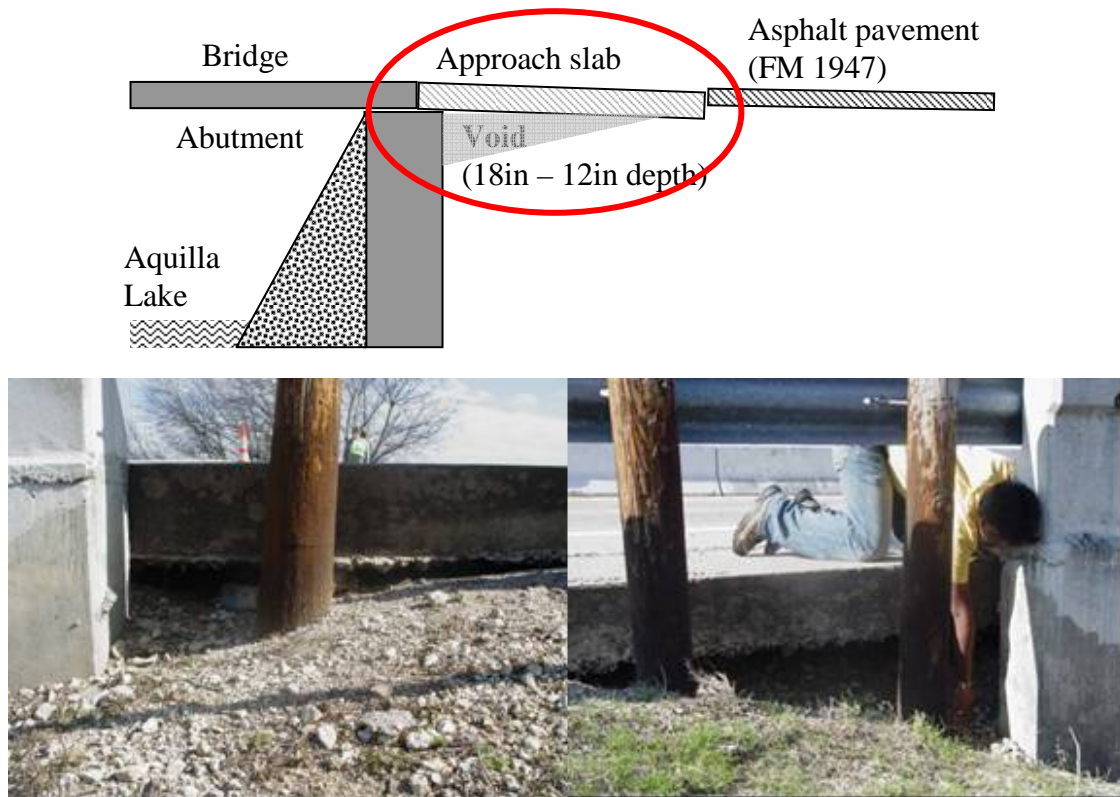


Figure 2.66 Schematic of the approach slab with developed void under the bridge at FM 1947 Hill County, Texas

Figure 2.67 depicts the position of the approach slab during and after the injection process. During and immediately after the injection process, researchers observed a few minor hairline cracks on the approach slab as shown in Figure 2.68. The minor cracks on the surface of the approach slab during this injection operation are relatively common and they will not lead to further distress of the approach slab. The post performance of this method is very crucial to address the expansion of these hairline cracks and movements of repaired approach slabs. A simple field monitoring study including elevation surveys and visual inspection of these minor cracks would reveal the effectiveness of this technique.



Figure 2.67 Position of approach slab during and after the Urethane injection process



Figure 2.68 Hairline crack observed on the approach slab during the urethane injection

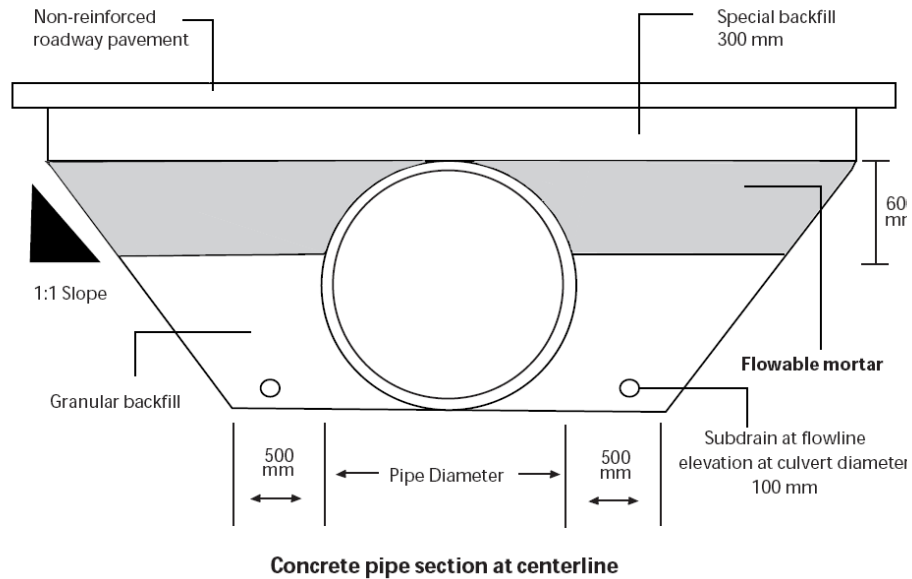
As per the discussions with TxDOT engineers in Houston, the process was quite effective. Several Houston sites that were visited were repaired utilizing this injection method ten years ago and they are still functioning adequately. The work reported in the Houston District was instrumental in the development of the TxDOT Special Specification for the use of the urethane injection method for lifting the distressed approach slabs.

2.5.3.4 Flowable fill

Flowable fill or controlled low-strength material is defined by ACI Committee 229 as a self-compacting, cementitious material used primarily as a backfill in lieu of compacted fill. The flowable fill has other common names, such as, unshrinkable fill, controlled density fill, flowable mortar, flowable fill, plastic soil-cement and soil-cement slurry (Du et al., 2006). This controlled low-strength filling material is made of cement, fly ash, water, sand, and typically an air-entraining admixture (NCHRP, 597). A significant requisite property of flowable fill is the self-leveling ability, which allows it to flow; no compaction is needed to fill voids and hard-to-reach zones (Abu-Hejleh et al., 2006). Therefore, the flowable fill is commonly used in the backfill applications, utility bedding, void fill and bridge approaches (Du et al., 2006).

A primary purpose of using flowable fill is as a backfill behind the abutment. CDOT has used the flowable fill backfill behind the abutment wall in an effort to reduce the approach settlements since 1992 (Abu-Hejleh et al., 2006). The other new applications for the flowable fill are for use as a subbase under bridge approaches and a repair work of the approaches (Du et al., 2006). Historically, the application of using flowable fill as a subbase was first employed in Ohio by ODOT (Brewer, 1992).

In Iowa, the flowable fill is a favorable backfill used as a placement under the existing bridges, around or within box culverts or culvert pipes, and in open trenches (Smadi, 2001). Smadi (2001) also cited that the advantages of flowable mortar are not only due to its fluidity, but also due to its durability, requiring less frequent maintenance. Moreover, the flowable mortar is also easily excavated. Therefore, the maintenance works, if required, can be done effortlessly (Smadi, 2001). Figure 2.69 shows details of flowable mortar used under a roadway pavement.



Note: Illustration is not to scale.

Figure 2.69 The flowable mortar used under a roadway pavement (Smadi, 2001)

In Texas, the flowable fill was used for the first time for repairing severe settlements of bridge approaches at the intersection of I-35 and O'Conner Drive in San Antonio in 2002 by TxDOT (NCHRP, 597; Du et al., 2006). For this practice, TxDOT used a specialized mixture using flowable fill, which consisted of sand, flyash and water; no cement (Williammee, 2008). The compressive strength of cored samples indicated that the long-term strength and rigidity of the flowable fill were strong enough to serve this purpose (NCHRP, 597). After the mixture proportions were adjusted to have adequate flowability for the application, the flowable fill has shown a great success for repairing the approaches (Du et al., 2006 and Williammee, 2008). Recently, the flowable fill was used in the Fort Worth District in place of a flexible base beneath the approach slab. The 3 ft. deep flex base is prepared with Type 1 cement (2.4% by weight) as a base material as shown in Figure 2.70.

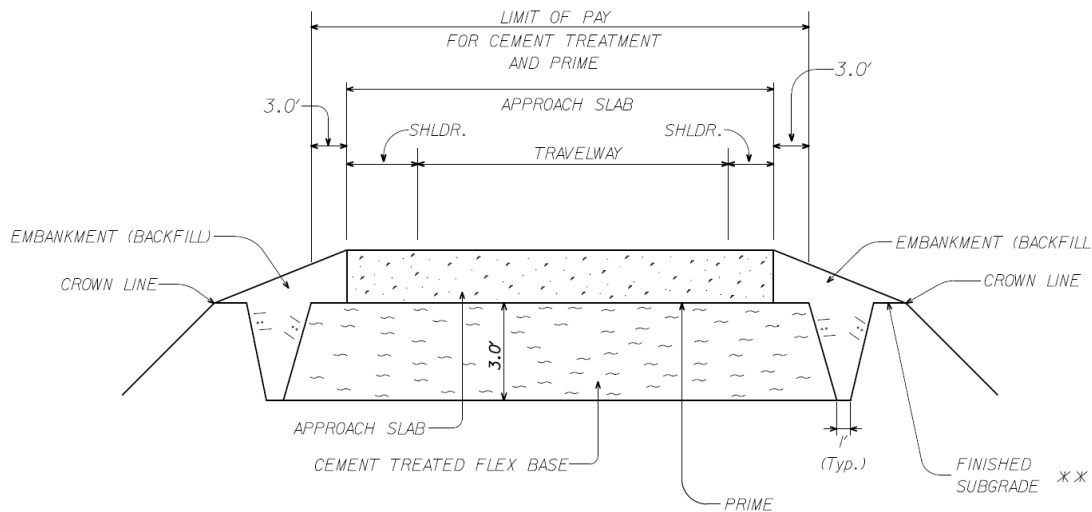


Figure 2.70 The flowable fill used as a base material (Du, 2008)

2.5.4 Other Methods

Several other techniques are also available to mitigate the settlement problem caused in the approach slab area and these techniques are discussed in the following.

2.5.4.1 Precambering

If the approach pavement settlement cannot be controlled economically, a pre-cambered roadway approach may be applied (Tadros and Benak, 1989). Hoppe (1999) recommended implementing pre-cambering of bridge approaches for up to a 1/125 longitudinal gradient. The pre-cambering is used to accommodate the differential settlement that will inevitably occur between a structure constructed on deep foundations and adjoining earthworks.

Briaud et al. (1997) recommended pre-cambering with gradient values of less than 1/200 of the approach slab length to compensate for the anticipated post-construction settlements. The pre-cambered design utilizes a paving notch that supports a concrete slab. The notch must be effectively hinged, which allows the concrete slab moving radially (see Figure 2.71). The flexible pavement over the slab will absorb some movement below it but not to a great extent (Briaud et al, 1997). The pre-cambered approach system also requires an accurate assessment of settlement potential (if possible). The pre-cambered approach design

2.5.4.3 Expanded Polystyrene (EPS) Geofoam

Expanded Polystyrene (EPS) Geofoam is a lightweight material made of rigid foam plastic that has been used as fill material around the world for more than 30 years. This material is approximately 100 times lighter than conventional soils and at least 20 to 30 times lighter than any other lightweight fill alternatives. The added advantages of EPS Geofoam including reduced loads on underlying subgrade, increased construction speed, and reduced lateral stresses on retaining structures has increased the adoptability of this material to many highway construction projects. More than 20 State DOTs including Minnesota, New York, Massachusetts, and Utah adopted the EPS Geofoam to mitigate the differential settlement at the bridge abutments, slope stability, alternate construction on fill for approach embankments and reported high success in terms of ease and speed in construction, and reduced total project costs.

Lightweight EPS Geofoam was used as an alternate fill material at Kaneohe Interchange in Oahu, Hawaii while encountering a 6m thick layer of very soft organic soil during construction. 17,000 m³ of EPS Geofoam was used to support a 21 m high embankment construction (Mimura and Kimura, 1995). They reported the efficiency of the material in reducing the pre- and post-construction settlements. Figure 2.72 shows the construction of the embankment with the EPS Geofoam.



Figure 2.72 Emergency Ramp and High Embankment constructed using the EPS Geofoam at Kaneohe interchange in Oahu, Hawaii

2.5 Summary

This chapter presented a thorough review of the literature review on settlement at the bridge approach. The definition of the settlement at the bridge approach problem is firstly presented following with the magnitude of the bump tolerance. Afterward, major mechanisms causing the bump problem are introduced. The primary sources of the problem broadly divided into four categories are material properties of foundation and embankment, design criteria for bridge foundation, abutment and deck, construction supervision of the structures, and maintenance criteria. (Hopkins, 1969, 1985; Stewart, 1985; Greimann et al., 1987; Laguros et al., 1990; Kramer and Sajer, 1991; Ha et al., 2002; Jayawikrama et al., 2005; White et al., 2005, 2007).

Major focus of this chapter was given to several techniques used to mitigate the bump problem, which was presented into two main sections; the techniques for new bridge construction, and the measures for distressed approach slabs. The techniques for new bridge construction can be divided into various groups such as improvement of foundation soil, improvement of backfill material, design of bridge foundation, design of approach slab, and effective drainage and erosion control methods. Several techniques fallen into these groups can be listed; for example, Excavation and replacement, Preloading and surcharge, Dynamic compaction, Stone and Lime Columns, Geopiers, Concrete Injected Columns, Deep Soil Mixing Columns, Geotextiles/Geogrids, Geocells and etc.

The maintenance measures for distressed approach slabs are normally used as remedial measures after problems are detected. The most important techniques fallen into this category are pressure grouting under the slab, slab-jacking or mud-jacking technique, the Urethane method, and compaction or high pressure grouting. It can be noted that many of these measures could be also applied for improvement of backfill material in new bridge constructions.

CHAPTER 3

SELECTION OF SETTLEMENT MITIGATION METHODS

3.1 Introduction and Dissertation Research Objective

From a comprehensive study presented in Chapter 2 resulting in many techniques are proven to be viable to mitigate the settlement at the bridge approach problem. Some techniques presented in the literature reviews are feasible to mitigate the problem, but not practical to study in this research. The main objective of this dissertation research is to evaluate two methods that can be used to control approach slab settlements in the real field conditions. Therefore, in this chapter, an attempt is made to select two methods to mitigate settlements underneath the approach slabs. Selection process is done by performing the following two tasks.

In the first task, a survey questionnaire was distributed to all 25 Districts to collect each TxDOT Districts' practices with respect to this approach settlement problem. The results from the survey are very valuable to understanding the problems encountered and the solutions used to minimize the bumps at the end of the bridges.

In the second task, a ranking analysis of viable techniques was done by using four criteria including 'Technique Feasibility', 'Construction Requirements', 'Cost Considerations' and 'Overall Performance'. After each mitigation method has been considered and analyzed according to the aforementioned criteria, the mitigation techniques were ranked, and two of the recommended methods were considered for the evaluation in this research.

3.2 TxDOT Districts' Surveys

As part of this survey task, a survey of all the Districts in the Texas Department of Transportation was performed to collect and understand the problems encountered and the solutions used to minimize the bumps at the end of the bridges.

The researchers distributed a survey questionnaire to all 25 Districts and a total of 16 District responses were received. In a few cases, responses from different engineers from the same District were received. All these results were tabulated and summarized as followings:

a) *Most Districts have encountered bridge approach settlement/heaving problems.*

As shown in Figure 3.1, it can be seen that 17 out of 18 Districts (94%) have encountered the bridge approach settlement. Among the 17 Districts, 6 Districts (33%) have experienced both settlement and heaving problems, while 11 Districts (61%) have only encountered the bridge approach settlement. The Odessa District reported that they have no problems either with bridge approach settlement or heaving.

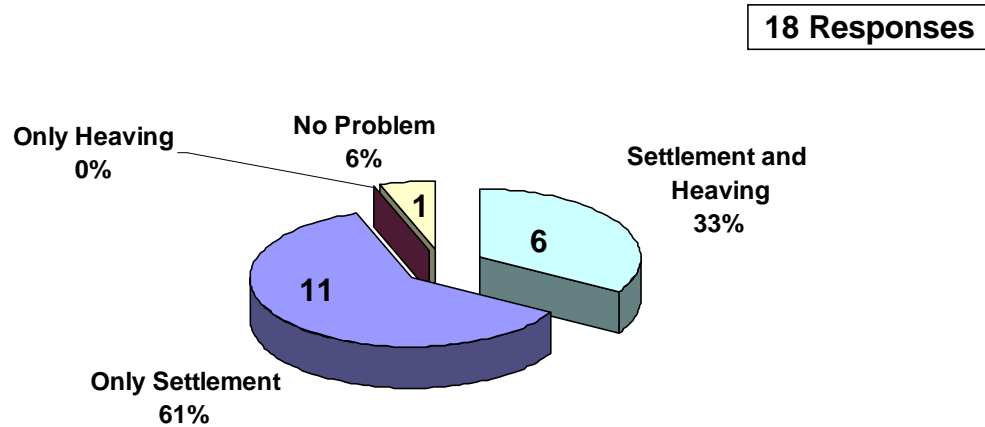


Figure 3.1 Number of districts that encountered bridge approach settlement/ heaving

b) *Majority of the Districts noted this problem from visual observations to identify the bump problem in the field.*

Figure 3.2 presents further responses from 17 Districts, who noted the bridge approach settlement/heaving. These responses related to the procedures followed for

identifying the heave/settlement problem at the bridge approaches. All of 17 responded Districts noted this problem from visual observations. Some other forms of identification of this problem were through evaluation of rideability and from the receipt of public complaints as mentioned by 15 and 10 Districts respectively. Only two (2) Districts have reported that they have used Rideability (International Roughness Index) measurements whereas three (3) other Districts have noted that they used other methods including notification from Maintenance Offices to identify the problem.

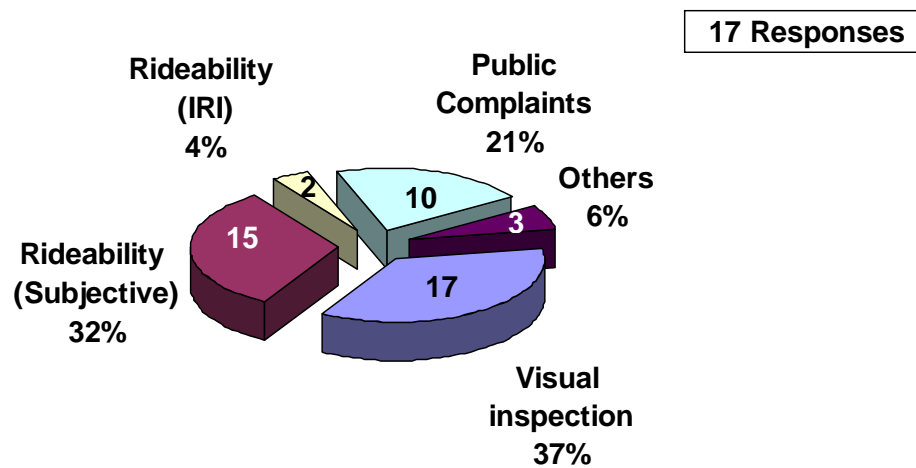


Figure 3.2 Procedure to identify the problem in the field

c) *Minority of Districts conducted any forensic examinations on the distressed approaches to identify potential cause(s) of the problem.*

For the question related to whether a District has conducted any forensic examinations on the distressed approaches to identify potential cause(s) of the problem, most of Districts (53%) reported in the negative (Figure 3.3).

17 Responses

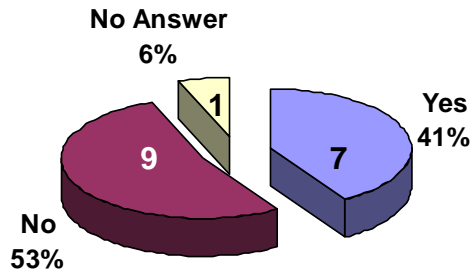


Figure 3.3 Number of Districts that conducted any forensic examinations on the distressed approaches to identify potential cause(s) of the problem

d) *The compaction of the fill was considered as a major factor contributing to the approach settlements in the District*

Figure 3.4 shows various factors that the Districts attributed to the settlement or heaving problem. It should be noted that the Districts were asked to select more than one response. As a result, the total responses do not total seventeen. The following summarizes each of the factors and the number of responses received:

- Natural subgrade: 6 responses
- Construction practices: 13 responses
- Drainage and Soil erosion: 12 responses
- Void formation: 10 responses
- Compaction of Fill: 15 responses
- Others: 3 responses mentioned poor design in old practices and sulfate problems.

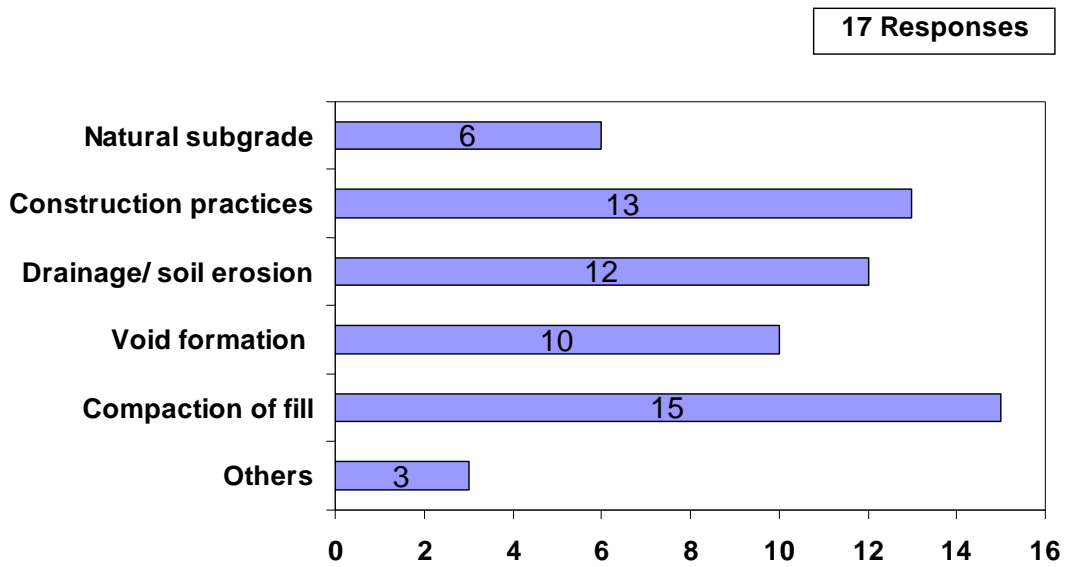


Figure 3.4 Factors attributed to the approach settlement problems

e) *Geotechnical investigations on embankment fill and foundation subgrade material are normally performed by Districts.*

Fifty nine percent (59%) of the respondent Districts noted that they typically perform geotechnical investigations on fill and foundation subgrades (Figure 3.5).

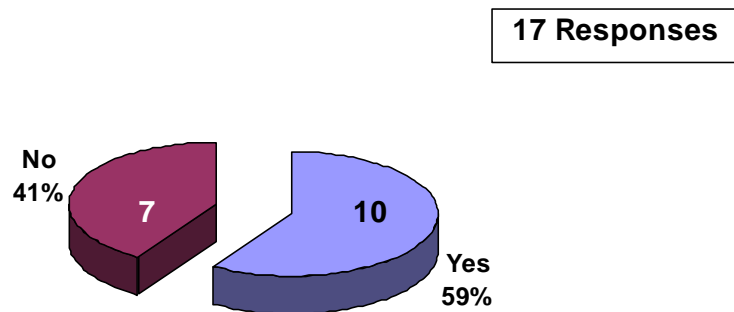


Figure 3.5 Number of Districts that perform a geotechnical investigation on embankment fill and foundation subgrade material

f) *Various PI specifications are used in the selection of embankment fill material by the Districts*

Figure 3.6 shows various PI specifications listed by the Districts that they followed in the selection of embankment fill material. As per Figure 3.6, the maximum PI of the fill material used by select Districts was around 40 while most of them required it to be less than 25.

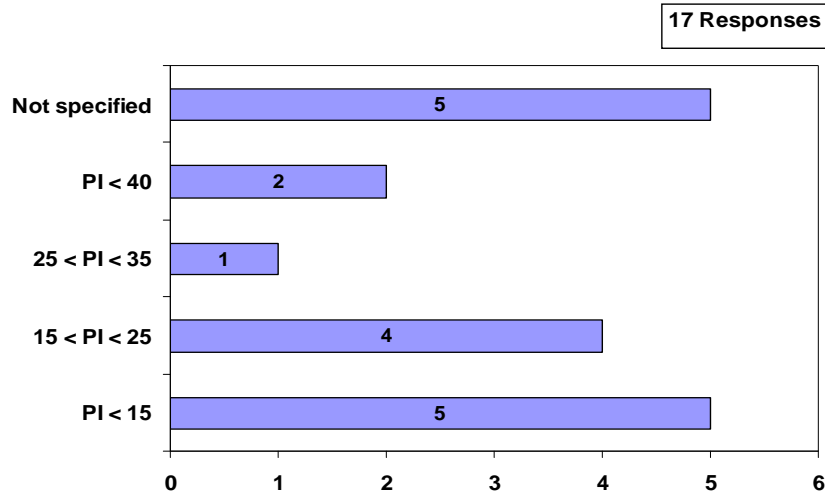


Figure 3.6 PI value required for embankment material

g) *The Nuclear Gauge are normally used to perform Quality Assessment (QA) on compacted fill material*

Figure 3.7 presents Districts' responses related to Quality Assessment (QA) studies performed on compacted fill material. Figure 3.7 results show that 15 out of the 17 Districts (88%) noted that they have used the Nuclear Gauge for compaction Quality Assessment (QA) studies. Seven (7) Districts used sampling and laboratory testing, while only one (1) District used the dynamic cone penetrometer (DCP) for the same purpose.

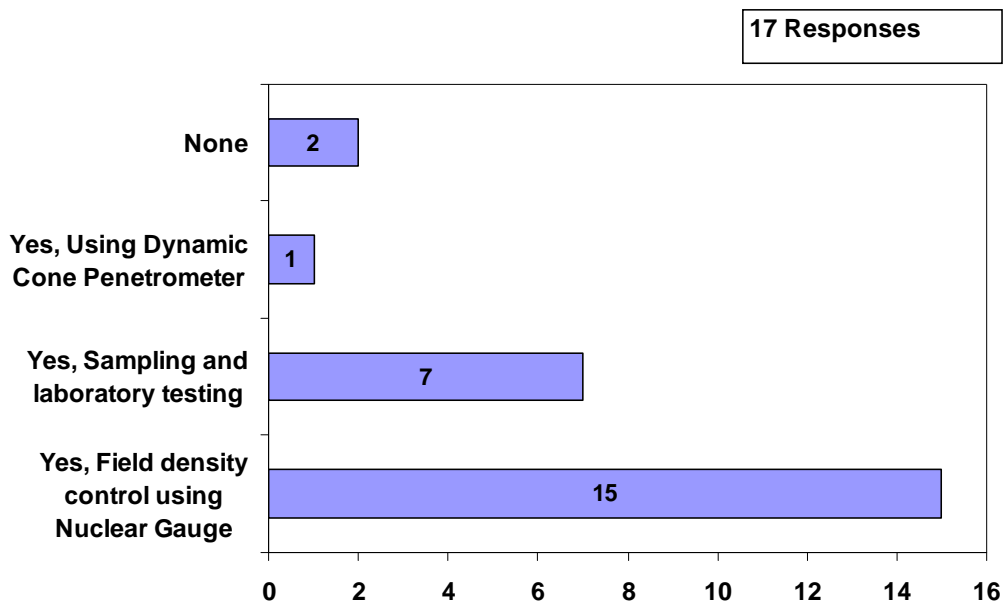


Figure 3.7 Number of Districts conducting Quality Assessment (QA) studies on compacted fill material

h) The level-up or milling of the approach slab is a frequently used maintenance measure by the majority of the TxDOT Districts

Figure 3.8 lists various remediation methods used by the Districts to repair the heave/bumps. Survey results revealed that the level-up or milling of the approach slab is a frequently used maintenance measure by the majority of the TxDOT Districts (17 out of 18 respondents, 94%). With respect to its performance, only 3 Districts noted that this method is working well, 8 Districts as good and 6 Districts as fair. Use of Urethane injection was the second choice by the Districts as ten Districts (55%) have selected this as their remedial measure. With respect to its performance, Districts rated this technique as a very well (2 Districts), good (2 Districts) and well (2 Districts), while 4 Districts rated this method as fair. Other remedial measures include reconstruction of the approach slab, treatment of the subgrade, chemical treatment of the backfill, and the installation of effective drainage and reinforced backfill material. Performance rating of these methods is listed in the same figure.

Two other Districts responded that they have employed other methods such as pressure grouting and cement stabilized sand.

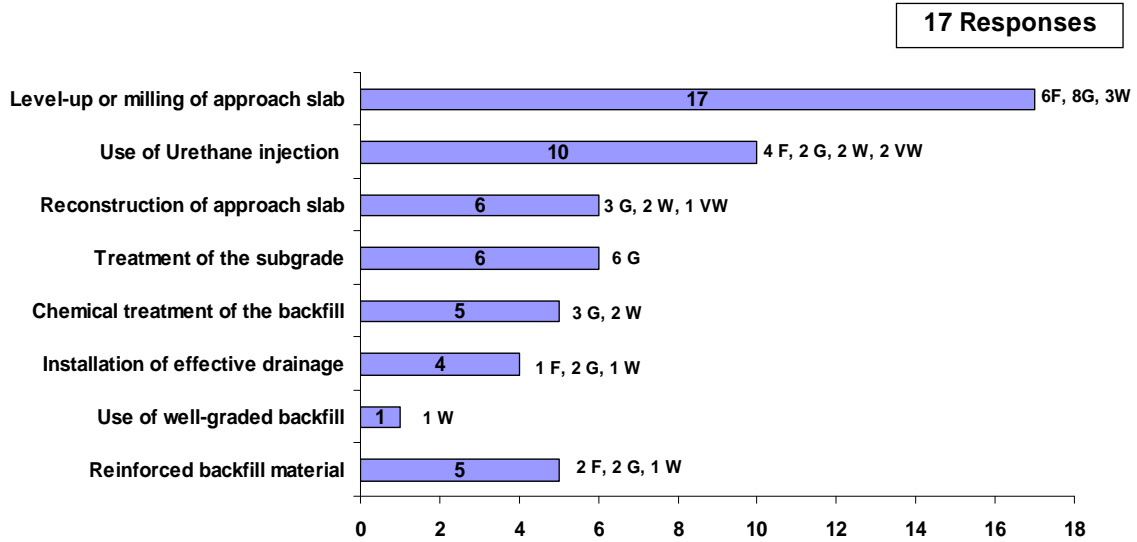


Figure 3.8 Remedial/maintenance measures taken in responded districts and its performance (Note: VW – Very Well; W – Well; G – Good; F – Fair)

i) *Most of the Districts recommend controlling the PI value for fill material used for embankments.*

Table 3.1 gives the information that controlling the PI value is the most recommended method given by the Districts in this survey, either by using chemical treatment in the subgrade and backfill or by using density control compaction. The other recommendations are using rock embankment under the approach slab, select fill material, using 2 sacks of concrete at approach and backwall and even quality control during embankment construction.

j) *Turf growth is typically implemented as a remedial method to control the erosion/slope failure problems.*

Figure 3.9 shows that 5 out of the 17 Districts (30%) responding have employed Turf growth and Geosynthetics methods to control the erosion/slope failure problems, while 5 other Districts have implemented only Geosynthetics to manage the problem. Six (6) Districts have

done nothing and some Districts have chosen other methods, such as, rock riprap, flatten the slope, flexible reinforcement, improve drainage, water intrusion and erosion control. Nevertheless, none of 17 Districts has chosen the baling method to control the problem.

Table 3.1 Recommendations for fill material used for embankments

District	Recommendations for fill material used for embankments
Abilene	PI \leq 15, or lime treat to reduce PI \leq 15
Austin	<ol style="list-style-type: none"> 1. Use rock embankment under the approach slabs to prevent settlement issues with success. 2. PI requirements to insure non-plastic materials.
Brownwood	<ol style="list-style-type: none"> 1. Select fill for drainage behind abutment walls. 2. Cement or lime treat subgrade
Dallas	Graded backfill material with PI 10 to 25 with density controlled compaction
El Paso	2 sacks of concrete at approach slabs and backwall
Fort Worth	<ol style="list-style-type: none"> 1. Test embankment for compliance with requirements at beginning of the bridge, end of the bridge, and at 25' intervals for a distance of 150' from each bridge end. 2. Embankments are supposed to be constructed to the final subgrade elevation prior to the excavation for abutment caps and approach slabs. 3. Additional density testing of roadway embankments near bridges
Houston	<ol style="list-style-type: none"> 1. Lower the LL/PI 2. Good compaction 3. Cement stabilized backfill
Laredo	Item 132
Pharr	Cement stabilized backfill
Waco	Cement stabilized backfill

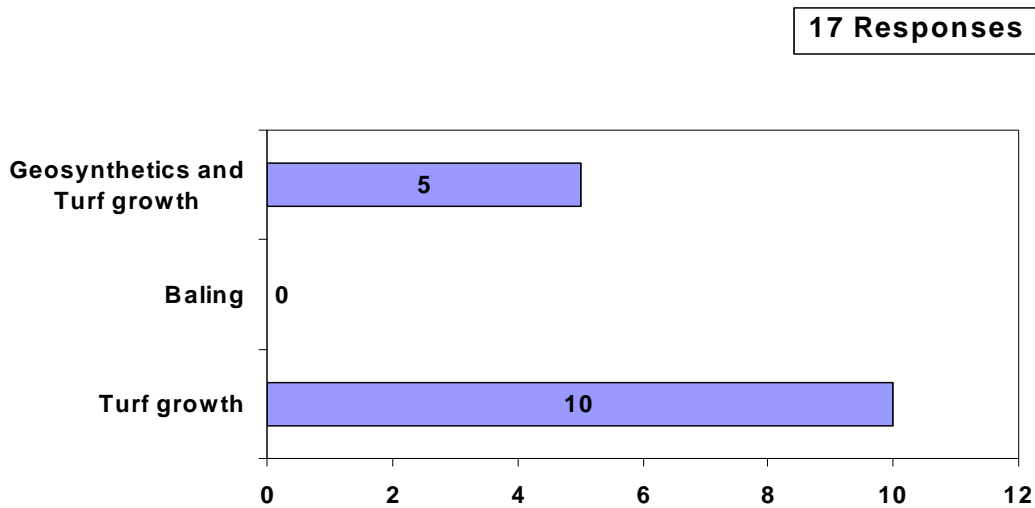


Figure 3.9 Methods to control the erosion/slope failure

3.3 Ranking Analysis of Mitigation Techniques

The non-parametric ranking analysis was performed in this task to rank the techniques presented from the literature review, which can be divided into two groups. One group focuses on novel methods used for foundation and fill improvement, while another group deals with techniques normally used for approach slab maintenance. The first group focuses on novel methods used for foundation and fill improvement and these methods include Deep Soil Mixing (DSM), Continuous Flight Auger (CFA) piles, MSE wall, and other methods. The second group deals with techniques normally used for approach slab maintenance such as Hot Mix Asphalt (HMA) overlays, slab replacement, Urethane injection and others. Four criteria including 'Technique Feasibility', 'Construction Requirements', 'Cost Considerations' and 'Overall Performance' are considered and for each criterion, a ranking was assigned to each method.

For technique feasibility, three levels of ranking (shown in parentheses) were considered and these were: 1) they have been already implemented and proven as well design methods; 2) technique is effective but still under research; 3) and they are ineffective. Table 3.1 presents the ranks given for the methods listed in each group. All methods of the

first group are novel and yet to be evaluated and hence they are assigned a rank of two (2). Ranks given in Group Two are also presented in the same table.

Three criteria used in 'Construction Requirements' are: 1) requires mobilization of heavy equipment; 2) and requires quality control during construction. Cost ranking was based on the costs of the construction for performing the field work. The last factor for the ranking analysis is based on the Overall Performance of each method. This rank was based on the available literature. Table 3.1 presents all these ranks for each method.

In conclusion, after each mitigation method has been considered and analyzed according to the four criteria, the mitigation techniques were ranked. The results show that for the novel foundation and fill improvement, six methods show early promise and can be recommended to be evaluated in this research, while for the maintenance measures the mud/slab jacking, grouting and Urethane injection shown promise and hence considered for further research evaluation.

Table 3.2 Ranking analysis of mitigation techniques for bridge approach settlement.

New or Maintenance Measure	Mitigation method	Technique Feasibility (a)			Construction Requirements (b)			Cost Considerations (c)			Overall Performance			Is this method recommended for present research?
		Ineffective	Effective but under research	Proven, well design method	Low	Medium	High	Low	Medium	High	Not proven	Ineffective	Effective	
Novel Methods for Foundation and Fill Improvement	MSE Walls/GRS		✓				✓			✓	✓			✗
	Geofoam		✓			✓			✓	✓	✓			✓
	Lightweight Fill		✓			✓			✓	✓	✓			✓
	Flowable fill		✓		✓			✓				✓		✓
	Deep Soil Mixing (DSM)		✓		✓				✓			✓		✓
	Continuous Flight Augercast piles (CFA)		✓				✓		✓			✓		✗
	Concrete Injection Columns (CIC)		✓				✓			✓	✓			✗
	Geopiers		✓				✓		✓			✓		✓
Maintenance Measures	HMA overlay			✓		✓		✓			✓			✗
	Mud/ Slab jacking		✓		✓			✓				✓		✓
	Slab replacement			✓		✓			✓			✓		✗
	Grouting			✓	✓				✓			✓		✓
	Urethane injection		✓		✓					✓			✓	✓

3.4 Summary

This chapter presents the results of TxDOT's districts survey and a ranking analysis. The ranking analysis was done concurrently with a district survey, which reveals each TxDOT Districts' practices with respect to the approach settlement problem. The results from both the analysis and the survey are useful in this study. From the aspects of understanding of the bump problems encountered in each District and the techniques available to minimize the bump problem, five methods including Geofoam, Deep Soil Mixing, Geopiers, Lightweight Fill and Flowable Fill are recommended as foundation and fill improvement methods to be evaluated in this research, while the mud/slab jacking, grouting and Urethane injection are also recommended for maintenance measures evaluation.

Since the objective of the research is to investigate the methods that could be comprehensively evaluated from controlling approach slab settlements of new bridge construction. Two methods, one for foundation treatment and the other for embankment modification are considered for the present dissertation research evaluations. The next chapters describe these evaluation studies on both methods for settlement control.

CHAPTER 4
DESIGN OF DEEP SOIL MIXING (DSM) FOR SETTLEMENT CONTROL

4.1 Introduction

As discussed in chapter 3, the soil-cement treatment (DSM) was chosen as one of the viable techniques to improve engineering properties of clayey soft soils beneath a bridge embankment in this study. One site of a bridge at the IH 30 in the North of Arlington, Texas was selected to evaluate the application of this technique in real field conditions. An embankment on the south side of the bridge was constructed over the DSM treated test section, while other side of the bridge was constructed on a local stiff soil with a conventional method (i.e. without the DSM treatment). This section is treated as a control section.

In this chapter, the subsections describe the procedure(s) developed for the design of the DSM columns.

4.2 Procedure for Design of DSM Columns

4.2.1 Theoretical Formulation

The design of DSM columns for the field section is based on the settlement prediction model for treated soils originally proposed by Rao et al. (1988). The model was also used to predict soil settlements occurred in the DSM test section. The prediction of the settlement is based on the overburden pressures, thickness of soil layers and the properties of soil in each layer. The equation used to predict the soil settlement is shown in the following:

$$7. \Delta h = \sum_{i=1}^n \frac{C_{s,i} h_i}{1 + e_{o,i}} \log \frac{p'_{i,i}}{p'_{p,i}} + \sum_{i=1}^n \frac{C_{c,i} h_i}{1 + e_{o,i}} \log \frac{p'_{f,i}}{p'_{p,i}} \quad (4.1)$$

The equation of settlement consists of two terms. When the overburden pressure is less than the pre-consolidation pressure, the first term of the equation is only used for the settlement

prediction, while the second term is disregarded. The second term is included as shown in the equation when the overburden pressure is greater than the pre-consolidation pressure. The $C_{s,i}$, $C_{c,i}$, $e_{o,i}$, $p'_{f,i}$, $p'_{p,i}$, $p'_{i,i}$ and h_i are recompression index, consolidation index, initial void ratio, final effective stress (overburden \pm any changes in total stress), preconsolidation stress, initial stress overburden, and thickness of each layer 'i', respectively (Figure 4.1).

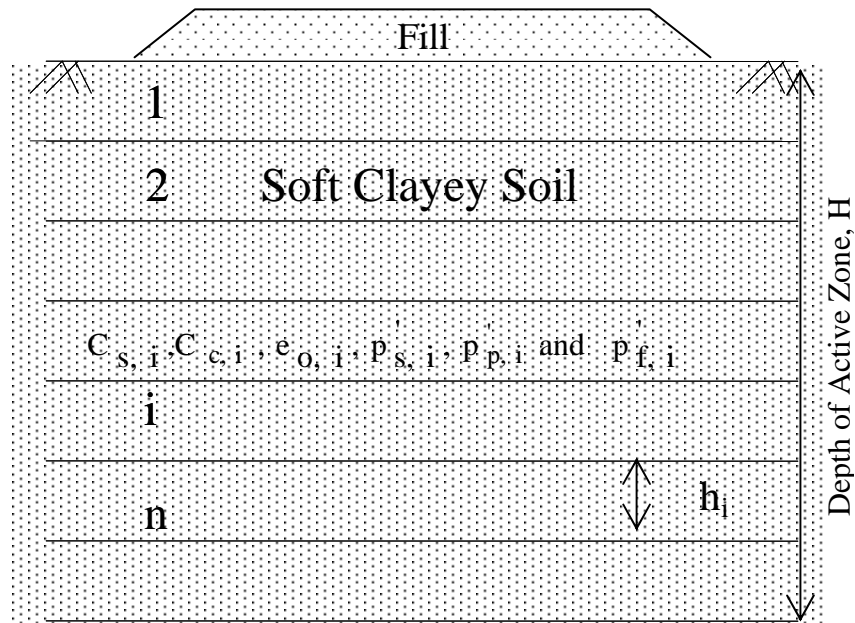


Figure 4.1 Schematic of untreated ground depicting layers for settlement prediction

Most of variable values, $C_{s,i}$, $C_{c,i}$, $e_{o,i}$, $p'_{p,i}$, are obtained from the 'constant volume' type oedometer tests which are already discussed in Chapter 3. The final overburden stress, $p'_{f,i}$, is calculated accounted for the overburden stress as well as any net changes in total stresses from either traffic loading or surcharge loading as weight of embankment itself. It is assumed that the ground water level is far below the considered soil strata and will not affect the water content in the soil strata.

From the Equation 4.1, the settlement in the DSM-soil composite section can be predicted by the following equation.

$$\Delta h = \sum_{i=1}^n \frac{C_{r,i}^{comp} h_i}{1 + e_{o,i}^{comp}} \log \frac{p'_{i,i}}{p'_{p,i}} + \sum_{i=1}^n \frac{C_{c,i}^{comp} h_i}{1 + e_{o,i}^{comp}} \log \frac{p'_{f,i}}{p'_{p,i}} \quad (4.2)$$

Where the parameters $C_{r,i}^{comp}$, $C_{c,i}^{comp}$, and $e_{o,i}^{comp}$ are the composite properties of soil layer 'i' in the treated ground (Figure 4.2). These parameters are estimated as shown below, based on the treated and untreated soil properties determined from the laboratory studies.

$$C_{r,i}^{comp} = C_{r,i}^{col} \times a_r + C_{r,i}^{soil} \times (1 - a_r) \quad (4.3)$$

$$C_{rc,i}^{comp} = C_{r,i}^{col} \times a_r + C_{c,i}^{soil} \times (1 - a_r) \quad (4.4)$$

$$C_{c,i}^{comp} = C_{c,i}^{col} \times a_r + C_{c,i}^{soil} \times (1 - a_r) \quad (4.5)$$

$$e_{o,i}^{comp} = e_{o,i}^{col} \times a_r + e_{o,i}^{soil} \times (1 - a_r) \quad (4.6)$$

The symbols with 'soil' in the superscript indicate untreated soil properties and those with 'col' represent soil-cement column properties. The effect of DSM treatment is taken into account for estimating the values of composite parameters, which are then determined by estimating the weighted average of the treated and untreated soil properties as per their area ratio, α_r . The parameter α_r (area ratio) is defined as the ratio of the area of treated columns to the total area and used as the weighting factor.

Equation 4.2 is further simplified assuming that: (1) the initial void ratio ($e_{o,i}$) and bulk unit weights for both the untreated and treated sections are the same and constant with the depth, and (2) the composite properties, C_i^{comp} is constant with depth. Settlement equation is typically used in 3 case scenarios as per the magnitudes of the overburden and pre-consolidation pressures. These are presented in the following:

Case 1; When $p'_{f,i} \leq p'_{p,i} \leq p'_{col}$

$$\Delta h_1 = \sum_{i=1}^n \frac{C_{r,i}^{comp} h_i}{1+e_{o,i}} \log \frac{p'_{f,i}}{p'_{p,i}} \quad (4.7)$$

Case 2; When $p'_{p,i} \leq p'_{f,i} \leq p'_{col}$

$$\Delta h_2 = \left\langle \sum_{i=1}^n \frac{C_{r,i}^{soil} h_i}{1+e_{o,i}} \log \frac{p'_{p,i}}{p'_{i,i}} + \sum_{i=1}^n \frac{C_{c,i}^{soil} h_i}{1+e_{o,i}} \log \frac{p'_{f,i}}{p'_{p,i}} \right\rangle x(1-a_r) + \left(\sum_{i=1}^n \frac{C_{r,i}^{col} h_i}{1+e_{o,i}} \log \frac{p'_{f,i}}{p'_{i,i}} \right) x(a_r) \quad (4.8)$$

Case 3; When $p'_{p,i} \leq p'_{col} \leq p'_{f,i}$

$$\Delta h_3 = \left\langle \sum_{i=1}^n \frac{C_{r,i}^{soil} h_i}{1+e_{o,i}} \log \frac{p'_{p,i}}{p'_{i,i}} + \sum_{i=1}^n \frac{C_{c,i}^{soil} h_i}{1+e_{o,i}} \log \frac{p'_{f,i}}{p'_{p,i}} \right\rangle x(1-a_r) + \left\langle \sum_{i=1}^n \frac{C_{r,i}^{col} h_i}{1+e_{o,i}} \log \frac{p'_{p,i}}{p'_{i,i}} + \sum_{i=1}^n \frac{C_{c,i}^{col} h_i}{1+e_{o,i}} \log \frac{p'_{f,i}}{p'_{p,i}} \right\rangle x(a_r) \quad (4.9)$$

In the present design example of bridge embankment loading, the calculation for settlement happening in cases 2 and 3 can be neglected since the overburden pressure due to a summation of traffic loading and embankment fill weight is not expected to be greater than the preconsolidation pressure of the underlying soil.

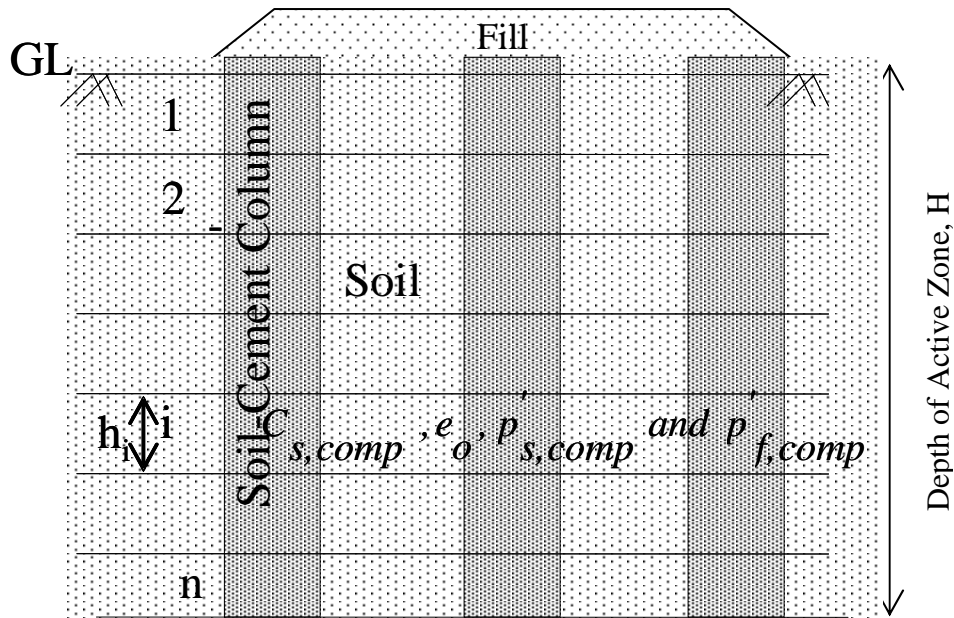


Figure 4.2 Schematic of composite ground depicting layers for heave prediction

4.2.2 Design Steps

Based on the settlement prediction models in Equations 4.1 through 4.9, the design steps shown in the flow chart (Figure 4.3) are followed for determining the diameter, length and spacing of the DSM columns for mitigating the settlement distress causing from soft soil subgrades: The design steps involved are as follows:

1. Determine the compression index (C_c) and reconsolidation index (C_r), pre-consolidation pressure, initial overburden pressure, initial void ratio and total unit weight of the untreated soil specimens retrieved from each soil layer at the site. Consolidation tests were conducted as per the ASTM D2435-04 method to estimate the compression indices of the soils and the preconsolidation pressures expected from the soils on the site. In case of the soil having several strata, the tests should be carried out on each individual layer.
2. The representative soil properties, such as, consolidation index, reconsolidation index, preconsolidation pressure, initial void ratio and bulk unit weight can be determined as the weighted average of the individual properties of the soil layers from the surface to the maximum active depth.
3. Estimate the amount of settlement Δh_{unt} , of the untreated ground by using Equation 4.1.

4. Establish the acceptable settlement, Δh_{tr} , for a given project. According to TXDOT bridge design, the permissible settlement for bridge approach slab is 2.0 in. (5 mm), while in other state the allowable values may be various. If the calculated settlement of the soil before treatment (estimated in Step 2) is less than the allowable level, soil treatment will not be necessary. Otherwise, the next succeeding steps should be followed to design and establish the DSM treatments for the project site. The costs involved with the field treatments are inversely proportional to the magnitudes of the established permissible settlement used in this step. The lower the permissible settlement, the greater number of the DSM columns required; consequently, the higher the costs is involved with the ground treatment. Δh_{tr} of less than 2 in.(5 mm) is needed in order to mitigate the bump at the end of the bridge.
5. Find the appropriate amount of chemical stabilizers for soil-cement columns by repeating the tests mentioned in Step 1 on soil specimens stabilized with different quantity of additives. The main objective of this is to minimize the representative compression index value of the soil-cement specimens. The desirable criteria of an adequate amount of additives adding into the soil are 1) reducing the compressive index value of the treated soil compared with one of the untreated soil, 2) increasing the preconsolidation pressure of the treated soil compared with one of the untreated soil.
6. Estimate the treated area ratio required for the project for reducing the overall settlement of the treated soil to a permissible settlement value prescribed in Step 3. Based on the recompression and compression indices of the untreated soil measured in Step 1 and the permissible settlement in Step 3, the following appropriate Figure 4.4 is used to estimate the area treatment ratio. This area treatment ratio is used in the following equations to estimate the column spacing. The figure presents various predicted settlement (which is equivalent to permissible settlement for the design exercise) versus area ratio plots for given recompression and compression index value. Equation 4.7 is used in the preparation

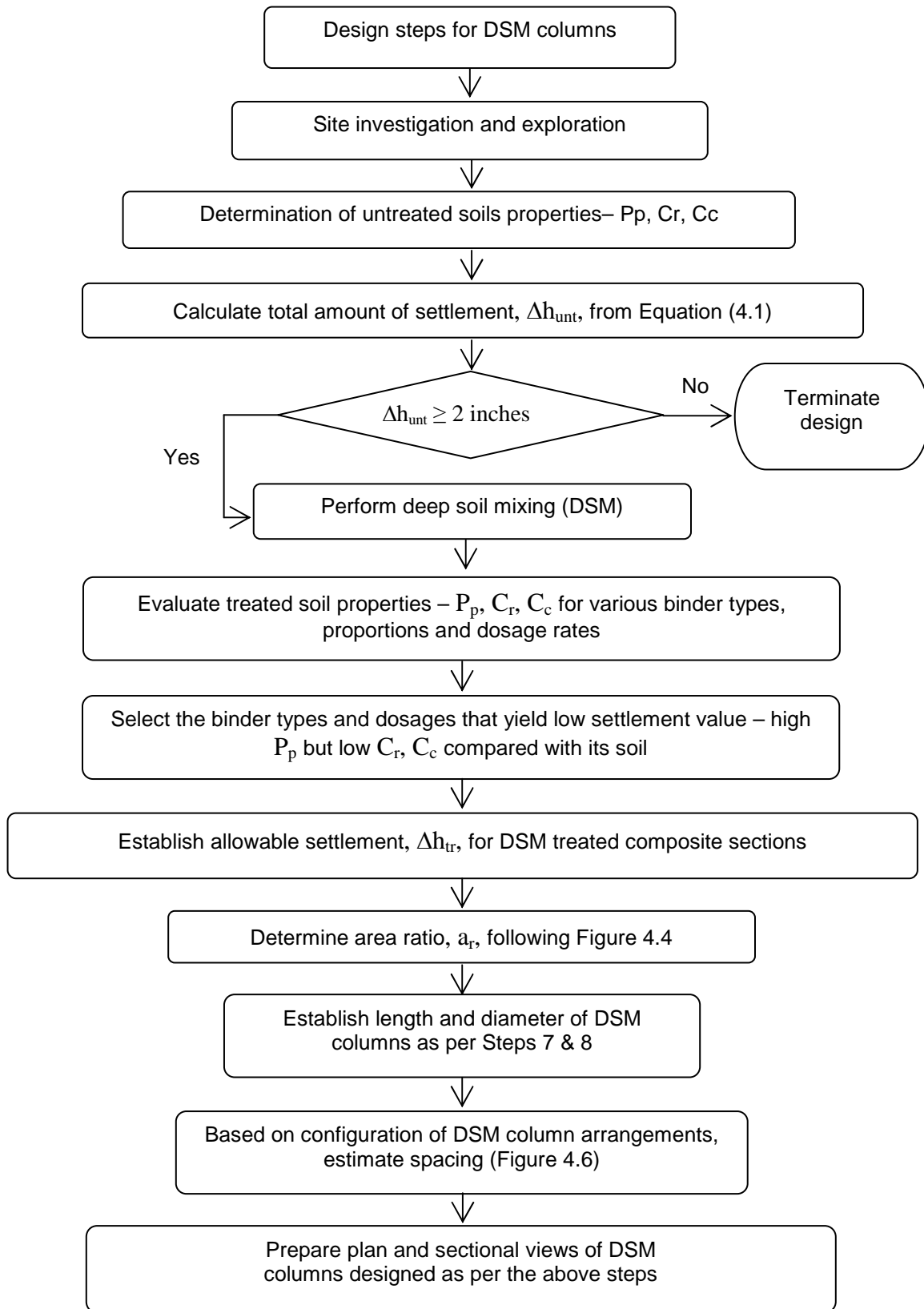


Figure 4.3 Design flow chart for DSM treatment

of these figures. Please note that this equation for area ratio already accounts for composite consolidation properties of the treated and untreated ground. Binders and dosage rates that yield very low settlement characteristics (Step 3) are only recommended for field implementation.

7. If the recompression and compression index of the untreated soil lies in between those that were used in the development of the design charts, then a linear interpolation method should be followed by using two charts, one lower than the consolidation index value under consideration and the other above the consolidation index value.
8. The diameter of the DSM column is either already known or pre-established based on the DSM rigs used by the hired DSM contractor in the field. If the diameter information is not known at the time of design, then the DSM columns can be designed for various diameter sizes. A DSM column size can then be selected based on the overall costs of the DSM work for the project site. For example, a DSM contractor with a rig capable of making smaller diameter columns may charge a lesser amount for mobilization costs than a DSM provider with larger diameter rigs. Hence, the DSM column diameter is based on either locally available DSM rigs or on cost considerations. In this practice, the diameter of 4.00 ft (1.2 m) is recommended by the DSM contractor.

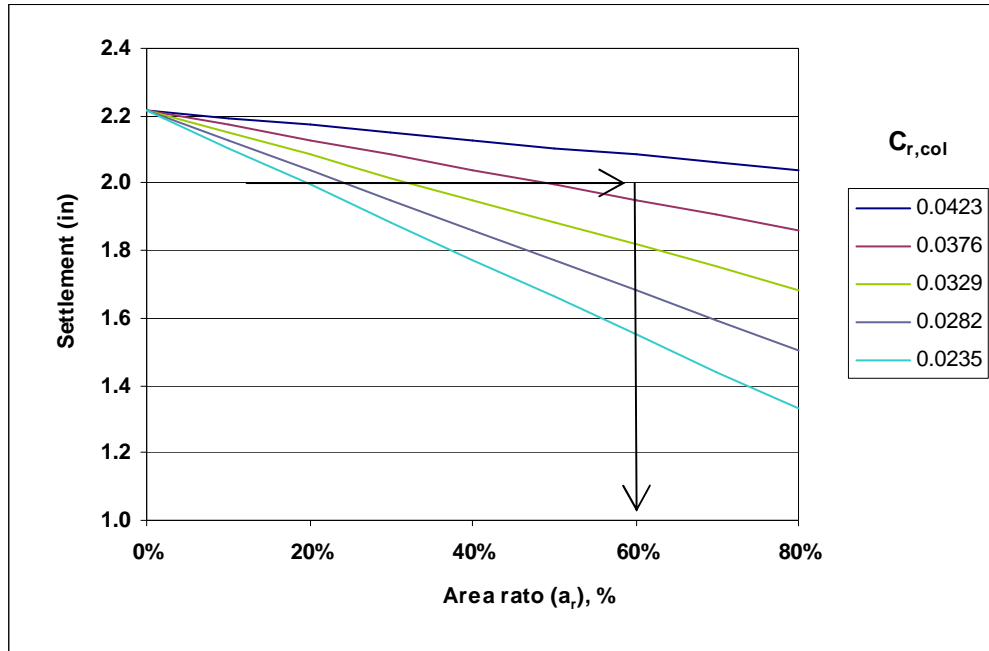


Figure 4.4 Design charts for estimating DSM area ratios for $C_{r,soil} = 0.047$ and $C_{r,col}$ 50-90% of $C_{r,soil}$

9. The length of the DSM column is usually designed by considering the depth of the soft soil stratum. It is recommended that the bottom of DSM columns should be located on a hard non-expansive stratum. The depth of soft soil stratum and elevations of each soil layers can be determined by bore logs which were done on site. Based on the survey results, it was found that there are three kinds of soil laid beneath the construction area. The top soil layer is clay with the thickness of 20 ft (6 m), the second layer beneath clay stratum is sand with the thickness of 5 ft (1.5 m) and the last layer is hard shale. Therefore, according to the recommended criterion the length of DSM columns should be designed as 25 ft (7.5 m), approximately laid on a top of shale layer.
10. Establish the configuration of the DSM columns in the field. In general, two configuration types - 'square' and 'triangular' - are used in practice. Figure 4.5 depicts the schematics of both configurations. Based on the area ratio, a_r derived in Step 5, and the diameter of the DSM columns, the optimum spacing of DSM columns can be determined by using either Figure 4.6 or Figure 4.7.

11. In the case of multi-axial rigs, treated area under multiple shafts can be idealized as an equivalent circle and then the same spacing calculation can be followed as per the above step.
12. Lastly, the final plans and section details shall be prepared using the above designed or established DSM column diameter, length and spacing information. The spacing should be rounded to a lower bound value since this ensures that the overall design is more conservative as lower bound rounding of the spacing results in higher area ratios than determined from the design chart.
13. The plan and sectional views developed following the above design procedure for construction of prototype test sections are presented in the following section.

4.2.3 Design Specifications of Materials for DSM Treated Test Sections

4.2.3.1 Below are the specifications of materials, including binders and water, arrived at following the laboratory studies for construction of the DSM columns.

1. Only cement is recommended for DSM construction
2. A dosage rate of 160 kg/m^3 (10 pcf) is recommended.
3. A water-binder ratio of 4.0 or lower is recommended.

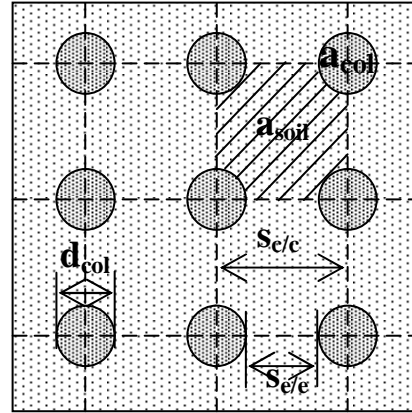
Based on these specifications, the total required quantities of binders and water for both test sections are estimated.

SQUARE ARRANGEMENT:

$$a_r = \frac{a_{col}}{a_{soil} + a_{col}}$$

$$= \frac{\text{area of column}}{\text{area of square}} = \frac{\left(\frac{\pi d_{col}^2}{4}\right)}{s_{c/c} \times s_{c/c}}$$

$$s_{c/c} = \sqrt{\frac{\pi}{4a_r}} d_{col}$$



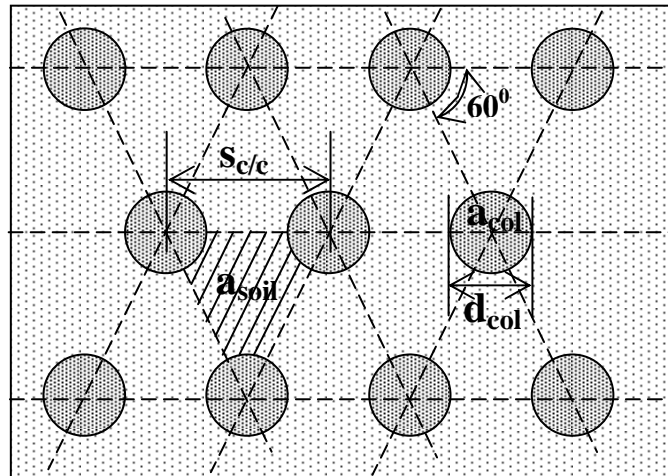
(4.10)

TRIANGULAR ARRANGEMENT:

$$a_r = \frac{1/2 a_{col}}{a_{soil} + 1/2 a_{col}}$$

$$= \frac{1/2 \text{ area of column}}{\text{area of equilateral } \Delta e}$$

$$= \frac{1/2 \left(\frac{\pi d_{col}^2}{4}\right)}{1/2 \times s_{c/c} \times \sqrt{3}/2 \times s_{c/c}}$$



$$s_{c/c} = \sqrt{\frac{\pi}{3.464a_r}} d_{col}$$

(4.11)

Figure 4.5 Configurations of DSM columns and corresponding equations for column spacing

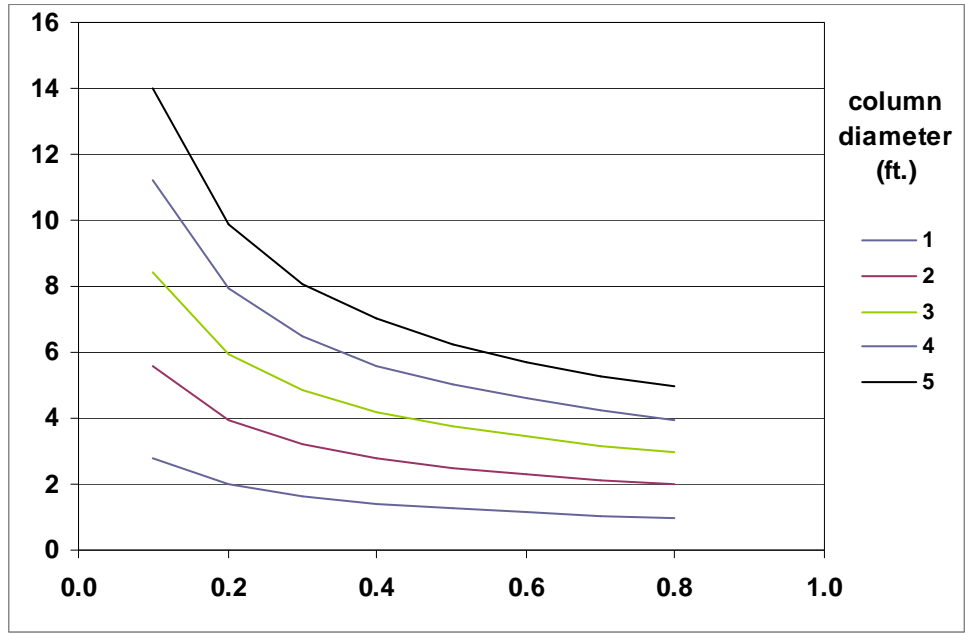


Figure 4.6 DSM column spacing details for Square Pattern

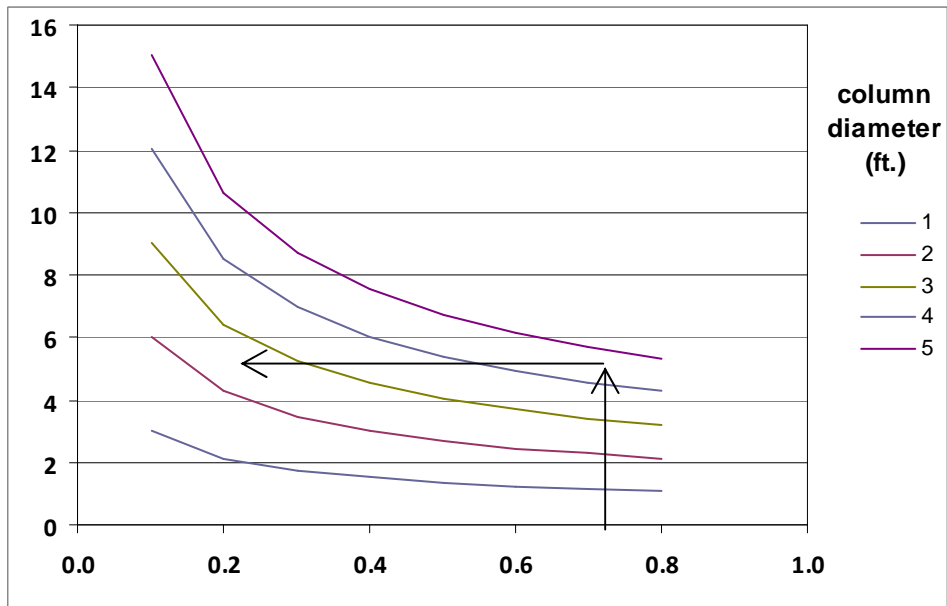


Figure 4.7 DSM column spacing details for Triangular pattern.

4.2.3.2 Specifications of DSM Column Geometry and Arrangement

As shown in Figure 5.6b, a triangular arrangement of the DSM columns is considered and with the area ratio of 0.50 the center-to-center distance of column spacing should be 5.5 ft (1.65 m). The column dimensions, as aforementioned in Step 9 are 4 ft (1.20 m) in diameter and 25 ft (7.5 m) in length.

4.3 Summary

This chapter presents the stepwise procedure developed for the design of the DSM columns based on the heave prediction model proposed by Rao et al.,1993. Following the provided specifications of materials used in construction and the stepwise procedure, the specifications of DSM column, column geometry and its arrangement can be determined.

CHAPTER 5
LABORATORY INVESTIGATIONS FOR DSM AND LIGHT WEIGHT FILL STUDIES

5.1 Introduction

This chapter presents two laboratory investigations performed simultaneously, which are presented in three sections, site selection and soil sampling, experimental test program, and discussion of laboratory results. The first section gives details of two sites used in this study. The second section describes the details of tests performed on embankment fill and natural foundation soils. As discussed in the literature review, the factors responsible for the bump problem are not similar and vary from site to site. Therefore, the natural foundation soils and embankment materials from each site were tested to evaluate their compressibility properties.

Several promising techniques were analyzed through a ranking analysis and the results are shown in Table 3.2 in Chapter 3. Two methods, lightweight fills and deep soil mixing (DSM) methods were primarily focused for the research investigations. An expanded clay shale (ECS) was used as the lightweight embankment fill material and it is characterized as an embankment material, whereas soil-binder mixes as the DSM were tested for their suitability as being a foundation soil. In this section the details of tests performed on embankment fill and natural foundation soils along with detailed test procedures followed, soil-binder mix design methods and specimen preparation procedures simulating the DSM technology are also provided. All the engineering tests performed are in compliance with the procedures outlined by Texas Department of Transportation (TxDOT) and the American Society of Testing Materials (ASTM) standards, wherever applicable. The laboratory results of several soils obtained from various test sites selected for this project study are presented in the last section.

5.2 Site Selection and Field Soil Sampling

Two new bridges in Arlington, Texas were chosen to study the selected mitigation techniques to control approach slab settlements. The DSM treatment was used at one site to improve the weak foundation soil underneath the bridge across the interstate highway IH30 site in North Arlington, Texas. The plan view of the site and the layout of the proposed DSM treatment zone are shown in Figure 5.1. The shaded zone represents the weak soil zone under the bridge embankment. In this case, a 25 ft. (7.5 m) height embankment was constructed on the DSM treated ground. The DSM treatment is shown in the hatched portion. Undisturbed and disturbed soil samples were collected from two soil borings along the center line of the bridge..

In another site in south of Arlington, Texas, lightweight aggregate was proposed to utilize as a fill material for an approach embankment of a bridge along state highway 360 (SH360). In this case, the foundation soil was not treated with any deep stabilization methods, except, a few inches of lime stabilization of subgrade soils for pavement construction was considered. The layout of the proposed bridge site of SH360 is shown in Figure 5.2. Natural soil samples were collected from soil borings made along the median of the proposed highways. The ECS aggregate material was obtained from the stockpile in Dallas district and brought to the geotechnical laboratories at UT Arlington for analyses.



Figure 5.1 Details of weak soil and DSM treatment, IH 30 site, Arlington, TX

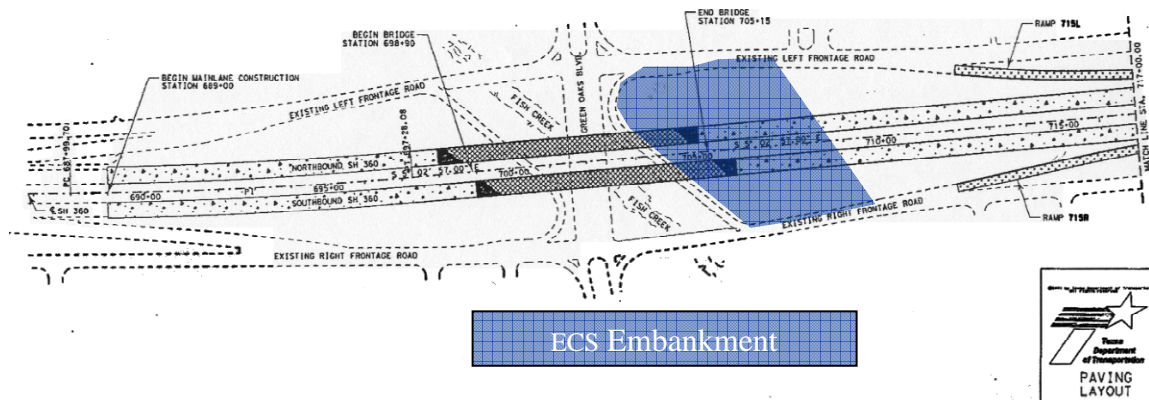


Figure 5.2 Details of ECS Bridge Site, SH 360, Arlington, TX

The soil samples either from embankment fill or from subgrade soil were brought to investigate their properties in a laboratory. For site SH 360, north side of bridge embankment was constructed with a select fill while the south side was constructed with ECS as a lightweight fill material. Therefore, the engineering properties of ECS and select embankment fill were investigated. The different properties of both materials are considered here as critical factors for understanding the differences in settlement magnitudes monitored at bridge approaches at both sides of the bridge. For the site IH30, the DSM technique was employed only to improve the subgrade soil and select fill was used to construct the embankment fill material. Thus, properties of the embankment fill, natural subgrade soil and modified subgrade soil are characterized. For treated soil, the soil-cement samples of subgrade material with the same water-cement-soil contents as constructed in the field were reproduced in a laboratory environment to find the properties of DSM specimens.

Another site in Houston (State Highway or SH6) was studied briefly as this site was constructed with Geopiers to mitigate settlements. However, these are not done as a part of this research program and hence only minor details are only included here for illustrative purposes.

To evaluate the physical and engineering properties of the representative soils, a series of laboratory tests were designed and conducted. To classify the soils, grain size analysis was carried out according to Tex-110-E method; Atterberg Limit tests were performed according to Tex-104-E, Tex-105-E and Tex-106-E. Compaction characteristics were determined in

accordance with Tex-113-E method. The test procedures stipulated in ASTM D-2435-96 was used to determine the compressibility characteristics of the soils. The linear shrinkage strain (Tex-107-E), free swell test (ASTM-D2166), and unconfined compression tests (ASTM-D2166) were also performed. The details of these tests are presented in the following sections.

5.3 Experimental Program

This section presents the details of test procedures followed to conduct the index and engineering tests outlined in the previous section on the control soils. The details of the experimental studies carried out on different samples as summarized in Table 5.1.

Table 5.1 Summary of tests performed on natural/artificial soils

Test performed	SH 360, Arlington, TX		IH 30, Arlington, TX			
	Expanded Clay Shale (ECS)	Selected Fill (emb.)	Selected Fill (emb.)	Foundation Soil (control section, B2)	Foundation Soil (study section, B1)	Soil-Cement Moisture (DSM)
Grain Size Analysis	✓	✓	✓	✓	✓	
Atterberg Limit Test			✓	✓	✓	
Standard Compaction Test		✓	✓			
Linear Shrinkage Strains		✓	✓	✓	✓	✓
One-Dimensional Free Swell Tests		✓	✓	✓	✓	✓
One-dimensional Consolidation Test	✓	✓	✓	✓	✓	✓
Direct Shear Test	✓					
Unconfined Compression Strength (UCS) Test		✓	✓	✓	✓	✓

5.3.1 Sample Preparation

The sample preparation for determination of Atterberg Limits was done according to the wet preparation method described in Tex-101-E method. In this procedure, the soil sample was first soaked in tap water for a period of 24 hours as shown in Figure 5.3(a) and then washed the sample through a No. 10 sieve (2 mm). The portion of the sample passing the No. 10 sieve was again washed through a No. 200 (0.075 mm) sieve until at least 95% of the material passed through the sieve. The soil samples were transferred into a Plaster of Paris bowl with filter and allowed to dry until the water content was below the liquid limit. To enhance the process of drying, an electric fan was used as shown in Figure 5.3(b). When the sample was divided into wedges, it indicated that the soil was ready for the above-mentioned tests.

5.3.2 Atterberg Limit Tests

Atterberg limit tests include the determination of liquid limit (LL) and plastic limit (PL) of a soil to understand the consistency properties of the soil. According to addition of water to a soil, the state of the soil changes from dry, semisolid, plastic and finally to liquid. The water content at the boundaries of these states are known as shrinkage (SL), plastic (PL) and liquid (LL) limits, respectively. The LL is a boundary having its water content at which the soil flows and the PL is determined as the water content at which the soil starts crumbling when rolled into a 1/8-in. (3.2 mm) diameter thread. These tests are somewhat operator sensitive and take time to perform. The numerical difference between LL and PL values is known as the plasticity index (PI) (Tex-106-E) and characterizes the plasticity nature of the soil.

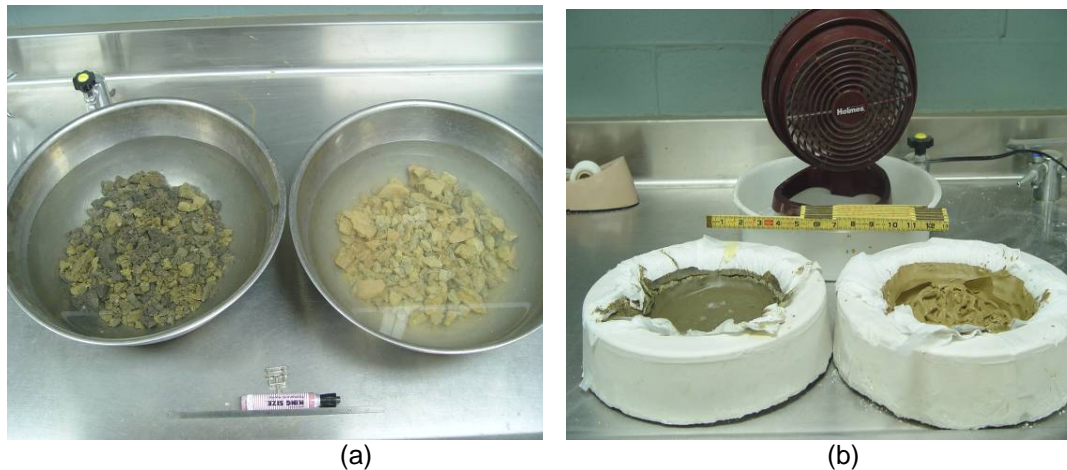


Figure 5.3 Sample preparations by wet analysis for soil classification and determination of Atterberg Limits (a) Soaking stage and (b) Drying stage

Representative soil samples were prepared following the aforementioned procedure and are subjected to Atterberg Limit tests to determine the LL and PL following Tex-104-E and Tex-105-E, respectively. The water content of the samples during the tests was measured using the ignition oven drying method based on the repeatable data as reported by the Tex-103-E method.

5.3.3 Standard Proctor Compaction Test

To determine the compaction moisture content and dry unit weight relationships of the selected fill of embankment, the standard Proctor compaction tests were performed. These results were also used to prepare the specimens for unconfined compression strength tests and consolidation tests for the selected fill specimens. Several samples of the same soil with different water content were compacted in accordance with Tex-114-E procedure. After the wet density and actual water content of each compacted sample were measured, the dry density of soil for each sample was calculated. The compaction curve could be drawn by plotted dry density and water content values of each soil sample. The optimum moisture content of the soil is the water content at which the soils are compacted to a maximum dry unit weight condition. Soils with a dense state exhibiting a high shear strength but low compressibility suit to support civil infrastructures. Compaction tests were conducted on all types of soils to determine moisture

content and dry unit weight relationships. According to TxDOT design for the embankment higher than 30 ft, the embankment fill must be constructed with 98% optimum moisture content. Following are the expressions for determining both wet unit weight and in-situ natural water content:

$$\text{Bulk unit weight, } \gamma_w \text{ (kg/m}^3 \text{ or pcf)} = \frac{W_b}{v} \quad (5.1)$$

$$\text{In situ natural water content, } w_n \text{ (\%)} = \frac{W_b - W_d}{W_d} \quad (5.2)$$

$$\text{Dry unit weight, } \gamma_d \text{ (kg/m}^3 \text{ or pcf)} = \frac{\gamma_w}{1 + w_n} \quad (5.3)$$

Where W_b = wet weight of soil

W_d = dry weight of soil

and v = volume of soil samples.

5.3.4 Determination of Linear Shrinkage Strains

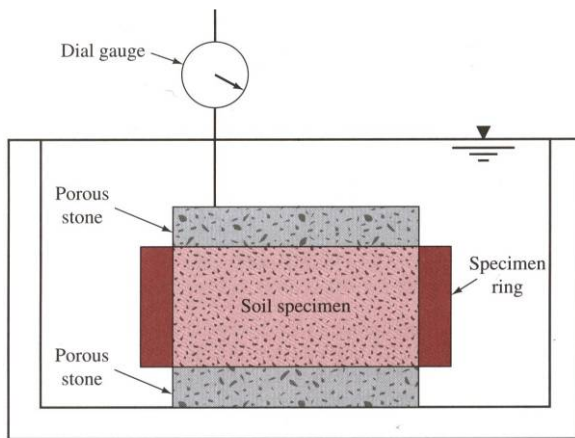
As explained in Tex-107-E test procedures, the soil specimens for shrinkage test were mixed with sufficient water until soil became slurry at the LL state. The soil slurry was then placed into a linear shrinkage mold of dimensions, 4 in. long \times 0.75 in. wide (102 mm long \times 19 mm wide). The inner surfaces of the mold were greased sufficiently to reduce the friction between the specimen and inner surfaces upon subjecting the specimen to drying. Care was taken while placing the soil into the mold so that the entrapped air was removed. The surface was then leveled with the top of the mold using a spatula and the specimens were air dried at room temperature until a color change was observed. The mold was then transferred into an oven set at 110 ± 5 °C for 24 hours. The change in length was determined accurately using Vernier calipers and the linear shrinkage strain (L_s) was calculated in percentage as follows:

$$L_s = \frac{\Delta L}{L_0} \times 100 \% \quad (5.4)$$

Where ΔL is change in length, and L_0 is original length of specimen.

5.3.5 One-Dimensional Free Swell Tests

One-dimensional free swell strain tests were conducted in accordance with ASTM D-4546. Each soil specimen was kept in a conventional oedometer steel ring of size 2.5 in. (64 mm) in diameter and 1 in. (25 mm) in height. The inner face of the consolidation ring was lubricated to minimize the friction during free swell. Prior to the testing, the free swell specimens were kept in a humidity room for moisture equilibrium purposes. The samples were taken out from the humidity room and weighed along with the oedometer ring prior to the testing. Porous stones and filter papers were placed on both top and bottom of the specimen to facilitate movement of water into the soil. The specimens were then transferred into a container and filled with water in order to soak the specimen under a no load condition. The amount of upward vertical movement (heave or swell) of the specimens was recorded at various time intervals by placing a dial gage on the top porous stone. Figure 5.4 shows a schematic sketch of the one-dimensional free swell test setup used in the present study. The recording of readings was continued until no further movement was measured for at least one day. Soaked specimens were then carefully removed.



(a)



(b)

Figure 5.4 Free swell test (a) Schematic Sketch (Das, 2002) and (b) Test Setup

from the ring, weighed, oven dried, and weighed after drying in order to calculate the moisture content of the saturated specimen. The swelling of the expansive soil, measured as strain, is termed as the free swell index (FSI).

5.3.6 Unconfined Compression Strength (UCS) Test

The UCS tests were performed on soil samples collected from different sites to determine the strength properties of the soil samples. The unconfined compression test is a special form of a triaxial test in which the confining pressure is zero. The test can be conducted only on clayey soils which can withstand without confinement. Test was performed as per ASTM-D2166. In this test, a cylindrical specimen with dimensions 1.3 in. in diameter and 2.8 in. in height was prepared. The specimen was first placed on a platform and then raised up until it came in contact with the top plate (Figure 5.5). Once the specimen reached the position, it was loaded at a constant strain rate of 2% which is a typical value for testing clayey soils. As the load approached the ultimate failure load, cracks began to appear on the surface of the specimen. Both deformation and corresponding axial loads on the specimen were recorded using a data acquisition system software, and were used further to plot a stress-strain graph corresponding to the values of load and deformation. Stress is obtained by dividing the load by the cross sectional area of the sample, whereas strain is obtained by dividing deformation by the original height of the specimen.

The data retrieved from the computer program contain load (Q) and deformation (δ) and the same was analyzed for maximum unconfined compressive strength (q_u) in psi or kPa. The following expressions show the computation of stress (σ) and strain (ϵ) corresponding to the load-deformation data.

$$\epsilon = \delta/L \quad (5.5)$$

$$\sigma = Q/A_c \quad (5.6)$$

$$\text{and } q_u = \sigma_{\max} \quad (5.7)$$

Where δ = change in length, L = length of the specimen and A_c = Corrected area of cross-section of the specimen and is equal to $A/(1 - \epsilon)$; A is the initial cross-section area.



Figure 5.5 UCS tests performed in a triaxial test setup

5.3.7 One-dimensional Consolidation Test

The One-dimensional consolidation tests were performed in this study. The main objective of this test is to find the compressibility of saturated fine-grained soils, which is considered as a time-dependent phenomenon. In the tests, soil specimens were laterally restrained by a conventional oedometer steel ring of size 2.5 in. (64 mm) in diameter and 1 in. (25 mm) in height, while axially loaded with total stress increments. Each load increments were maintained until excess pore water pressures were completely dissipated.

One-dimensional consolidation tests were conducted in accordance with ASTM D-2435-96. For subgrade specimens, they were prepared at their natural in-situ densities obtained from the sampling methods, while the soil embankment samples were prepared at a 98% of dry density from the standard compaction test. Porous stones and filter papers were placed on both the top and bottom of the specimen to facilitate water dissipation from the soil. Then, specimens were

transferred into a container and filled with water in order to inundate the specimens. During the inundation period, normally 24 hours, the specimens were under a seating load of 100 psf (4800 kN/m²) in order to be certain that the specimens became saturated no swelling occur prior to the loading. An automated consolidometer test setup(s) was used to perform this test. Figure 5.6 shows the consolidation test setup used in this research study. The load increments were programmed and specimen deformations were automatically recorded by GeoJac System until the end of the test. At the end, the specimens were then carefully removed from the ring, weighed, oven dried, and weighed after drying in order to calculate the moisture content of the saturated specimens. Then, void ratios were calculated using height of solids method and plotted with vertical stress to obtain the compression index of the specimens.

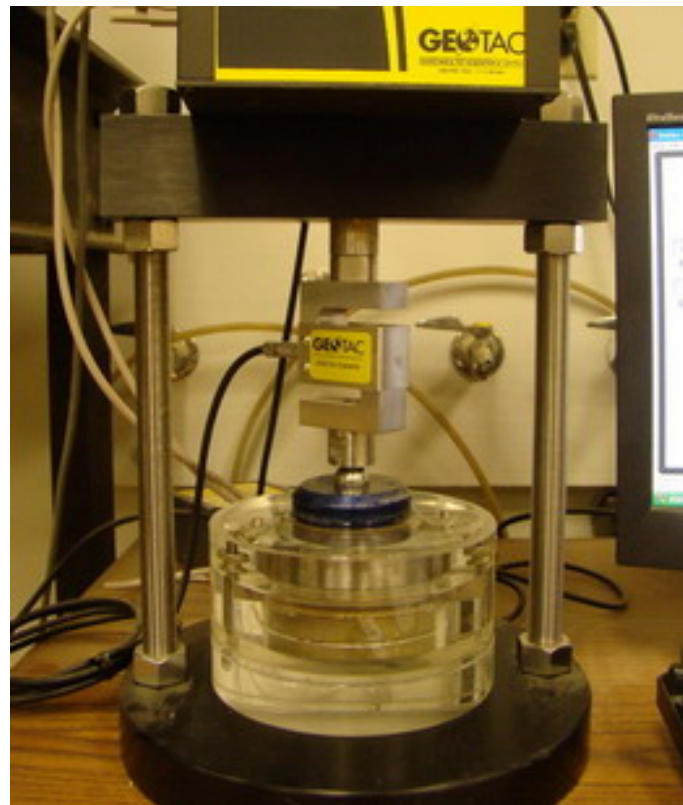


Figure 5.6 Consolidation test setup

5.3.8 Deep Soil Mixing Related Laboratory Studies

Deep soil mixing related studies were performed on soil samples collected from IH 30 site. The binder used in this study is Type I Portland cement. The soil-cement binder mixes were prepared in the laboratory environment to simulate the mix designs that has been used in the field. These studies were carried out to understand the behavior of weak foundation soil treated with DSM columns. The compressibility properties and strength properties of the soil-cement mixes were undertaken for this purpose. Following sections explain the procedures followed to prepare the soil-binder mixes by quantifying different material constituents of the matrix soil.

5.3.8.1 Preparation of Soil Samples

This section explains the steps involved in calculating the quantities of soil, cement and water for DSM columns followed by the test procedures used for preparing soil and soil-cement specimens.

5.3.8.1.1 Soil Quantity

The in-situ soil properties including bulk unit weight and water content of the soil were estimated from samples obtained from site exploration (sample borings). Following are the expressions used for determining the bulk unit weight and in situ moisture content.

$$\text{Wet unit weight, } \gamma_b \text{ (kg/m}^3 \text{ or pcf)} = \frac{W_b}{v} \quad (5.8)$$

$$\text{In-situ natural water content, } w_n \text{ (\%)} = \frac{W_b - W_d}{W_d} \quad (5.9)$$

$$\text{Dry unit weight, } \gamma_d \text{ (kg/m}^3 \text{ or pcf)} = \frac{\gamma_b}{1 + w_n} \quad (5.10)$$

where W_b , W_d and v are wet weight, dry weight and volume of soil samples, respectively.

The wet weights were obtained as soon as the samples were brought to the laboratory. The dry weights were obtained after placing soil samples in an oven for 24 hrs. The weight of dry soil mass required for preparing either an untreated or treated soil sample for one UCS, free swell specimen or consolidation test are as follows.

$$\text{Dry weight of soil for sample mix, } W_s = \gamma_d \times V \times N \times \eta \quad (5.11)$$

where V is the volume of specimen mold (shown in Table 5.2), N is the number of specimens and η is the extra mass to account for any loss of material during preparation, which can be in the range of 1.1 to 1.2.

Table 5.2 Details of Specimen Molds Used

Mold	Dimensions, in. (cm)	Volume, in. ³ (cm ³)
UCS	1.3 (3.30) × 2.8 (7.11)	3.65 (60.72)
Free Swell Strain and One-Dimensional Consolidation	2.5 (6.35) × 1 (2.54)	6.25 (80.44)
Linear Shrinkage Bar	4.0 (10.2) × 0.75(1.9) × 0.75(1.9)	2.25 (36.82)

5.3.8.1.2 Cement Quantities

In case of DSM columns, following are the expressions for calculating the quantities of cement given the dosage or content in terms of kg/m³. The cement dosage (α in kg/m³) is defined as the amount of dry weight of cement required for stabilizing 1 m³ of soil in-situ; i.e., bulk volume. The amount of cement required to treat the soil quantity is as follows:

$$W_c = \alpha \times V \times N \times \eta \quad (5.12)$$

5.3.8.1.3 Water Quantity

The amount of water in the soil samples were calculated from the in-situ natural water content (w_n) for untreated subgrade soil. For the embankment fill material, the water content in

soil samples were obtained from the compaction curve at 98 percent of maximum density from the standard Proctor tests of it.

Therefore, weight of water for sample mix,

$$W_w = w_n \times \gamma_d \times V \times N \times \eta \quad (5.13)$$

In case of DSM, water used as slurry must be added into the sample. The additional weight of water in accordance with water binder (w/b) ratio can be calculated from,

$$\text{Weight of water from w/b ratio, } W_{w, \text{slurry}} = w/b \times W_b \quad (5.14)$$

This ratio typically varied from 0.8 to 1.3 in the present study. Therefore,

$$\text{Total amount of water for preparing soil-binder mix, } W_T = W_w + W_{w, \text{slurry}} \quad (5.15)$$

5.3.8.2 Soil-Cement Mix Design - Example Calculations

This section explains the typical sample calculations carried out in the present study to obtain the required amount of material for soil-cement specimen for a consolidation test.

Already known in situ bulk unit weight and moisture content of the foundation soils were directly used in these calculations. The data obtained from standard proctor tests was used to determine the molding water content (i.e. moisture content corresponds to 98% of maximum dry unit weight) wherever necessitated.

A soil sample obtained from sample boring number 1 was used in these calculations. The sample dimensions for a consolidation tests are 2.5 in. or 6.35 cm in diameter and 1 in. or 2.54 cm in height. The following shows sample calculations:

Average in situ bulk unit weight, γ_b :	1,800	kg/m ³
Average in situ water content, w_n (%):	19.59	%
Average dry unit weight, γ_d (from Eq. 5.3):	1,510	kg/m ³
Dry weight of soil, W_s (from Eq. 5.11):	145.17	gms
Binder dosage, α or a_w :	160	kg/m ³
Binder quantity, W_c (from Eq. 5.12)	12.87	gms
Water-binder ratio (w/b):	1.0	

Weight of water from w/b ratio for mixing, $W_{w, \text{slurry}}$ (using Eq. 5.14): 12.87 gms
 and weight of water from in situ water content, W_w (from Eq. 5.13): 24.20 gms
 Total water quantity for mixing (W_T) (from Eq. 5.15): 37.07 gms

Note: In this sample calculations, the number of specimens prepared out of the soil-binder mix are only one and hence, $N = 1$; In the estimation of dry soil mass, an extra amount of soil (η) will be catered for any loss of material during the sample preparation. In the present calculations, this percentage of soil is considered as 10% (i.e. $\eta = 1.1$).

5.4 Discussion of Test Results

5.4.1 Physical Properties of Subgrade Soils

5.4.1.1 Atterberg limit tests

Atterberg limit tests were performed on representative soil samples collected from each site. The soils were classified based on Unified Soil Classification System (USCS) and the results for soil samples collected from IH 30 was presented in Tables 5.3.

From the results shown in Table 5.3, it can be seen that all soil specimens obtained from soil borings number 1 and 2 and the selected fill are classified as low plasticity clays. The embankment was constructed using local native soil. The information is confirmed by the values of liquid limit, plastic limit and plastic index, which are not significantly different between values of the embankment and values of both subgrade soils.

Table 5.3 Physical properties of control soils from site IH30

Property	Test Designation		IH 30		
	TxDOT	ASTM	$B_{\text{Treated Section}}$	$B_{\text{Control Section}}$	SF
Liquid Limit (LL)	Tex-104-E	ASTM D4318	38	39	43
Plastic Limit (PL)	Tex-105-E	ASTM D4318	20	15	18
Plasticity Index (PI)	Tex-105-E	ASTM D4318	18	24	25
Specific gravity	Tex-108-E	ASTM D854	2.70	2.70	2.70
USCS classification	Tex-142-E	ASTM D2487	CL	CL	CL

The in-situ natural moisture content (w_n) and bulk unit weight (γ_b) for the subgrade soils from site IH30 were determined after the undisturbed specimens were brought from the construction site to the laboratory. The water content at soil bore number 1 and 2 are 19.6% and 15.5 % respectively. The bulk unit weights of the representative samples are 115 pcf (1.85 g/cm^3) and 122 pcf (1.95 g/cm^3), in respective for soil bore number 1 and 2.

Figure 5.8 presents the grain size distribution curves for both the ECS and the select fill materials. The ECS is a uniformly graded coarse grained material with little fines and has a coefficient of uniformity (C_u) = 2.8 and coefficient of curvature (C_c) = 2.6. ECS can be classified with the letter symbol GP based on the unified soil classification system (USCS). The normal fill or the control soil has a C_u = 18.9 and C_c = 0.61 along with a liquid limit = 29% and a plasticity index = 5. The select fill soil has been classified as silty sand with a letter symbol SM according to the USCS.

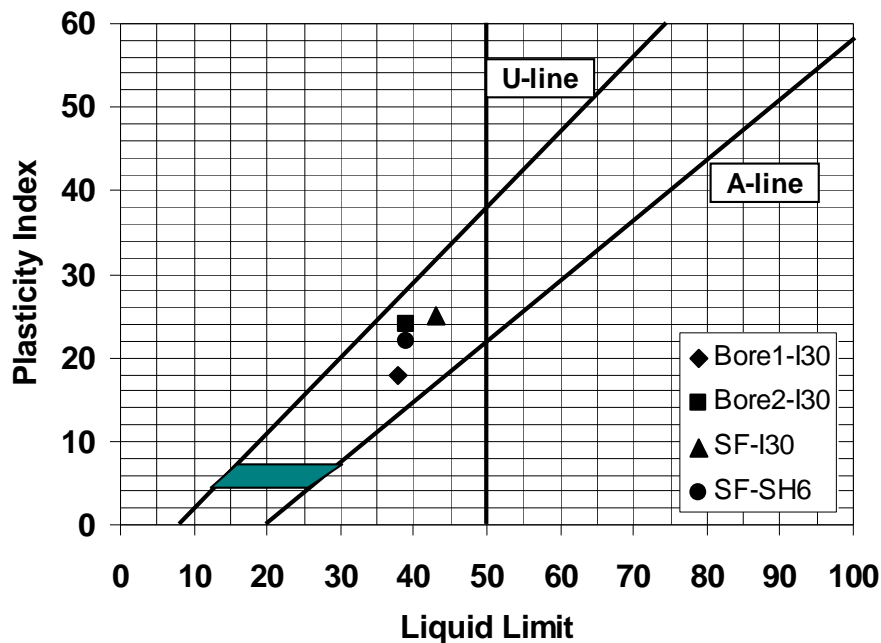


Figure 5.7 Casagrande's plasticity chart and type of soil samples

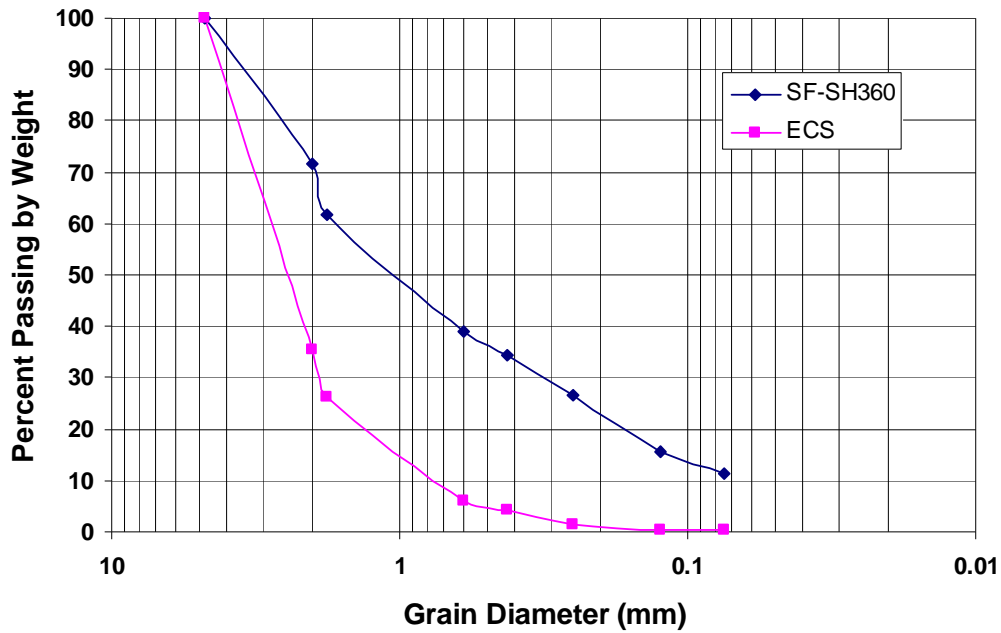


Figure 5.8 Grain size distribution curves of soil samples from site SH360

5.4.1.2 Standard Proctor Test

Compaction tests were performed to establish moisture-density relationships especially for the selected fill of embankment on all three bridge sites. The optimum moisture content (OMC) of the soil is the water content at which the soil is compacted to a maximum dry density (MDD) condition. As shown in Figures 5.9 and 5.10, at the water content at 98% of maximum dry density condition the selected fill on site LH30 has water content of 12% at the dry unit weight of 107 pcf (1.70 g/cm³), while selected fill SH360 has a water content of 10.6% at dry unit weight of 134 pcf (2.14 g/cm³). These values of water content and dry density were used further to investigate the compressibility and strength properties of the selected fill materials.

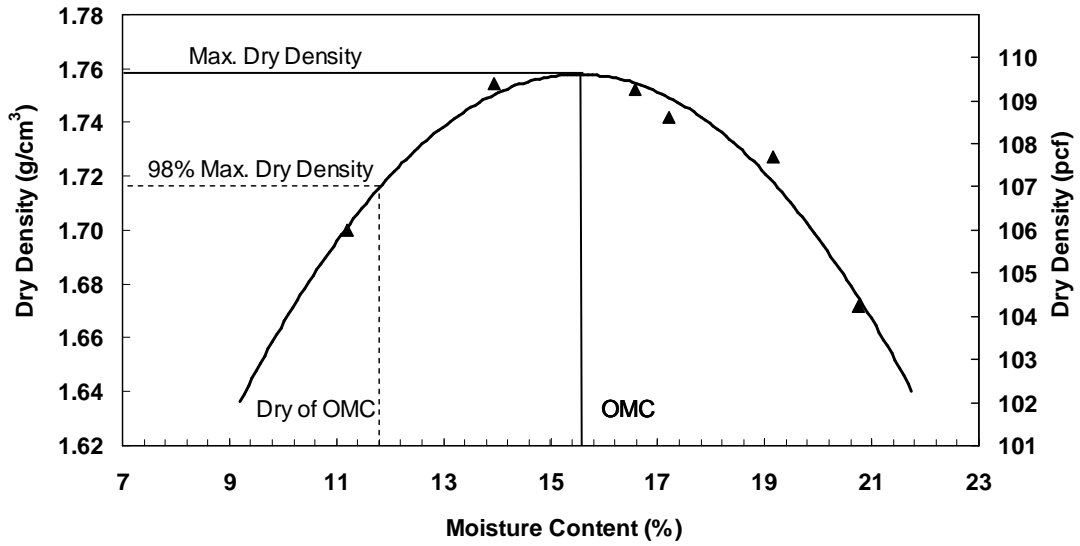


Figure 5.9 Standard Proctor curve of selected fill from site IH30

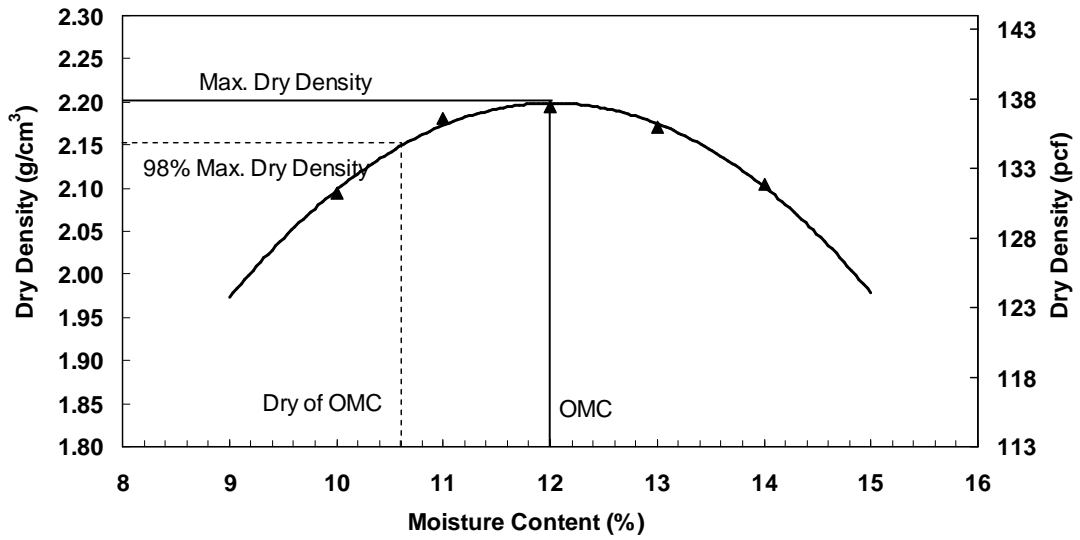


Figure 5.10 Standard Proctor Curve of selected fill from site SH360

5.4.2 Engineering Properties of Soils

5.4.2.1 Swell and Shrink Properties

The free swell (F_s) strains of the soil specimens bore number 1, number 2 and selected fill from Sites IH 30 are 4, 12 and 9%, in the same order, while the strain value of the selected fill specimen from site SH 360 and SH 6 are 9 and 2.2%, respectively. The percent of free swell with time is reported in Figure 5.11 and these results indicate that the maximum swell was recorded in about 480 minutes under saturated conditions. However, it must be noted that swelling time of bore number 1 from site IH 30 was 20 days but the whole data was not plotted due to a limitation of the Figure. The ECS and soil-cement sample showed their low swell strain values. Contrary to the conventional hypothesis, the maximum swell strains are recorded for specimens from bore number 2 and selected fill are different even both soil specimens have the same PI value. Therefore, the swell properties do not correlate well with PIs of soils.

The shrinkage strains from the linear shrinkage bar tests (Tex-107-E) were performed on representative soil samples from the three bridge sites and the results are shown in Table 5.6. Opposing from the results of swell strain values, the shrinkage strain values show more correlated to values of PI of each soils. Specimens from borehole number 1 (PI=18) from site I30 has the shrinkage strain values of 5.51, while specimens from borehole number 2 (PI=24) and selected fill (PI=25) have the strain values of 11.81 and 14.76, respectively. The same tendency can be seen from selected fill soil from SH 6, which has PI value of 22 and the strain value of 12.67.

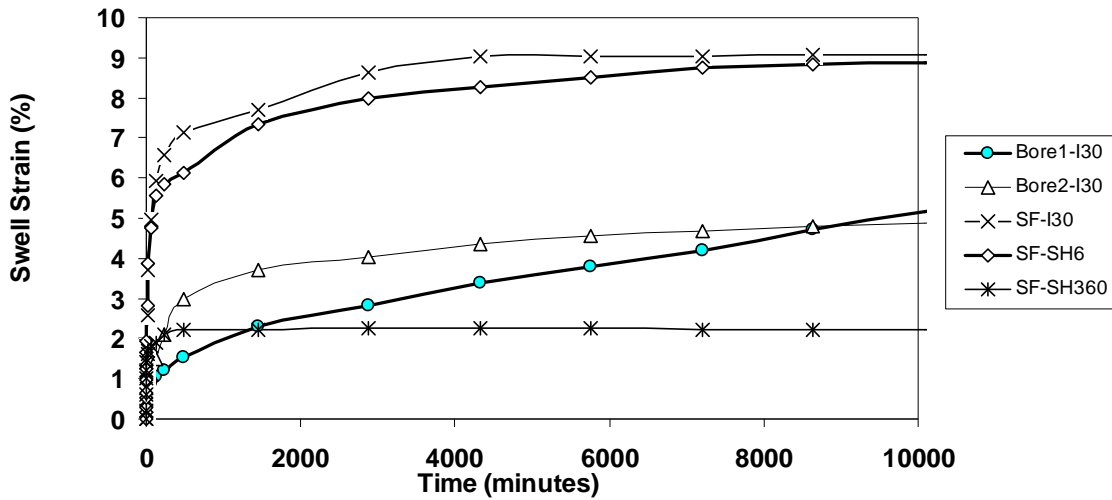


Figure 5.11 Free swell test results from studied sites

5.4.2.2 Compressibility Properties

After the one-dimensional free swell tests had been performed per ASTM D-2435-96 and the void ratios had been obtained, the load increments and specimen deformations were plotted in a semi-log scale. The compression and recompression index of soil specimens, C_c and C_r respectively, were achieved by calculating the slope of the compression and recompression curves. The values of C_c and C_r of soil specimens are shown in Table 5.4 and consolidation curves are shown in Figures 5.12 and 5.13.

It can be seen from Table 5.4 that the compression index of subgrade soil from bore number 1 has both compression (C_c) and recompression (C_r) indices more than values from bore number 2. However, both of these soil properties from bore number 1 were improved after the soil had been modified with cement. From this treatment method, the C_c value reduced from 0.390 to 0.263 and C_r value reduced from 0.046 to 0.035. Furthermore, the soil-cement mix can also increase the pre-compression pressure (σ_r) of the specimens. From Figure 5.12, it is clearly seen that the σ_r increased 3 times from 5,000 psf to 15,000 psf than untreated soil. It can lead to a conclusion that at the same amount of load acting upon the soil-cement and untreated soil, the soil-cement will have less amount of settlement than a natural soil due to less C_c and

more σ_r values. As shown in Table 5.4, selected fill specimens from three sites have low C_c and C_r values due to the reason that the soil was compacted to reach 98% of its highest density. For a granular material like the ECS, as expected, both C_c and C_r values of this material are very low.

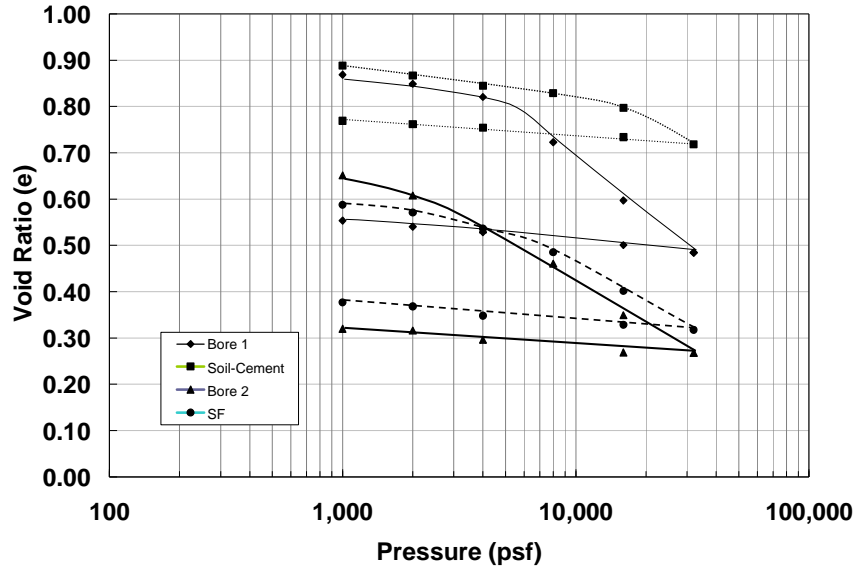


Figure 5.12 Consolidation curves of soil specimens from site IH30

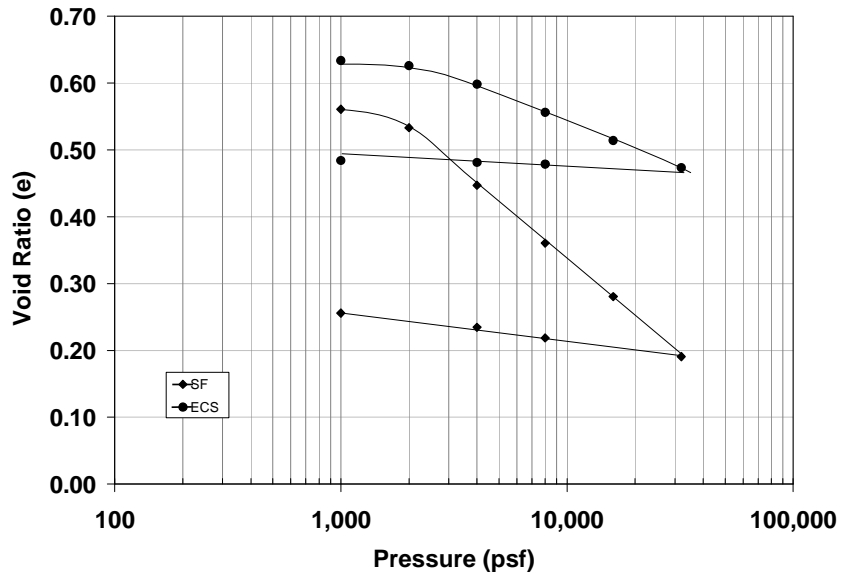


Figure 5.13 Consolidation curves of local and ECS soil specimens from site SH360

5.4.2.3 Strength and Stiffness Properties

The strength of the cohesive soils from three bridge sites was evaluated through unconfined compression Strength (UCS) tests. These tests were performed in accordance with the procedure explained in sections 5.3.6. The unconfined compressive strength (q_u) is estimated from Equations (5.6), (5.7) and stress-strain curve as shown in Figure 5.14. The average values of q_u are also shown in Table 6. The UCS values of soil specimens from site IH 30, for bore number 1 is 1.02 tsf (range from 0.87 to 1.18 tsf), from bore number 2 is 0.80 tsf (range from 0.63 to 0.96 tsf), for selected fill is 1.02 (range from 1.43 to 1.64 tsf) and for soil-cement sample is 7.04 tsf (range from 8.2 to 8.8 tsf). The UCS values of selected fill specimens from site SH360 are 2.47 tsf (range from 2.1 to 2.67 tsf).

It can be seen that ground improvement either by chemical or mechanical method can increase unconfined compressive strength values. The untreated subgrade soils have a low value of unconfined compressive strength, while treated subgrade soil as a soil-cement specimen has a strength value of 7.04 tsf, which is a higher than almost 7 times the value of untreated soil.

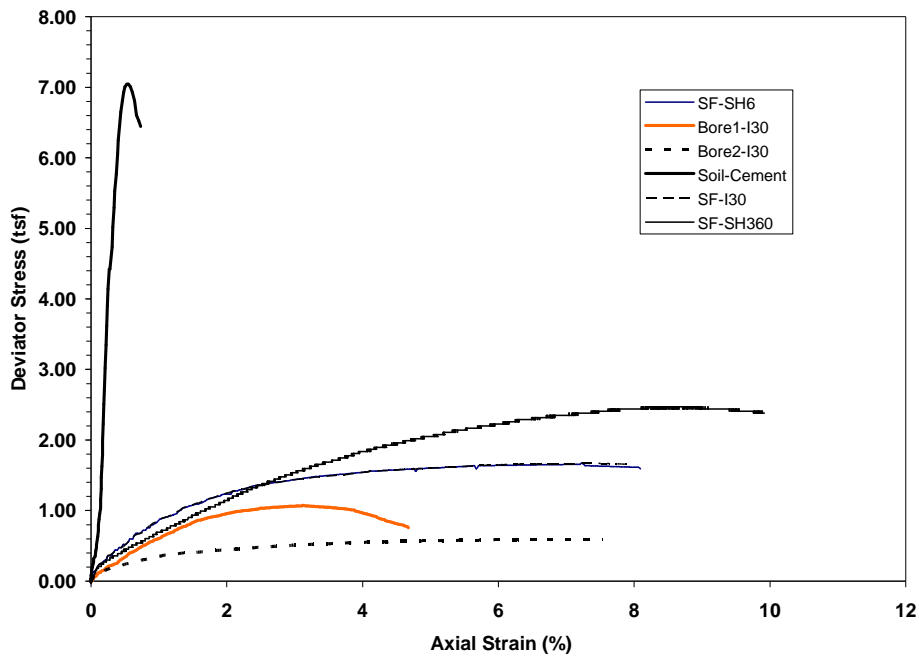


Figure 5.14 Stress-strain curves of soil specimens from unconfined compression tests.

Table 5.4 Engineering properties of soil specimens from Sites IH 30 and SH 360

Property	IH 30				SH 360	
	B1 (treated Section)	Soil- Cement (B1)	B2 (Control section)	SF	ECS	SF
Swell Index (%)	13	2	4	9	0	2.2
Linear shrinkage strain (%)	5.51	1.57	11.81	14.76	n.a.	n.a.
Compression Index (C_c)	0.392	0.263	0.307	0.265	0.141	0.280
Recompression Index (C_r)	0.046	0.035	0.037	0.047	0.012	0.039
Unconfined Compressive Strength (tsf)	1.02	7.04	0.80	1.67	n.a.	2.47
c	n.a.	n.a.	n.a.	n.a.	74.5	n.a.
ϕ	n.a.	n.a.	n.a.	n.a.	49	n.a.

Note: n.a. -not available

B1 - Bore at treated section

B2 - Bore at control section

5.5 Summary

This chapter presents a series of laboratory tests conducted on natural materials and manufactured materials obtained from two different bridge sites to evaluate their compressibility and strength characteristics. For the natural soils, all of the soil samples obtained were classified based on the unified soil classification system as low plastic clays with an average PI of 25, only the select fill used on north side of SH 360 bridge was classified as sandy silt (SM). The compressibility characteristics of the materials tested are found to be in permissible limits, with the lowest value from ECS material (select fill used at ECS site, SH 360). Furthermore, it can be concluded that the physical soil properties can be improved through soil-cement treatment (DSM). It is found that the soil-cement treatment improves not only the compressibility characteristics of the foundation soils, but also the strength of the material. The results obtained from the laboratory works in this chapter are needed for the design of mitigation techniques and later performance validation studies of the numerical analysis.

CHAPTER 6

CONSTRUCTION AND INSTRUMENTATION OF DSM AND ECS SECTIONS

6.1 Introduction

As discussed in Chapter 3, this research selected two methods as viable techniques to mitigate the settlement at the bridge approach problem. The first technique is using DSM columns for improvement of deep seated expansive soils beneath highways, while another technique is using the ECS as a lightweight fill material from embankment construction to reduce a dead load exerting on the soft soil subgrade. To evaluate the application of those two techniques in real field conditions, a study of DSM and ECS test sections were performed in two different locations with some instrumentation placements. In addition to the investigation on the treated test sections, a control section without any treatment on each site was also performed. In conclusion, each mitigation method has its own test site, and each test site has one test and one control section. The instruments used include horizontal inclinometer, vertical inclinometer, sondex and rod extensometer to investigate the settlement transpired in the fields.

This chapter presents the procedures for the construction and instrumentation practices in the fields on both sites as described in following sections.

6.2 Sites Descriptions

6.2.1 DSM Columns, IH 30, Arlington, Texas

As noted in chapter 4, a new bridge on I-30 in Arlington, Texas was constructed on a weak foundation system that was stabilized with the deep soil mixing or DSM columns as a mitigation technique to improve the weak foundation soil. Soil cement columns of 4.0 ft (1.2 m) diameter with a spacing of 5.5 ft (1.7 m) center to center spacing were constructed in the test site and the layout of the DSM treatment shows as a dotted area in Figure 6.1. The shaded zone represents the weak soil zone under the bridge embankment.



Figure 6.1 Details of weak soil and DSM treatment, IH 30 site, Arlington, TX

6.2.2 ECS Backfill Material, SH 360, Arlington, Texas

The ECS was used as a backfill material to construct the northbound lanes of a new bridge structure constructed at south end extension of SH-360. The total quantity of the ECS constructed in this project was 26,242 yd³ (20202 m³). This site was considered as an example of fill treatment for a new bridge construction.

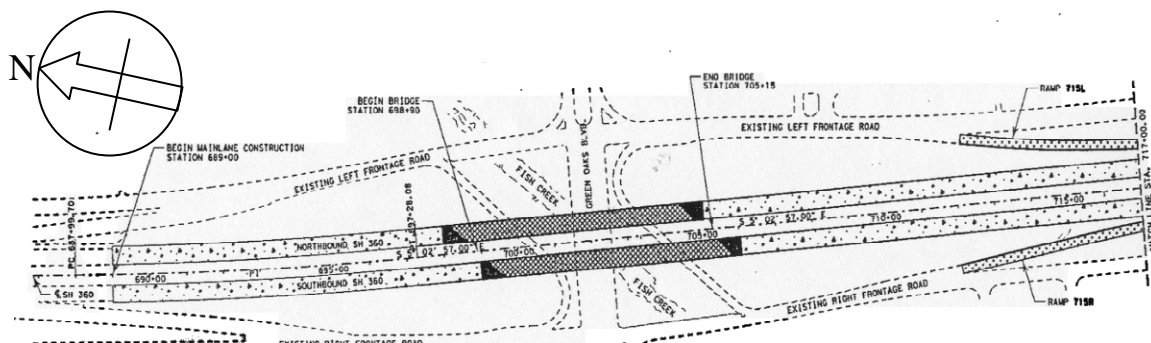


Figure 6.2 Details of ECS Bridge Site, SH 360, Arlington, TX

6.2.3 Geopier, SH-6 across US-90 A, Houston, Texas

Geopier is another mitigation method which was used to support MSE walls and embankments of the SH-6 Bridge site constructed over US-90A in Houston, Texas. The Geopier columns have a diameter of 30 in. (75 cm) and their length vary from 12 to 25 ft (3.5 to

7.5 m). The sites of both locations, North bound entrance ramp and South bound exit ramp, are shown in Figure 6.3. This site was not a major focus of this research as it was constructed and monitored much earlier than the initiation of this research. Hence no major conclusions are reported with respect to Geopier technology and only observations related to approach settlements are only reported with respect to this application.

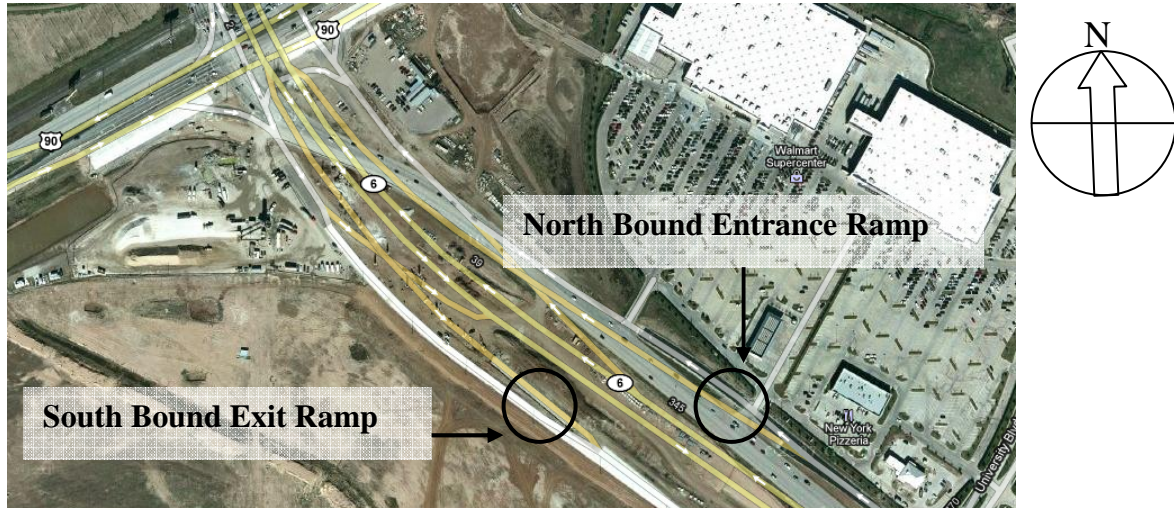


Figure 6.3 Details of Geopier Bridge Site, SH-6 and US 90A, Houston, TX

The following sections provide detailed descriptions of both DSM and light weight fill material used at the construction sites, respectively.

6.3 Design Specifications of Materials and Geometry Details for DSM Treated Test Sections

The following provides the specifications of materials used in construction of the DSM columns. The plan and sectional views showing geometrical specifications are also presented below.

6.3.1 Specifications of Binder Materials

Below are the specifications of materials, including binders and water, arrived at following the laboratory studies for construction of the DSM columns:

1. Binder was composed of 100% of Ordinary Portland cement Type I/II.
2. A binder dosage rate of 160 kg/m^3 (10 pcf) was used.
3. A water to binder ratio of 4:1 was recommended for field grout preparation.

6.3.2 Specifications of Geogrid

Table 6.1 describes specification details of the Geogrid and anchor rods used during construction of the DSM test sections.

Table 6.1 Details the Geogrid

Type	Biaxial Geogrid
Tensile Strength	20 kN/m or of 1400 lb/ft (both in machine and cross-machine directions)
Material	Polypropylene

6.3.3 Specifications of DSM Column Geometry and Arrangement

According to the design of DSM columns in chapter 4, the DSM columns were constructed as a triangular arrangement with a center-to-center column spacing of 5.5 ft (1.65 m) with an area ratio (a_r) of 50%. The column dimensions are 4 ft (1.2 m) in diameter and 25 ft (7.5 m) in length or until the tip of the columns seating on a hard shale layer. The sectional and plan views of the DSM treated sections are depicted in Figure 6.4. The perspective plan view of the DSM construction is shown in Figure 6.5.

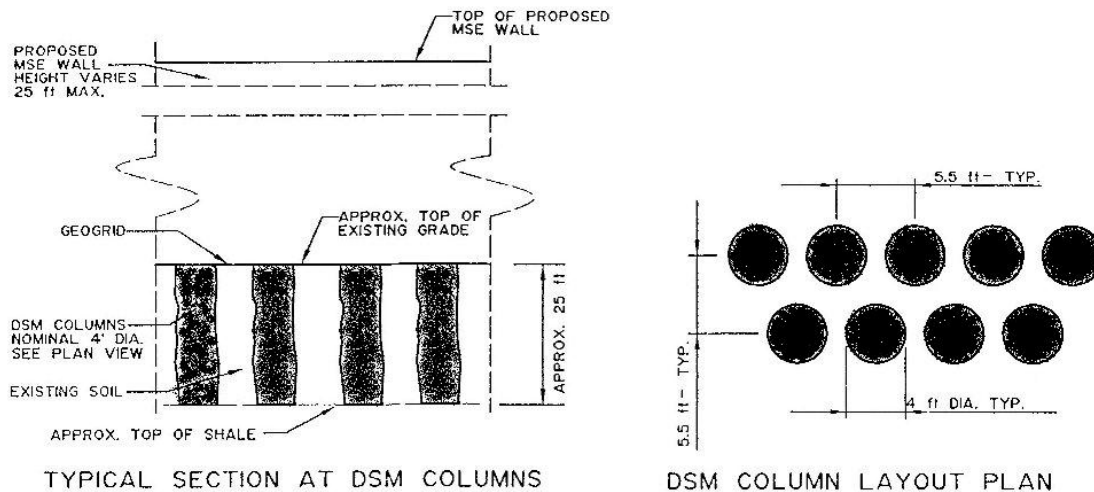


Figure 6.4 Sectional details of DSM columns at Site IH30

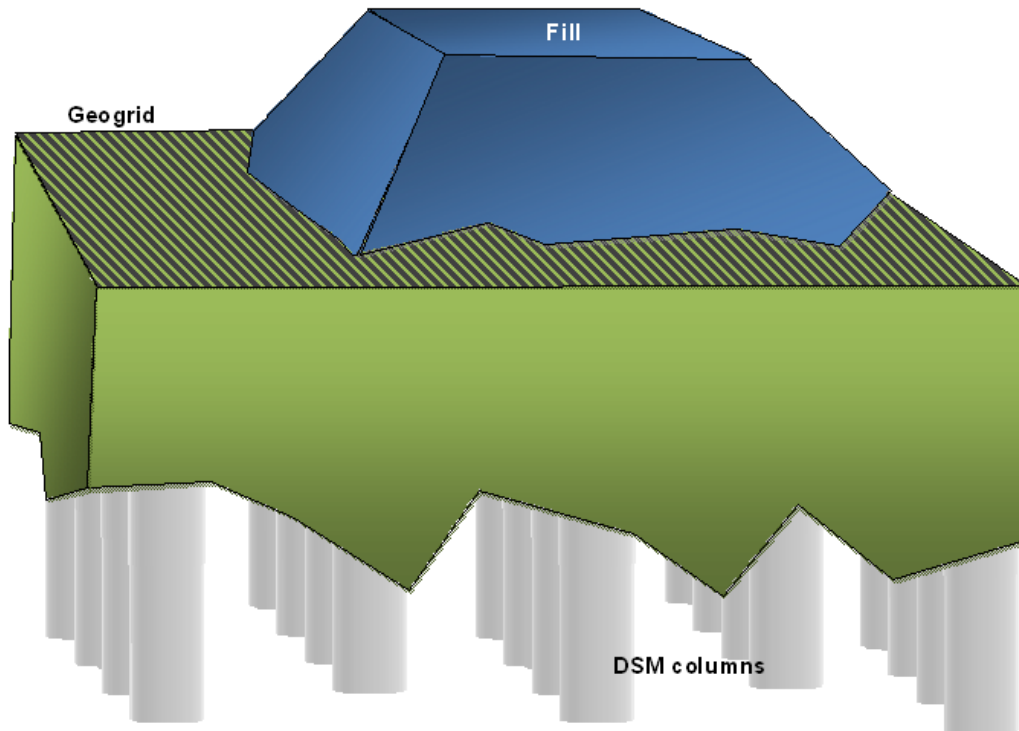


Figure 6.5 A typical perspective view of DSM treated-geogrid-reinforced test section

6.4 Construction of DSM Columns

The construction procedure of the DSM column installation according to the DSM Work Plan Report (RECON, 2007) is presented in the following steps.

1. Following the design recommendation, the survey was done to establish the proper position of the DSM elements. In this step, the center points of each row of DSM columns were surveyed and staked.
2. Before starting the construction of the DSM columns, a hydraulic auger mounted on an excavator was used to remove soil from ground surface at each location of the DSM columns to create space to accommodate soil-cement spoil collection.
3. After the pre-augering, the auger was positioned over the DSM center mark, then 4-ft diameter hole was bored to the required depth (25 ft or until reach the shale strata).

4. The binder slurry of cement was prepared in a large mixing tank at the project site. The quantity of water was measured with a flow meter, while the cement was measured with a flow scale. The colloidal mixer was used to produce the grout. The cement and water was circulated and agitated. The finished grout would be pumped to the holding tank.
5. During the DSM operation, the grout was pumped with high-pressure-progressive cavity pumps, which have a capacity of 100 gpm at pressure 100 psi. The grout was pumped from the holding tank through a hose to a grout swivel on top of the mixing tool shaft. The swivel allows the grout to flow through the shaft and exit through ports on mixing tool, while the tool is rotating. The grout flow rate was monitored at the pump with a flow meter, and was regulated by “bypassing” a portion of the grout flow to the holding tank.
6. The hydraulic drill was mounted with a crawler to systematically advance, rotate and withdrawal the four ft diameter mixing tools. Grout was injected through the bottom of the mixing tool during the initial penetration of the augers, or during subsequent stroking of the element.
7. Upon reaching the soil-cement element, mixing and stroking would continue at adequate speed and duration to mix all loose, soft and unmixed soil prior to final withdrawal of the mixing tool.

6.5 Construction of the Embankment with ECS

The light weight aggregate fill, expanded clay shale or ECS was used to construct the embankment of the bridge on the highway SH360 in Arlington, Texas. The ECS was delivered to the bridge site in trucks like natural fill materials. Then, it was spread uniformly in horizontal by tracked vehicles in layers not exceed 12 in. thick. Each layer was compacted using vibratory compaction equipment with 10 tons static weight. A minimum of 3 passes is required to ensure full compaction. The best method of site control is by measuring the settlement of the

compacted layer, which should not be more than 10% of the layer thickness or 1.2 in. Totally, a quantity of 26, 242 yd³ was used in the embankment construction in the project.

6.6 Construction of the Geopiers

The Geopier was purposed to support MSE walls and embankments of the SH-6 Bridge constructed over US-90A in Houston as shown in Figure 6.3. The researcher was not involved during design procedures; however, has a permit to investigate the efficiency of the Geopier in providing sufficient support for its above structures.

According to geotechnical data obtained from the TxDOT, the subsurface soils on site below the embankments are soft clay soils. Base on the subsurface soil data, the results from the stability analysis of the embankment slope show that the factors of safety in a long term condition are between 1.0 and 1.1, which are lower than 1.25 (a minimum factor of safety required by TxDOT). Moreover, the results from the settlement analysis show that the settlements at the retaining wall of the 20-ft-high embankments give a yield of 4.6 in. and with a differential settlement between the edge and corner of 1.3 in. Therefore, to reduce the amount of settlement the Geopier foundation reinforcement was selected to support approach pavements. Details of Geopier methodology are defined as in the following and this information is taken from a Geotechnical Investigation Report (Rep. No. 01-128GH-0, HVJ Associates, 2003)

1. For the North Bound Entrance Ramp with wall heights ranging from 8.0 ft to 13.0 ft:
 - a. Install Geopier elements at an area ratio of 0.06 (two rows of Geopier elements with a spacing of 8.0 ft by 8.0 ft with a zone extending back from the wall face a distance of 10.0 ft. Shaft lengths of 15.0 ft long are required to control settlement and satisfy the bearing capacity and slope stability requirement.

- b. Install Geopier elements at a spacing of 12.0 ft on-center beneath the center portion of the embankment. Shaft lengths of 12.0 ft are required to control settlement.
- 2. For the North Bound Entrance Ramp with wall height ranging from 13.0 ft to 18.0 ft:
 - a. Install Geopier elements at an area ratio of 0.19 (three rows of Geopier elements with a spacing of 5.0 ft by 6.0 ft with a zone extending back from the wall face a distance of 10.0 ft. Shaft lengths of 25.0 ft are required to control settlement and satisfy the bearing capacity and slope stability requirement.
 - b. Install Geopier elements at a spacing of 12.0 ft on-center beneath the center portion of the embankment. Shaft lengths of 25.0 ft are required to control settlement.
- 3. For the South Bound Exit Ramp with wall heights ranging from 8.0 ft to 12.5 ft:
 - a. Install Geopier elements at an area ratio of 0.12 (three rows of Geopier elements with a spacing of 5.0 ft by 9.5 ft with a zone extending back from the wall face a distance of 10.0 ft. Shaft lengths of 15.0 ft are required to control settlement and satisfy the bearing capacity and slope stability requirement.
 - b. Install Geopier elements at a spacing of 12.0 ft on-center beneath the center portion of the embankment. Shaft lengths of 15.0 ft are required to control settlement.
- 4. For the South Bound Exit Ramp with wall heights ranging from 12.5 ft to 17.6 ft:
 - a. Install Geopier elements at an area ratio of 0.25 (three rows of Geopier elements with a spacing of 4.75 ft by 5.0 ft with a zone extending back from the wall face a distance of 10 ft. Shaft lengths of 20 ft are required to

control settlement and satisfy the bearing capacity and slope stability requirement.

- b. Install Geopier elements at a spacing of 12.0 ft on-center beneath the center portion of the embankment. Shaft lengths of 20 ft are required to control settlement.

The construction of Geopier Rammed Aggregate Piers is described in the Geopier Reference manual (Fox and Cowell 1998) and in the literature (Lawton and Fox 1994, Lawton et al. 1994, Lawton and Merry 2000, and Wissman et al. 2000). First, the weak subsurface soils are drilled to get a bore of 30 inch-diameters. Second, to construct the Geopier element the selected aggregate is filled into the bore and then rammed with a beveled tamper with thin lifts, normally about one ft in thickness. Then, the next aggregate filling interval is preceded until the element reaches its required height. The procedures to construct the Geopier are shown in Figure 6.6. The ramming action causes the aggregate to compact vertically as well as to push laterally against the matrix soil. Consequently, the very dense aggregate piers with a high stiffness are formed and resulting in a significantly increased composite stiffness of soil within the Geopier-reinforced zone. In this project, the Geopier was constructed using open-graded stone to afford radial drainage to the piers. The radial drainage of excess pore pressure acts as vertical drains to increase the time rate of settlement.

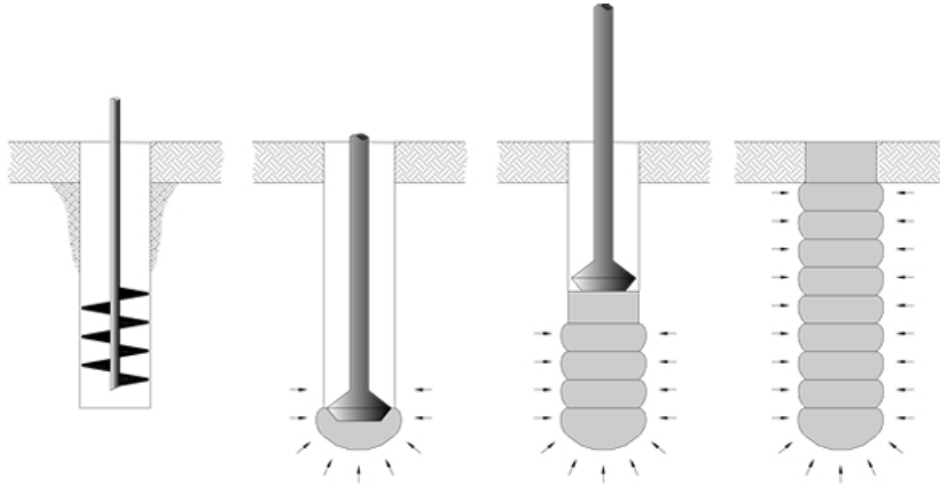


Figure 6.6 Rammed aggregate pier construction process (Sentez Insaat, 2010)
<http://sentezinsaat.com.tr/en/geopier-system.html>

6.7 Instrumentation

In evaluating the field performance of the mitigation techniques in preventing the settlement problem, instrumentation plays an important role in understanding the performance of the structure with time. In the present study, different types of instrumentation were installed in all three sites test sections to observe the performance of the viable techniques to prevent the settlement problem.

The performance evaluation of the mitigation techniques is achieved through regular data collection and analysis related to surface and underlying soil movements with time both in the vertical and horizontal directions. The instrumentation used at IH 30, DSM site are shown in Figure 6.7 and this includes horizontal inclinometer, vertical inclinometer, rod extensometer and sondex, while on site SH 360, ECS site, only vertical inclinometers were installed as shown in Figure 6.8. For a bridge site in Houston, the locations of installed sondex systems and vertical Inclinerometers were used and the locations of instrument are shown in Figure 6.9. Data collections were performed regularly at twice a month at sites IH 30 and SH 360 in Arlington, and once a year at the site SH 6 in Houston. The subsequent sections present the details of the instruments used and the installation procedures followed.

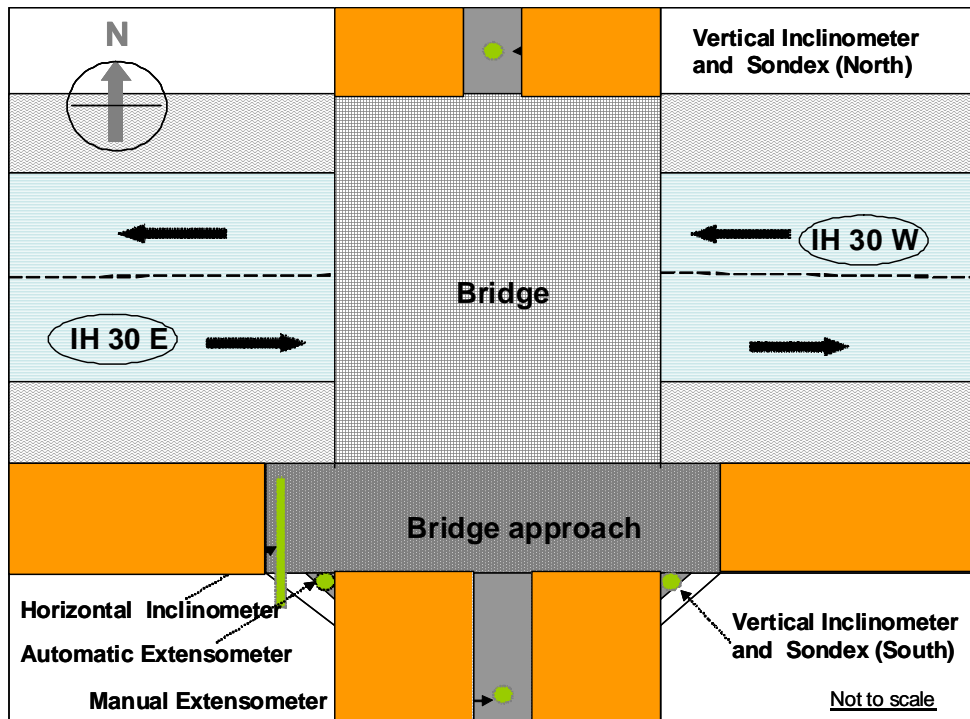


Figure 6.7 Instrumentation details on IH 30, Arlington, Texas

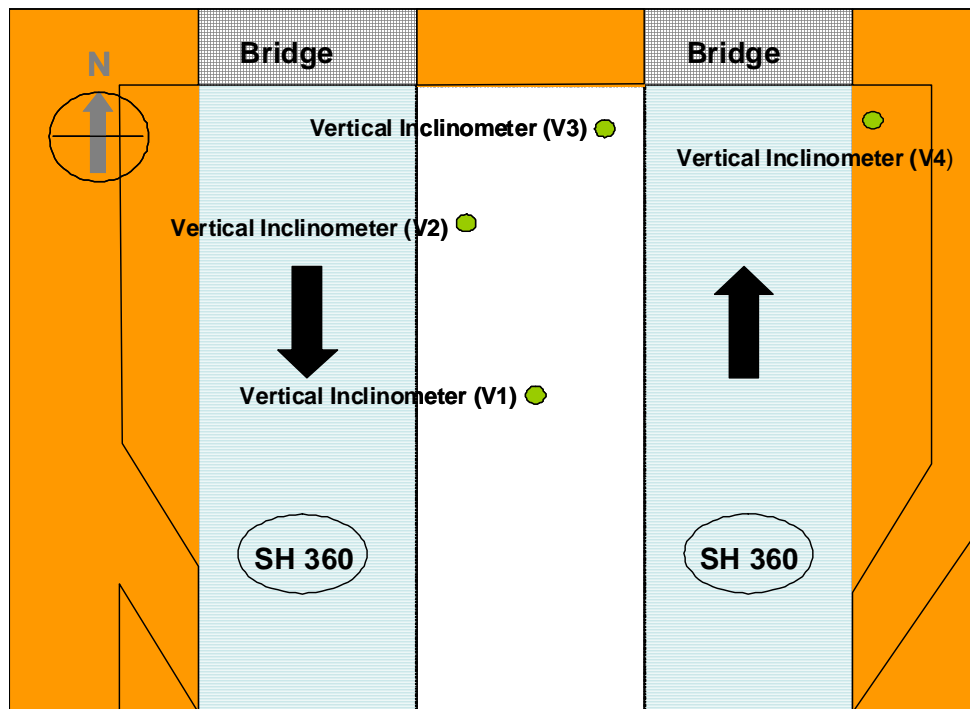


Figure 6.8 Instrumentation details on SH 360, Arlington, Texas

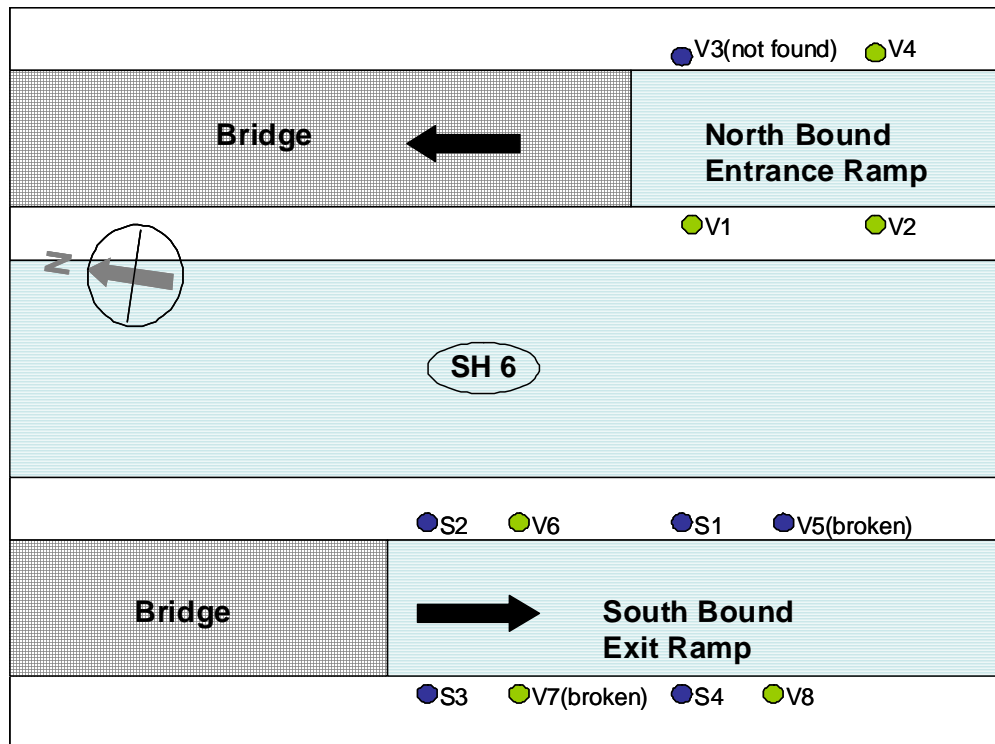


Figure 6.9 Instrumentation details on SH 6, Houston, Texas

6.7.1 *Inclinometers*

Inclinometers are defined as the devices for monitoring surface and subsurface deformations in a perpendicular direction to the axis of a flexible plastic casing by means of a probe passing through the casing (EM 1110-2-1908 – US Army Corps). The inclinometer casing is an ABS (acrylonitrile-butadiene-styrene) plastic pipe, which inside has 4 groves perpendicular with each others as shown in Figure 6.10. The casings are available in various diameters 1.9 in. (4.8 cm), 2.75 in. (7.0 cm) and 3.34 in. (8.5 cm). The small diameter casings (1.9 in.) are suitable for measuring small deformations, therefore they are not chosen for monitoring soil movements in this study. Whereas, the 2.75 and 3.34 in. diameter casings are suitable for monitoring moderate to large deformations and are suitable for application in construction projects (foundations, embankments, slopes, landslides and retaining walls). In this research, the 3.34 in. diameter pipe was selected to be a casing for horizontal inclinometer probes, while the 2.75 in. diameter casing was using as the vertical inclinometer probes. The casings used in

this project have a length of 10 ft (3 m). Therefore, for the casing installation longer than 10 ft (3 m) the casings are assembled by pushing the female end of one casing into the male end of another, as shown in Figure 6.11. Typical details of the casing are also depicted in Figure 6.11 (a). More details about repairing and assembling the casings can be found in Slope Indicator (2010). The following subsections present the principles involved, installation details and subsequent monitoring procedures of both vertical and horizontal inclinometers.

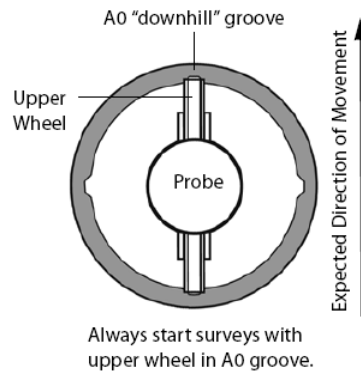


Figure 6.10 Details of inside inclinometer casing and a probe (Slope Indicator, 2006).

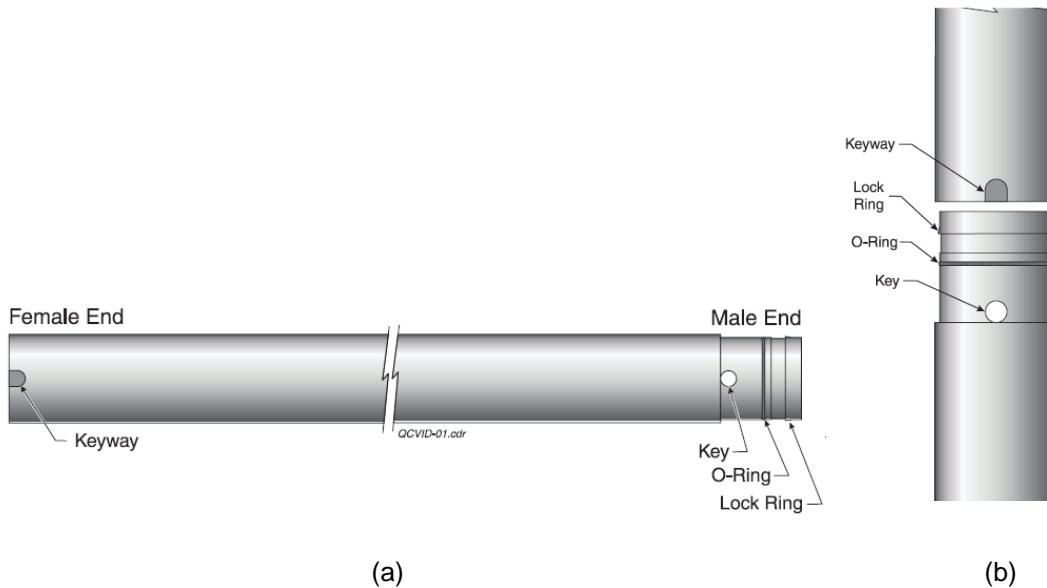


Figure 6.11 (a) Details of inclinometer casing and (b) Assembling procedure (Slope Indicator, 2009).

6.7.1.1 Vertical Inclinerometers

An inclinometer probe is used to monitor the lateral deformations of engineering structures (foundations, embankments, landslides, slopes, retaining walls etc.) by passing it through the inclinometer casing. The inclinometer probe uses its two force-balanced accelerometers inside the probe to measure the inclination of the axis of the casing pipe with respect to the vertical. The details of the probe and planes of measurement are shown in Figure 6.12. The two accelerometers help in measuring the lateral movements in both the A and B directions, as shown in Figure 6.12(b). The plane in which the deformations are measured along the wheels is the A-axis, while the one perpendicular to the wheels is the B-axis. Therefore, it is necessary to align one set of grooves along the expected direction of movement during casing installation. The components included in the inclinometer unit are a flexible plastic guide casing, a portable probe, labeled control cable, readout unit and a pulley assembly.

The principle involved in measuring the lateral deformations using a vertical probe is as follows. The probe measures the angle of inclination of the inclinometer casing axis with respect to the vertical which is then converted into lateral movement using a sine function. From Figure 6.13, deviation, δ_i , at an interval 'i', is

$$\delta_i = L \times \sin \theta_i \quad (6.1)$$

To obtain the profile of the casing the deviation at each interval is calculated by summing the values from bottom of the casing until that interval ($\sum \delta_i$), as shown in Figure 6.13.

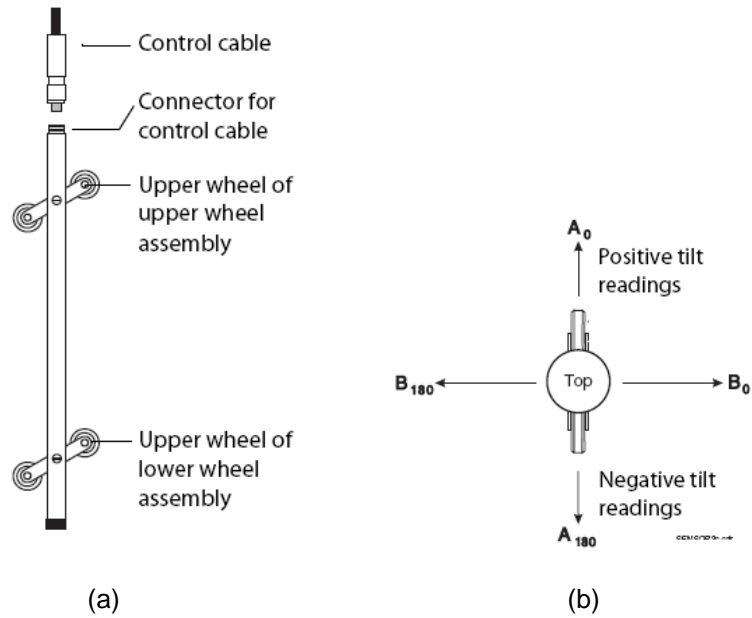


Figure 6.12 Details of inclinometer probe (Slope Indicator 2000); (a) Components and (b) Measurement planes.

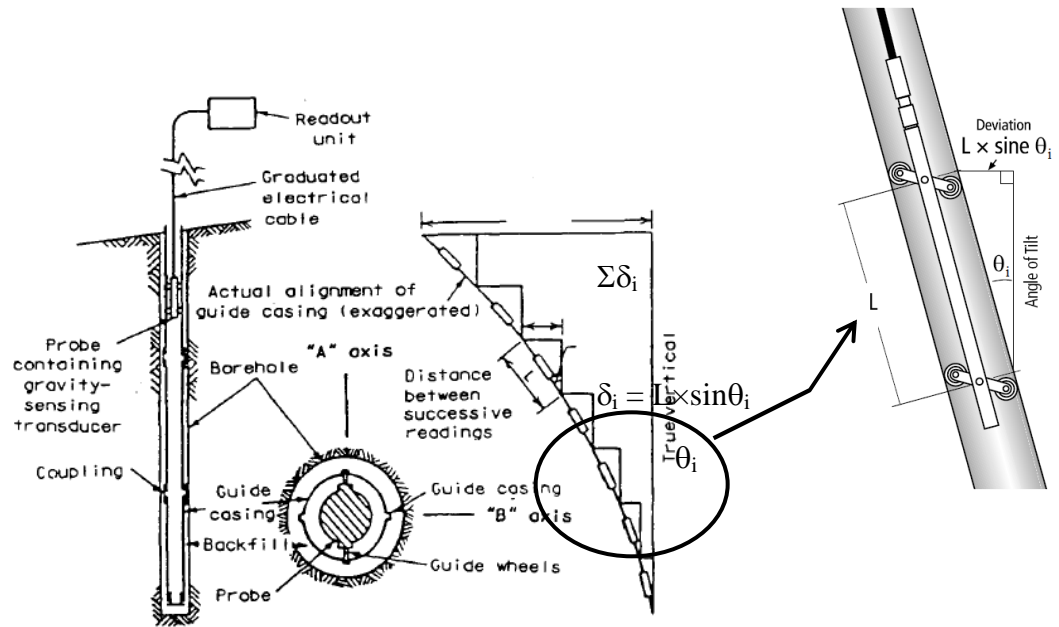


Figure 6.13 Principle in inclinometers for measuring deformation (Dunncliff, 1988)

In the present study, on site IH30, two vertical inclinometers were installed in the DSM treated section, while one was installed in the control embankment. Two locations near the side slopes of the treated embankment were selected considering the importance of the location that will address erosion performance issues of treated area. The depth of installation, from the surface of fill to the shale strata, is varied from 52 to 54 ft (15.6 to 16.2 m).

The step by step procedure followed for installation of vertical inclinometers is as follows:

1. After the locations of inclinometer were selected, boreholes were drilled using an auger as shown in Figure 6.14. While drilling, it is important to maintain the verticality of the borehole throughout the monitoring depth.
2. Before inserting the first casing, the bottom of the casing was closed using a bottom cap as shown in Figure 6.15.
3. After the bottom of borehole reached the required depth, the inclinometer casing was inserted into the borehole (Figure 6.16). The casing was assembled during the casing installation with the pipe clamping technique (Figure 6.17). A bentonite-cement grout mix was used to fill the gap between casings and bore during this procedure (Figure 6.18). The grout mix is prepared at the site in a slurry form and delivered into the gap using a grout pipe or a hose. A well prepared grout mix should be free of lumps and thin enough to pump; at the same time it should be able to set in reasonable time, but too much water will result in shrinking the grout, leaving the upper portion ungrouted (Slope Indicator, 2000). Because of the low consistency of the grout mix, it is expected to maintain the continuity without any air pockets locked in between along the depth.
4. At the time of filling the gap with the grout mix, it is necessary to make sure the inclinometer casing is prevented from floating due to buoyancy forces. In the present study, this is achieved by filling the casing with water as shown in Figure 6.19.



Figure 6.14 A selected location was bored to install the inclinometer casing



Figure 6.15 A bottom of the casing was plugged with a bottom cap



Figure 6.16 The casing installation after reaching the required drilling depth

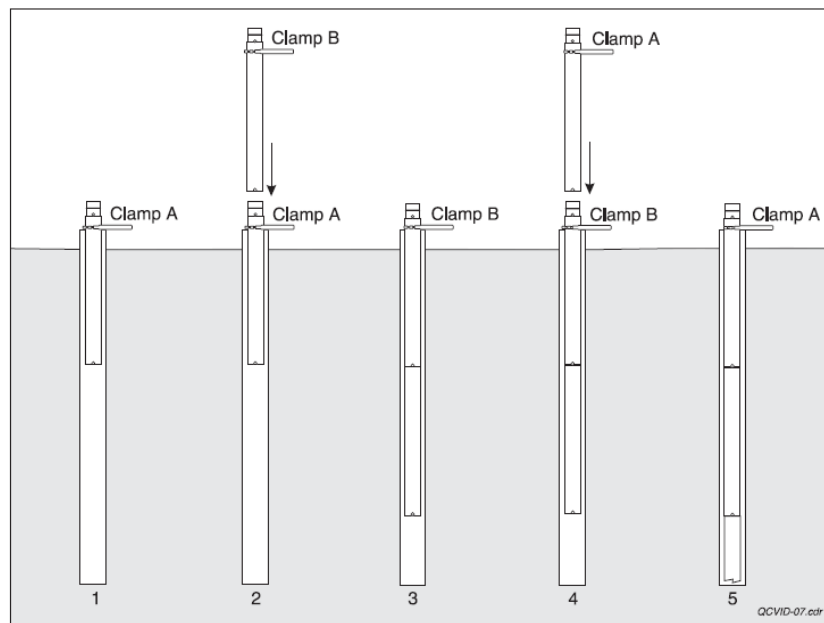


Figure 6.17 The pipe clamping techniques required for casing installation
 (Slope Indicator, 2009)
 (<http://www.slopeindicator.com/pdf/manuals/qc-casing-installation-guide.pdf>)



Figure 6.18 The gap between casings and bore was filled with grout mixing



Figure 6.19 Water was filled into the casing to avoid floating due to buoyancy

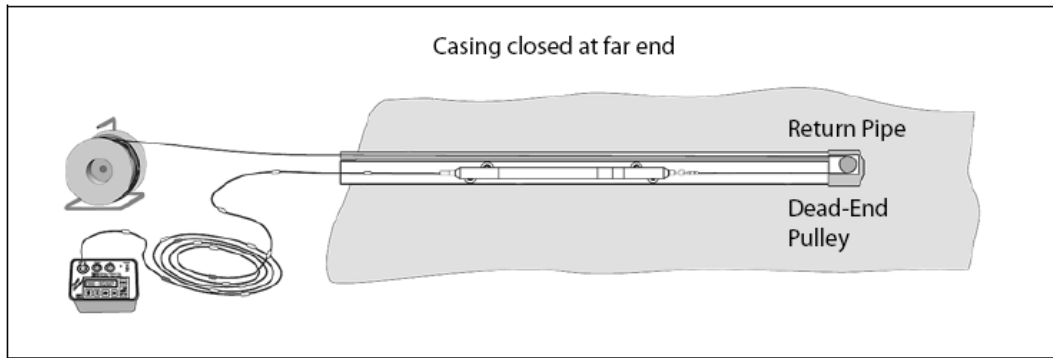
5. The proportions of bentonite-cement grout mix should be adjusted such that the 28-day strength is similar to the strength of the in situ soils. The proportions of bentonite, cement and water recommended for stiff and soft in situ clayey soils can be found in Slope Indicator (2000). As soon as the installation of the casings and construction of the test section is completed, the initial profile of the casing is obtained by running the inclinometer probe through the casing. Readings should be taken from bottom to top by initially lowering the probe to the bottom of the casing and then pulling it upwards to each interval. The details of monitoring and data collection procedures are presented in the following chapter.

6.7.1.2 Horizontal Inclinometer

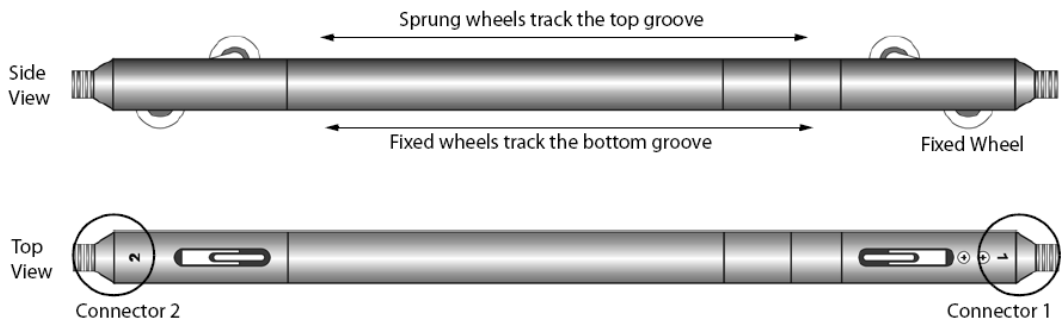
Typical applications of horizontal inclinometers include measurement of settlement and/or heave under storage tanks, embankments, and dams etc. In the present study, horizontal inclinometers were used to monitor the vertical surface movements in the DSM treated composite test sections. This was achieved by passing a horizontal probe through the casing. Two inclinometer casings of diameter 3.34 in. (8.5 cm) were installed in the treated section on the south side of the bridge. They were placed under the bridge approach slab, traffic moving in the eastward direction. The casings have a total length of 80 ft (3.33 m), which covers the highway pavement, a pedestrian walkway and a side slope.

The components of the horizontal inclinometer include the horizontal probe, graduated control cable, pull cable, and a readout unit. The schematic of the horizontal inclinometer unit setup and details of the horizontal probe are shown in Figure 6.20. The wheels on one side of the probe are fixed and are always kept in the bottom groove of the casing during an inclinometer survey. The principle involved in measuring vertical movements is the same as that used for the vertical inclinometer probe. Unlike the vertical probe, the horizontal probe contains one force-balanced accelerometer and measures the deviation of the casing axis along the plane of wheels from the horizontal. The profile of the casing can be obtained by plotting the

measurements at each interval along the length of the casing. Any change in the profile of the casing compared to the initial profile from subsequent surveys indicates the surface movements.



(a)



(b)

Figure 6.20 (a) Schematic of horizontal inclinometer setup and (b) Horizontal probe

The following steps describe the procedure followed for installation of the horizontal inclinometers:

1. Trenches of size 1.5 × 2 ft (0.5 × 0.6 m) are excavated at selected locations along the width of the test sections as shown in Figure 6.21. As per the Slope Indicator manual (2005), a small gradient of 5% is maintained along the length of the casing for drainage purposes.
2. The trenches are then cleaned and a layer of sand is placed for proper seating of the inclinometer casing.

3. Casings are laid carefully into the trenches, while assembling from one end until the required length is reached and simultaneously a stainless steel cable is pulled through the casing. In the present study, casing closed at far end installation type was selected as shown in Figure 6.20 (a).
4. At the time of assembling the casings, one set of grooves were aligned vertical to the ground surface to measure surface movements. The procedure for assembling the inclinometer casings are the same as that explained in the above section.
5. To check the alignment of the grooves at the junction of two casings, it is recommended to run the probe through the casing from the near end to far end and back again.



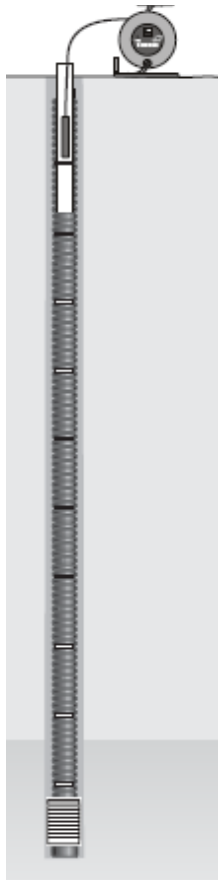
Figure 6.21 A trench was excavated at the selected location.

6. Care was taken to avoid any debris and dirt from entering the casing during installation.
7. Finally, the trenches were backfilled and the casing ends were closed using caps. The ends should always be kept closed, except at the time of survey, to prevent any debris from entering the casing during the monitoring period

6.7.2 Sondex Settlement System

The Sondex Settlement system is used along with inclinometer casing to measure settlement and heave associated with excavation, construction, backfill, or tunneling operations. The Sondex system is installed by placing corrugated pipes, with which have stainless steel sensing ring attached around the pipes, outside of the inclinometer casing as shown in Figure 6.22 (a). Figure 6.22 (b) shows the components of the Sondex system include a Sondex readout and the corrugated. From the picture, it can be seen that the readout consists of a reel with a built-in voltmeter, a measured cable and a probe.

A depth measurement is done by reading from the survey tape, while the probe is being drawn through the center of the casing and a buzzer sounds when a ring is detected. The probe contains a reed switch which closes when a sensing ring is detected, sounding a buzzer on the reel. The annular space between the borehole wall and the corrugated pipe is backfilled with soft grout, coupling the pipe to the surrounding ground, so that the corrugated pipe and rings move with settlement or heave. Settlement and heave are calculated by comparing the current depth to the initial value.



(a)



(b)

Figure 6.22 (a) A typical Sondex installation (b) Sondex system components

Before the casing installation, corrugated pipes were placed on the vertical casing up to the design depths as shown in Figure 6.23. Each corrugated pipe was attached to the casing with mastic and vinyl tape, except for the bottom corrugated which was riveted (Figure 6.24)



Figure 6.23 A corrugated pipe was placed on the vertical casing at a design depth



Figure 6.24 A corrugated pipe was attached on the casing with (a) mastic tape and (b) rivet

6.7.3 Rod Extensometer System

The rod extensometer is installed in boreholes to monitor settlements in foundations, subsidence above tunnels, displacements of retaining structures, and deformations in underground openings. As shown in Figure 6.25, the main components of a rod extensometer are anchors, steel rods inside protective pipe, and a reference head. The anchors are installed downhole with rods spanning the distance from the downhole anchors to the reference head at

the surface. The rods are placed inside the protective plastic pipe to prevent bonding between rods and grout backfill. Readings are obtained at the reference head by measuring the distance between the top (near end) of the rod and a reference surface either manually by a digital depth micrometer or automatically by VW sensors. A change in this distance indicates that movement has occurred. The resulting data can be used to determine the zone, rate, and acceleration of movements, and to calculate strain. Anchors are selected to match field conditions; in this study the groutable anchor suitable for rock was selected.

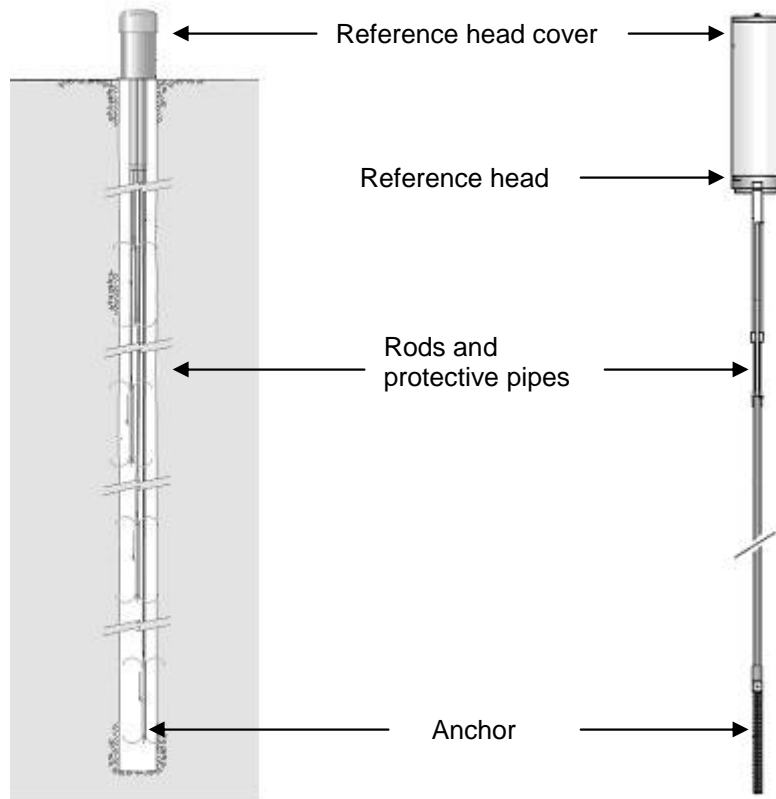


Figure 6.25 Main components of Rod extensometer system

In the present study, two rod extensometer systems were installed at IH 30 site in the south embankment. The mechanical one was installed in the median, while the electrical one was installed close to the approach slab as shown in Figure 6.7. To measure the soil movement occurring in different locations below the embankment surface, each of extensometer system

has 4 sets of steel rod and an anchor installed at the depths of 10, 20, 40 and 50 ft, respectively. Since the deepest anchor was embedded in the shale layer and presumed to be stable, this anchor was used as a bottom reference in the settlement analysis. The settlement calculation must be done by subtracting each value of the other anchors from the change value for the deepest anchor. The details of the calculation analysis can be found in the rod extensometer manual (Slope indicator, 2004).

The step by step procedure to install the rod extensometer system is presented in the following:

1. After the locations of rod extensometer were selected, boreholes were drilled using an auger until the auger tip reached 1 ft below the hard shale layer. In the mean time, the extensometer assembly was carried out.
2. The rod assembly are shown in Figure 6.26, and the procedures are as followings;
 - a. Cut 10 in. (254 mm) off the protective pipe
 - b. Screw anchor adapter into anchor
 - c. Fit rod into anchor adapter, then tighten set screws
 - d. Slide rubber sleeve over anchor adapter
 - e. Screw special pipe coupling onto anchor adapter
 - f. Glue protective pipe into special pipe coupling
3. After the rod assembly was finished, other rods and protective pipes were added until each rod reached required length. The rod and pipe connecting was done as followings;
 - a. Glue coupling onto protective pipe
 - b. Screw on length of rod and tighten
 - c. Slide protective pipe onto rod and glue into coupling
 - d. Continue until correct rod length is obtained
 - e. Cut the last length of protective pipe so that it ends 17 in. (430 mm) below

the top of the rod. Then slide the pipe onto the rod and glue into coupling.

4. When all rods had their length as required depths, the 17-inch-top-part of the rods were installed. The procedures are depicted in Figure 6.27 and described as followings;
 - a. Slide telescoping joint onto rod.
 - b. Glue coupling onto protective pipe.
 - c. Press sensor adapter onto rod and tighten both set screws.
 - d. Pull telescoping joint up over sensor adapter.
5. Once the rod preparation was finished, all rods were connected with the reference head. The components of the reference head are shown in Figure 6.28. The reference head has two half, a top and a bottom one. The center hole in the bottom half is threaded to accept all-thread rod, while the hole in the top half has no threads. The procedures to assemble the reference head are shown in Figure 6.29 and described below;
 - a. Fit bottom half of reference head over telescoping joints.
 - b. Fit O-rings onto the telescoping joints.
 - c. Seat O-rings in reference head, where the unused positions in the reference head are plugged.
 - d. Screw all-thread rod into bottom half of reference head.
 - e. Fit top half of reference head onto bottom half.
 - f. Place steel reference plate onto reference head, and then fasten it with nut.
6. After the rods and the reference head were connected, the whole set of the instrument was placed into the borehole as shown in Figure 6.30.
7. Rope was used to hold up the assembly of rods and reference head in the required position (Figure 6.31). Then, a bentonite-cement grout mix was used to fill the gap between casings and bore during this procedure. The grout mix is prepared at the

site in a slurry form and delivered into the gap using a grout pipe or a hose. For the automatic reading system, the Vibrating Wire displacement sensors were installed in the last step after the grouting had finished. Instead of the procedure mentioned in step 5, the installation of automatic reading sensors were done following these procedures;

- a. Screw sensor clamp in to reference head (Figure 6.32)
- b. Screw sensor shaft into adapter at top of rod (Figure 6.33)
- c. Connect readout to displacement sensor
- d. Move sensor up or down to achieve desired initial reading.
- e. Tighten set screws on sensor clamps

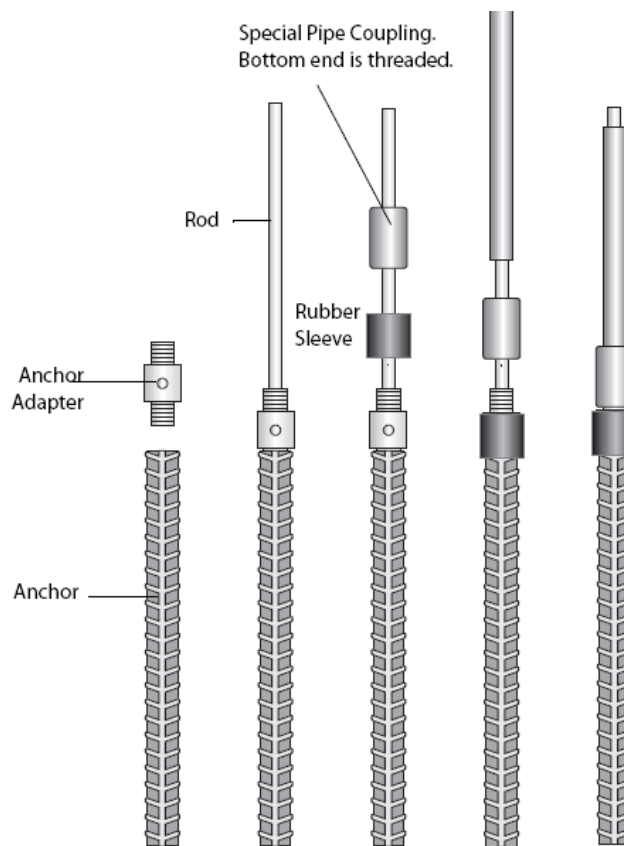


Figure 6.26 The procedures in rod anchor assembly

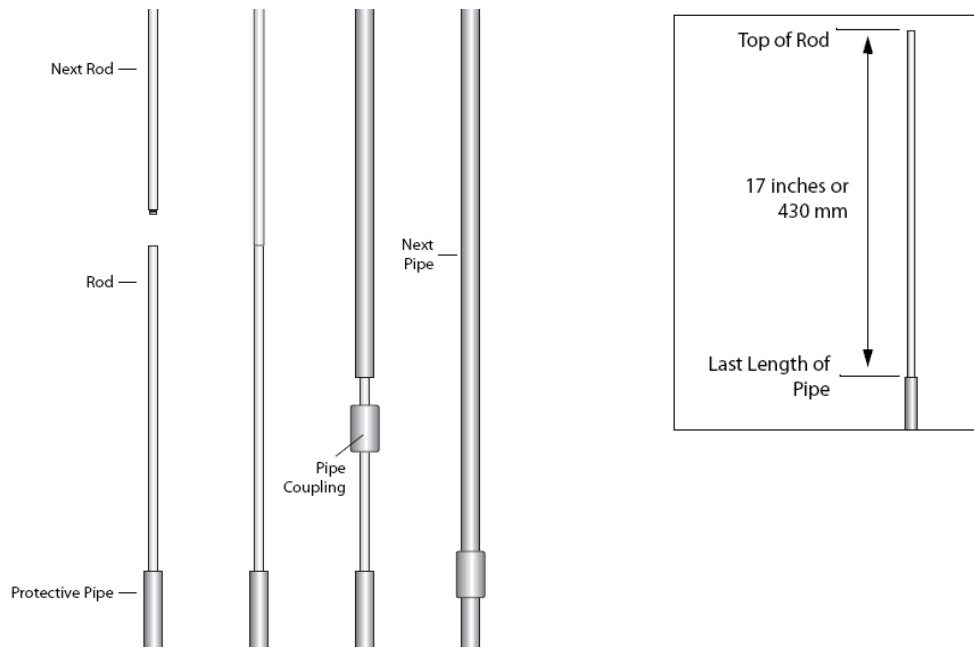


Figure 6.27 The procedures in adding rods and protective pipes

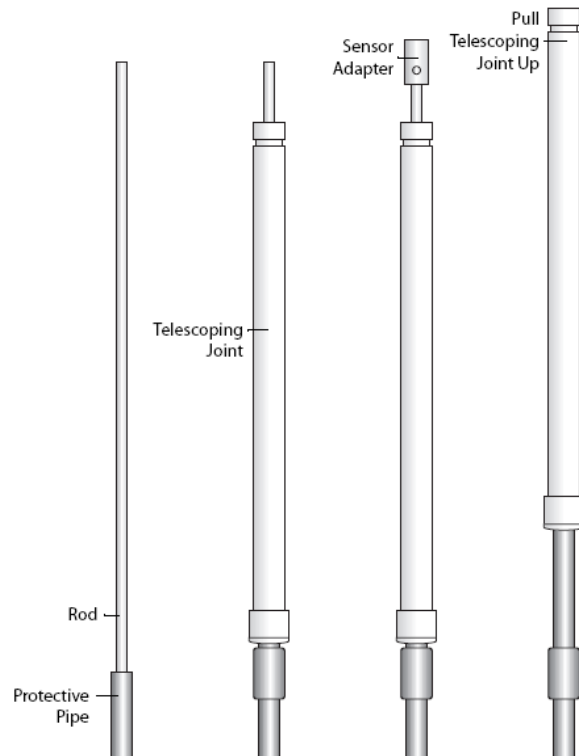


Figure 6.28 The procedures in installing the top part of the rods.

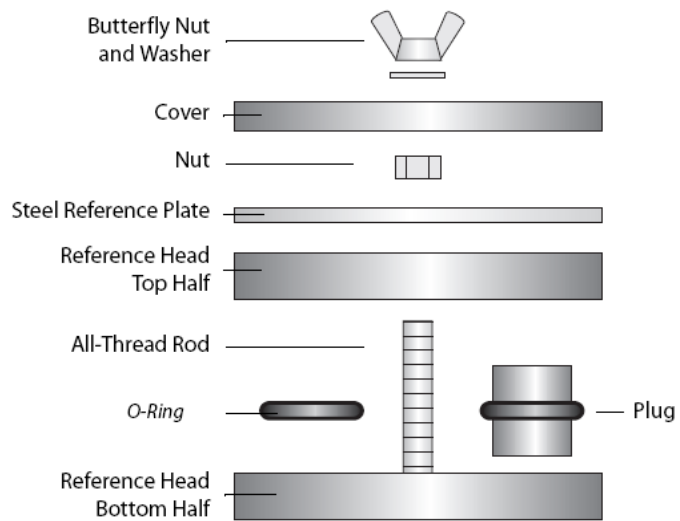


Figure 6.29 The components of reference head

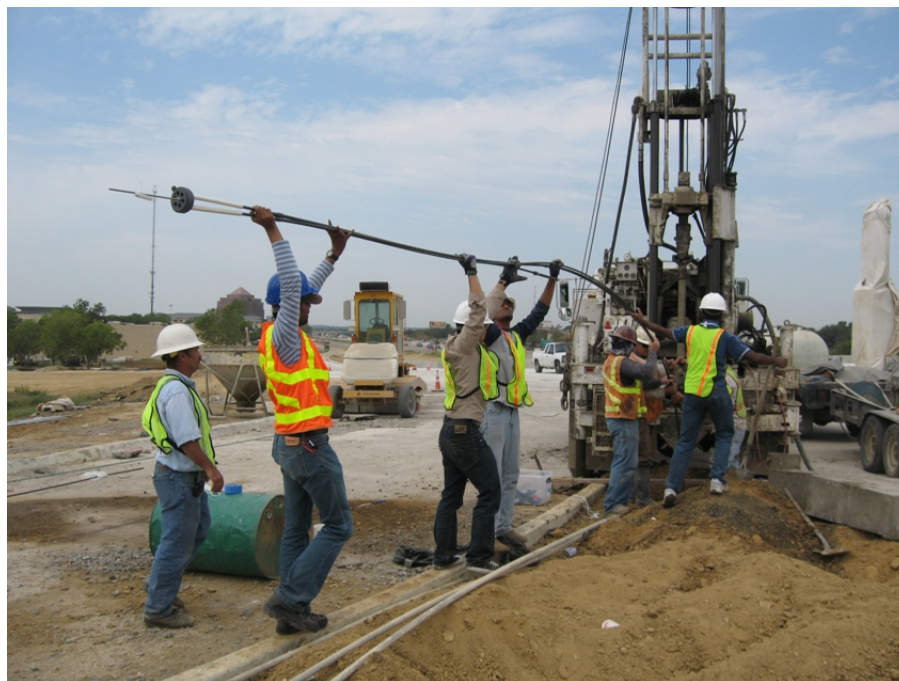


Figure 6.30 The set of assembled rods and reference head were put into the hole.



Figure 6.31 The set of assembled rods and reference head was held up by rope



Figure 6.32 The VW sensor adapters were screwed into the reference head

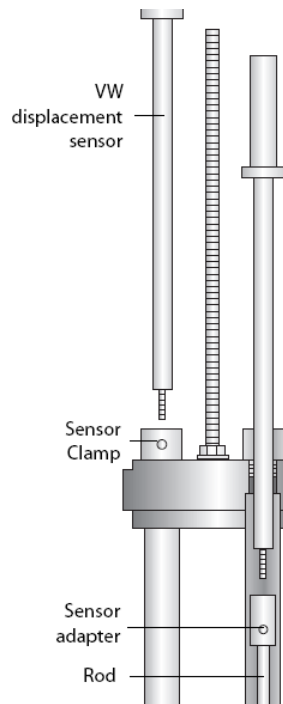


Figure 6.33 The VW sensors were screwed into their adapter

At ECS site, only vertical inclinometers were installed. For settlement monitoring, the total station surveys were performed. After instrumentation was completed, field data was collected at regular intervals. Data collection and analysis are presented in the later sections.

6.8 Summary

This chapter mainly presents construction and instrumentation procedures on the studied sites. To prevent the substantial settlement occurring, three different mitigation techniques were used in the bridge embankment construction. For site IH 30, the DSM was chosen to improve the strength of subgrade beneath the embankment; the ECS was selected to use as a backfill of an embankment on site SH 360 due to its lightweight property, while the Geopier was chosen to support the MSE wall and embankment ramp of the bridge on site SH 6. The instrument used in this research is also presented in this chapter. Many types of tools, for example, horizontal inclinometer, vertical inclinometer, Sondex system and Rod extensometer

system, were installed on different sites to collect the soil movement data in the fields. First, details and principles of the equipment are given and then followed by the installation of it.

CHAPTER 7

ANALYSIS OF FIELD MONITORED DATA

7.1 Introduction

As already discussed in previous chapters, two mitigation techniques were selected in this research to investigate their effectiveness in lessening the differential settlement on the bridge approach slabs. To evaluate the effectiveness of each technique, field instrumentations were performed on test sections. Field performance data was collected at regular time periods from November 2008 to September 2010. Collected data primarily included both lateral and vertical displacements of the approach slab. Data was collected from various sources including horizontal inclinometer, sondex, rod extensometers, and elevation surveys that were used to extract the vertical movements experienced by the slab. The data from horizontal inclinometer and elevation surveys revealed the movements close to the surface, while data from rod extensometer and sondex provided ground movements at various embedded depths. The results obtained were used to analyze in this chapter. The field data and its analysis are presented in detail.

7.2 Performance Evaluation of DSM Stabilization Treated Section

7.2.1 DSM treated section

7.2.1.1 Vertical Soil Movements

DSM treatments were studied on the bridge sections built on IH30 near the center lane exit. Instruments for settlement monitoring included elevation surveys for the vertical movements of soils and two horizontal inclinometers for vertical movements and these studies were performed periodically. Additionally, two rod extensometers were also installed in the same embankment on the DSM treated section. The rod extensometer is an instrument having steel rods connecting between the base at the soil surface and their anchors are buried in the

soil. The extensometer readings indicate the displacement readings occurring in the soil below either by measuring the vibratory frequencies happening in the rods or by using a digital gauge that measures the movements at the rod heads.

Sondex type displacement instrumentation was also installed at this site. This sondex functions similar to the rod extensometer and was used here to monitor the vertical soil movements of various depth segments. The sondex was installed by placing corrugated pipes with stainless steel sensing rings outside the inclinometer casing. The sondex readings were recorded by lowering the probe through the center of the vertical casing, and the readings were collected when the probe passes through the magnetic rings.

7.2.1.1.1. Horizontal Inclinometer

At the IH30 site in Arlington, two horizontal inclinometer casings of 3.34 in. (8.5 cm) diameter were installed underneath the bridge approach slab on the DSM treated section, which is located on the south embankment of the bridge at two locations as shown in Figure 7.1. The details of the horizontal inclinometer probe and casing installation procedures were discussed and presented in the previous chapter. Figure 7.2 shows the horizontal inclinometer installation.

The data readings were surveyed regularly for every two to three weeks to study and observe the settlement behaviors of the treated sections. A standard survey of the horizontal casing included two passes of the probe through the casing with the help of the pull-cable, as shown in Figure 7.3. In the first pass, the labeled end of the probe was connected to the control cable (Figure 7.3 a) and for the second pass the labeled end of the probe was connected to the pull-cable (Figure 7.3 b). Figure 7.3 shows the schematic of horizontal inclinometer surveys (Slope Indicator 2004). The data during the survey were collected and stored using a data storage unit known as DataMate. Thereafter, the collected data was transferred from the Datamate to the computer with software and the results were plotted and viewed with the Digipro program.

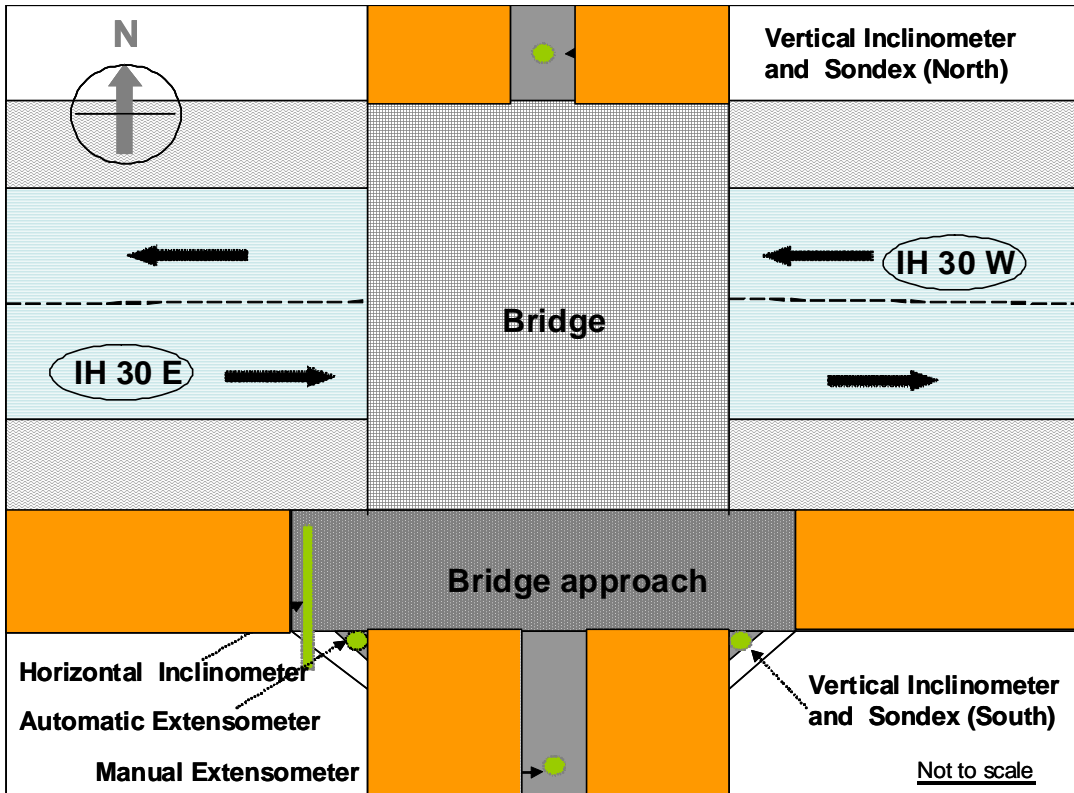


Figure 7.1 Instrumentation on IH30 DSM site, Arlington, Texas

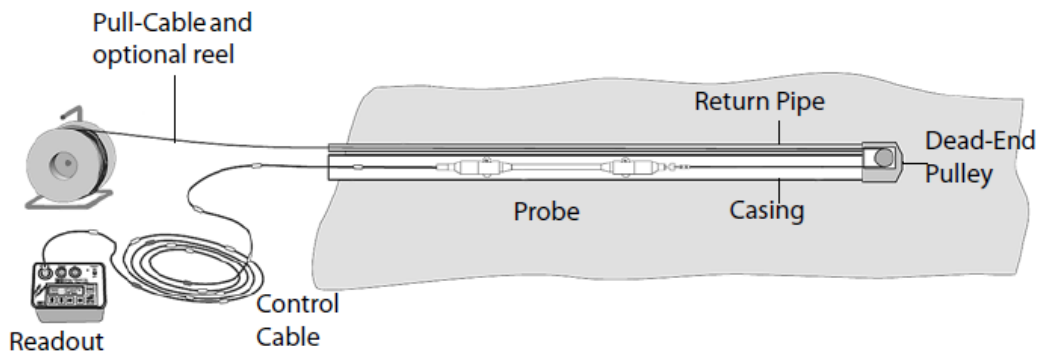
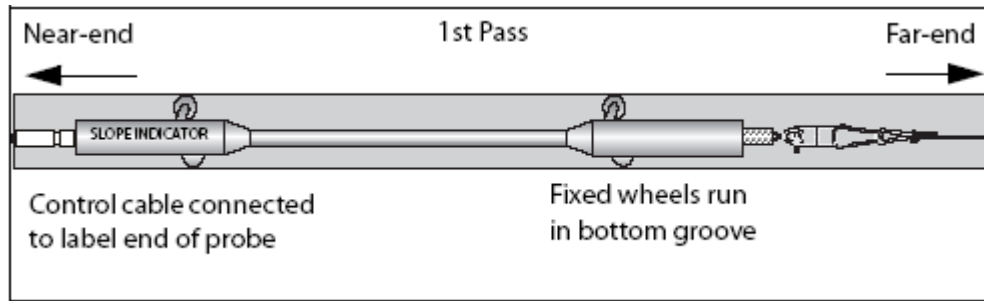
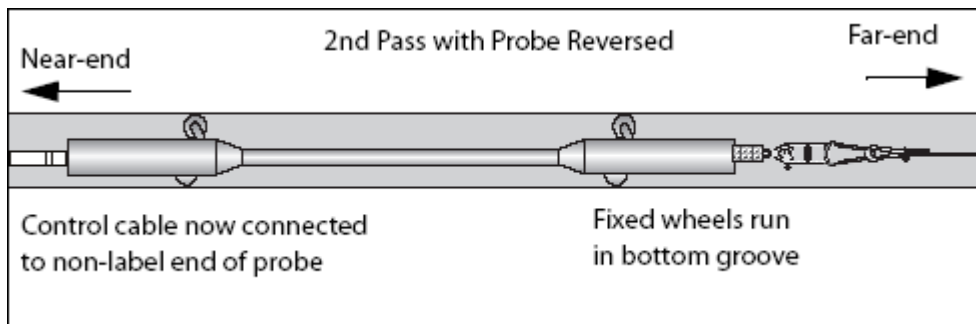


Figure 7.2 The closed-end installation of the horizontal inclinometer (Slope Indicator 2004).



(a)



(b)

Figure 7.3 The horizontal inclinometer readings scheme (a) 1st Pass (b) 2nd Pass (Slope Indicator 2004).

As mentioned, two horizontal inclinometer casings were originally installed at this site. However, after the installation, one inclinometer located near the east end of the embankment was broken during the construction of the approach slab. Due to difficulty in repair or fix this casing (Figure 7.4), this one was not accessed for settlement monitoring in the subsequent monitoring work.

The data readings of the other inclinometer casing on the west side were performed periodically in every two-three weeks. The readings were obtained with an inclinometer probe and a data logger as shown in Figure 7.5.



Figure 7.4 The location of the broken casing



Figure 7.5 Inclinometer data retrieves

The data is presented in the form of graphs plotted between the horizontal inclinometer displacements in inch versus length of the probe in foot. Each plot normally shows the change of casing profile at that moment when compared with the initial one at the time of installation which was used as a reference. Since the displacements occurred in every fortnight, it is too complicate to show or to discuss all the results; therefore, the displacements recorded on monthly basis are used and plotted on the graphs. The horizontal inclinometer casing on this site has a total length of 78 ft; 32 ft was laid beneath a fill slope and a pedestrian side walk, 20 ft was laid under a highway pavement, and 26 ft as laid underneath an approach slab. However, the total length of the casing was reduced to 48 ft in December, 2009, since it was broken at the length of 48 ft from its open end. The data collection was eventually terminated in April, 2010 due to the loss of the cable broken off due to probable rusting.

To clarify the plots of the cumulative displacement, the displacement data are presented separately into two graphs. Both graphs show the soil movement data happened over the last three years, but use a different date as their reference in the movement calculation (before and after the approach slab construction finished). Figure 7.6 shows cumulative displacements along a casing length of 78 ft from July, 2008 to December, 2009 (during a construction of the approach slab), whereas Figure 7.7 presents the displacement data occurred after the construction of the slab had been finished (used November 2008 data as a reference). The displacement data occurred after the casing was broken is presented separately later.

From the profile of inclinometer readings as shown in Figures 7.6, the following observations are noted:

- The inclinometer profiles before and after of the approach slab construction had shown some major changes in the soil movements underneath the embankment sections.

- On November 8, 2008, in the first 8 ft, the straight line of the casing can be noticeable. The reason is this part of the inclinometer pipe was damaged during the construction of the embankment and the approach slab. Since the broken part located near the pipe end, the researcher was not able fix or repairs the problem. A new 10 ft casing was brought to replace the damaged one, and thereafter it was cut to keep the whole length of the pipe to be 78 ft.
- The maximum displacement on the inclinometer casing occurred at a length of 48 ft from the open end and the magnitude of this displaced was 1.70 in. This value was with respect to the initial position of the casing at the time of installation.
- In total, four humps with displacements more than 1 in. along the inclinometer casing are noticed. These humps show that the casing profile had dramatically changed from the straight-line at the time of installation to the humps soon after the construction completion. The locations that have camel-hump curves are the points that significantly changed in the curvature between right and left sides of the localized points. The bending at these convex or concave points also shows high strains occurring between their top and bottom parts of the casing, and this induces high stresses. Therefore, the humps along the casing can be considered as the weak points in the casing and adjacent subsoils, which can result in the breaking of the casing.
- More settlements can be noticed at the lengths from the opened end till the length of 32 ft. This length of the casing was laid along the slope and the pedestrian sidewalk.

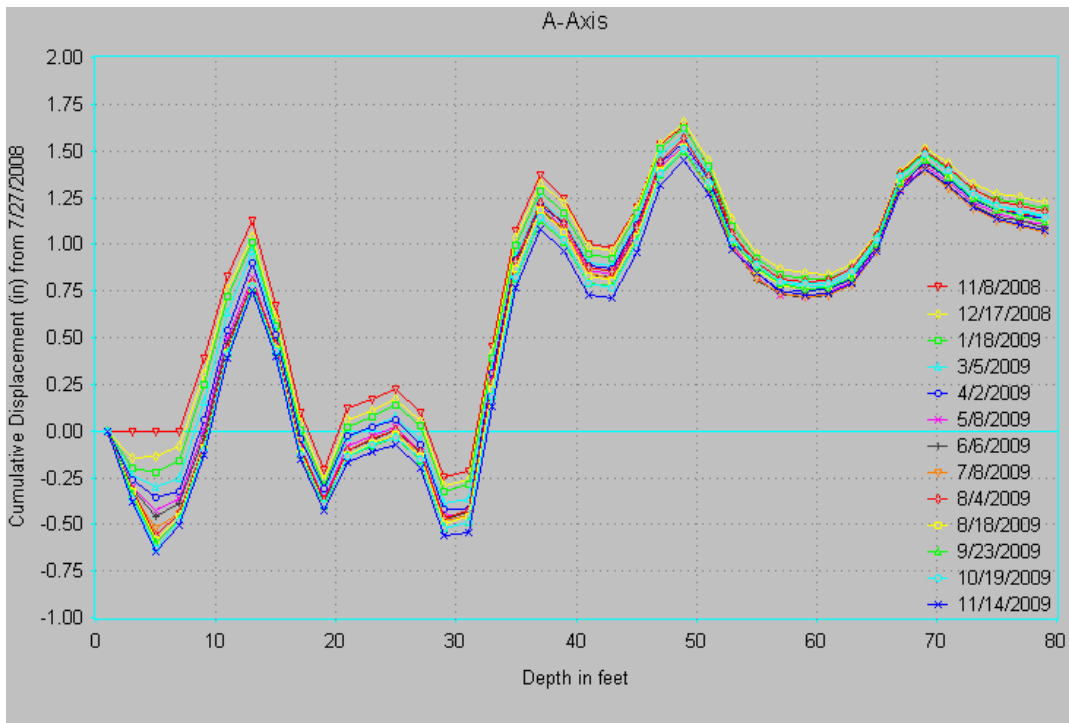


Figure 7.6 The cumulative displacements from 11/8/2008 to 11/14/2009 (compared with a casing profile before the construction of the approach slab finished)

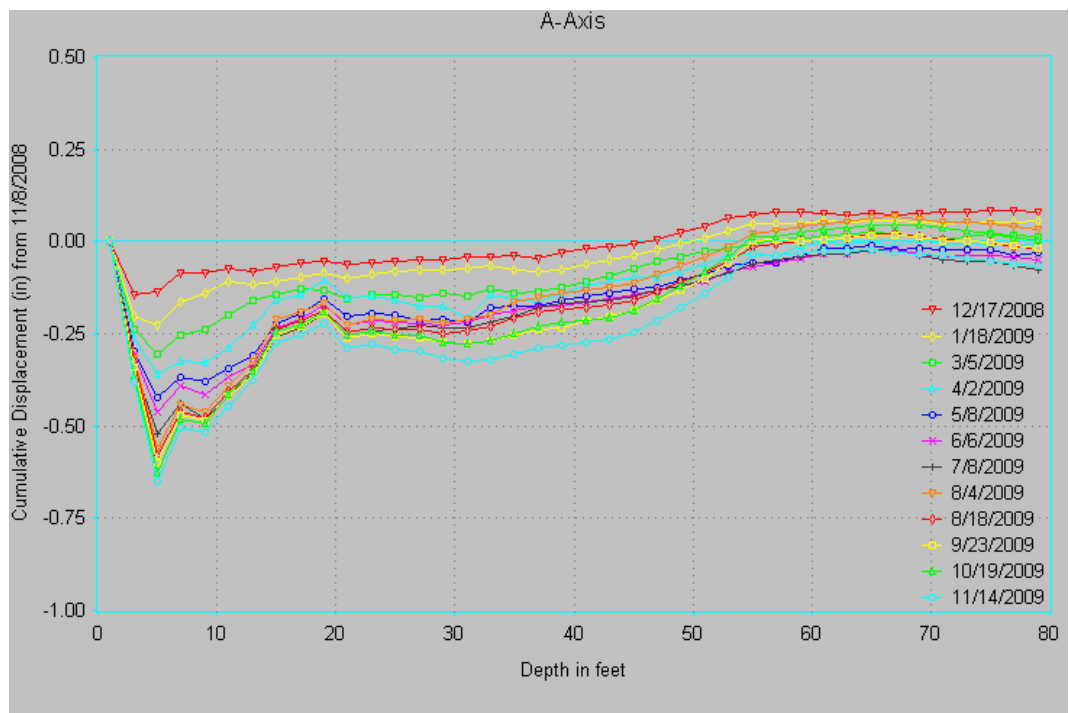


Figure 7.7 The cumulative displacements from 11/23/2008 to 4/14/2010 (compared with a casing profile after the construction of the approach slab finished)

- It can be observed during the site visits that the traffic on the approach slab is more than the same on right-turn pavement section, the casing profile and the data monitored show that the settlements occurred in the approach slab section are lower than the other side. This reveals that the slab can mitigate the amount of the settlement induced from the traffic load.

From the profile of inclinometer readings shown in Figure 7.7, the following observations can be noted:

- After the construction of the embankment and the approach slab, considerable movement of the casing can be seen in a zone of slope fill at the lengths between 0 and 20 ft. This trend happened only in the first six months, and thereafter less amounts of settlements were observed. Unlike another section under the pedestrian and traffic pavement, the soil movements kept increasing according to time.

Figures 7.8 and 7.9 present soil movements after the breaking of the casing:

- From Figure 7.8, it can be clearly seen that the casing was broken at the point where the highest hump was recorded.
- Most of the settlements occurred within the first twelve month, whereas only small amount of the soil movements was recorded in the last four months before the readings were terminated.

From Figure 7.9, it is clearly seen that after the construction of the approach slab, the maximum amount of the settlement occurred under the highway pavement is 0.50 in. and the minimum settlement value is 0.25 in. Moreover, it can be noticed that the highest value of the settlement is 0.75 in. and it happened in the slope fill area, which has the lowest compaction effort and this was not in the approach slab location.

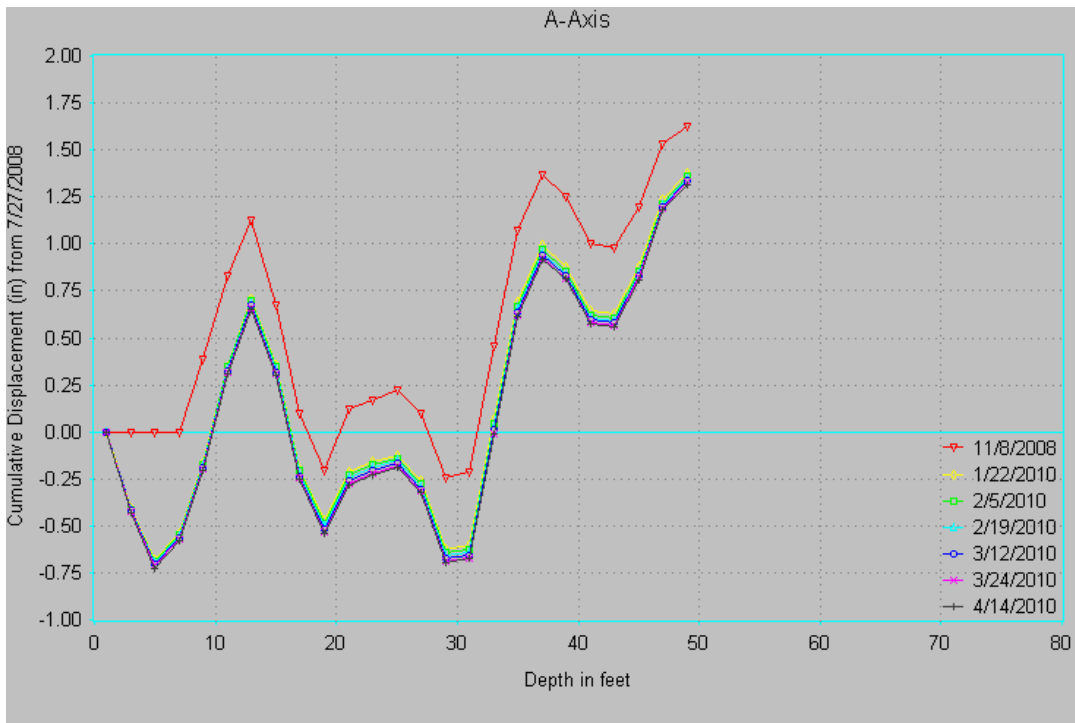


Figure 7.8 The cumulative displacements from 11/8/2008 to 4/14/2010 (compared with a casing profile before the construction of the approach slab finished)

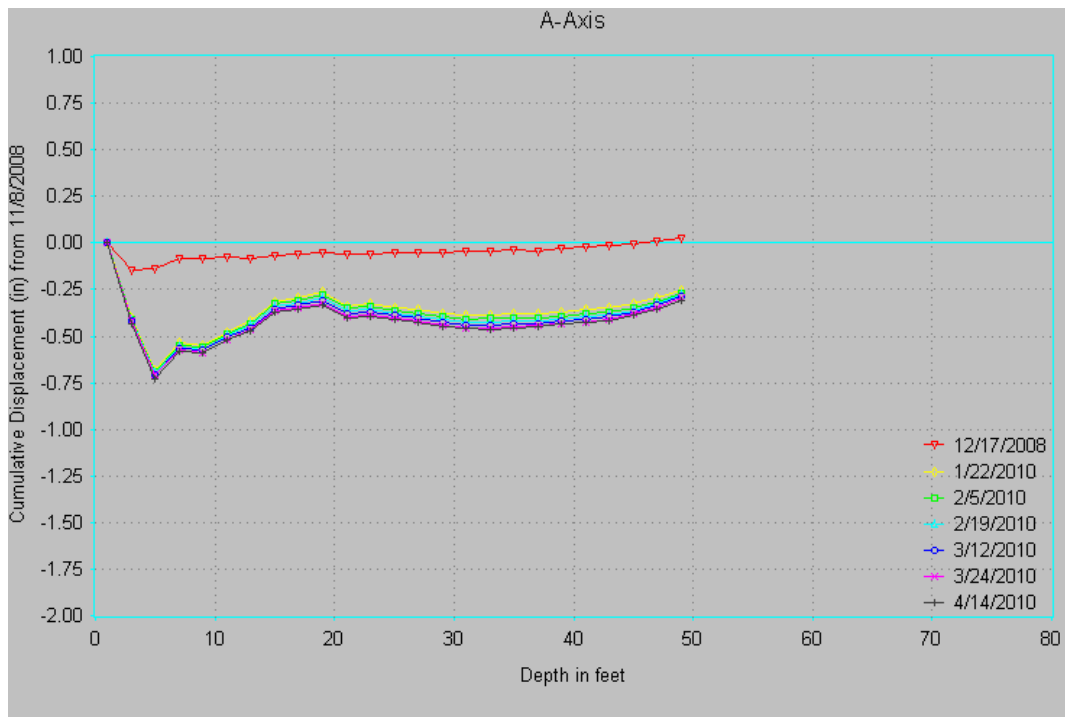


Figure 7.9 The cumulative displacements from 12/17/2008 to 4/14/2009 (compared with a casing profile after the construction of the approach slab finished)

The elevation surveys were also performed at a location close to a highway pavement both in treated and untreated section by using a Total Station (TS) device, which has a resolution of 0.1 in. (0.25 cm). Generally, the data obtained from the surveys are the elevation data compared to one Benchmark (BM) value, which was fixed and located far from the area of the study to avoid any influencing circumstances affecting on the BM elevation. The collected elevation data are presented in Table 7.1. To determine the vertical movements of the selected points, the elevation values at any date of survey must be subtracted by the value at the initial reading. For example, the movement in a treated section on March 20, 2009 is equal to 0.12 ft. The positive value shows that the selected point was settled.

7.2.1.1.2. Automatic Reading Rod Extensometer Surveys

As already mentioned, one rod extensometer with automatic reading capabilities was installed at the site. The rod extensometer was installed to monitor settlements occurring in the embankment fill of the bridge and the natural subgrade foundation. As already discussed in the previous chapter, the main components of a rod extensometer are anchors, steel rods inside protective pipe, and a reference head. The anchors are installed down-hole with rods spanning the distance from the down-hole anchors to the reference head at the surface. Further details about the rod extensometer installation can be found on slope indicator website (<http://www.slopeindicator.com/instruments/ext-rod.html>).

The frequency occurred in the steel rods were obtained at the reference head by the VW readout and then stored in a data logger. Thereafter, the readings were downloaded to a notebook computer using vibrating wire or VW Quattro Logger Manager Software, and then these readings were converted to distance in length units by using calibration factors as shown in Equation 7.1.

Table 7.1 Elevation survey data on test section site IH30

Date	Elevation of the interested point (ft)	Soil settlements	
		ft	mm
24-Jun-08	29.74	0	0
13-Aug-08	29.70	0.04	12.19
2-Oct-08	29.67	0.07	21.34
25-Oct-08	29.66	0.08	24.38
23-Nov-08	29.65	0.09	27.43
30-Dec-08	29.63	0.11	33.53
13-Feb-09	29.63	0.11	33.53
6-Mar-09	29.62	0.12	36.58
20-Mar-09	29.62	0.12	36.58
6-Jun-09	29.61	0.13	39.62
8-Aug-09	29.60	0.14	42.67
21-Sep-09	29.60	0.14	42.67
8-Dec-09	29.60	0.14	42.67
8-Feb-10	29.59	0.15	45.72
14-Apr-10	29.59	0.15	45.72
13-Jun-10	29.59	0.15	45.72
22-Sep-10	29.58	0.16	48.77

$$\text{Readings}_{(\text{Engineering Unit})} = (A \times F^2) + (B \times F) + C \quad (7.1)$$

Where F is the sensor reading in Hz; A, B, and C are coefficients listed on the sensor calibration sheet.

By using VW Quattro Logger Manager Software, the readings obtained from the field were presented both in frequency and converted distance units. These readings were then used

in a spreadsheet program to plot distance information as shown in Figures 7.10 and 7.11.

The readings that are taken at the extensometer head level and these are used to calculate changes in the distances between reference elevation and each anchor. When the reference head is located on stable ground, movements of the anchor can be calculated relative to the reference head. However, in this research, the reference head is not stable, and thus the deepest anchor was used here as the reference elevation. In this case, the data were calculated and inverted. The movements of each anchor were calculated relative to the bottom anchor. The calculation procedures are presented in the following:

- Construct a table of changes by subtracting the initial reading from subsequent readings for each anchor. This shows movements relative to the reference head as shown in Figure 7.10.
- Since the reference anchor is the deepest anchor, the data must be inverted to show movements relative to the deepest anchor, which is done by subtracting the changes for each anchor from the changes at the deepest anchor as shown in Figure 7.11.

Figure 7.10 shows changes in length of the extensometer rods, whose anchors were laid in the different levels. These movements are the displacements of the anchors relative to the reference head. The positive displacements show those rods are extended; on the contrary, the negative changes mean the lengths of the rods are shortened. All in all, it can be seen from Figure 7.10 that the changes in the length of the rod indicate that there were some movement occurring in the soils surrounding the extensometer. However, Figure 7.10 does not present the information indicate the direction of the soil movements at the different depths. Therefore, the readings are analyzed further by inverted calculation.

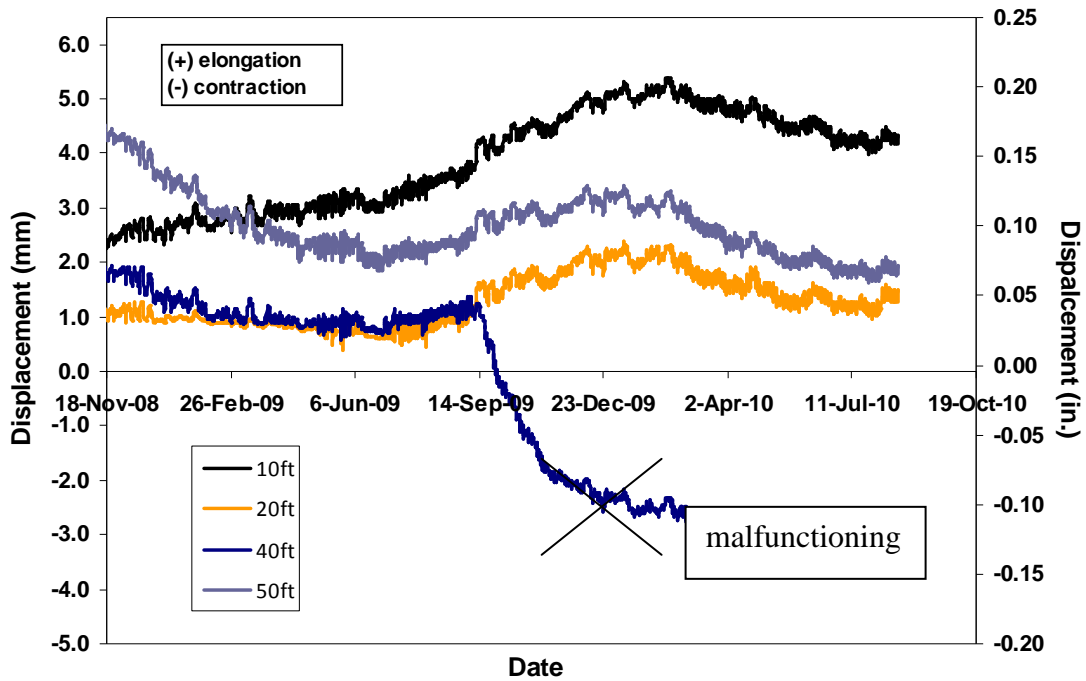


Figure 7.10 The changes in length of the extensometer rods

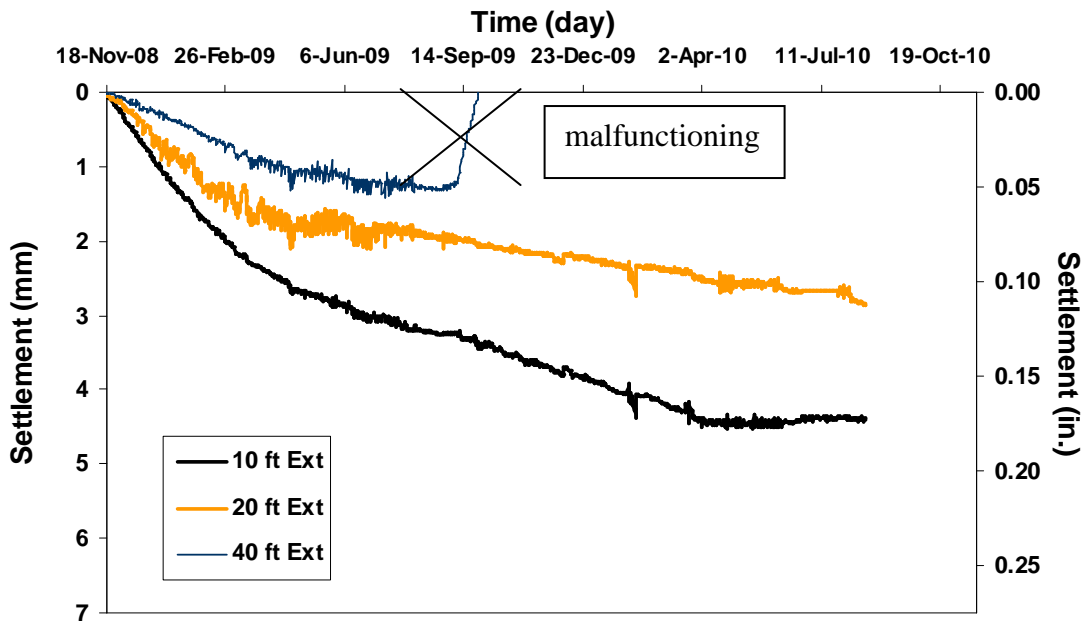


Figure 7.11 The soil displacement having the bottom rod anchor as a reference

From Figure 7.11, when using a bottom anchor as a reference, it is clearly seen that the soils at the level 10 and 20 ft from the top of the embankment settled. Moreover, it can be seen that the rate of the settlements were high in first four months (November, 2008 to March, 2009), and afterwards it gradually decreased until April 2010. From April 2010, the levels of the anchors at 10 and 20 ft from the embankment surface have become steady. For the rod anchored at 40 ft depth, in the first 10 months, the movements of the soil at this depth had shown the same behavior as the ones at depths of 10 and 20 ft as seen it Figure 7.11. However, there was an abrupt change of the direction of the movement started from September, 2009. This indicated the malfunction of the VW at the depth of 40 ft, and therefore the displacements data from this depth was not used for the settlement analysis.

7.2.1.1.3. Manual Reading Rod Extensometer Surveys

Another rod extensometer of manual type was installed on site at a different location on the same south embankment. However, instead of installing automatic reading one this rod extensometer was a manual reading type. Generally, the main components of both types of rod extensometer are the same, except that there are no VW sensors to detect displacements in the manual extensometer. Therefore, a digital depth micrometer was used to get the displacements occurred at the head of each rods as shown in Figure 7.12.

As same as the automatic extensometer, the observation readings are used to calculate changes in the distance between the reference elevation and each anchor by using the deepest anchor as the reference for calculation. The readings data were inverted, and movements relative to the deepest anchor are done by subtracting the changes for each anchor from the changes at the deepest anchor as shown in Figure 7.13.

Figure 7.13 shows the more comprehensive picture on how the soil settlements might have occurred in the embankment. It can be seen that the settlement occurred in the embankment and these values were increasing with time. Also, at the deeper location, the higher settlement could be monitored. In addition, the plots from Figures 7.11 and 7.13 also reveal the time-settlement relation from the manual and automatic extensometers are concurred.

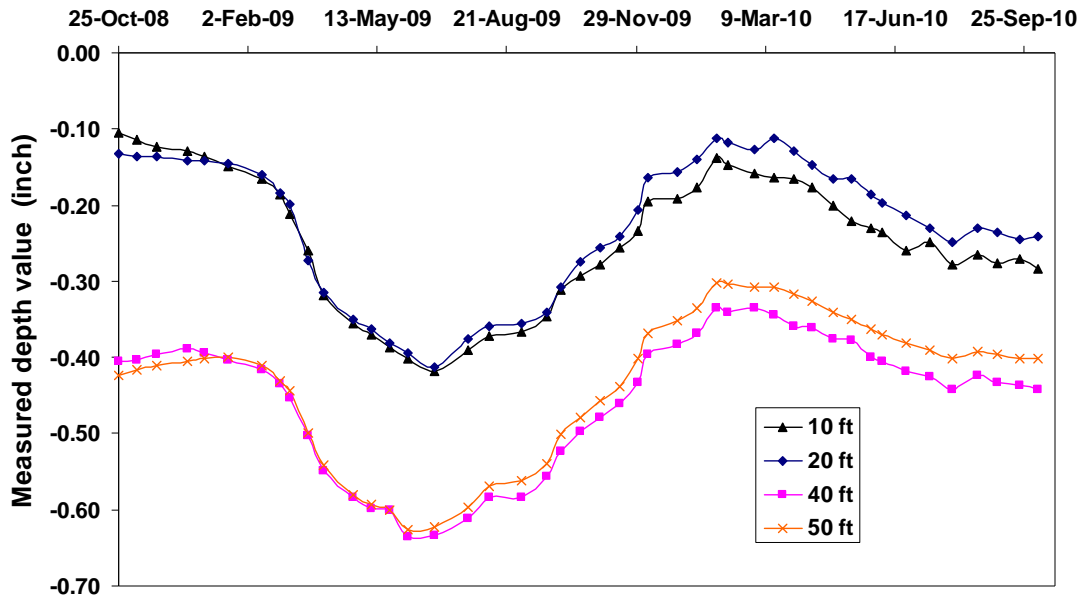


Figure 7.12 The depth values of the rod head measured by digital gauge

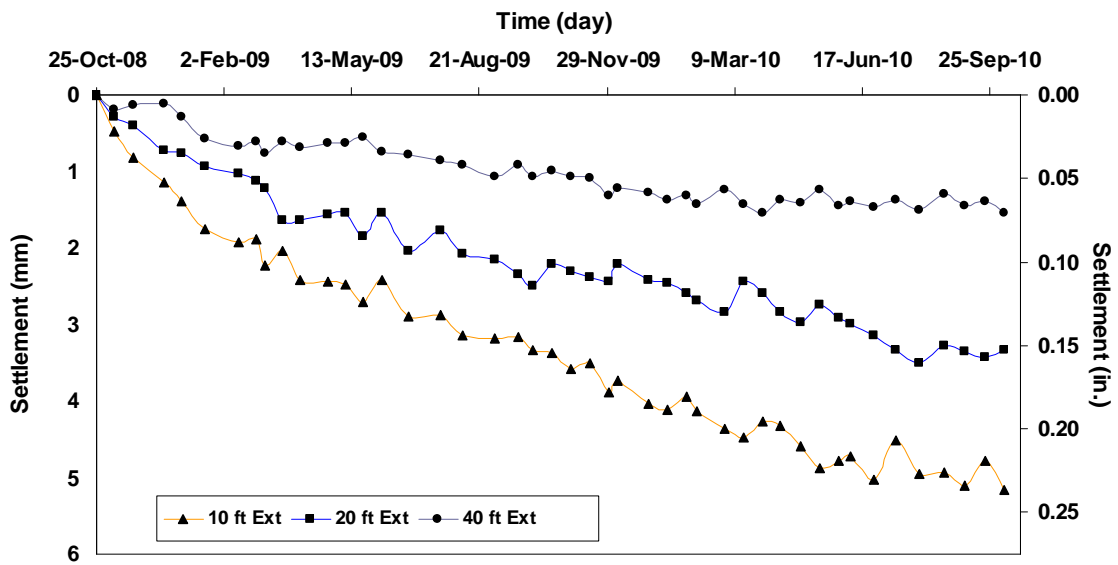


Figure 7.13 The soil displacement having the bottom rod anchor as a reference

The maximum settlements of manual extensometer at the depth of 10, 20 and 40 ft are about 0.20, 0.10 and 0.05 in., respectively. These numbers have small differences from the settlements measured in the automatic extensometer; this can happen due to a human error during the readings using the depth dial gauge.

7.2.1.1.4. Sondex readings

The sondex devices were installed on IH30 DSM site with vertical inclinometer casings. The readings were performed by lowering the probe through the center of the vertical casing. When the probe passes through the sensor rings, a buzzer sound will emanate and the readings will be collected on the tape as shown in Figure 7.14

The sondex was installed at the same time as with the vertical inclinometer installation and has an aim to detect soil settlements larger than the capacity of the extensometer. Therefore, the data obtained from the sondex is normally fewer accurate compared with data obtained from the extensometer.



Figure 7.14 The sondex instrument and the readings

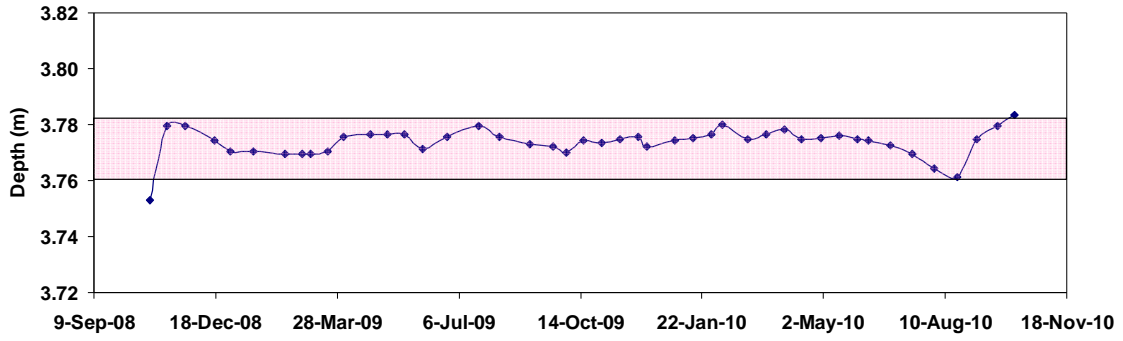
The bottom ring was fixed on the vertical casing by bolts, the other rings were still able to move according to soil movements surrounding it. Therefore, the bottom ring was chosen as a reference for the displacement calculation and the vertical movements can be obtained similar to the steps performed in the extensometers. However, the data obtained from sondex are not

accurate as the rod extensometer due to two following reasons. First, the readings of sondex were performed by the movement of the probe through sensor rings, which induced magnetic field and the buzz around it. The schematic movement in inducing the magnetic field depends on the speed of the probe. If the movement speed is low, the magnetic field will not be induced, and therefore the buzzing will not be sounded. However, if the movement is too rapid, then the readings on tape will be done erroneously. Second, with the scale on measuring tape of 0.01 ft (0.12 in.) the readings cannot be obtained as accurate as in the rod extensometers. Therefore, the readings of each depth must be performed three times to obtain the arithmetic average value for being a representative of the depth. The plots of the average measured depth and time are shown in Figures 7.15 and 7.16. Figures 7.15 (a), (b), (c), and (d) show the average depth readings in the treated embankment in the South at the depth of 10, 20, 40 and 50 ft, respectively.

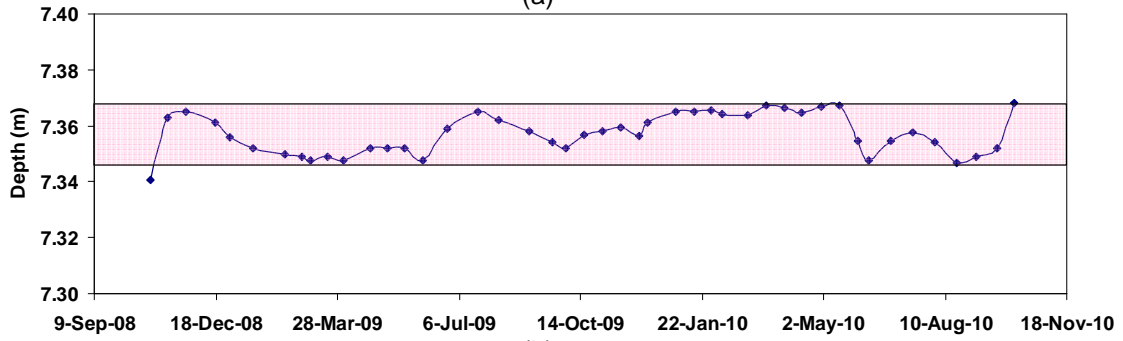
From Figures 7.15, it can be seen that the vertical movements occurred in the embankment on the treated DSM area are fallen in the small range, normally within 0.8 in. (0.02 m). The results show that no large settlements can be detected in both the embankments on treated and on untreated native material during the study period.

7.2.1.2 Lateral Soil Movements

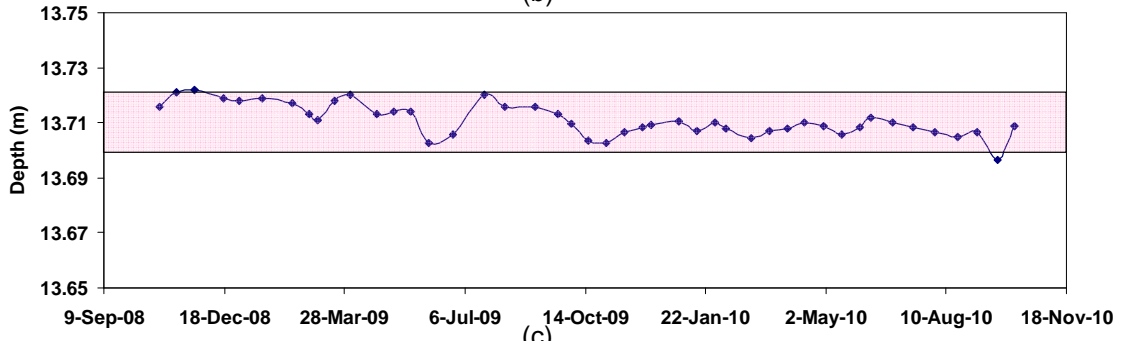
To monitor the lateral movements occurring within the embankment, two vertical inclinometer casings were installed on site IH 30 as already shown in Figure 7.1. The lateral soil movement can not only be an indication showing the instability of the slope, but also a factor in deteriorating the structure above. Therefore, both vertical inclinometer casings were installed at the locations close to the approach slabs and also close to the slopes. This will measuring horizontal movements in the embankment, and also for monitoring the effect of horizontal movements on the settlements of the approach slabs.



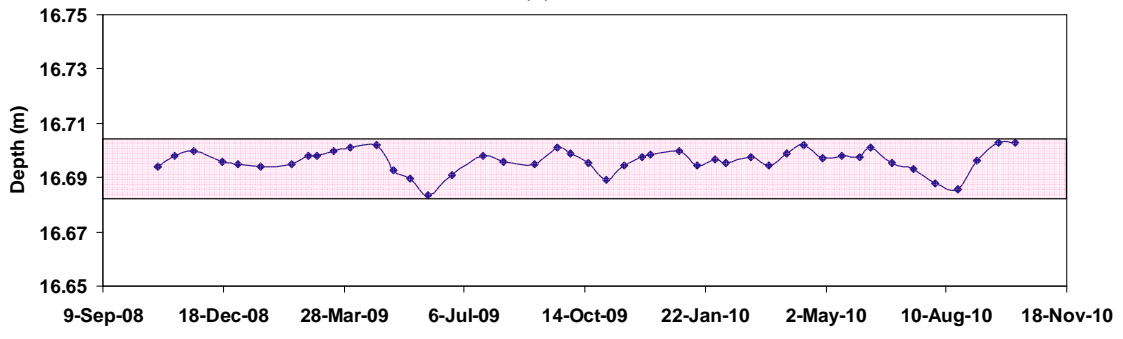
(a)



(b)



(c)



(d)

Figures 7.15 The average depth readings in the test embankment at the depth of (a) 10, (b) 20, (c) 40, and (d) 50 ft

7.2.1.2.1. Vertical Inclinator Surveys

On the site IH30, one vertical inclinometer was installed in a treated section in the south embankment of the bridge. The vertical inclinometers are used to monitor the soil movement in horizontal. Normally, the readings were performed at periodic intervals as same as in the readings of horizontal inclinometer. To perform the readings of the vertical inclinometer the orientation of the probe in each reading is essential, since the orientation will state the direction of the casing movement. Therefore, the data readings were always performed by keeping the orientation of the probe A0 on the downhill direction as shown in Figure 7.16.

The Inclinator surveying was performed by sending the inclinometer probe into the casing in the A-direction and the upper wheel of the probe was in the A0 groove as shown in Figure 7.17. The data at each depth interval were then collected and stored using a Digitilt DataMate connected to the inclinometer probe. The readings, thus, stored in the DataMate were downloaded to a computer using a DataMate Manager (DMM) software. Plots, as shown in Figures 7.18 were developed using the DigiPro software.

Results from the vertical inclinometers showing the lateral movement of soils in the test section at site IH 30 is presented in Figures 7.18. In the Figure, it can be seen that the overall movements in the treated embankments are very small and less than 0.1 in. in both directions. These low movements in the lateral direction are attributed to high confinements of the soils surrounding the inclinometer casings. From Figure 7.18, it can be seen that the soil movements in the both directions are swaying back and forth through the period of the readings. This behavior can be attributed to the installation of the inclinometer casing in the treated soil sections close to the approach slab, and away from the embankment slope. Moreover, the inclinometer is located at the corner of the highway intersection surrounded with traffic in all directions. Therefore, the traffic from all directions can affect the movement of the inclinometer.



Figure 7.16 The vertical inclinometer reading

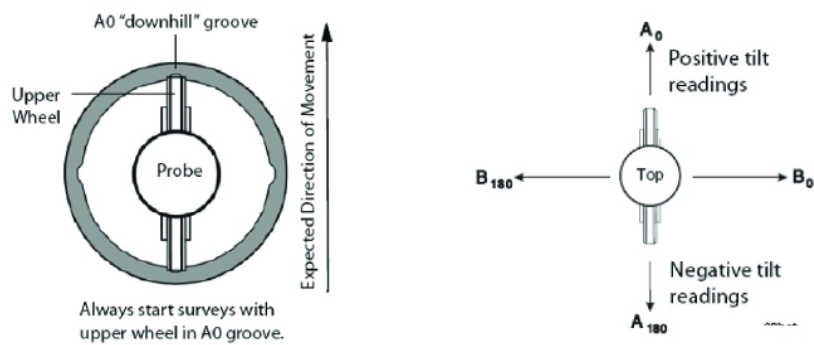


Figure 7.17 Orientation of probe within inclinometer casing (Slope Indicator)

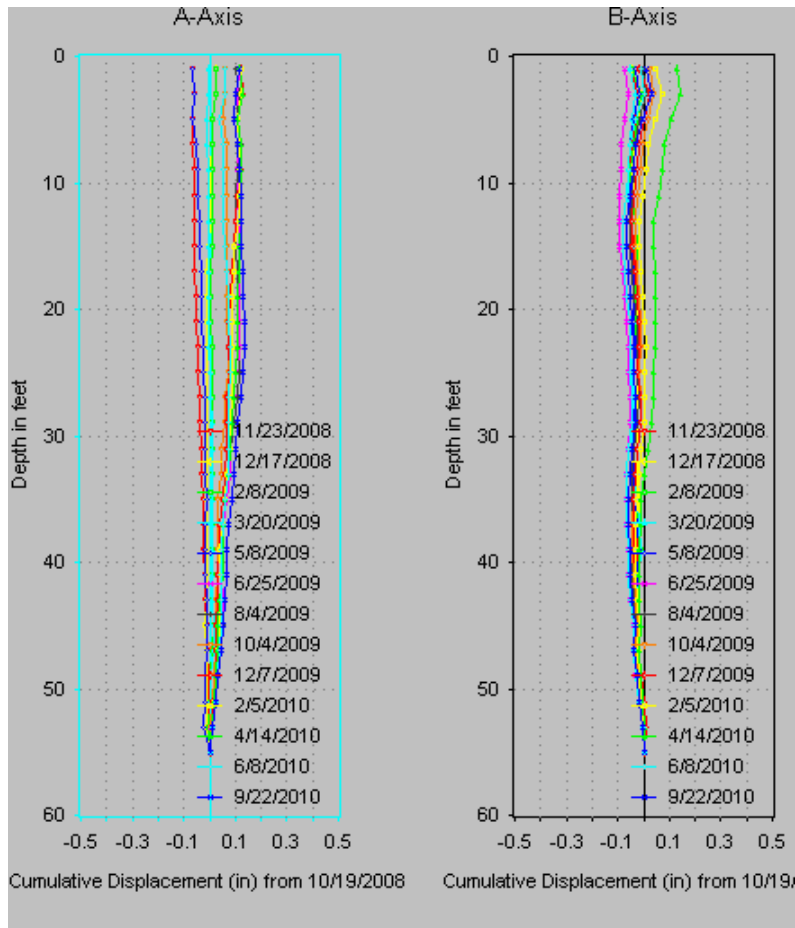


Figure 7.18 Lateral soil movements in the test section during 10/19/2008 to 8/4/2010

7.2.2 Control Section

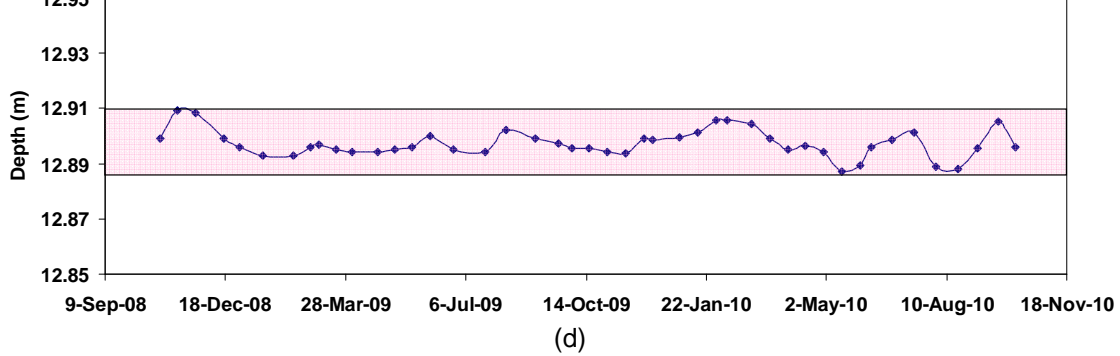
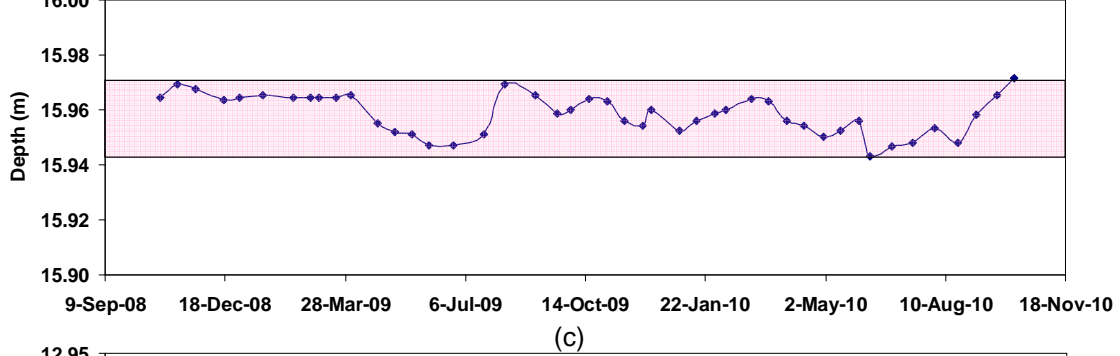
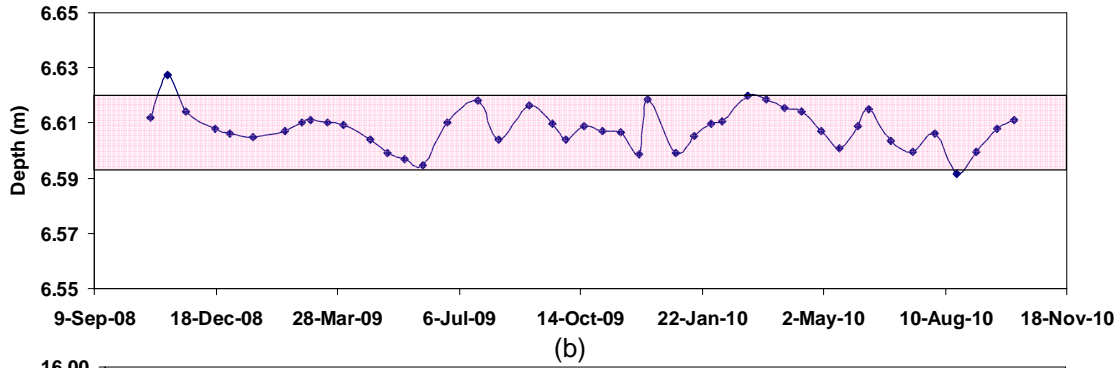
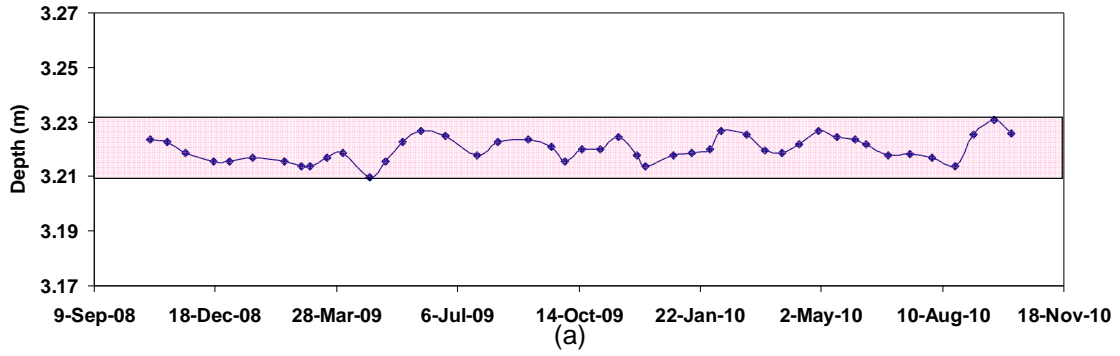
7.2.2.1 Vertical Soil Movements

In the control section, the sondex readings and the elevation surveys were performed to obtain the vertical soil movement data. The elevation survey results are presented in Table 7.2., which shows that the control embankment settled about 86 mm within 3 years.

The vertical movements were also monitored by using sondex, and the collected data are plotted and presented in Figure 7.19. From the figure, it can be seen that the depth readings of each sensor rings are varied during the period of the study. However, the depth reading variations within a range of 0.8 – 1.2 in. (0.02-0.03 m) are small and can lead to a conclusion that no large settlement can be detected in the control section.

Table 7.2 Elevation survey data on control section site IH30

Date	Elevation of the interested point (ft)	Soil settlements	
		ft	mm
24-Jun-08	32.07	0	0
13-Aug-08	32.03	0.04	12.19
2-Oct-08	31.99	0.08	24.38
25-Oct-08	31.95	0.12	36.58
23-Nov-08	31.91	0.16	48.77
30-Dec-08	31.89	0.18	54.86
13-Feb-09	31.88	0.19	57.91
6-Mar-09	31.87	0.20	60.96
20-Mar-09	31.86	0.21	64.01
6-Jun-09	31.84	0.23	70.10
8-Aug-09	31.84	0.23	70.10
21-Sep-09	31.83	0.24	73.15
8-Dec-09	31.82	0.25	76.20
8-Feb-10	31.81	0.26	79.25
14-Apr-10	31.81	0.26	79.25
13-Jun-10	31.80	0.27	82.30
22-Sep-10	31.79	0.28	85.34



Figures 7.19 The average depth readings in the untreated embankment at the depth of (a) 10, (b) 20, (c) 40, and (d) 50 ft

7.2.2.2 Lateral Soil Movements

One vertical inclinometer was installed in the median of the control section between two directions of the traffic and the monitoring results are shown in Figure 7.20.

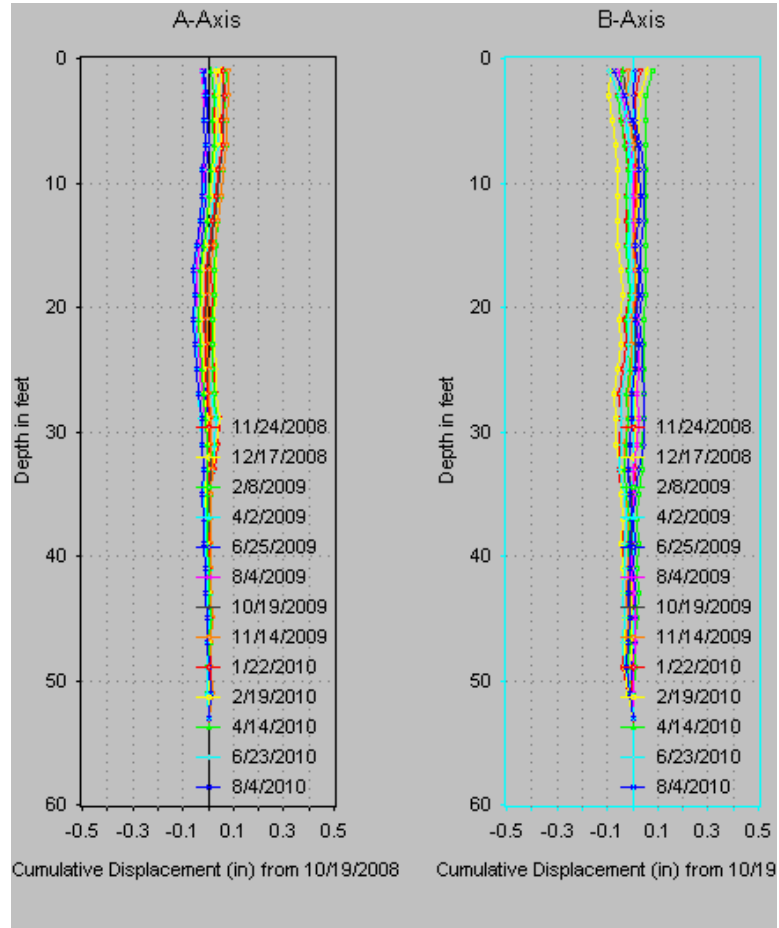


Figure 7.20 Lateral soil movements in the control embankment during 10/19/2008 to 8/4/2010

Similar to the lateral movements monitored in the test section, the swing-movements can be also noticed in the B-axis in the vertical inclinometer casing installed in the control embankment in the North as shown in Figure 7.19. Since the casing is located at the centre in the highway median, the traffic from both directions in the B-axis could have equally affected the soil movement behavior. Therefore, the casing moved from one side to another with the small displacements.

Although the casing still had sway-movements during the monitoring period, the displacement clearly moved towards the downward slope of the embankment. With the horizontal movement of 0.1 in. within 2 years, this amount of movement can be characterized as small and this could be attributed to two factors. First, the casing was installed close to an approach slab in an area with a gradual slope of 4.0% which is not too steep. Second, the embankment was well constructed and hence may have lesser soil movements. To summarize, the variations of the casing profiles with a very small movement less than 0.1 in. indicate that the lateral movements are not critical in the assessment of deep soil treatment methods in mitigating approach slab settlements.

7.2.3 Settlement Comparisons between DSM Treated Section and Untreated Section

In order to provide a clear idea about the differences of the soil displacements occurred over the treated and untreated sections, the data performed on both control and DSM sections at IH 30, DSM site is summarized and presented in Tables 7.3 to 7.6.

From Table 7.3, it can be seen that the settlements occurred beneath the approach slab is equal to 0.25 in. It should be noted here that the settlement from the horizontal inclinometer is less than the same value obtained from elevation surveys, since these two readings were started at different time periods. The settlement value from elevation survey (Table 7.4), which was initiated in June 2008, is less than the value from the horizontal inclinometer, which was started in November 2008. In addition, the data in Table 7.4 also reveals that the embankment in the control section experienced higher settlements than in the test or treated section.

Table 7.3 Measured vertical displacements in treated and untreated sections

	DSM treated section	Untreated section
Horizontal Inclinometer (in.)	0.25	-
Elevation surveys (in.)	1.92	3.36

Table 7.4 Elevation survey data in treated section and untreated section

Date	Soil settlements (in.)	
	DSM treated section	Untreated section
24-Jun-08	0.00	0.00
13-Aug-08	0.48	0.48
2-Oct-08	0.84	0.96
25-Oct-08	0.96	1.44
23-Nov-08	1.08	1.92
30-Dec-08	1.32	2.16
13-Feb-09	1.32	2.28
6-Mar-09	1.44	2.40
20-Mar-09	1.44	2.52
6-Jun-09	1.56	2.76
8-Aug-09	1.68	2.76
21-Sep-09	1.68	2.88
8-Dec-09	1.68	3.00
8-Feb-10	1.80	3.12
14-Apr-10	1.80	3.12
13-Jun-10	1.80	3.24
22-Sep-10	1.92	3.36

Table 7.5 presented the measured depth data monitored from sondex. It can be noted that the variations of the depth readings at both sections are very small. Although the variations of the depth readings at the level 2nd and the 3rd in the untreated section are larger than the values in the treated section, those deviations are considered small. Hence, the data from sondex is used to consider the existence of the settlements, with small range of deviation in the depth readings.

Table 7.5 Depth of sensor rings from Sondex readings in treated and untreated sections

	DSM treated section	Untreated section
-at the 1 st depth (m)	3.77 + 0.01	3.20+ 0.010
-at the 2 nd depth (m)	7.36 + 0.01	6.61+ 0.015
-at the 3 rd depth (m)	13.71+ 0.01	15.96+0.015
-at the 4 th depth (m)	16.70+ 0.01	12.90+0.010

The lateral movements of soil in both control and test embankments are presented in Table 7.6. It can be seen here that only small lateral displacements could be monitored from the vertical inclinometers. With movements monitored during the period of study, it can see that the lateral soil movements in the embankment are not critical in this study.

Table 7.6 Measured lateral displacements in treated and untreated sections

	DSM treated section	Untreated section
Lateral displacements (in.)	+ 0.1	+ 0.1

7.3 Performance Evaluation of Light Weight Expanded Clay Shale or ECS Fill

7.3.1 ECS Test Section

7.3.1.1 Vertical movements

On the ECS site, no horizontal inclinometer was installed to monitor the vertical soil movement. Therefore, the elevation survey were performed to measure the displacement happened in the embankment. The elevation survey data are presented in Table 7.7, which shows that the ECS embankment experienced a settlement of about 1.45 in. (37 mm).

7.3.1.2 Lateral Soil Movements

On site SH30, there were four vertical inclinometer casings installed in a test section in the south embankment of the bridge. On this site, the vertical inclinometers are used to monitor the soil movement in horizontal in different locations as shown in Figure 7.20. To perform the readings, the orientations of the readings in all vertical casing were in the North-South

alignment. The reason that the reading orientation was not followed the direction of the slope as suggested in the manual is the location varieties of the installed casings. Figure 7.21 shows that although the inclinometer casings V1, V2 and V3 were installed in the median of the highway, the casings V1 and V2 are located far from the slope of the embankment, while the casing V3 is located near the slope of the embankment. Moreover, the casing V4 was installed in the embankment between two slopes. Therefore, in this case it is more convenient to arrange the orientation of the probe while reading in the North-South direction. As a result, the data readings were always performed by keeping the orientation of the probe A_0 toward to the North. Normally, the readings were performed in every fortnight.

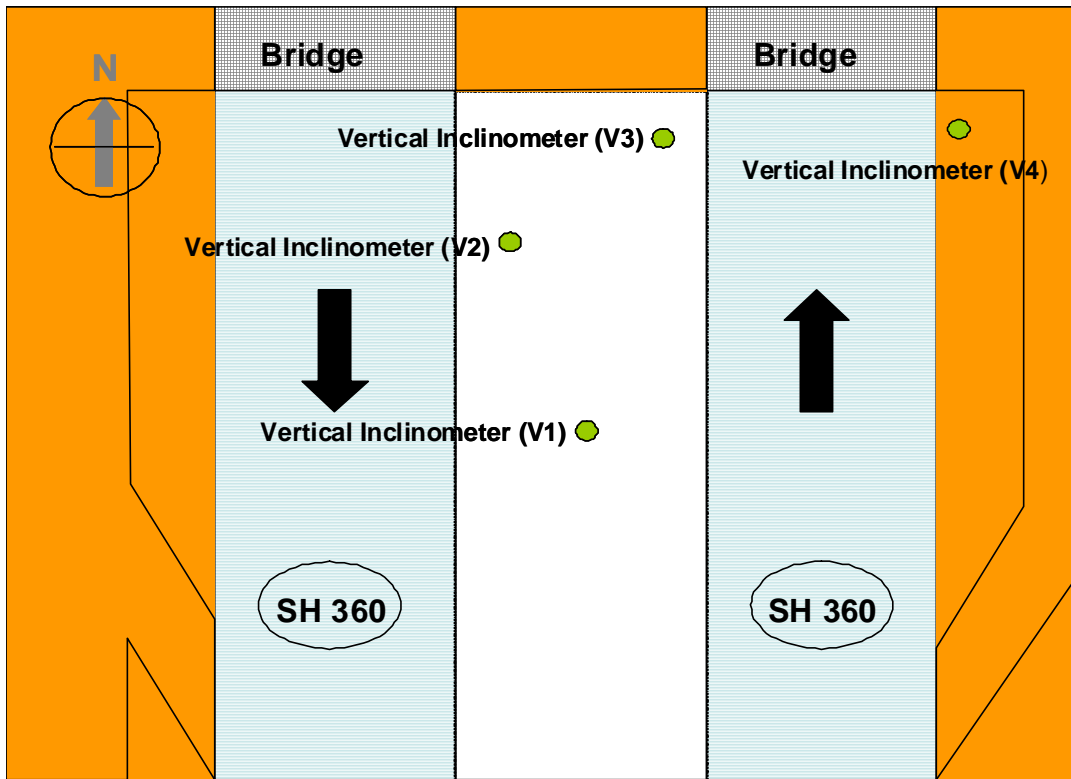


Figure 7.21 Instrumentations on SH 360, Arlington, Texas

Table 7.7 Elevation survey data on Test section site SH360

Date	Elevation of the interested point (ft)	Soil settlements	
		ft	mm
16-Jul-06	1.41	0.00	0.00
14-Aug-06	1.39	0.02	6.10
18-Sep-06	1.37	0.04	12.19
14-Oct-06	1.36	0.05	15.24
17-Nov-06	1.35	0.06	18.29
10-Dec-06	1.35	0.06	18.29
15-Jan-07	1.34	0.07	21.34
17-Feb-07	1.34	0.07	21.34
20-Mar-07	1.34	0.07	21.34
13-Apr-07	1.33	0.08	24.38
20-May-07	1.33	0.08	24.38
3-Sep-07	1.33	0.08	24.38
16-Dec-07	1.32	0.09	27.43
18-Jun-08	1.32	0.09	27.43
19-Sep-08	1.31	0.10	30.48
17-Dec-08	1.31	0.10	30.48
18-Jan-09	1.31	0.10	30.48
20-Mar-09	1.31	0.10	30.48
2-Sep-09	1.30	0.11	33.53
6-Nov-09	1.30	0.11	33.53
8-Feb-10	1.30	0.11	33.53
5-Apr-10	1.30	0.11	33.53
14-Apr-10	1.30	0.11	33.53
8-Jun-10	1.29	0.12	36.58

Figures 7.22 - 7.23 show the lateral movements of the inclinometer casings occurred within 4 years. Figure 7.22 (a) reveals the soil movements occurred around the casing V1, which is located at the middle of highway median. It can be observed that the lateral movements happened both in the A-axis and B-axis along this casing were less than 0.1 and 0.5 in., respectively. The very small movements in the A-axis were due to the location of the installation, which is located far away from the slope. Therefore, only small scales of soil movements could be observed. On the contrary, in the perpendicular direction the larger amount of the movements can be seen and also toward the left. Normally, if the casing is located at the middle of the highway median where the amount of the traffic from both directions are not much different, there must not be any displacements can be observed. However, since the casing was installed between embankments constructed with two types of materials (RAP on the left and ECS on the right), soil behaviors responded to the load conditions differently. In this case, soil moved from one side constructed with the ECS to another side constructed with the RAP.

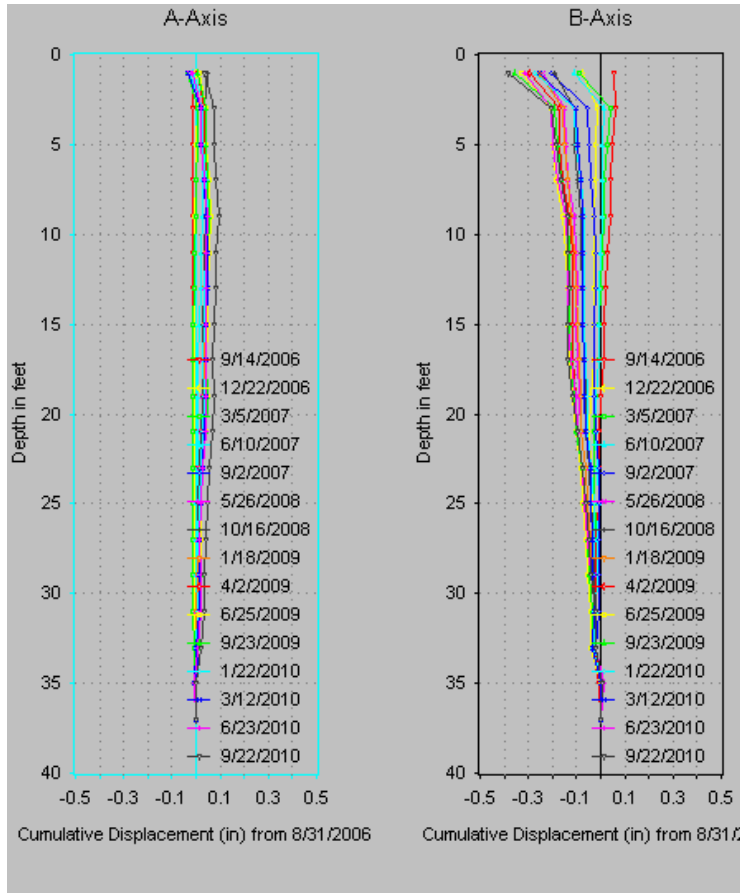
Figure 7.22 (b) shows the soil movements happened in the casing V2, which was installed closed to the left embankment as shown in Figure 7.21. From the Figure 7.22 (b), it can be seen that scale of the soil displacements in both axis were almost the same at 0.5 in. Considering movements in the A-axis, the direction of soil displacements are backward against to the slope, while in the B-axis, the direction of lateral displacements is in the deposit direction completely different from the displacement in the casing V1. This result may be related to a reason that the casing V2 was installed close to the left embankment more than the right one and the installation location exerts stronger influence than the type of construction material.

Figure 7.23 (a) shows the soil displacement occurred in the vertical casing V3. It can be noticed from the Figure that the lateral displacements have the magnitude about 0.75 in. in both directions. The plot also reveals that the soils around the casing V3 moved away from the slope but toward to the nearer highway. To explain those movement behaviors, it is also necessary to

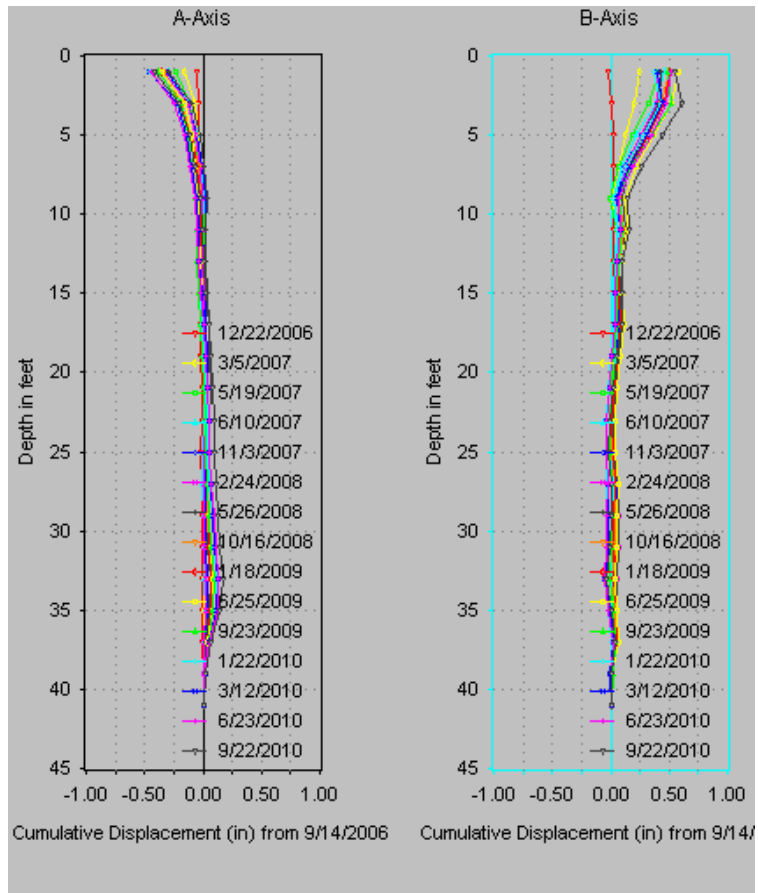
consider the soil displacements occurred around the casing V4, which was installed on another side of the embankment.

From Figure 7.23 (b), it can be seen that the casing V4 has lateral movements more than 2 in. in the A-axis and 5 in. in the B-axis. The movements of 5 in. in the B-axis are not only observed in the plot, but also visualized during site visit as shown in Figure 7.24. The magnitudes of these movements are more than the allowable horizontal movement of 1 in. From Figure 7.23 (b), it can be also noticed that the movements in both directions are normally occurred within the depth of 15 ft from the surface, which can be seen as a rotation of the slope. In addition, the maximum displacement (2 in.) happened in the first year after the construction, especially during winter and spring. Possible reasons for these movements could be heavy rainfall induced soil erosion at the surface and resulted in lateral movements of the slope.

The amount of the lateral movements occurred around the casing V4 have also induced the movements occurred in the casing V3. This phenomenon can be visualized at the surface of the highway pavement. As shown in Figures 7.25 (a) and (b), it can be seen that there is a gap occurred close to the bridge between the highway pavement and the shoulder. However, no gap could be observed between the shoulder and the casing V3 platform, Figure 7.26. This means the soils moving from the median to the highway towards the outer slope. Therefore, the V3 platform could be still close to the shoulder. On contrary, a wide opening observed close to the pavement indicates that the more distance from the median, the more horizontal movements could occur. The opening on the highway allowed more precipitation flowing into the embankment and this could induce erosion, which made the settlement problem become more severe. As seen in Figures 7.27 (a) and (b), there is an opening with a width of 1 in. and the settlement of the slope of 2 in. can be observed next to the abutment.

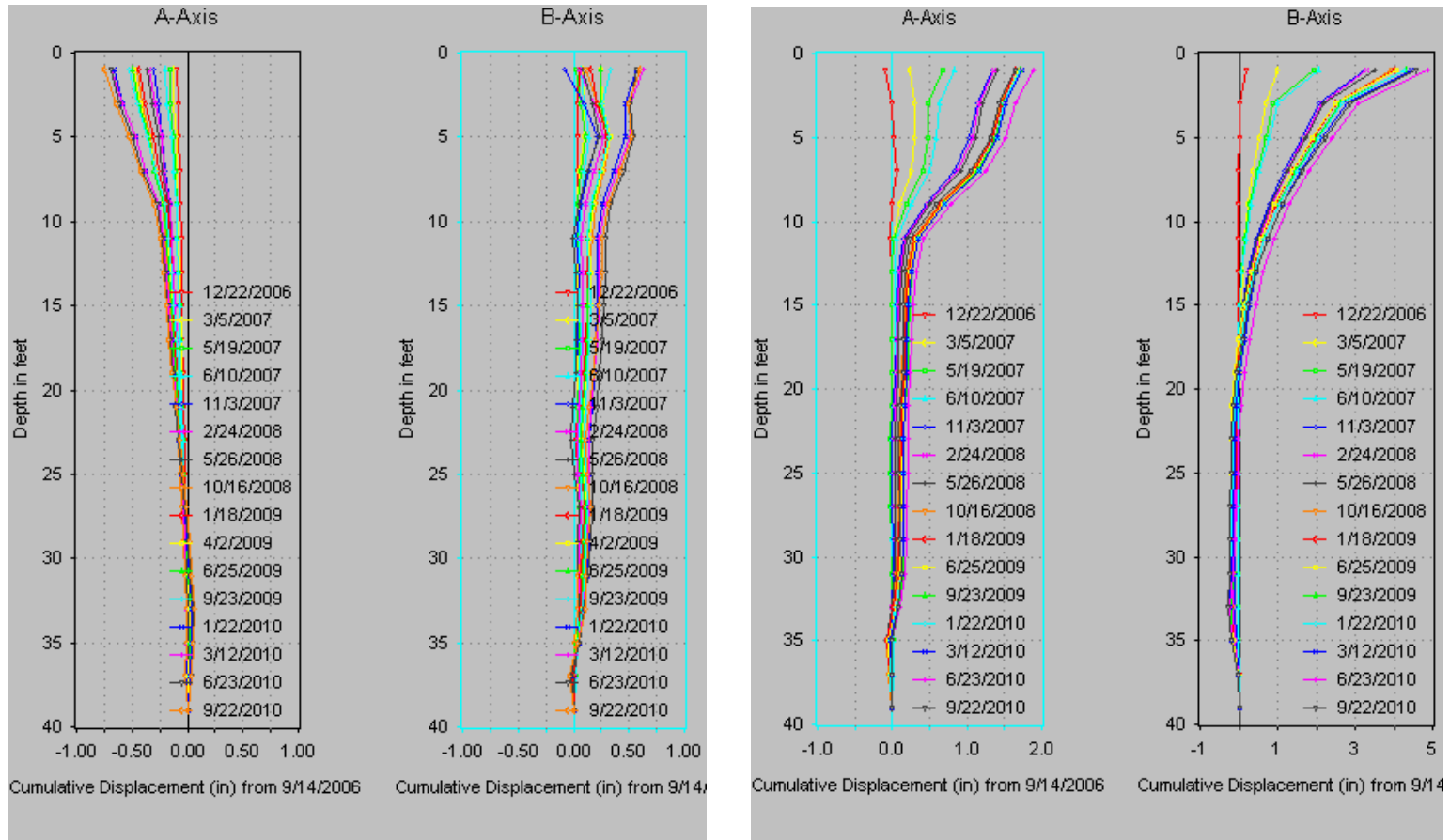


(a)



(b)

Figure 7.22 Lateral soil movements during 8/31/2006 to 8/4/2010 in the vertical inclinometers (a) V1, (b) V2



(a) (b)
 Figure 7.23 Lateral soil movements during 8/31/2006 to 8/4/2010 in the vertical inclinometers (a) V3, (b) V4



Figure 7.24 Lateral movement of the platform casing V4



(a)



(b)

Figure 7.25 Opening observed between highway pavement and its shoulder



Figure 7.26 The casing V3 platform close to highway shoulder



(a)

(b)

Figure 7.27 Opening observed close to abutment of the bridge

7.3.2 Conventional Fill Section

7.3.2.1 Survey Elevation

In the conventional fill section, elevation surveys were also performed to obtain the road profile by using a Total Station (TS). The collected elevation data are shown in Table 7.8. The elevation data is useful for comparing the settlements happened between the control and the test section as shown in the following section.

7.3.3 Comparisons of Data between ECS test section and control section

It can be seen from Table 7.9 that during the study duration, there were settlement occurred in the control section more than the test section, which can be visualized that the pavement near the bridge approach in the control section constructed with conventional fill was already overlaid by asphalt to mitigate the bump problem as shown in Figure 7.28.



Figure 7.28 Bridge approach in the control embankment was overlaid by Asphalt to mitigate the bump

Table 7.8 Elevation survey data on the control section site SH 360

Date	Elevation of the interested point (ft)	Soil settlements	
		ft	mm
16-Jul-06	-6.98	0.00	0.00
14-Aug-06	-7.00	0.02	6.10
18-Sep-06	-7.01	0.03	9.14
14-Oct-06	-7.03	0.05	15.24
17-Nov-06	-7.05	0.07	21.34
10-Dec-06	-7.06	0.08	24.38
15-Jan-07	-7.07	0.09	27.43
17-Feb-07	-7.08	0.10	30.48
20-Mar-07	-7.09	0.11	33.53
13-Apr-07	-7.10	0.12	36.58
20-May-07	-7.11	0.13	39.62
3-Sep-07	-7.14	0.16	48.77
16-Dec-07	-7.15	0.17	51.82
18-Jun-08	-7.16	0.18	54.86
19-Sep-08	-7.18	0.20	60.96
17-Dec-08	-7.19	0.21	64.01
18-Jan-09	-7.22	0.24	73.15
20-Mar-09	-7.22	0.24	73.15
2-Sep-09	-7.23	0.25	76.20
6-Nov-09	-7.24	0.26	79.25
8-Feb-10	-7.24	0.26	79.25
5-Apr-10	-7.25	0.27	82.30
14-Apr-10	-7.25	0.27	82.30
8-Jun-10	-7.24	0.28	85.34

Table 7.9 Comparisons of settlement data on the control and ECS sections on site SH 360

Date	Soil settlements (in.)	
	Test section	Control section
16-Jul-06	0.00	0.00
14-Aug-06	0.24	0.24
18-Sep-06	0.48	0.36
14-Oct-06	0.60	0.60
17-Nov-06	0.72	0.84
10-Dec-06	0.72	0.96
15-Jan-07	0.84	1.08
17-Feb-07	0.84	1.20
20-Mar-07	0.84	1.32
13-Apr-07	0.96	1.44
20-May-07	0.96	1.56
3-Sep-07	0.96	1.92
16-Dec-07	1.08	2.04
18-Jun-08	1.08	2.16
19-Sep-08	1.20	2.40
17-Dec-08	1.20	2.52
18-Jan-09	1.20	2.88
20-Mar-09	1.20	2.88
2-Sep-09	1.32	3.00
6-Nov-09	1.32	3.12
8-Feb-10	1.32	3.12
5-Apr-10	1.32	3.24
14-Apr-10	1.32	3.24
8-Jun-10	1.44	3.36

7.4 Performance Evaluation based on Geopier Reinforcement

On site SH 6, there were eight vertical inclinometer casings and four sondex installed on this site as shown in Figure 7.29. All of the instruments were installed in treated sections both near the North-bound entrance ramp and the South-bound exit ramp. The sondex was only installed in the exit ramp, while eight vertical inclinometers were evenly installed in both ramps. On this site, the vertical inclinometers are used to monitor the soil movement in horizontal in different locations as shown in Figure 7.29 and the sondex were used to monitor the soil movement in the vertical direction. To perform the readings in the vertical inclinometer, the orientations of the readings were performed as a direction outward of the ramp (A0 was on a far-away side to the ramp). This orientation would give a clear idea of the direction of soil movement compared with the ramp. One problem found on this site is the installed sondex and vertical inclinometers were damaged during the time of study. After the bridge construction was finished, the study areas were landscaped and mowed. Moreover, the installed instruments on this site were not well-protected with any covers as on site IH 30 and SH 360. Due to the aforementioned reasons, only readings in 4 inclinometers (V1, V2, V6, and V8) could be performed through the period of the study and then can be presented in this chapter.

Figures 7.30 - 7.31 (a) to (b) show there were only small scale lateral movements during the observation within the duration of two years monitoring (from October, 2008). Normally, the magnitude of lateral movements in both directions are less than 0.1 in., only at the casing V2, which has a lateral movement of 0.3 in. However, with those small amounts of the movements observed after the bridge construction had been finished in February 2008, it can lead to a conclusion that the Geopier could be a viable method to mitigate the soft soil movement underneath the embankments.

Since the traffic on the bridge is heavy and the researcher was not able to work on the highway shoulder. Therefore, the elevation survey was not performed on the site. Therefore, the researcher made a request to TxDOT ask for the IRI values performed on the ramps above in the study area on February 20, 2009. The results of the IRI between 117 and 124 (inch/mile)

reveal that the pavements were still in a good condition (IRI 250 inch/mile or 3.9 m/km indicates a very good riding quality). The numbers of the IRI values further confirm the good viability of the Geopier to support the embankment constructed over the soft soil. No modeling was attempted on this method as this work was primarily done prior to this research.

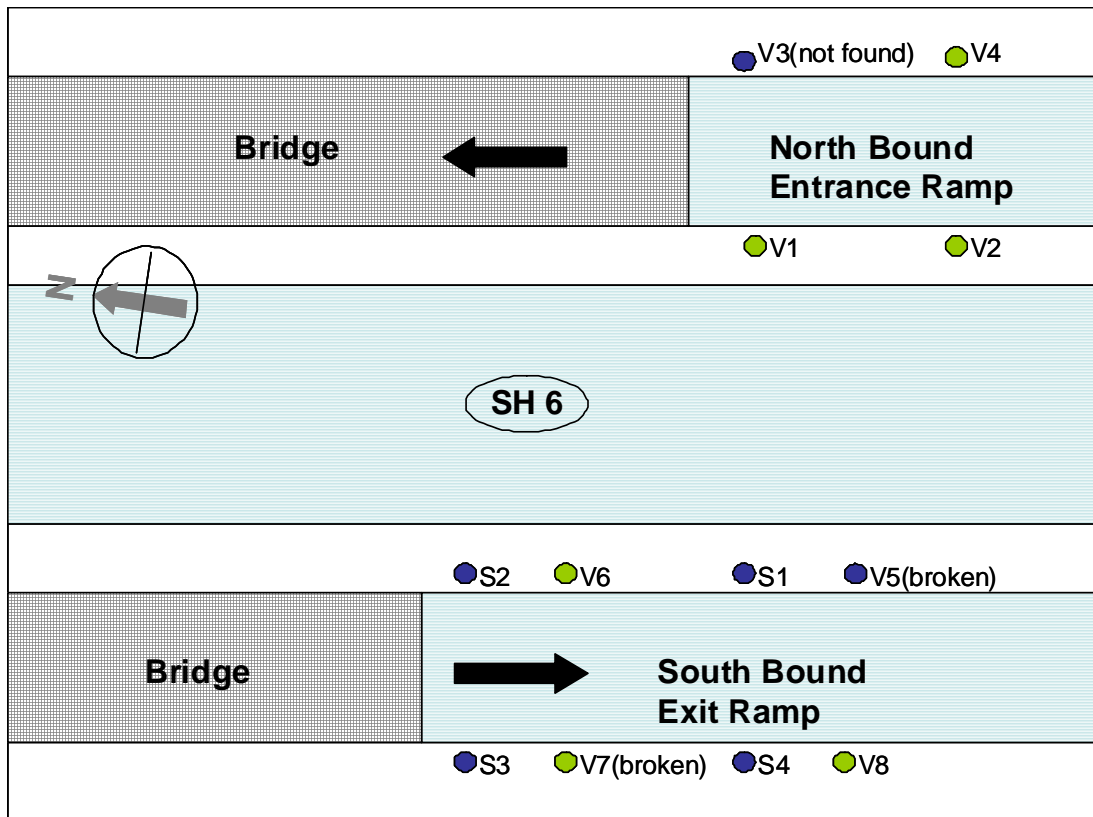
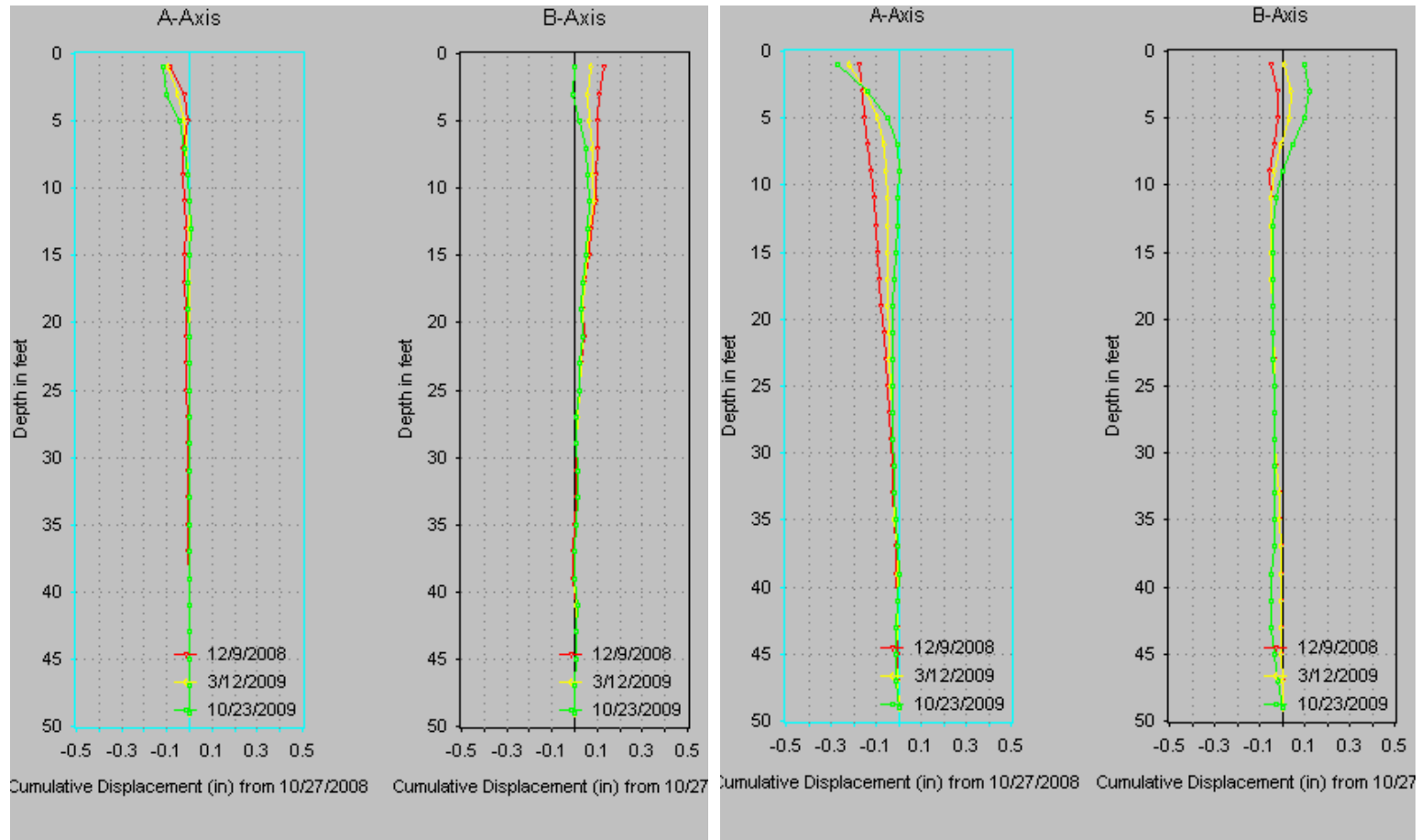
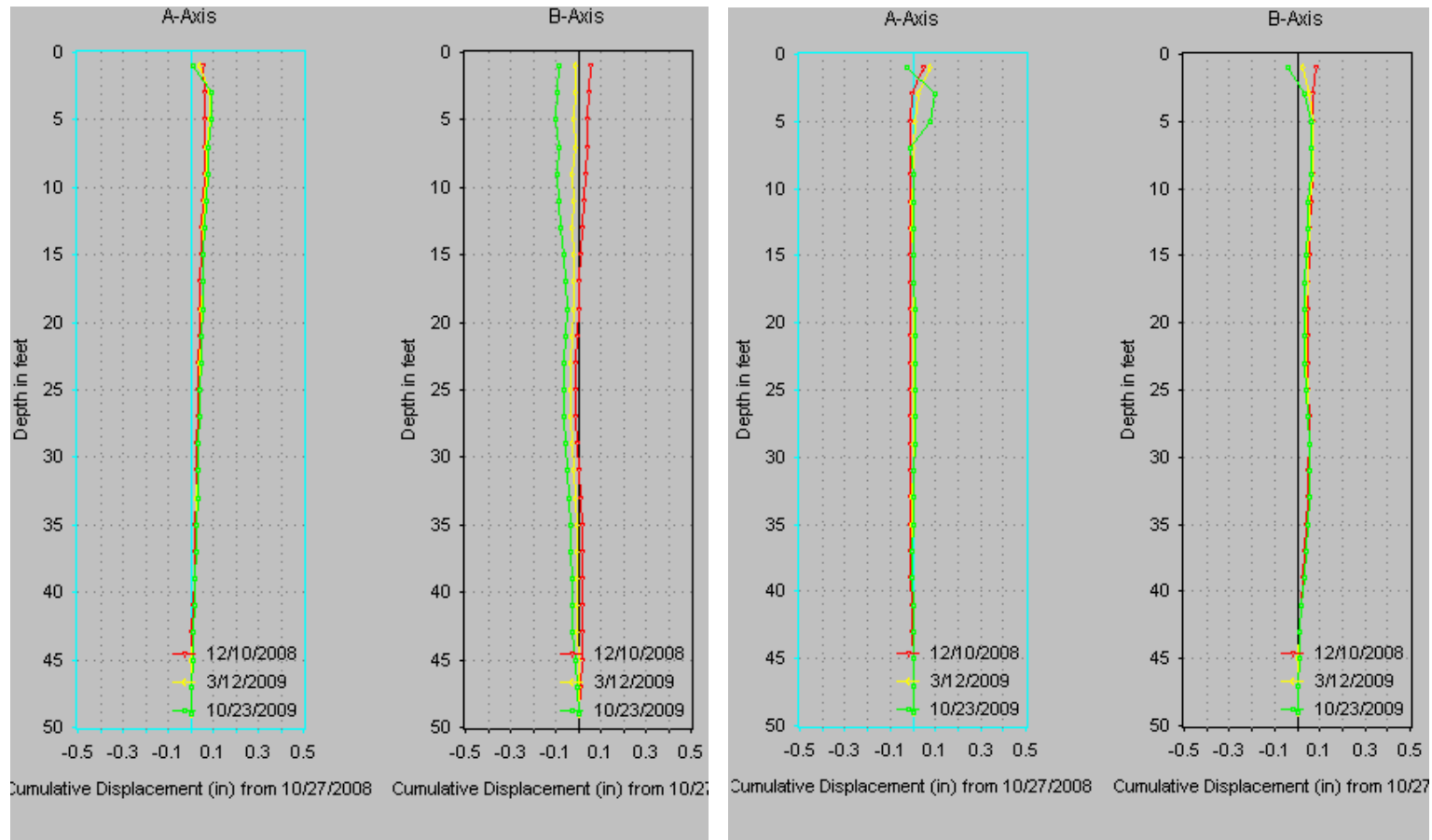


Figure 7.29 Instrumentation on SH6, Houston, Texas



(a) (b)
 Figure 7.30 Lateral soil movements during 10/27/2008 to 10/23/2009 in the vertical inclinometers (a) V1, (b) V2



(a) (b)
 Figure 7.31 Lateral soil movements during 10/27/2008 to 10/23/2009 in the vertical inclinometers (a) V6, (b) V8

7.5 Performance Comparison between DSM and ECS in Mitigating the Settlement

The elevation survey data from DSM and ECS sites were plotted to see the efficiency of each method in mitigating the settlement occurred in the embankments. As showed in Figure 7.32, it can be seen that both DSM and ECS can be used to reduce the magnitude of the settlement. With the same time duration, the embankment with DSM support had the settlement of 2.0 in. (50 mm), while the embankment without DSM experienced the settlement of 3.5 in. (90 mm). The same trend is also found in the embankment constructed with ECS, which had a settlement of 1.25 in. (30 mm.) only, while the embankment constructed with local fill had the settlement value og 2.5 in. (60 mm). It should be noted that it is quite difficult to compare the amount of the settlement occurred in two different sites even they were constructed on soft soil foundations. However, it can be seen from this study that both mitigation techniques can be employed to mitigate the settlement occurred at the bridge approach.

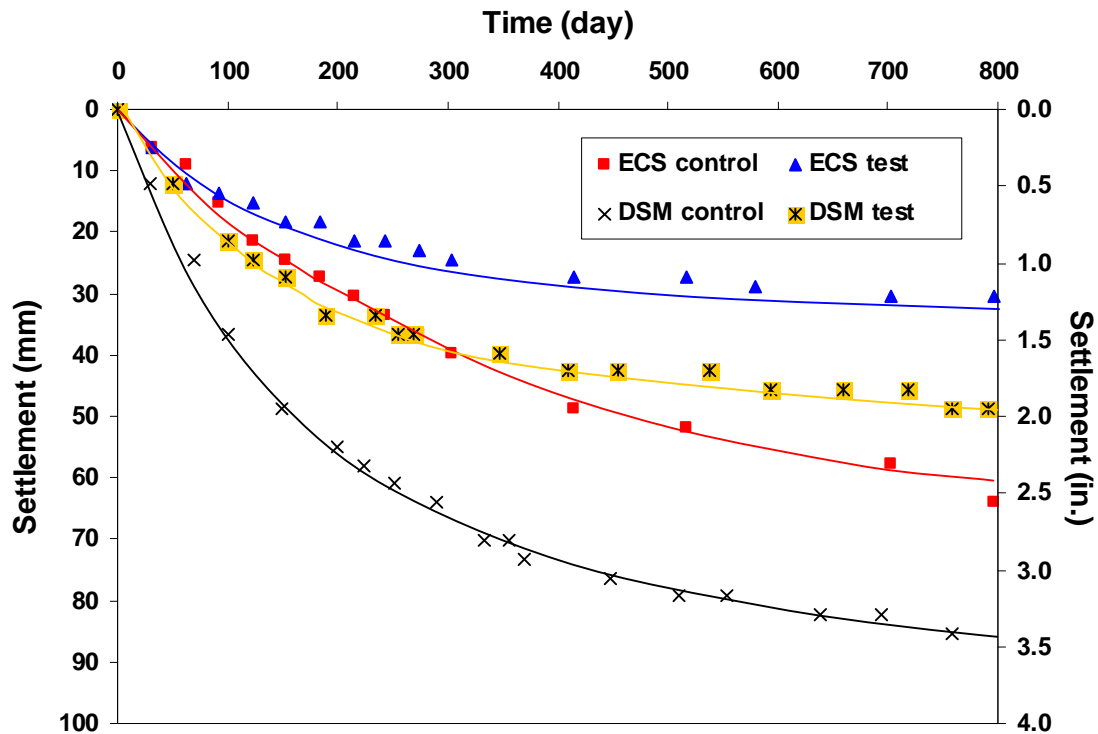


Figure 7.32 Monitored settlement values from DSM and ECS sites

7.6 Summary

This chapter presents the collected data obtained in the field during the site visits on DSM (IH 30, Arlington), ECS fills (SH 360, Arlington) and Geopier (SH 6, Houston) sections. Various types of instruments, for example, horizontal inclinometer, vertical inclinometer, rod extensometer, and sondex, were installed on sites to evaluate the effectiveness of each technique constructed on all three bridge sites, field studies were performed through field data collected periodically from November 2008 to September 2010. The instruments were used to monitor the soil movement either in horizontal or vertical directions in the different interested locations. At the DSM and ECS sections, two control sites with no treatments are instrumented and monitored.

In conclusion, on site DSM IH 30 horizontal inclinometer readings including elevation surveys were performed to monitor the vertical soil movements on the surface of the embankment. The inclinometer yielded the movements of soil data under the bridge approach slab, while the elevation survey directly gave the displacement on the pavement profile. These monitored data from the horizontal inclinometer addition and the elevation survey are useful to investigate the soil movements on the highway surface, and will be used further in the numerical model analysis in another Chapter. From the data collection, it can be seen that the soil beneath the approach slab has a maximum vertical displacement at the approach of 0.25 in. (6.35 mm), while a maximum value at the embankment slope is about 0.75 in. (19.05 mm). The most important factor resulting in this small difference of the settlement value is the accuracy of the instrument itself. While per reading the inclinometer has an accuracy of 0.006 in. (0.16 mm), the total station can give the accuracy only at 0.12 in. (3 mm) or 20 times larger than the inclinometer resolution .

The results from vertical movements monitoring show that only small movements less than 0.1 in. (2.54 mm) are observed in the embankment. The small movements may indicate that the lateral movements are not critical in the assessment of deep soil treatment methods in mitigating approach slab settlements.

On site ECS fill used on SH 360, only vertical inclinometers readings and elevation surveys were performed. Four vertical inclinometers were installed in different locations, at the centre of highway median, in the median but close to the highway, in the median but close to an embankment slope, and in the outer slope. The obtained data from the inclinometer readings show that there were large horizontal displacements could be detected in two vertical inclinometers V3 and V4, which were installed near the slope. The displacement of 5 in. (127 mm) in the lateral direction and 2 in. (50.8 mm) in the perpendicular direction indicates that settlement problem occurring in the embankment. In addition, with the results from elevation surveys the magnitude of the vertical settlement of 1.5 in. (38.1 mm) and 3.4 in. (86.4 mm) should be problematic, which can be seen that the bump already exists on the site. Many of the problematic movements could be visualized during the site visit. The lateral movement of the approach slab could be seen via the opening existing between highway pavement and its shoulder, also via the gap between the inclinometer platform and the highway shoulder. The soil erosion is considered as a main factor for the settlement occurred in the embankment, which may indicate the insufficiency water drainage system during the construction.

The data obtained in this chapter are not only useful to consider the efficiency of the mitigation methods, but they will also be used further in the comparison analysis between the field observations and the analytical predictions obtained from the numerical modeling analysis attempted in the next chapter.

CHAPTER 8

NUMERICAL MODELING

8.1 Introduction

This chapter presents the results of numerical studies attempted to understand the settlement behavior of the present embankments by using the commercial geotechnical finite element software (Plaxis Program). The results of the laboratory testing presented in Chapter 5 were used as the input model parameters in the numerical analysis, and the results from FEM analyses are used to compare with the measured data obtained from the field to validate the modeling analysis. The analysis was performed on two embankments, one supported with DSM columns (IH30, Arlington, Texas) and the other constructed with ECS material (SH360, Arlington, Texas). Once the modeling analysis with satisfaction comparison results obtained, the modeling was then extended to other embankment configurations by varying both heights and slopes of the embankment. The area ratios of the DSMs are varied in order to mitigate the settlements of the hypothetical sections. It should be noted that the unit in this analysis was done in metric system.

8.2 Finite Element Method (FEM)

The Finite element method (FEM) has been found to be the most powerful numerical techniques for solving problems in the mechanics of continuous media (Bugrov, 1975). Nowadays, the FEM plays an important role in all branches of engineering for the analysis and design of the structures (Bathe, 2003). The analysis is typically performed by transforming the physical problem, an actual structure and structural components, into a mathematical model (Bathe, 2003). By using a series of algebraic equations, the numerical models can be solved, and the quantities of interested parameters for example, stress, strain and deformation at the points of interest can be approximately obtained (Burd, 2004)

The FEM is generally consisted of nodes and elements to form a finite element mesh of the structures. A typical two dimensional mesh with 6 nodes is shown in Figure 8.1.

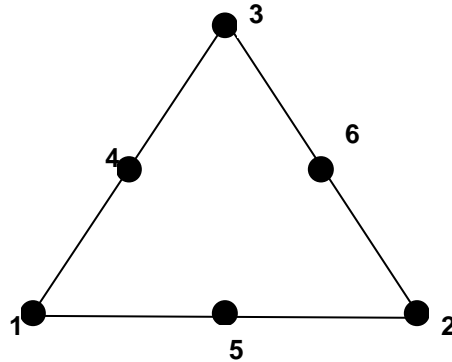


Figure 8.1 Six-node triangular element (Plaxis Manual)

The nodes are not only the points where more than one or two elements connect to the others, but also the points where values of the primary variable of interested parameter are calculated (Burd, 2004). In the FEM analysis, the values of the strain will be calculated and then interpolated in for the entire structure. Later, a relationship between stress-strain of a material behavior usually termed as a constitutive law is used to calculate the stress occurred in the mesh. Last, the force acting on each node obtained from the previous step will be calculated further to compute the nodal displacements by relating the nodal forces with the stiffness equations.

For the one dimensional (1-D) consolidation, the phenomenon can be described by the following differential equation:

$$\frac{\partial p}{\partial t} = c_v \frac{\partial^2 p}{\partial z^2} \quad (8.1)$$

Where

$$c_v = \frac{kE_{OED}}{\gamma_w}$$

$$E_{OED} = \frac{(1-\nu)E}{(1+\nu)(1-2\nu)}$$

$$Z = H - y$$

- k is permeability of soil
- E is the Young's modulus
- ν is the Poisson's ratio
- γ_w is unit weight of water
- E_{OED} is the oedometer modulus

The analytical solution for the above Equation 8.1 in a relation to p/p_0 as a function of time and position is presented by Verruijt (1983) and this equation is presented in the following:

$$\frac{p}{p_0}(z,t) = \frac{4}{\pi} \sum_{j=1}^{\infty} \frac{(-1)^{j-1}}{2j-1} \cos\left[(2j-1)\frac{\pi}{2} \frac{y}{H}\right] e^{\left[-(2j-1)^2 \frac{\pi^2}{4} \frac{c_v t}{H^2}\right]} \quad (8.2)$$

The results of both numerical and analytical method are presented in Figure 8.2. The dotted lines are the results from analytical method and the continuous lines are the results from numerical analysis. It can be seen that the results from both methods are close.

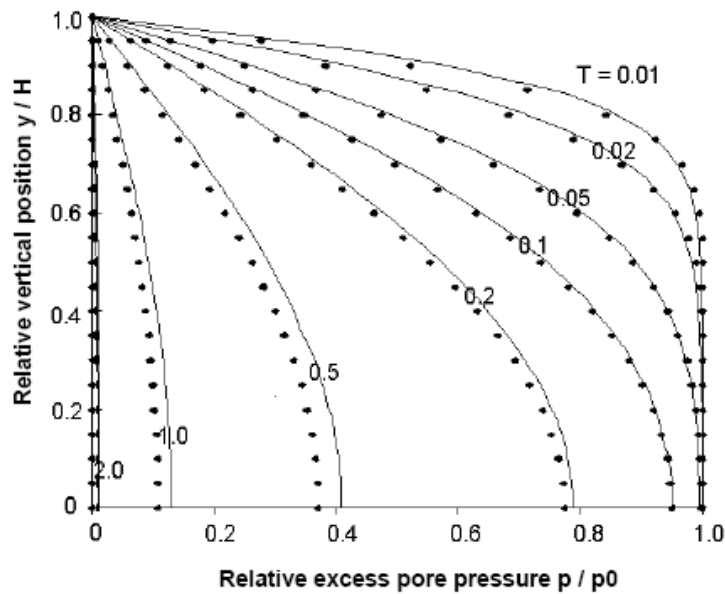


Figure 8.2 The results of excess pore pressure as a function of height from Numerical and analytical methods (Plaxis Manual)

8.3 Modeling of DSM Columns and Control Section, IH30, Arlington, Texas

8.3.1 Test embankment section

8.3.1.1 Geometry and boundary conditions of the DSM columns model

From the previous Chapters, a cross-section and subsurface profile of the embankment passing through the installed rod extensometer is shown in Figure 8.3. The embankment has a total height of 19 ft (6 m) from an existing ground surface and has a side slope of 1V:4H. This section was used in the model to analyze the soil movements occurred both within and underneath the embankment. The embankment was constructed on soft clay with a thickness of 26 ft (8 m) underlain by 10 ft (3 m) thick hard shale. Diameters of soil cement columns have a diameter of 4.0 ft (1.2 m) with a center to center spacing of 5.5 ft (1.67 m). However, in numerical analysis, instead of using the diameter of the DSM columns, the area-ratio (a_r) between DSM and natural soil was used, which was described in Chapter 4. The area ratio with the triangular arrangement using 4 ft diameter columns as per the Equation 8.3 (a_r) is 0.50.

$$a_r = \frac{\frac{1}{2}a_{col}}{a_{soil} + \frac{1}{2}a_{col}} \quad (8.3)$$
$$a_r = \frac{\frac{1}{2}\pi\frac{(4)^2}{4}}{\left(\frac{1}{2} \times 5.5 \times 5.5 \times \frac{\sqrt{3}}{2}\right)} = 0.48 \approx 0.50$$

The columns were constructed with their based placed over the top of the hard shale layer. Therefore, the length of the columns used in this numerical analysis was equal to the thickness of soft clay layer or 26 ft (8 m). The geometry of the embankment modeled together with the boundary conditions is shown in Figure 8.3.

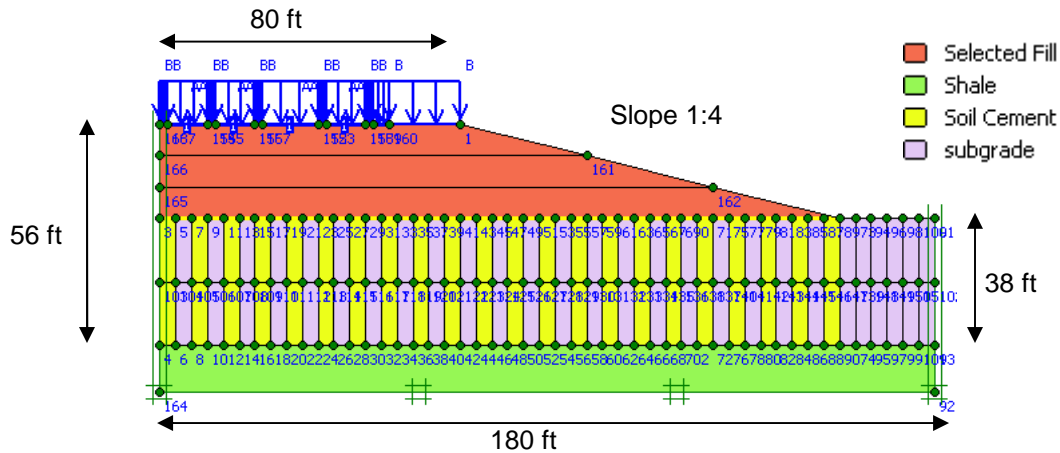


Figure 8.3 Geometry and boundary conditions of the DSM columns model

8.3.1.2 Material property values in a numerical analysis

A soft soil model was used in this study to simulate a natural soft clayey soil, while a hardening soil model was used to simulate the DSM treated foundation soils. Most strength and stiffness information of the deep-mixed and soft clay materials comes from the unconfined compressive strength tests. Secant values of Young's modulus of elasticity determined at 50% of the unconfined compressive strength E_u^{50} . The value of Poisson's ratio for the DSM section is equal to 0.25.

Since this research study is focused on long-term settlement behavior of the embankments supporting approach slabs, the short term embankment settlements during the construction stage were disregarded in the analysis. The analysis was thus done by using a consolidation based model, and the analysis was carried out until the ultimate pore pressure state was reached, or in other words, or until excess pore water pressure developed during embankment loading was completely dissipated. The behavior of the reinforced concrete approach slab was assumed as perfectly-plastic material. The displacement of the boundary at $x=0, y=0$ was restricted in all directions as well as the boundaries at the points of the base. The material properties used in the analysis are given in Table 8.1.

8.3.1.3 Discretization of the DSM treated section

The numerical analyses were performed using Plaxis software version 8.6. A two-dimensional, plain-strain model with 6-node triangular elements was used to model soil layers

and the DSM column elements as shown in Figure 8.4. The embankment in the model consists of 4 types of material, which are select fill, shale, soil cement, and natural subgrade soil. In Figure 8.4, Geogrid is also seen as a yellow line drawn between the embankment and its foundation. On the top left of the model, the approach slab is seen as a blue line, which has a length equal to the width of the slab in a field.

Table 8.1 Properties and model type of the materials used in the model analysis

	Unit	Select Fill	Soft clay	DSM columns	Hard shale
Model type		Soft soil model	Soft soil model	Hardening Soil Model	Hardening Soil Model
Moist density, γ_m	pcf	107	110	110	119
Sat. density, γ_s	pcf	124	122	122	138
Elastic modulus, E_{ref}^{50}	psf	-	-	365270	436496
Poisson's Ratio	-	-	-	0.2	0.2
Cohesion, c	psf	830	540	3130	8830
Friction Angle, ϕ	°	5	5	40	10
Permeability, k	ft/min	2×10^{-6}	2×10^{-6}	2×10^{-6}	2×10^{-6}
Compression Index, C_c	-	0.265	0.39	0.263	0.02
Recompression Index, C_r	-	0.010	0.047	0.041	0.003
Over Consolidation Ratio, OCR	-	-	2.5	5.0	10.0
Initial void ratio, e_o	-	0.60	0.80	0.80	0.50

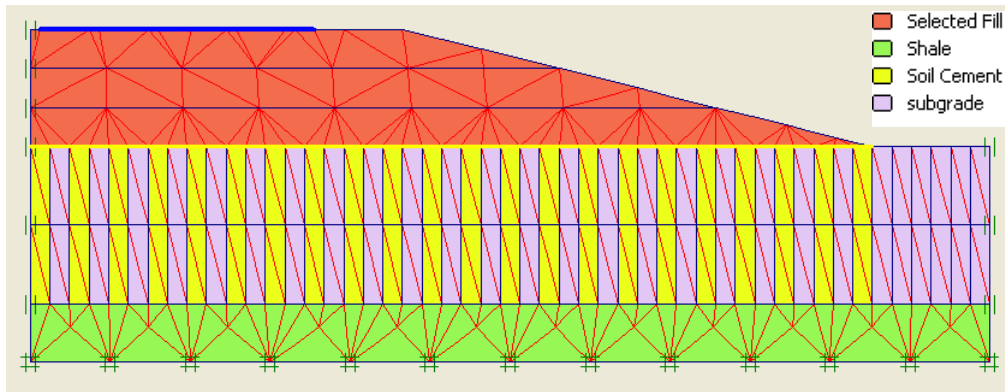


Figure 8.4 Nodes and elements in the DSM treated section

8.3.1.4 Settlement analyses

In the analyses, the total height of the embankment of 6 m was divided into three (3) layers to simulate different phases during the embankment construction as shown in Figure 8.5. In the modeling, each layer was filled in 25 days, and then the layer was left to be consolidated for another twenty five or 25 days. An initial overburden stress due to soil weight, a plastic calculation was used as a load input with multiplier factor of 1.0. Then, the same soil layer was left to be consolidated. This step was done to simulate the compaction effort performed in a real practice. After the last layer of the embankment was included, the whole embankment was compacted by a uniform load in phase number 11. The calculation of the settlement was reset after the construction of an approach slab had been completed in phase number 10. It should be noted that the model analyzed by using a gravity load of the material and the traffic load of 80 kN/m².

Identification	Phase no.	Start from	Calculation	Loading input	Time	Wa...	First	Last
Initial phase	0	0	N/A	N/A	0.00 ...	0	0	0
→ <Phase 1>	1	0	Plastic analysis	Staged construction	25.0...	1		
→ <Phase 2>	2	1	Consolidation ana...	Staged construction	25.0...	2		
→ <Phase 3>	3	2	Plastic analysis	Staged construction	25.0...	3		
→ <Phase 4>	4	3	Consolidation ana...	Staged construction	25.0...	4		
→ <Phase 5>	5	4	Plastic analysis	Staged construction	25.0...	5		
→ <Phase 7>	7	5	Consolidation ana...	Staged construction	25.0...	7		
→ <Phase 11>	11	7	Consolidation ana...	Staged construction	60.0...	11		
→ <Phase 10>	10	11	Consolidation ana...	Staged construction	70.0...	10		
→ <Phase 8>	8	10	Consolidation ana...	Staged construction	200....	8		
→ <Phase 12>	12	8	Consolidation ana...	Staged construction	1000...	8		
→ <Phase 9>	9	12	Consolidation ana...	Staged construction	2000...	9		
→ <Phase 6>	6	9	Consolidation ana...	Minimum pore pressure	1000...	9		

Figure 8.5 Calculation phase in the settlement calculation

To validate the results of the numerical analysis, there are five points selected for studying soil movements on top and within the embankment system. Point A was selected to study vertical displacements occurred in a pavement, while point E was chosen to obtain displacement data happened at the edge of the approach slab. Point B, C and D were the points located at the coordinates exactly at the same locations where the rod extensometers were anchored in the field, which are at the depths of the 10, 20, 40 ft (3, 6, and 13 m), respectively. In addition, another interesting location for analysis is at the edge of the approach slab and all these can be seen in Figure 8.6.

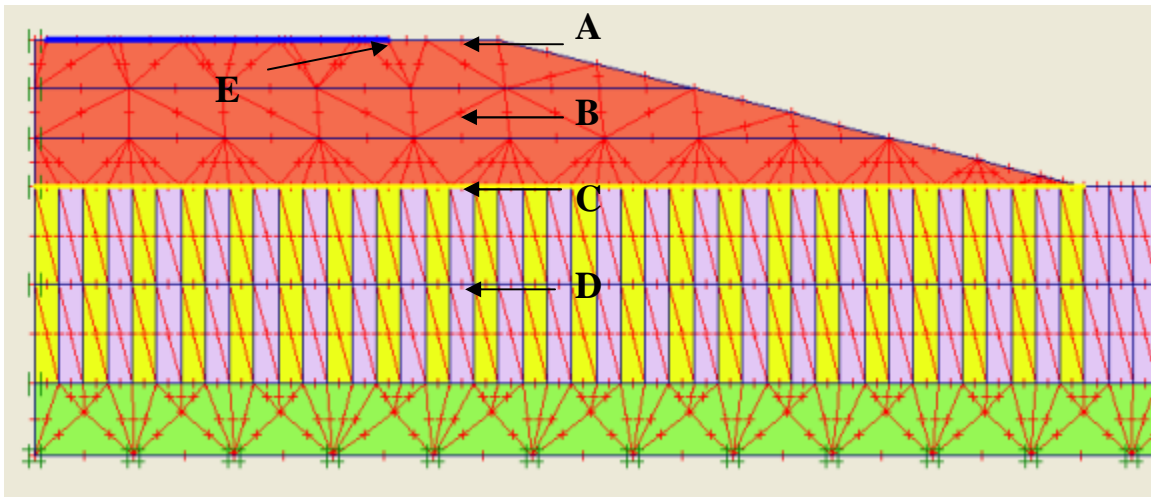


Figure 8.6 Observation points in the settlement calculation

8.3.1.5 Results of the FEM model analysis

The results from FEM model analysis are presented in Figures 8.7 to 8.10. Figure 8.7 presents the deformed mesh after the construction of the approach slab with a magnification scale of 1:20. The maximum displacement in this analysis is equal to 3.5 in. (0.090 m) and this occurred in the right side of the slab. The elements of DSM columns and natural subgrade soil are also deformed in the same area, which can indicate that the settlement of the subgrade soil can affect the displacement of the approach slab above it. The results of total displacements occurred in the embankment are shown in Figure 8.8. In this figure, it can be clearly seen that the maximum total displacement occurred on the right side of the slab, and the influenced area starts

from the top of the embankment until the depth of 20 ft (6 m) below the surface of natural subgrade. In addition, the affected area is mostly located under the embankment, while the soft subgrade beyond the embankment is not influenced much.

Figure 8.9 shows the horizontal soil movements. It can be seen that the horizontal movements occurred either under the embankment slope or beneath the approach slab, but not within the zone of observation. The vertical soil displacements are presented in Figure 8.10. It is obviously seen that the pattern of color shades from the results of vertical movements in Figure 8.10 is quite similar to the pattern from the results of total movements in Figure 8.8, which means the vertical movement is predominant factor in this study.

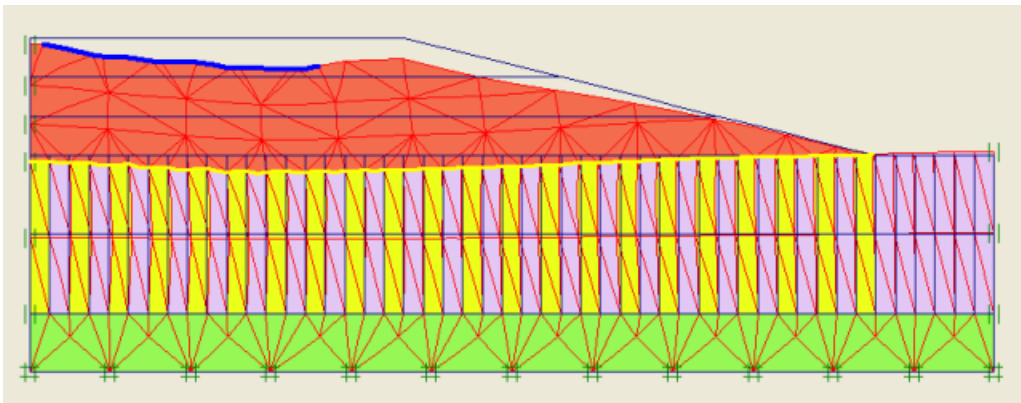


Figure 8.7 Deformed mesh of the model (scaled up 20 times)

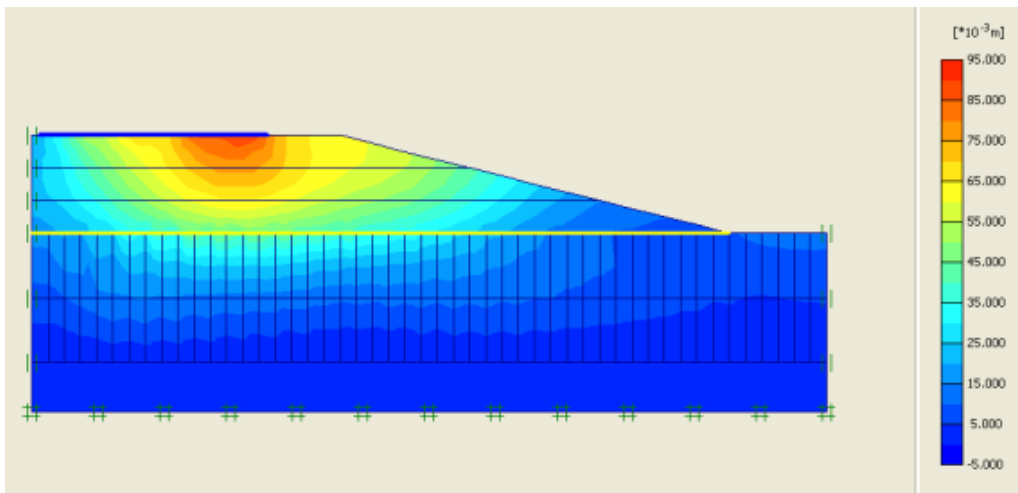


Figure 8.8 Total displacements in the embankment

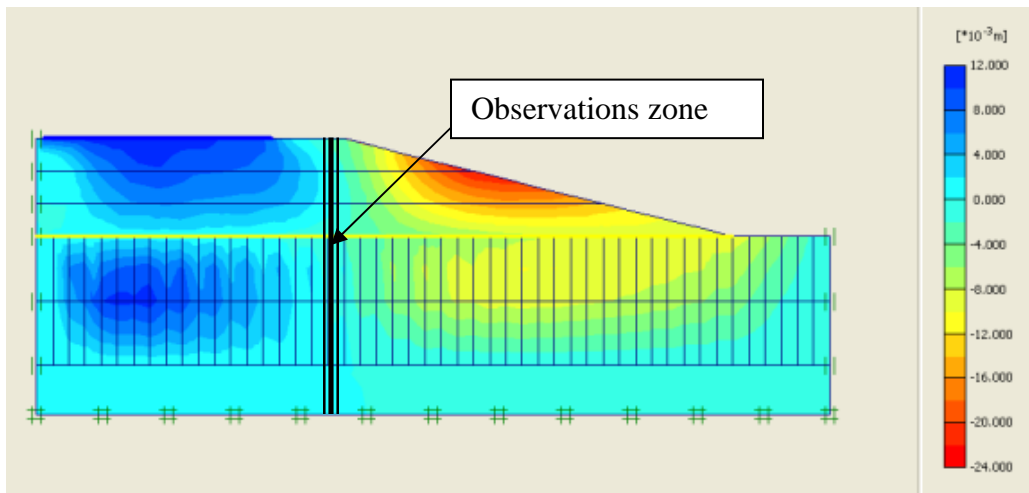


Figure 8.9 Horizontal displacements of the model

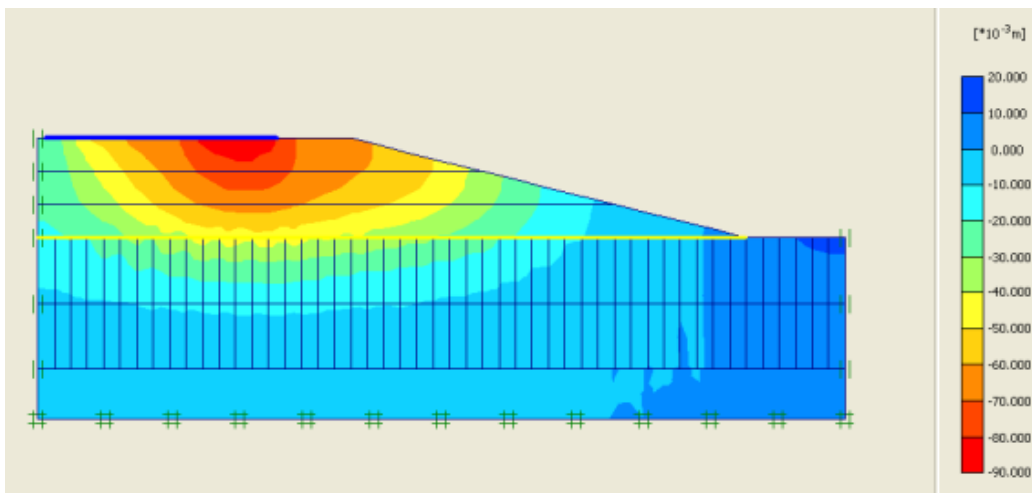


Figure 8.10 Vertical displacements of the model

8.3.1.6 Validation

In this section, the results of the model analysis are compared with the data from field studies. These comparisons are performed in order to validate the parameters used in the model analysis whether they can be good representatives of the real soils. Figures 8.11- 8.14 present the data comparisons, which are performed according to directions of soil movements, for example, 1) vertical displacements – used data obtained from horizontal inclinometer, elevation surveys, rod extensometer and sondex field monitoring studies, and 2) lateral movements – used data monitored from the vertical inclinometer surveys. If the comparisons showed good

agreement, then the validated model is planned to be used further for determining the ground improvement variables for variety of embankment designs.

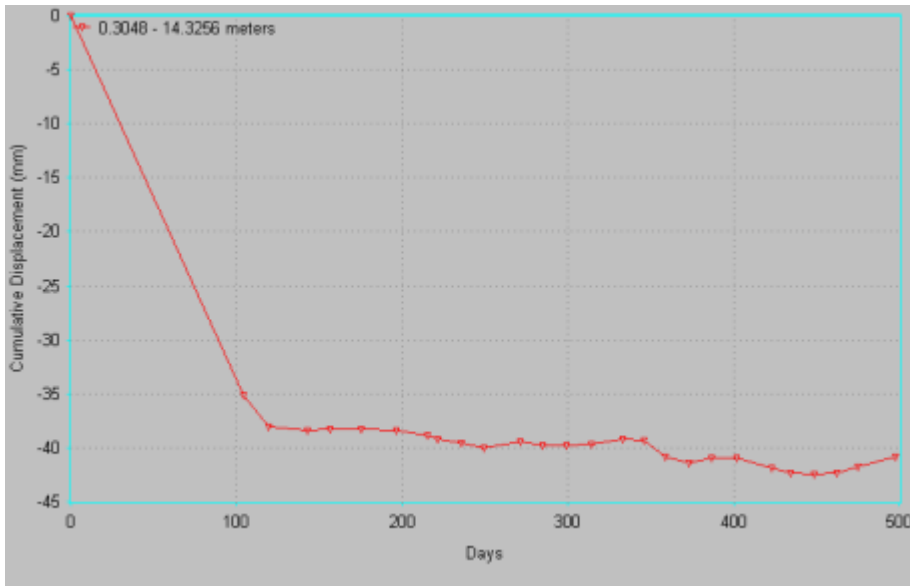
8.3.1.7 Comparisons in the vertical displacements

8.3.1.7.1 *Data comparisons with the horizontal inclinometer*

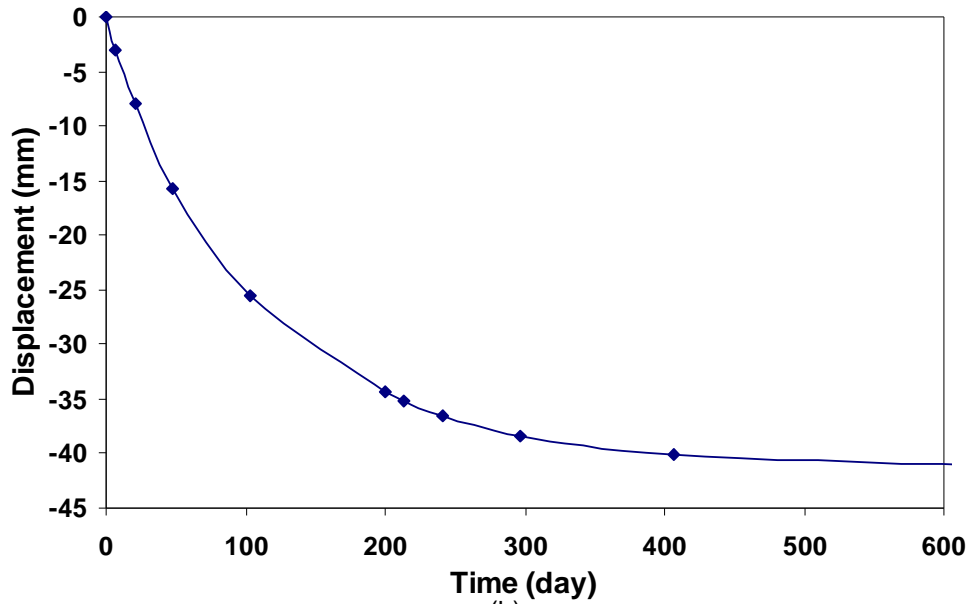
The data obtained from the horizontal inclinometer is the vertical displacements occurred beneath the approach slab and this is shown in Figure 8.11 (a). It can be seen from Figures 8.11 (a) that a total settlement of 1.38 in. (35 mm) occurred within 100 days after the installation of horizontal inclinometer, and thereafter the settlement gradually increased to 1.70 in. (43 mm) after completion of 500 days. Around that time, the inclinometer casing was broken and hence no more data was collected after that time period. The settlement trend can be seen in Figure 8.11 (b), the rapidly increase in settlement is seen in the first 100 days before the settlement gradually increased to the maximum settlement value of 1.65 in. (42 mm).

8.3.1.7.2 Data comparisons with the elevation surveys

Another data comparison is performed by plotting the data from the elevation surveys presented in Table 7.1 of Chapter 7 with the results from the numerical analysis. Comparisons can be seen in Figure 8.12. It can be noted that the time-settlements of the present comparison shows a good agreement with each other. Even though the settlement values from the recent elevation surveys are slightly larger than the results from the model, the prediction on the whole is still in agreement with the measured data.



(a)



(b)

Figure 8.11 Vertical displacements (a) from horizontal inclinometer (b) from numerical analysis

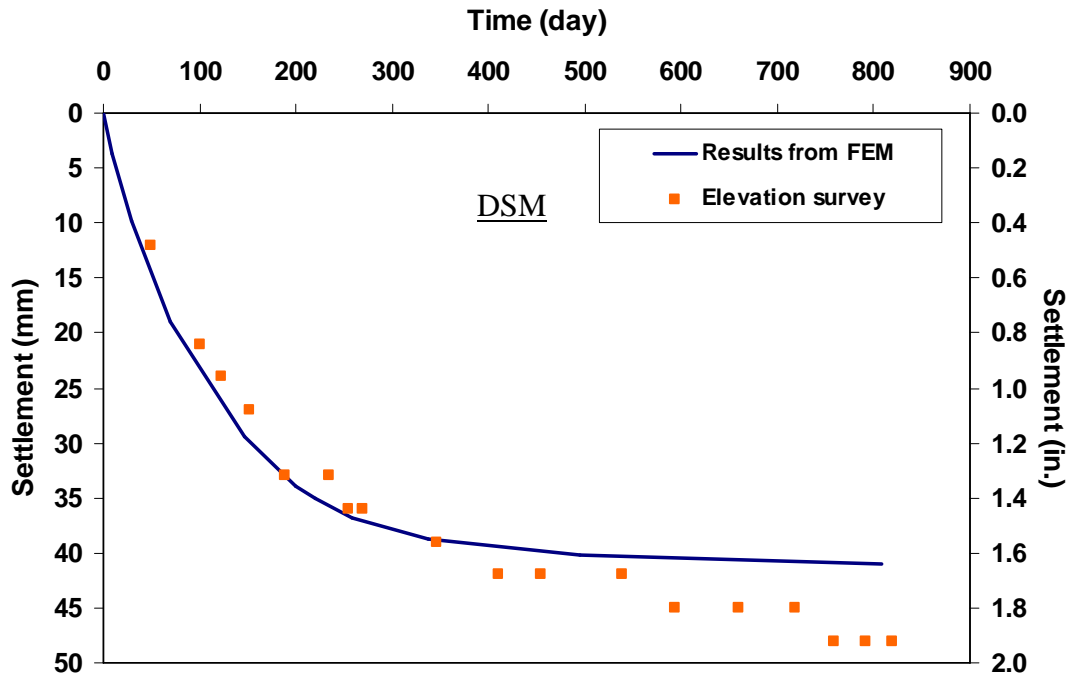


Figure 8.12 Comparison of vertical displacements in a treated section between data obtained from elevation surveys and results from numerical analysis

8.3.1.7.3 Data comparisons with the rod extensometers

Data obtained both from automatic and manual reading rod extensometers were plotted versus the results from the FEM numerical modeling as shown in Figures 8.13 and 8.14, respectively. From both figures, the settlements of soils at the different depths obtained from the FEM model have the same trends as the settlement values obtained from the field. The displacement values at the depth of 10 ft (3 m) are more than the measured values with a small difference of 0.04 in. (1 mm) between them. Overall it can be concluded that the settlement readings are in agreement with the numerical modeling results.

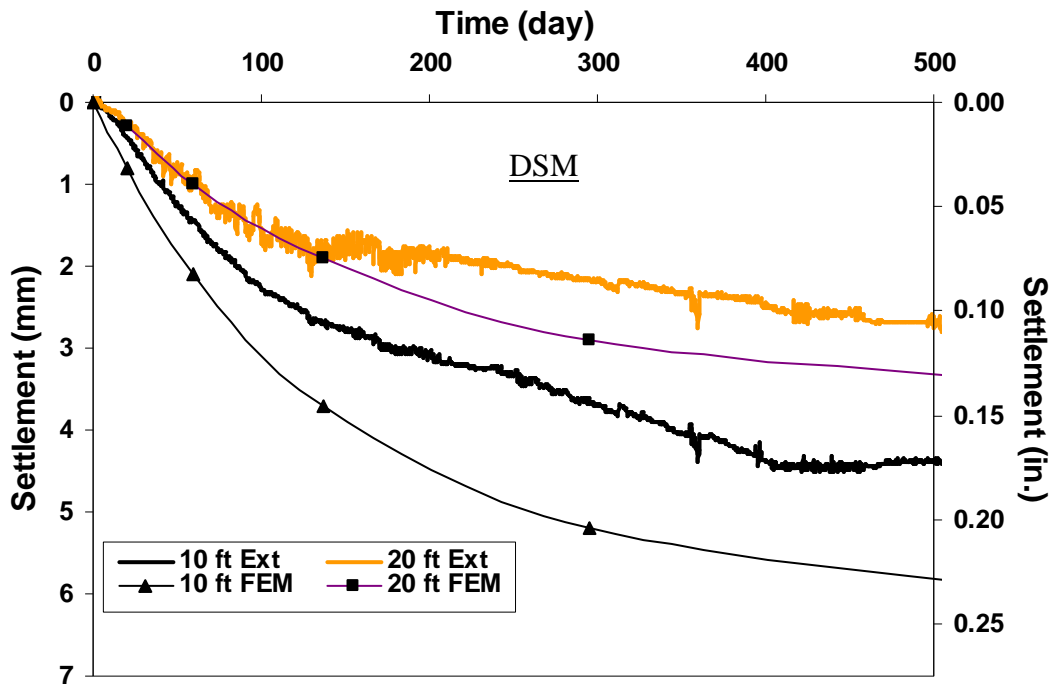


Figure 8.13 Comparison of vertical displacement values between data obtained from Automatic extensometer and results from numerical analysis

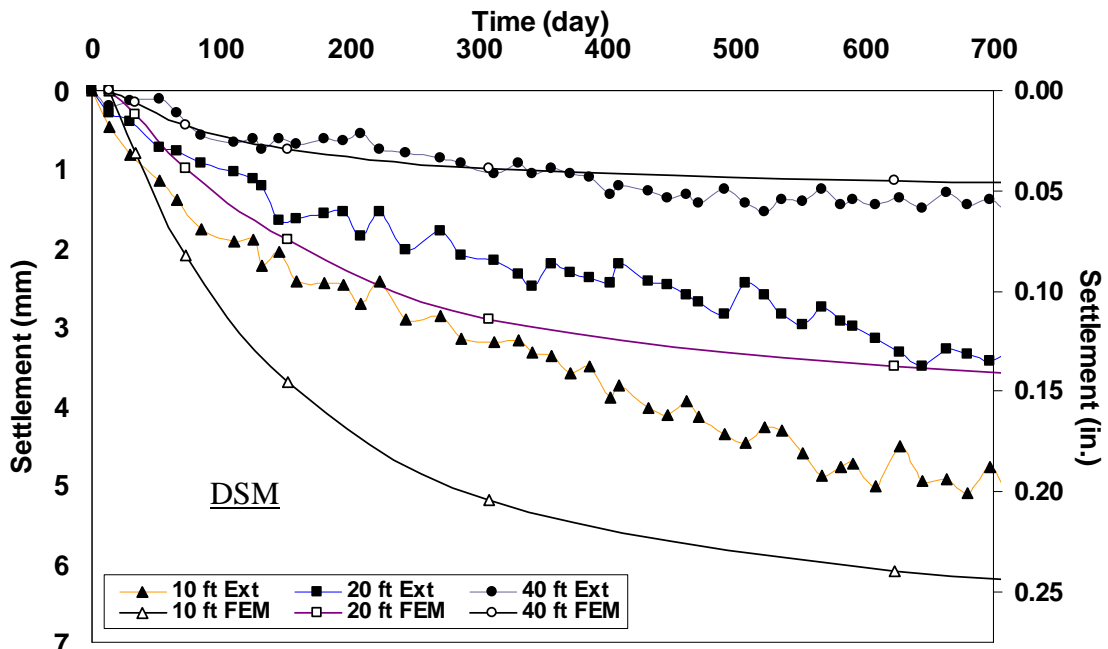


Figure 8.14 Comparison of vertical displacement values between data obtained from Manual extensometer and results from numerical analysis

8.3.1.7.4 Data comparisons with the sondex

From previous chapter 7, the readings of the sensor rings at all depths in the DSM treated embankment were swung up and down within 0.8 in. (20 mm). This oscillating reading value is obviously more than either the settlements monitored with the other instruments or the settlement results from the numerical analysis. Therefore, in this case no comparison is necessary to be performed, and the results from the FEM model can be considered in agreement with the data from sondex surveys.

8.3.1.8 Comparisons in the horizontal displacements

8.3.1.8.1 Data comparisons with the vertical inclinometer

The lateral movements measured from the vertical inclinometer surveys was plotted and compared with the results of numerical analysis in Figures 8.15 (a) and (b), respectively. As already mentioned in Section 8.3.5, the numerical analysis yields only small value of lateral soil movements in the area where the vertical inclinometers were installed. However, when the maximum value of 0.36 in. (9.28 mm) is compared with the lateral displacement in the direction of B-axis obtained from the field, it can be seen that the FEM analysis give the results close to the data from the field. Although, it is concluded from the previous chapter that the lateral movements are considered insignificant in the study of DSM site, the results of the numerical analysis can still prove that the soil parameters and other configurations used in the study have provided results that are in a good agreement with the performance of the test section and soils in the field.

8.3.2 *Control embankment section*

To comprehend how the DSM columns lessening the settlement in the embankment, the numerical analyses were also performed on a control embankment to understand settlement values in the control embankment, and then compare them with the values from the treated section analyses. The control section is the embankment located in the North side of the bridge. This embankment was constructed over the natural subgrade without any soil treatment or any support by the DSM columns. Therefore, this control embankment section is called as an

untreated section. In the untreated section, there was only a vertical inclinometer casing and sondex installed in the median of the four lane highway.

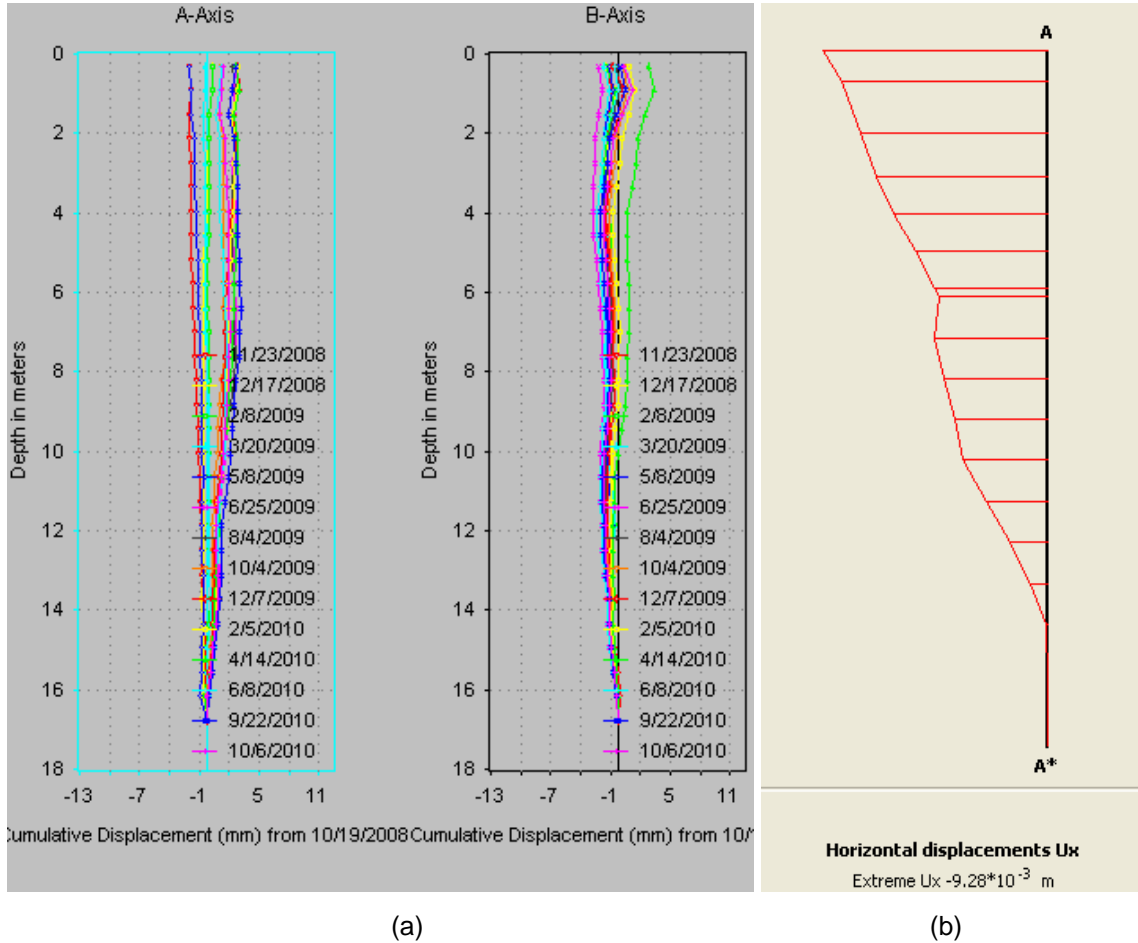


Figure 8.15 Lateral soil movements (a) from the vertical inclinometer (b) from results of the numerical analysis at the section of the inclinometer

8.3.2.1 Geometry, boundary conditions and discretization of the control section

The geometry and boundary conditions used in the untreated section are similar to ones in the treated section. This untreated embankment section has 4 lane traffic, 2 lanes for the northbound and others two for the southbound. Therefore, the embankment is symmetric and has a centre line on the left side as shown in Figure 8.16. Since the control section is the embankment without any support from the DSM columns, the numerical analyses on the control section are performed by removing the DSM elements and their input parameters out from the modeling, and then replacing the DSM elements with the soft subgrade and its properties as

shown in Figure 8.16. Apart from that changing number of the elements and nodes, and boundary conditions are the same as used in the treated section analyses.

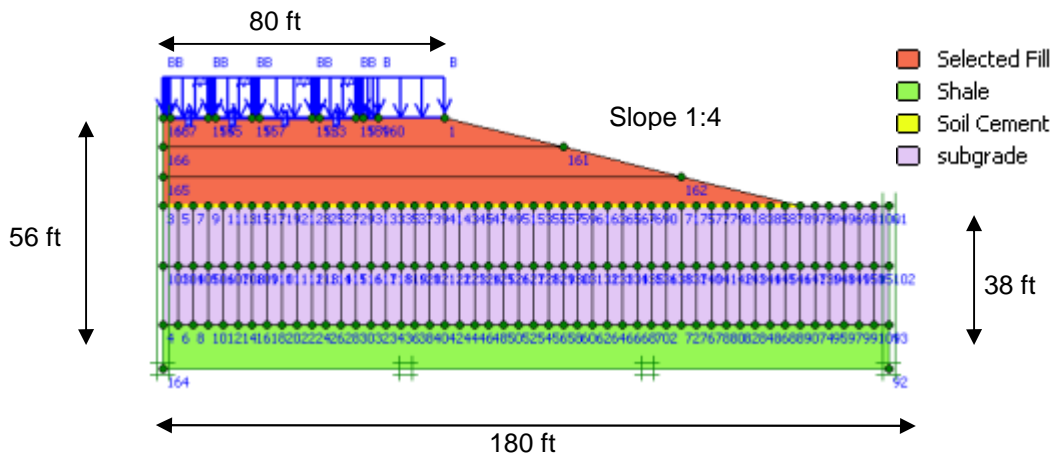


Figure 8.16 Geometry and boundary conditions of the untreated section in a model

8.3.2.2 Settlement analyses

In the settlement analyses, the embankment section with the total height of 6 m is divided into 3 layers similar to the DSM treated section. The duration of the construction phases, including calculation model, load multiplier factor, and traffic load in the treated section analysis are also used here. The difference from the treated section in this analysis was only the location of interesting points as shown in Figure 8.17.

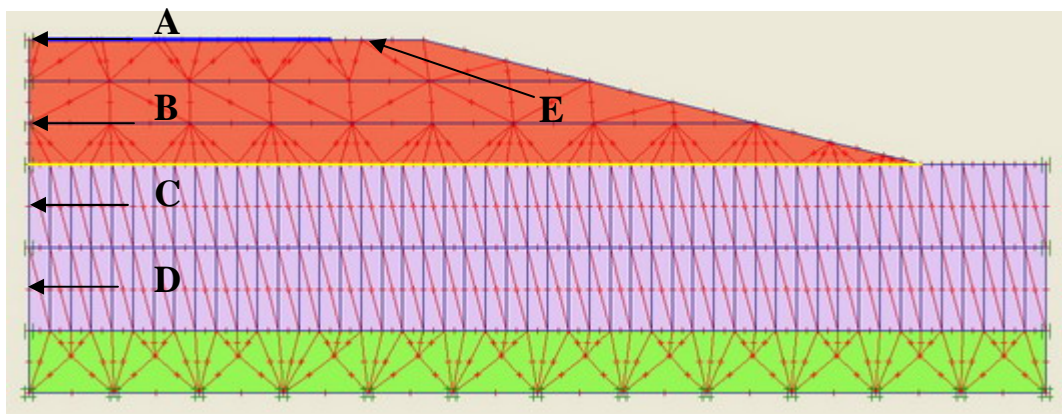


Figure 8.17 Observation points in the settlement calculation

Point A is a location of Control section where the elevation survey was performed, Point B, C and D are points where sensor rings of the sondex were collected, and these points are

selected such that they can be used for the settlement comparisons between the treated and untreated sections.

8.3.2.3 Results of the numerical analysis

Figures 8.18 – 8.21 show the results from numerical analysis. It can be seen from Figure 8.18 with the scale factor of 1 to ten times, the highest settlement in the analysis is equal to 11 in. (0.28 m) and this occurred near a slope of the embankment. Besides, it is clearly seen that the subgrade layer especially in the area under the crest of the embankment experienced more settlements than the outer slope area. The results of total displacements occurred in the embankment are shown in Figure 8.18.

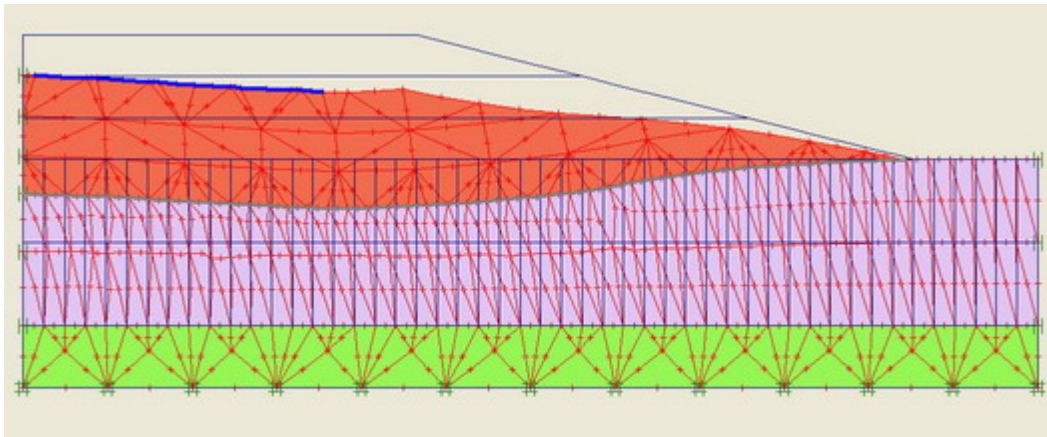


Figure 8.18 Deformed mesh of the model

In Figure 8.19, it is clearly seen that the maximum total displacement occurred at the top right of the embankment, and the influenced or stressed area starts from the top of the embankment to a depth of 20 ft (6 m) below the surface of natural subgrade and this observation is similar to the one noted from the treated section analysis. In addition, the affected area is mostly located underneath the embankment, while the soft subgrade beyond the embankment location has lesser influence.

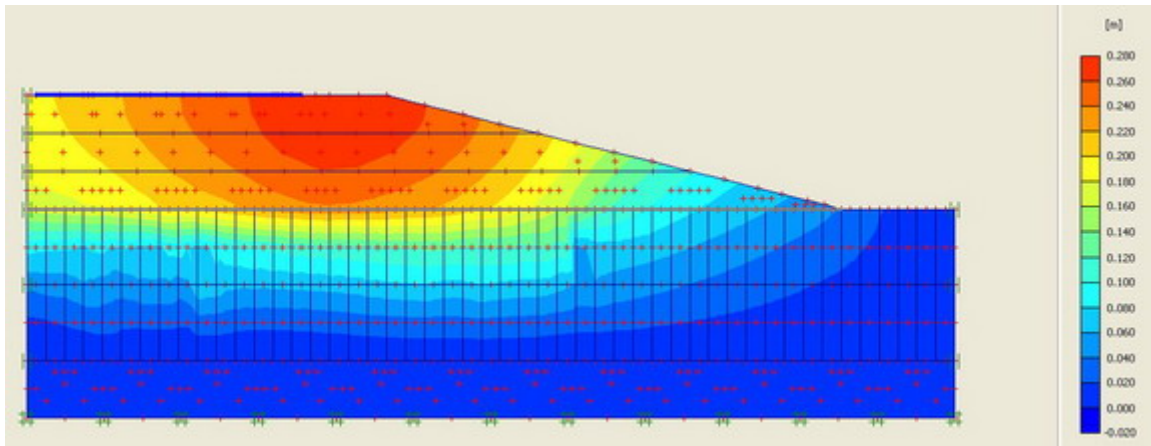


Figure 8.19 Total displacements in the embankment

Figure 8.20 presents the horizontal soil movements within and outside the embankment section. From the plot, it is seen that large horizontal soil movements occurred near the outer slope, whereas small movements can be seen in the area close to the centre line. Figure 8.21 presents the results of vertical soil displacements, which can be seen that they look similar to the results of total movements in Figure 8.19. The similarity of those two figures notifies that the vertical displacement is a predominant factor in the study.

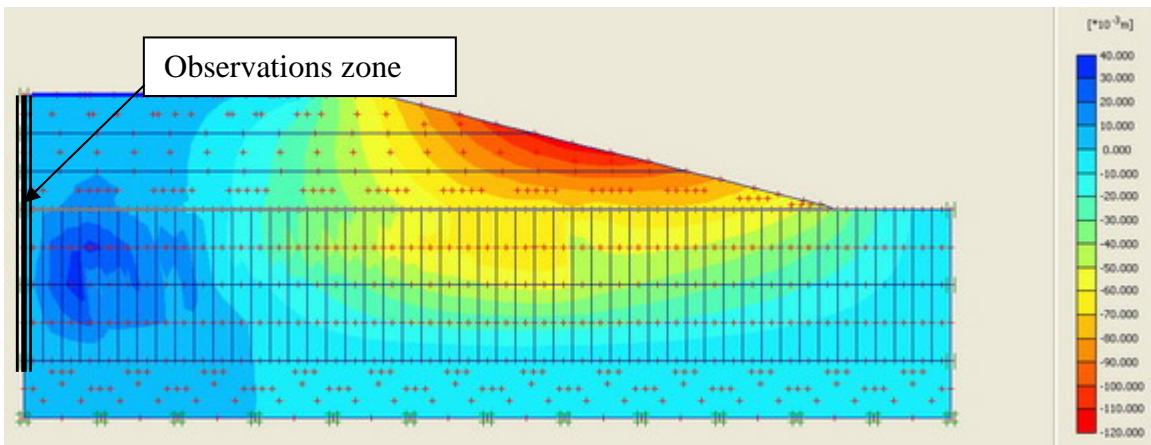


Figure 8.20 Horizontal displacements of the model

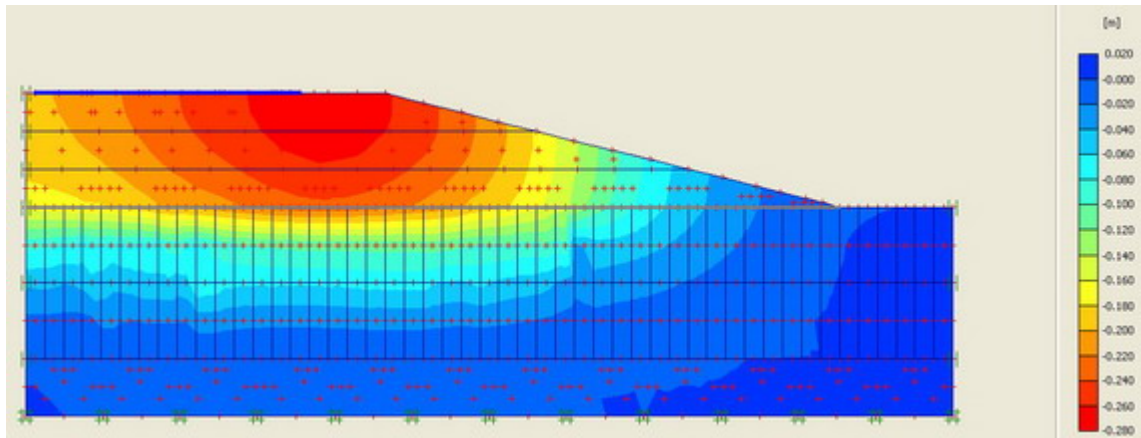


Figure 8.21 Vertical displacements of the model

8.3.2.4 Validation

The results from numerical analysis are compared with the monitored data from the field to evaluate whether the numerical model including its parameters are in agreement with the soil movement behavior in the field. As being done in the treated section, the data from elevation surveys and sondex are used to compare with the results of vertical soil movements from the FEM model, and the data recorded from vertical inclinometer were compared with lateral soil displacements. The data comparisons are presented in Figures 8.22 and 8.24. Figure 8.22 shows the graph plotted between vertical displacements from elevation surveys and the results from the numerical model. The comparison of lateral soil displacements is shown in Figure 8.24, which shows the monitoring data and the movements obtained from the numerical modeling using FEM software.

8.3.2.5 Comparisons in the vertical displacements

8.3.2.5.1 Data comparisons with the elevation surveys

The data from elevation surveys in Table 7.2 was plotted against the results of vertical soil displacements from the FEM model as shown in Figure 8.22. It can be mentioned that the time-settlement relationship from the numerical analysis is much higher than the time-settlement curve from the elevation survey. This result reveals that the numerical model used to predict the soil displacement in the control section was not fitted in the practice. This may come from that the section was chosen as a control section has soil properties different from the

assumption. After considering the location as shown in Figure 8.23, it can be seen that the monitoring point is not located in a weak soil zone, where the DSM is not required. The subgrade soil in this area has better properties than the subgrade soil in a treated section. Therefore, the

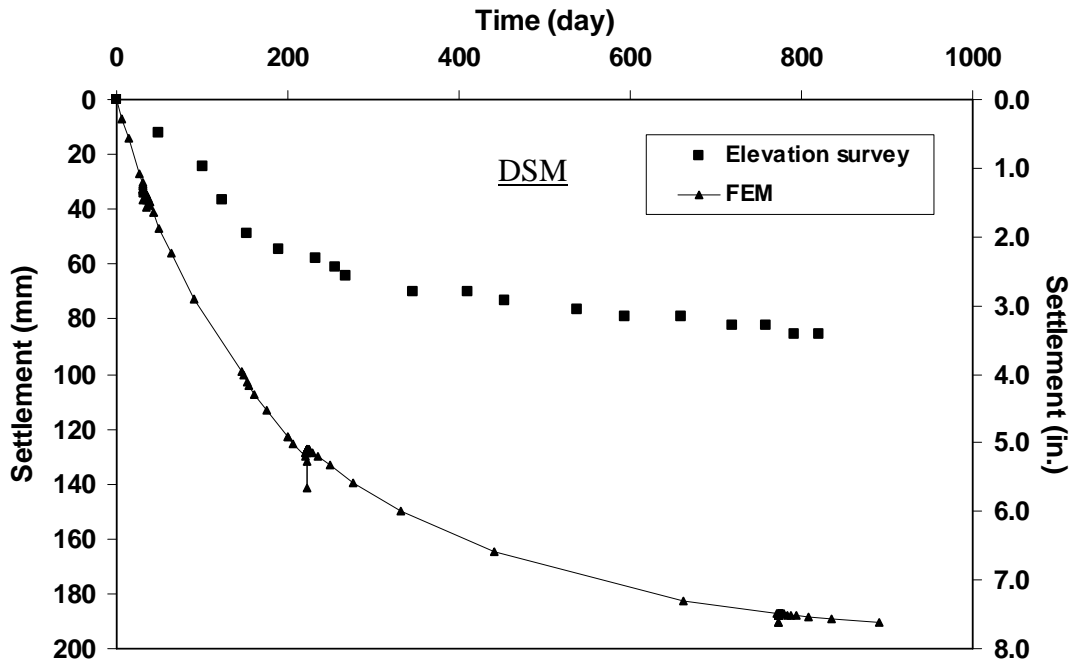


Figure 8.22 Comparison of vertical displacement in a control section values between data obtained from elevation surveys and results from numerical analysis

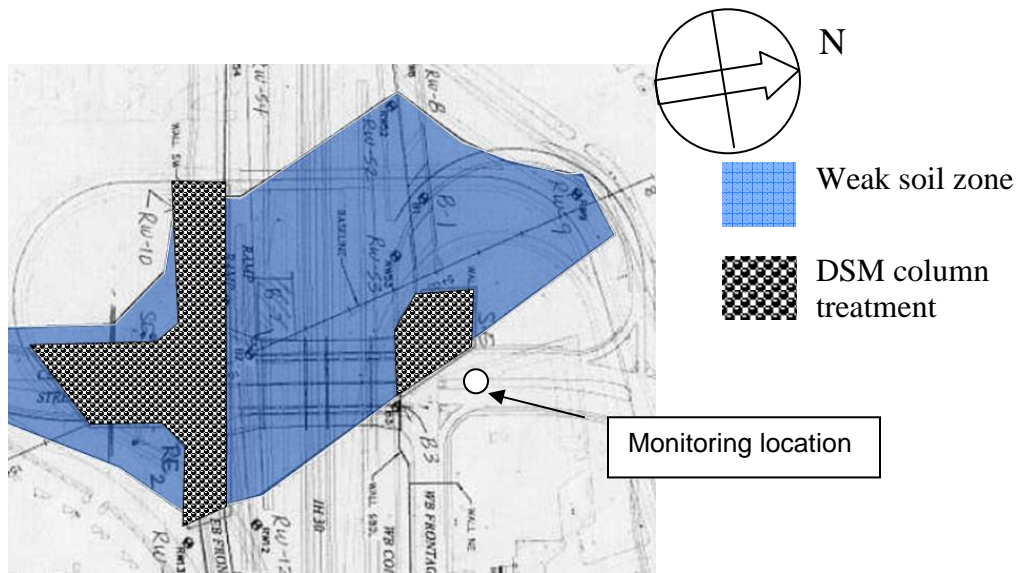


Figure 8.23 The monitoring location in a control section, IH 30 site, Arlington, TX

settlements from the observations are small when compared with the results from the numerical analysis, which used the weaker soil in the analysis. However, it can be seen that if the south embankment constructed without the DSM columns, the vertical displacement of 7.1 in. (0.18 m) could have been expected and worsen the settlements at the bridge approach.

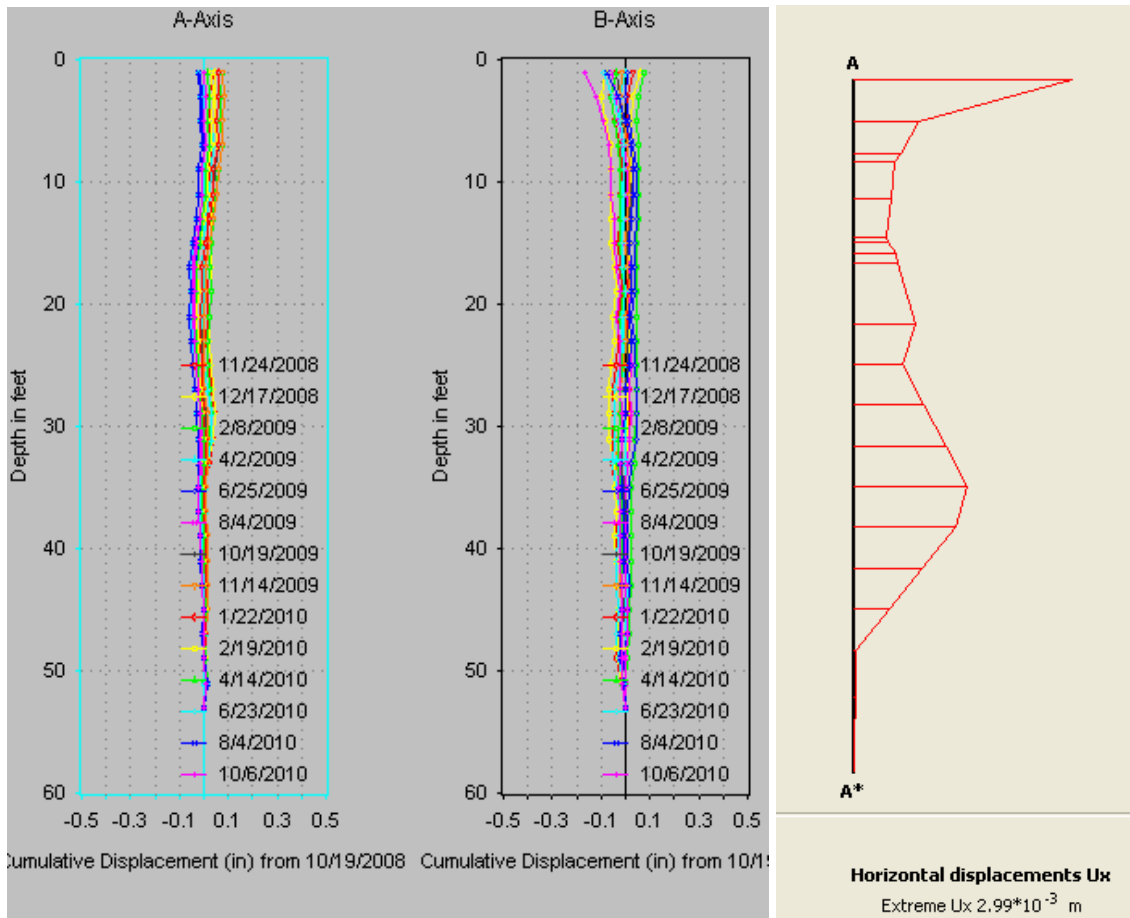
8.3.2.5.2 Data comparisons with the sondex

The comparison between the readings from Sondex and the results from the numerical analysis is not necessary to perform, since from the previous comparison it is already seen that the control section in a field is not a real representative of the untreated section. The untreated section has settlement values lesser than the amount of what it should have been due to stronger properties of the subgrade soil in the area. Therefore, in this case no comparison is presented, and the data from the sondex readings in Chapter 7 already revealed that even without the DSM columns, the vertical soil movements monitored in the field were fluctuated within a range of +/- 0.6 in. (1.5 cm), which is attributed to the strength of the subgrade soil in the North embankment.

8.3.2.6 Comparisons in the horizontal displacements

8.3.2.6.1 Data comparisons with the vertical inclinometer

Figures 8.24 (a) and (b) show the lateral movements measured in the vertical inclinometer and the results of lateral movements from numerical analysis, respectively. In this analysis, the lateral displacements in the A-axis from the vertical inclinometer are chosen for consideration, since it has the same movement direction as in the cross-section. Although it is seen that the magnitude of lateral displacements in both Figures are almost the same at 0.1 in. (2.54 mm) and 0.12 in. (2.99 mm), the comparison of them to validate the numerical model can be disregard. However, those two small displacement values reveal that the horizontal displacements are insignificant in this study.



(a) (b)
 Figure 8.24 Lateral soil movements (a) from the vertical inclinometer (b) from results of the numerical analysis at the section of the inclinometer

8.3.3 Comparisons of Vertical Soil Movements Occurred between Treated and Untreated Embankments

From the previous subsection, it is concluded that the horizontal soil movements are not significant in the study of DSM treated section. Therefore, only the soil movements in vertical direction are being considered. Since the subgrade soil in a control section is different from one in a test section, the comparison between the soil movements between both sections will be meaningless. Therefore, to see the effectiveness of the DSM columns in mitigating the settlement occurred in the embankment the data from elevation surveys on the treated embankment are used to compare with the results from numerical analysis performed on the control section. To do that, the vertical displacements at Point A shown in Figure 8.6 are compared with the

displacement values at Point E of Figure 8.17, and the comparison of the vertical soil movements is presented in Figure 8.25. It can be seen from the figure that the embankment with DSM columns experienced only one-fourth of magnitude of settlements occurred in the untreated embankment. This smaller settlement can reduce the bump problem that might occur under the bridge approach area.

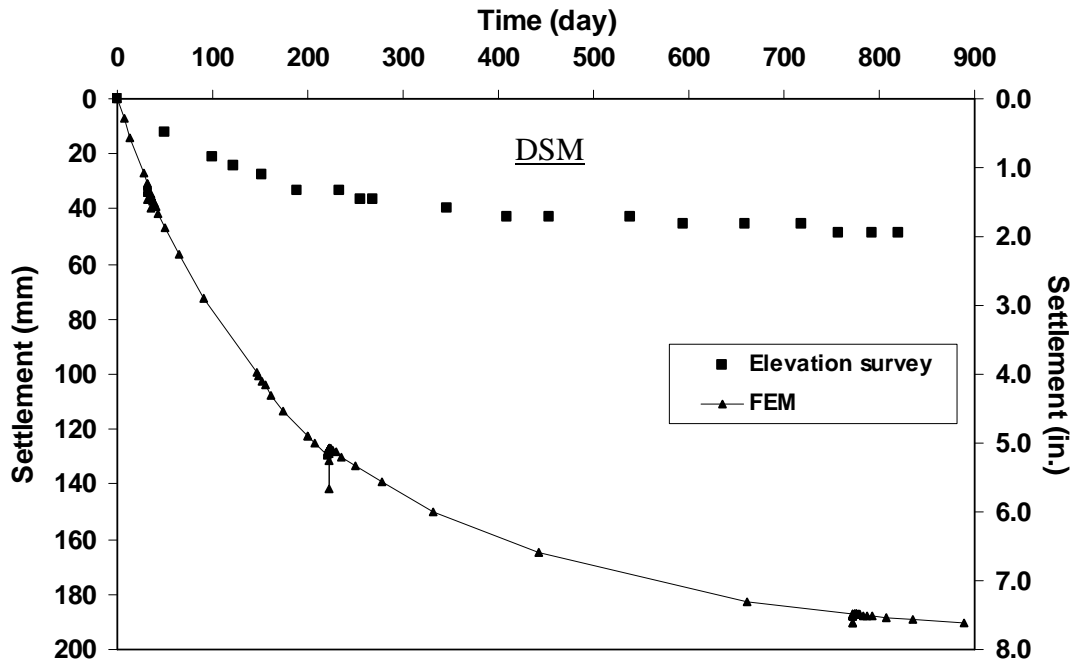


Figure 8.25 Comparison of vertical displacements between data obtained from elevation surveys in a treated section and results from numerical analysis in an untreated section

8.3.4 Analysis of Vertical Soil Movements

To predict a long term settlement, a hyperbolic method (Lin and Wong, 1999) was used in this study, and the hyperbolic equation is as follows:

$$\frac{t}{s} = \alpha + \beta t \quad (8.4)$$

- Where t = time from the start of embankment fill (day)
 s = measured settlement as any specific time t (mm)
 α = gradient of the straight line between t and t/s
 β = intersection of the straight line on the t/s axis

According to Eq. (8.4) the elevation survey data from both control and test section were plotted in with a function of time-settlement ratio as shown in Figure 8.26.

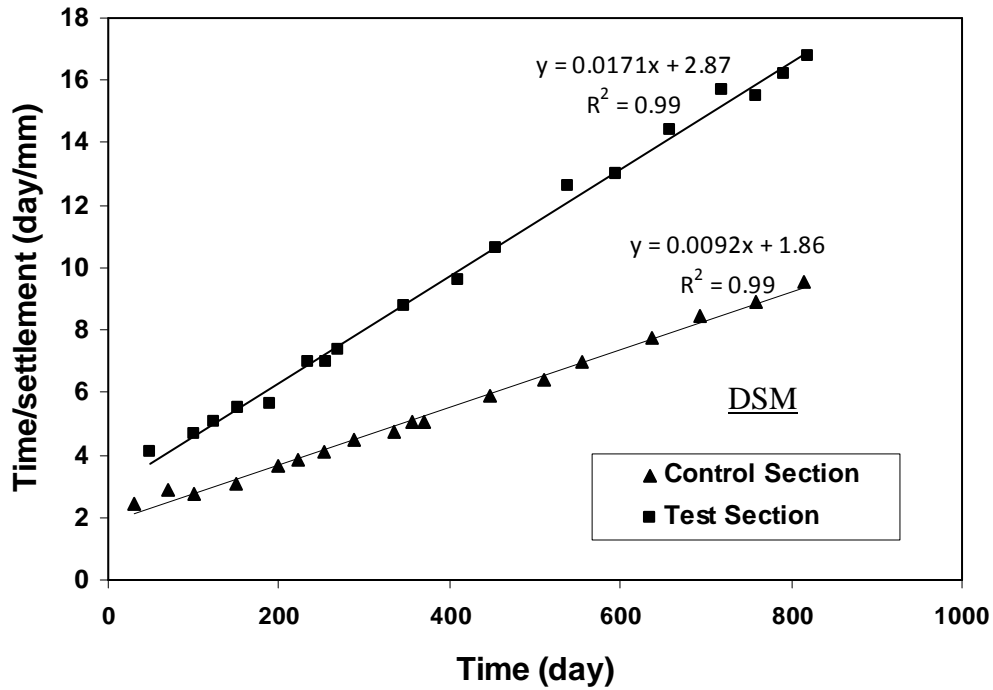


Figure 8.26 Regression equations from hyperbolic model to predict soil settlement values in both treated (test) and untreated (control) sections

With the regression equations shown in Figure 8.26 and the hyperbolic equation as in Eq. (8.4), the magnitude of soil settlements at a specific time (t) in the embankments can be obtained from the following Eq. (8.5).

$$s = \frac{t}{(\alpha + \beta t)} \quad (8.5)$$

Therefore, the soil settlement occurred at time (t) in a treated section is equal to:

$$s = \frac{t}{(2.87 + 0.0171t)} \text{ mm} \quad (8.6)$$

and the soil settlement occurred at time (t) in an untreated section is equal to:

$$s = \frac{t}{(1.86 + 0.0092t)} \text{ mm} \quad (8.7)$$

By solving Eq.(8.6), (8.7) and with the time increment of 10 days, the soil settlement occurred in both embankment at the specific time interval can be calculated. The results of the settlements prediction from hyperbolic model and FEM are shown in Table 8.2. From the table, it can be seen that if the settlement predictions are performed for 10 years, the settlement values in the treated section can be found at a value of 2.20 in. or 56 mm (hyperbolic model) and a value of 2.52 in. or 64 mm (FEM), while the value in the control section is equal to 4.06 in. 103 mm (hyperbolic model) and 10.63 in. or 270 mm (FEM). It should be noted that the settlement value of 270 mm in the control section was obtained when soft foundation soil as in the test section was used for the simulation. However, in practice the foundation soil in the control section is stiffer than in the test section; therefore, the predicted settlement values from the FEM are higher than values from elevation surveys and extrapolated data as seen in Table 8.2.

Table 8.2 Settlement predictions from the Hyperbolic model and the FEM

Settlements at year (in.)	Elevation surveys*	Hyperbolic model (extrapolated data)				FEM			
		2	2	10	20	30	2	10	20
Treated section	1.93	1.93	2.20	2.24	2.24	1.57	2.52	2.56	2.60
Control section	3.35	3.35	4.06	4.17	4.21	9.45**	10.63**	10.83**	10.91**

Noted - * Measured Data
 - ** Results from the simulation based on soil foundation in the treated section

From Figure 8.27, it is clearly seen that the results from extrapolation data and FEM for the test embankment are in agreement, while the results for the control embankment are quite different according to the aforementioned reason.

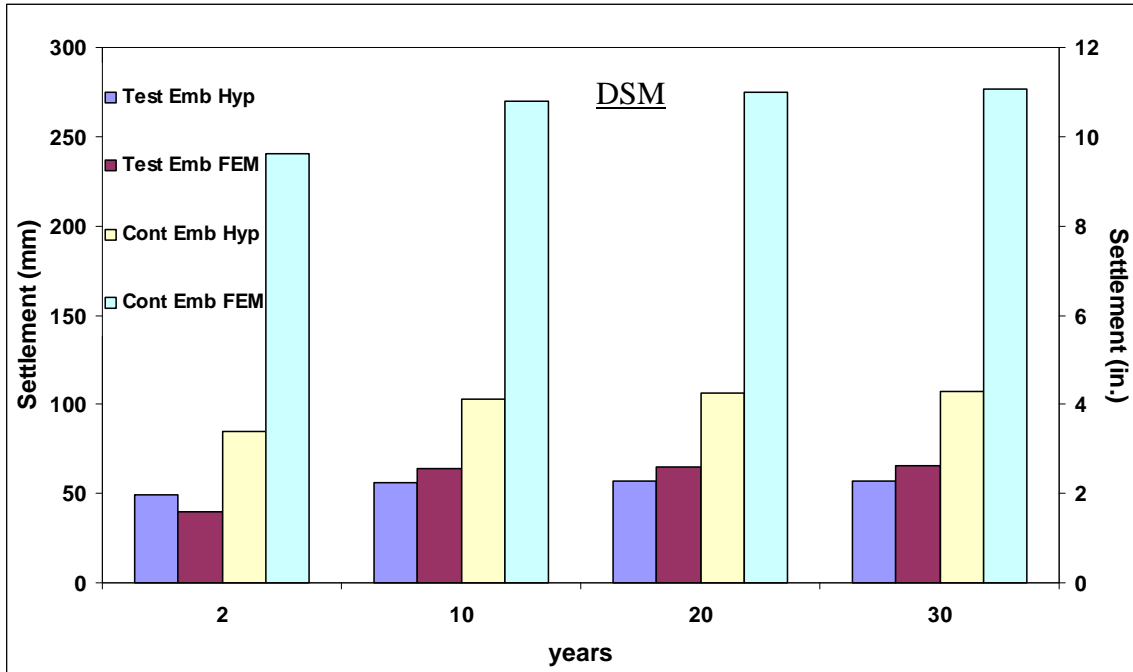


Figure 8.27 Settlement values from data extrapolation and FEM

8.3.5 Prediction of Soil Movements Occurred in the Treated Section with Variations of Embankment and DSM Configurations

To investigate the effects of embankment and foundation configurations on the settlement, parameters such as the area-ratio (a_r) between DSM and natural soil, slope and height of the embankment are varied for various scenarios.

8.3.5.1 Influence of area-ratio (a_r) between DSM and natural subgrade

The area-ratio (a_r) between DSM and natural soil is an important factor in reducing the settlements occurred underneath an embankment. Therefore, various values of the area-ratio (a_r) are used in the numerical analysis. Area-ratios of 0.3, 0.4, 0.6, 0.7 and 0.8 were inputted into the original embankment model, which has a height of 18 ft (5.5 m) and a side slope (V: H) of 1:4. Figure 8.28 shows a monitored point A and the embankment model with an area ratio of 0.3.

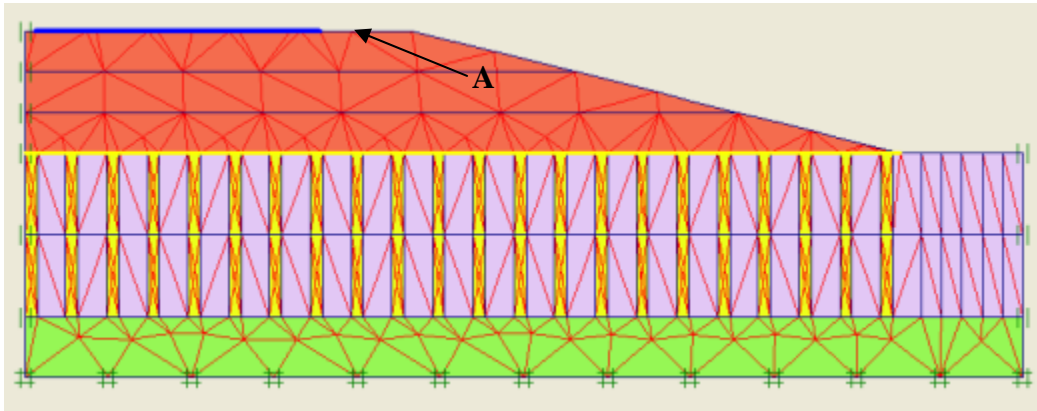


Figure 8.28 Nodes and elements in the DSM treated section with the area-ratio (a_r) of 0.3

The results from FEM analysis are presented in Figures 8.29 – 8.31. Figure 8.29 shows the deformed mesh of the embankment by scaling it up to 20 times. The maximum vertical displacement in this analysis is equal to 4.7 in. (0.12 m) and this occurred in the right side of the slab as shown in Figure 8.30. Figure 8.31 shows the horizontal displacement, it can be seen that the movements mostly occurred in the slope, but with a small magnitude of 0.015 in. (0.4 mm).

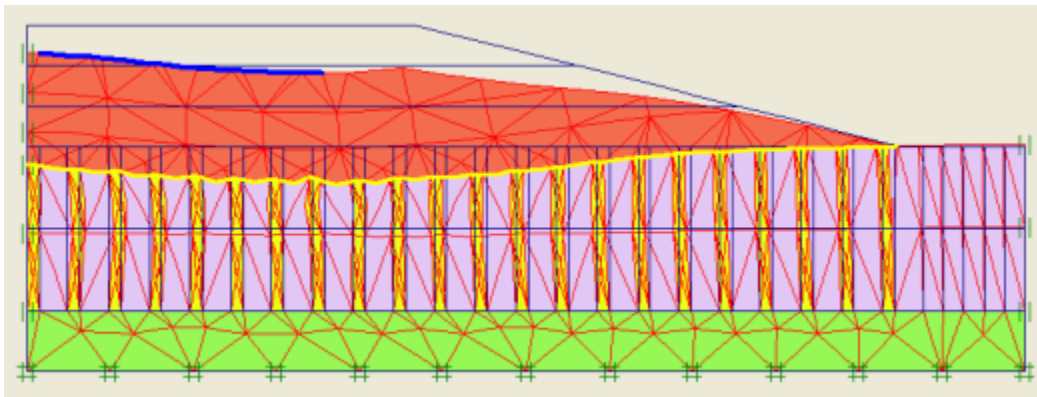


Figure 8.29 Deformed mesh of the DSM treated section with the area-ratio (a_r) of 0.3 (scaled up 20 times)

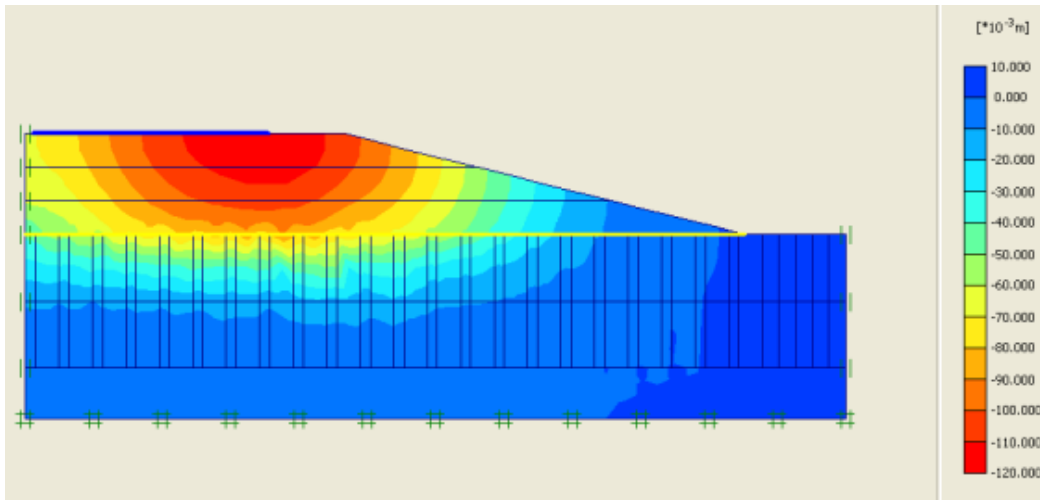


Figure 8.30 Vertical soil movements in the DSM treated section with the area-ratio (a_r) of 0.3

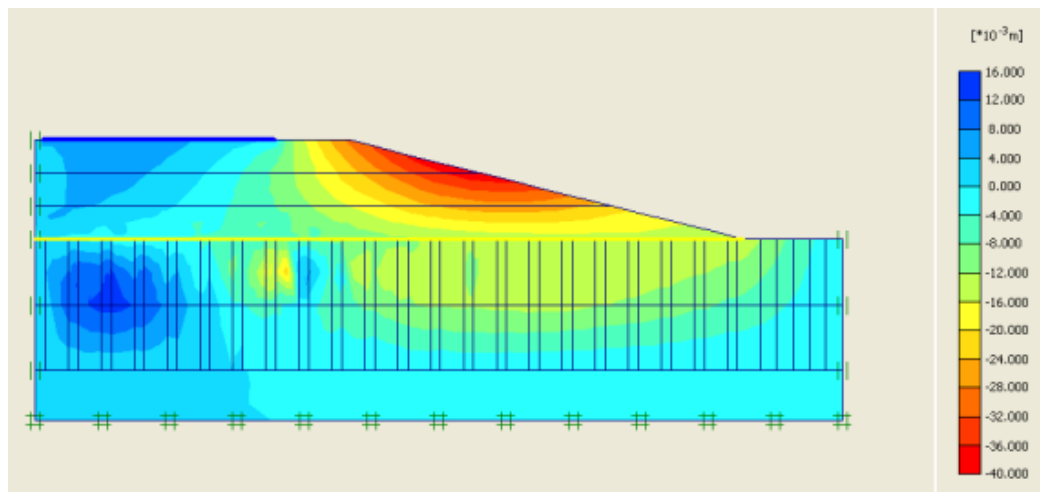


Figure 8.31 Horizontal soil movements in the DSM treated section with the area-ratio (a_r) of 0.3

The same procedure was also performed to find the vertical and lateral soil displacements for the area-ratio (a_r) of 0.3, 0.4, 0.5, 0.6, 0.7 and 0.8. The results of maximum displacements from the numerical analyses with various area-ratios (a_r) are presented in Table 8.3. It should be noted that the presented displacement values are the maximum soil movement occurred in any location in the embankment, which are different from the settlement values monitored on the pavement surface. Figure 8.32 shows a relationship between the soil settlement

monitored at Point A and time. It can be seen that the settlement can be reduced with an increase of the area-ratio of soil treatment.

Table 8.3 Maximum soil displacement of an embankment with various a_r

Area-ratio	Vertical displacement		Horizontal displacement	
	in.	mm	in.	mm
0.3	4.70	119.28	1.55	39.32
0.4	3.15	80.09	1.93	49.08
0.5	1.66	42.25	0.67	16.95
0.6	1.41	35.89	0.48	12.31
0.7	0.76	19.41	0.30	7.75
0.8	0.67	17.06	0.25	6.43

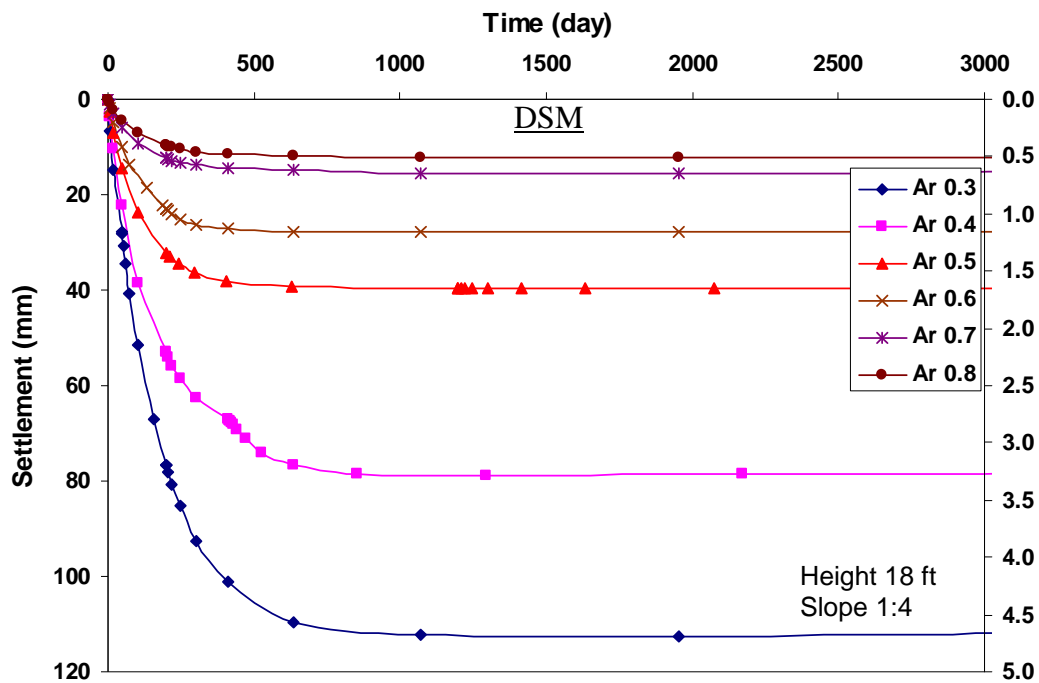


Figure 8.32 Time-settlement in the DSM treated section with various area-ratios (a_r) from 0.3 to 0.8

Figure 8.33 shows a relationship between soil settlements occurred in the DSM treated section with various area-ratios from 0.3 to 0.8. It can be clearly seen that the settlements reduce in a hyperbolic shape when the area-ratios increase from 0.3 to 0.8. The settlement has sharply decreased when area-ratio increased from 0.3 to 0.5, and thereafter the decrease is small. Therefore, it can be concluded that the most effective area-ratio in the DSM design should be between 0.5 and 0.7 for mitigating soil settlements in the embankments when DSM is used for soil treatment.

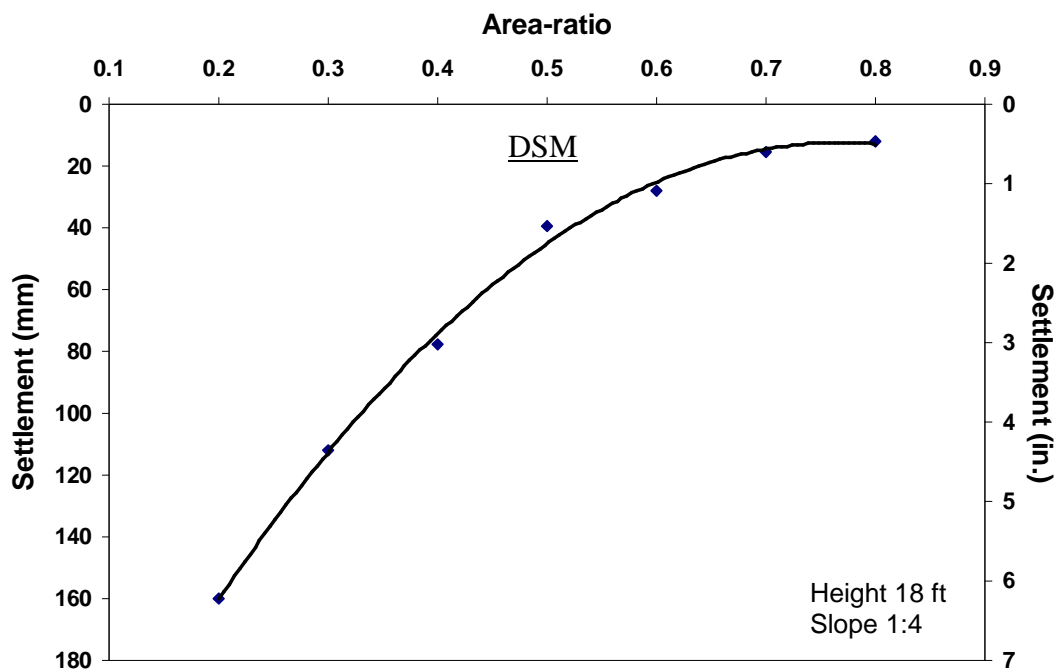


Figure 8.33 Settlement with various area-ratios (a.)

8.3.5.2 Influence of embankment slope

A stability of slope is another factor that can influence the movements of soils in the embankment. The embankment with a good stability, no failure plane occurred in the slope, the soil movements in this situation will depend solely on the consolidation phenomenon. On the contrary, the instability of the slope can induce more settlements in the embankment due to soil movements caused by the slope failure. Therefore, in order to study the effect of slope on the amount of the settlement in the embankment, the gradient of the embankment was changed with various V: H ratios, 1:1, 1:2, 1:3, 1:4, and 1:5. The embankment model in these analyses has a

height of 18 ft (5.5 m) and the area-ratio of 0.5. Figure 8.34 shows a monitored point A and the embankment model with a slope of 1:1 (V: H). It should be noted that the width of DSM columns treated area was changed from case to case depending on a distance from the center line to the toe of the embankment slope.

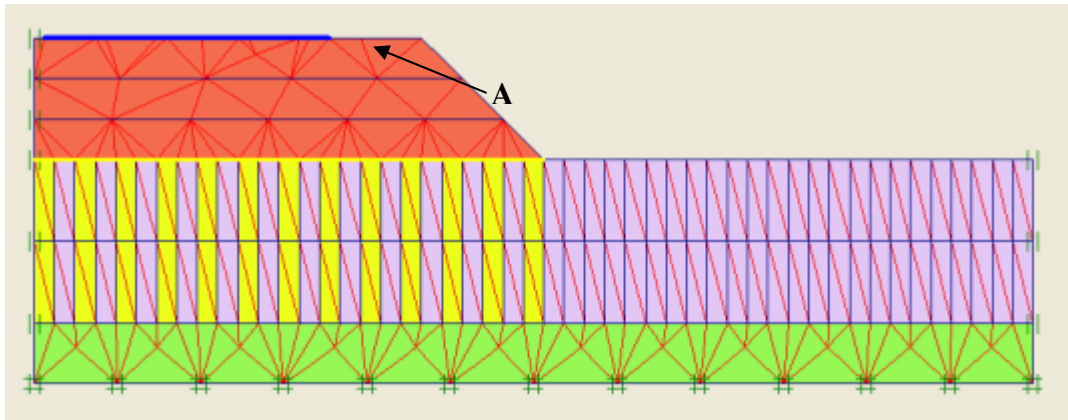


Figure 8.34 Geometry of DSM treated section with a slope (V: H) of 1:1

The results from numerical analysis are shown in Table 8.4. It can be seen that the soil displacements either in vertical or horizontal directions have only small differences when the embankment slope changes from 1:1 to 1:5.

Table 8.4 The maximum soil displacements with various embankment slopes

Slope (V:H)	Vertical displacement		Horizontal displacement	
	in.	mm	in.	mm
1:1	1.27	32.27	0.60	15.28
1:2	1.47	37.37	0.63	16.08
1:3	1.58	40.20	0.65	16.53
1:4	1.62	41.20	0.67	16.95
1:5	1.66	42.11	0.52	13.15

Figure 8.35 shows the deformed mesh of the embankment with a various slope by scaling up 50 times. As shown in Figure 8.35, it is clearly seen that no slope failure can be

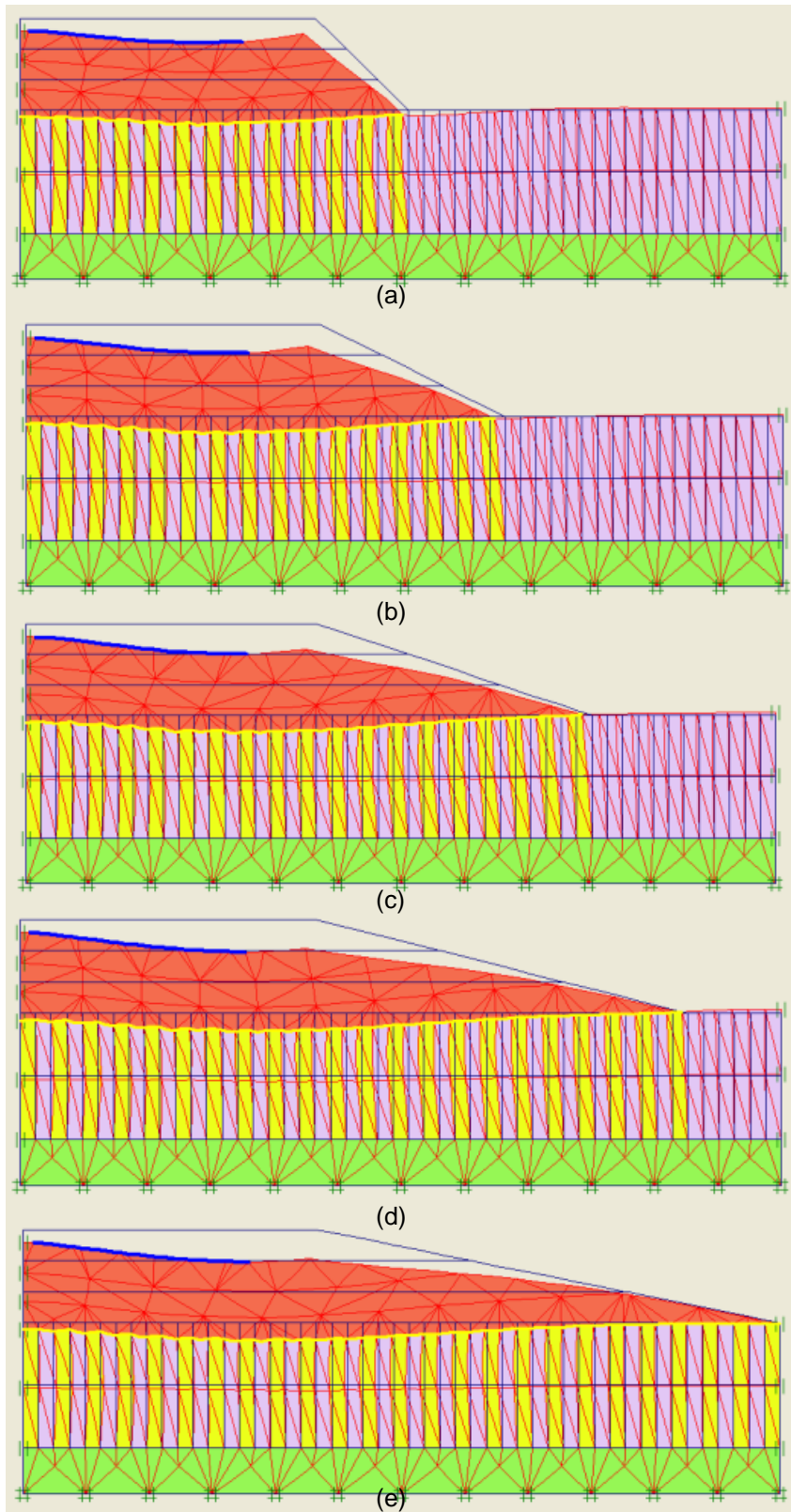


Figure 8.35 Deformed mesh show total settlements in the embankments with various slopes V:H; a) 1:1, b) 1:2, c) 1:3, d) 1:4, and e) 1:5

observed in any slope ratio values. As a result, the soil movement depends mostly on the weight of the embankment. It can be concluded that the slope of the embankment does not affect the magnitude of soil settlement in the treated embankment.

8.3.5.3 Influence of embankment height

Another analysis is performed here to investigate the height of embankment, affecting on the soil settlement. A various heights of the embankment were used in this study starting from 16, 18, 20, 22, 24, 26 ft (5.5, 6.0, 6.5, 7.0, 7.5 to 8.0 m.) Other parameters, slope and the area-ratio, are maintained at 1:4 (V: H) and 0.5, respectively, throughout the study. Figure 8.36 shows a monitored point A and the embankment model with a height of 24 ft (7.5 m) and slope of 1:4 (V: H). It should be noted that the width of embankment at its base and the width of DSM columns treated area must be changed from case to case in order to maintain the slope value at 1:4.

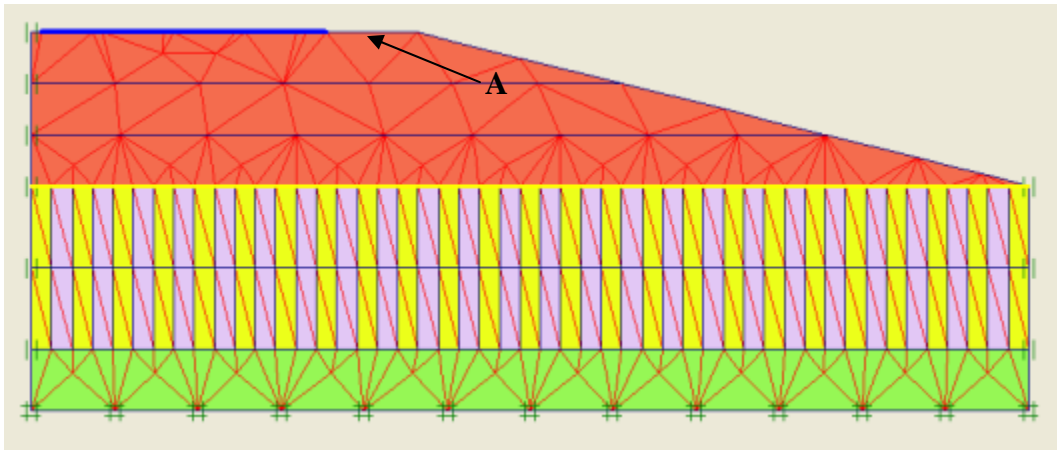


Figure 8.36 Geometry of DSM treated section with a height of 24 ft (7.5 m)

Figure 8.37 demonstrates how the height of the embankment affects on the settlement at Point A in the treated section. It can be seen from time-settlement curves in Figure 8.37 that the higher the embankment, the more soil settlements occurred as embankment height contributes to increase in overburden stress that induces soil settlements.

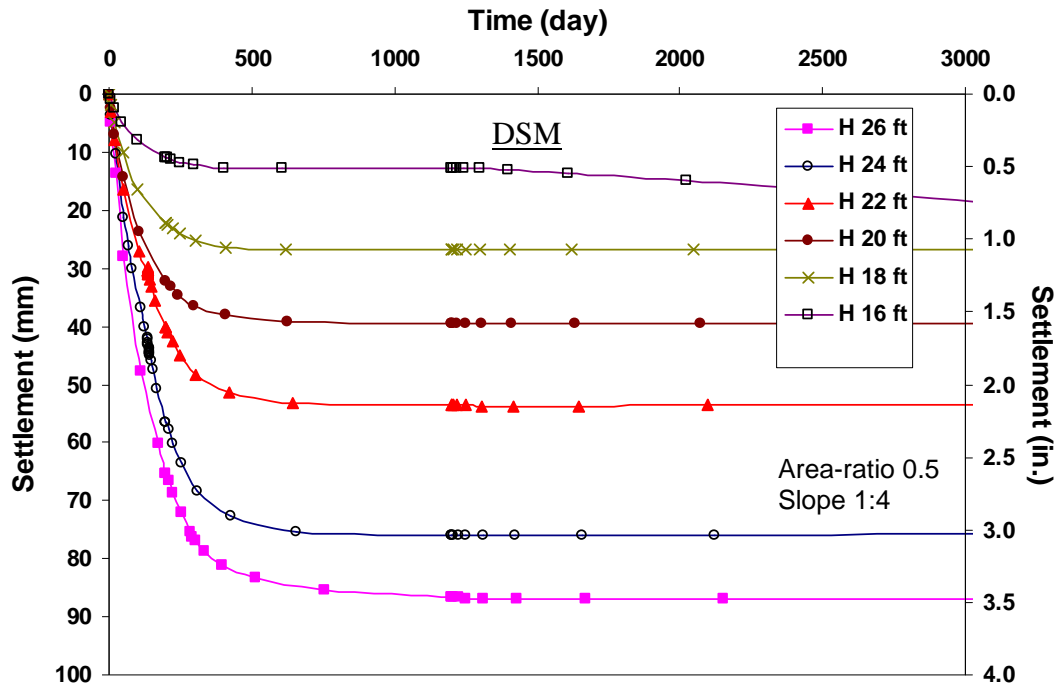


Figure 8.37 Time-settlement in the DSM treated section with various heights of embankment

8.3.5.4 Conclusion from variable studies

It can be concluded from the variable studies that two factors influencing the amount of the settlement in the embankment are the area-ratio of the DSM columns and natural subgrade, and the height of the embankment. With the same embankment geometry, the area-ratio can reduce the settlement occurred in the above structures. The effective area-ratio number found in this study is between 0.5-0.7. Although for the area-ratio less than 0.5 can lessen the settlement, the magnitude of the settlement is still not satisfied. While, the area-ratio number more than 0.7 the effectiveness of the increasing in the area-ratio number is reducing, the amount of the settlements with the area-ratio numbers in that range is slightly different and does not support the increase in cost of the area treatment.

8.3.5.5 Design chart for the DSM columns

From the variable studies, it is seen that the most influent factors for the settlement control in the DSM treated section are area-ratio and height of the embankment. Therefore, with variation of the two factors, a DSM design chart with area-ratios between 0.0 - 0.8 and height of embankment

between 16 - 30 ft (5.5 – 9.0 m) was established as shown in Figure 8.38. A design step-by-step procedure can be done in the following steps.

1. Establish the height of embankment required the DSM treatment.
2. Predict the settlement occurred in the embankment without any foundation treatment.
3. From the predicted settlement value, another settlement and area-ratio can be drawn by interpolation the existing curves shown in the Figure 8.38.
4. Establish a tolerate settlement occurred in the embankment.
5. With that allowable settlement value, a line is drawn parallel to the x-axis until it reaches with a curve of the established embankment height.
6. From the intercepted point, another line is drawn parallel to the y-axis. Thereafter, the minimum require area-ratio can be determined.
7. Length of the DSM columns can be established upon the site soil investigation data.
8. Diameter and arrangement of the DSM columns can be designed according to the market.
9. Number of DSM columns can be determined from the DSM diameter and its arrangement.

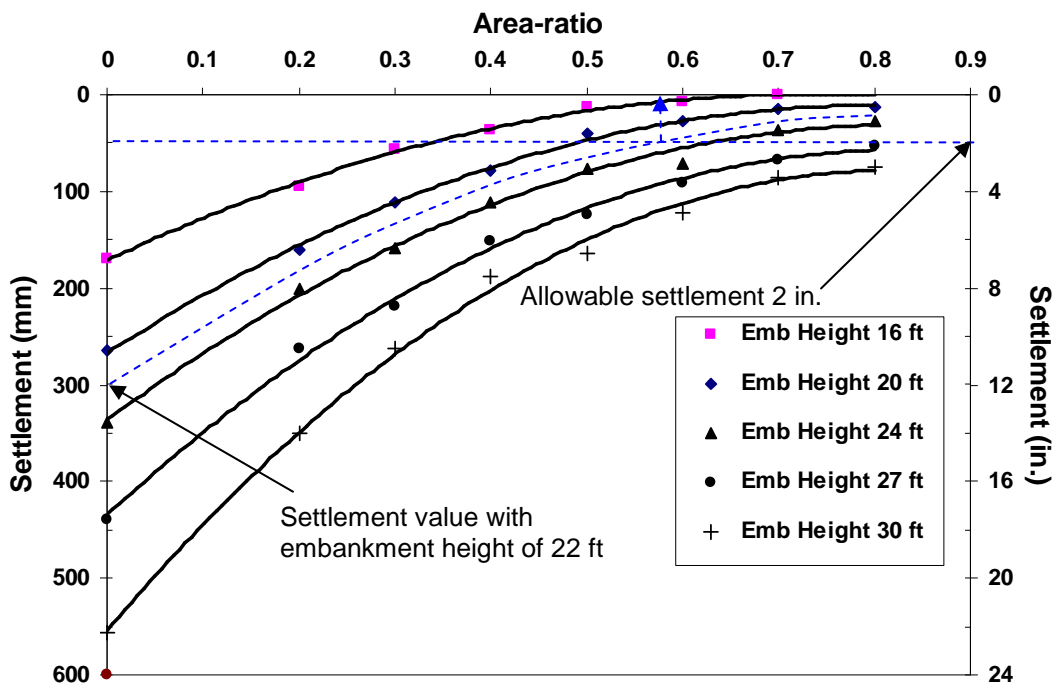


Figure 8.38 Design chart for DSM columns with various area-ratios and heights of embankment

8.4 Modeling of Light Weight Embankment System

8.4.1 ECS Embankment Section

8.4.1.1 Geometry and boundary conditions of the test section

A cross-section and subsurface profile of the light weight fill material namely expanded clay shale or ECS aggregate filled embankment is shown in Figure 8.39. The embankment has a total height of 30 ft (9 m) from an existing ground and a side slope of 2H: 1V. The embankment was constructed on a soft clay layer with a thickness of 16 ft (5 m), which is underlain by 10 ft (3 m) sand layer.

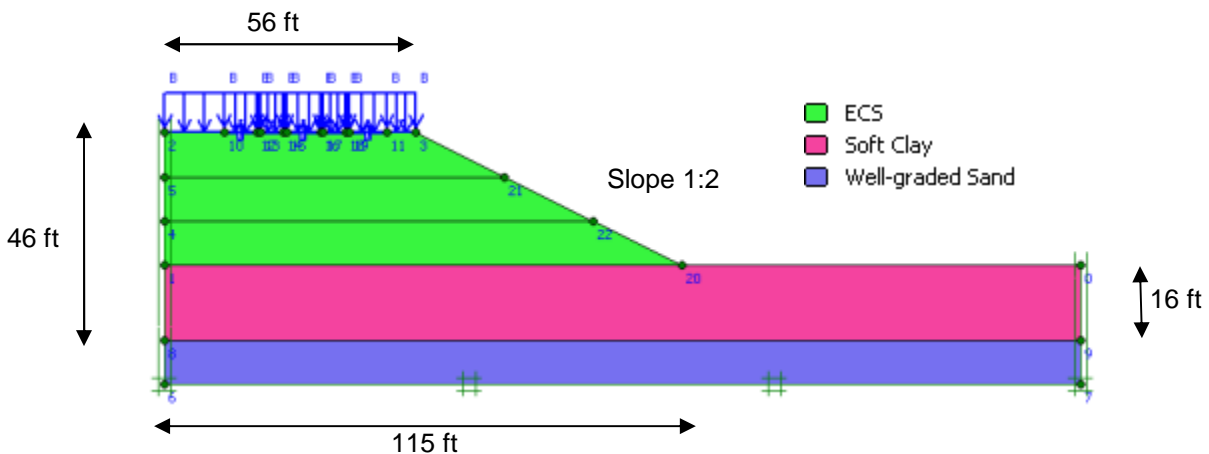


Figure 8.39 Geometry and boundary conditions of the ECS test section

8.4.1.2 Material property values in a numerical analysis

In this model analyses, a soft soil model is used to simulate soft clay material, while a Mohr Coulomb model is used to simulate ECS and well-graded sand materials. Most of the strength parameters derived from the laboratory study results presented in Chapter 5.

The analyses were performed to study the settlement behavior in a long-term duration due to a consolidation phenomenon. Therefore, the settlements occurred during the construction phases by using a plastic model are disregarded. The long-term settlement analyses are performed with a consolidation based model, and are carried out until the ultimate pore pressure state is reached, or in other words, until the dissipation of excess pore water pressure. The displacement of the boundary at $x=0$, $y=0$ was restricted in all directions as well as the

boundaries at the points of the base. The material properties used in the analyses are given in Table 8.5.

Table 8.5 Properties and model type of the materials used in the test section model analysis

	Unit	ECS	Soft clay	Well-graded Sand
Model type		Mohr-Coulomb	Soft soil	Mohr-Coulomb
Moist density, γ_m	pcf	38.7	89.3	96.7
Sat. density, γ_s	pcf	48.7	107.4	109.9
Elastic modulus, E_{ref}^{50}	psf	1×10^8	-	3.8×10^8
Poisson's Ratio	-	0.15	-	0.15
Cohesion, c	psf	1.57	0.94	0
Friction Angle, ϕ	°	49.5	5	33
Permeability, k	ft/min	2×10^{-3}	2×10^{-8}	1.2×10^{-4}
Compression Index, C_c	-	-	0.34	-
Recompression Index, C_r	-	-	0.023	-
Over Consolidation Ratio, OCR	-	-	3	-
Initial void ratio, e_o	-	-	0.80	-

8.4.1.3 Discretization of the test section

A two-dimensional plain-strain model with 6-node triangular elements is used to model the test embankment as shown in Figure 8.40. The embankment in the model consists of 3 types of materials, ECS, clay and sand. In Figure 8.40, the highway pavement is also seen on the top of the embankment model, as a blue line, which has a length equal to the width of the pavement in the field.

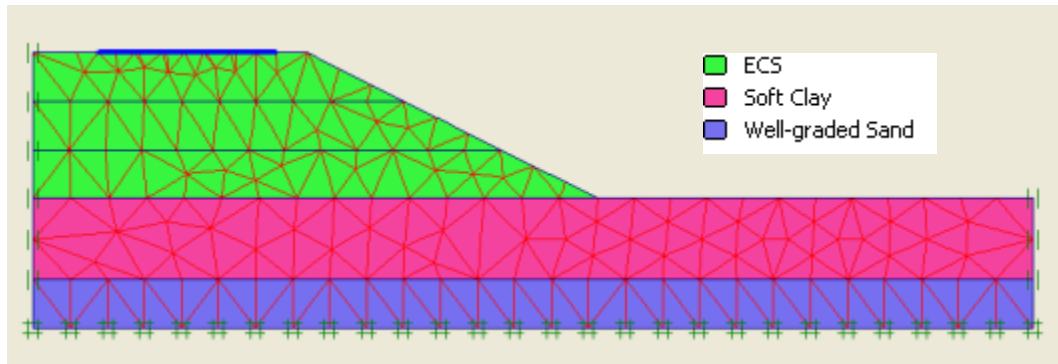


Figure 8.40 Nodes and elements in the test section

8.4.1.4 Settlement analyses

The total height of the embankment of 30 ft (9 m) was divided into 3 layers to simulate embankment construction phases in the analyses as shown in Figure 8.40. Figure 8.41 presents the construction phases in the numerical analyses. It can be seen from the figure that duration of the embankment construction in each layer was close to 25 days, and there after, the embankment was left to be consolidated for another 25 days. In an initial stage, the soil weight was used as a parameter that induced soil stress.

In the second stage, each layer in the embankment is modeled for consolidation. The embankment construction is simulated in that way until the whole embankment construction is completed. The simulation is done such that it replicates the compaction effort performed in real practice. After the completion of the last layer of the embankment, the whole embankment is compacted by applying uniform load in Phase number 8. The calculation of the settlement was reset after the construction of a highway pavement had been completed in Phase number 9. It should be noted that the model analyzed by using a gravity load of the material and the traffic load of 80 kN/m^2 .

Since only elevation surveys and vertical inclinometer monitoring were performed at the ECS site at the locations shown on Figure 8.42 (Points A and B). Therefore, those two points are selected to investigate the soil movements and to validate the results of the numerical analysis in this study.

Identification	Phase no.	Start from	Calculation	Loading input	Time	Wa...	First	Last
Initial phase	0	0	N/A	N/A	0.00 ...	0	0	0
✓ <Phase 2>	2	0	Consolidation ana...	Staged construction	25.0...	2	1	5
✓ <Phase 3>	3	2	Consolidation ana...	Staged construction	25.0...	3	6	7
✓ <Phase 4>	4	3	Plastic analysis	Staged construction	25.0...	4	8	21
✓ <Phase 5>	5	4	Consolidation ana...	Staged construction	25.0...	5	22	33
✓ <Phase 6>	6	5	Plastic analysis	Staged construction	25.0...	6	34	38
✓ <Phase 7>	7	6	Consolidation ana...	Staged construction	25.0...	7	39	61
✓ <Phase 8>	8	7	Consolidation ana...	Staged construction	70.0...	8	62	108
✓ <Phase 9>	9	8	Consolidation ana...	Staged construction	50.0...	9	109	146
✓ <Phase 13>	13	9	Consolidation ana...	Staged construction	1000...	13	147	276
✓ <Phase 12>	12	13	Consolidation ana...	Minimum pore pressure	1000...	13	277	277

Figure 8.41 Calculation phase in the settlement analyses

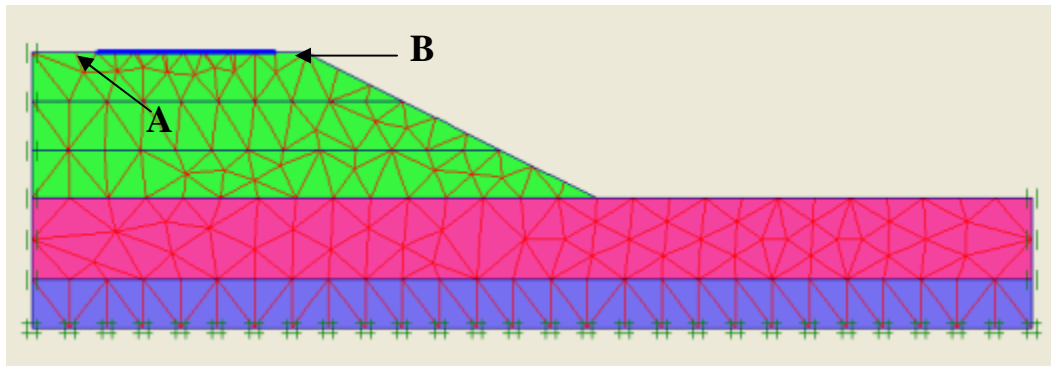


Figure 8.42 Observation points in the settlement calculation

8.4.1.5 Results of the numerical modeling analysis

The results from the FEM analysis are presented in Figures 8.43 – 8.46. Figure 8.43 shows the deformed mesh of the embankment with a displacement magnification scale of 1:50. The maximum long-term displacement in this analysis is equal to 1.89 in. (48 mm) and occurred in the left side of the embankment, which is seen in Figure 8.43. Besides, it can be clearly seen that the soft clay is the layer that experienced the highest amount of the settlement due to the consolidation, which induces the settlement occurred in the ECS embankment.

Figure 8.44 shows the results of total displacements occurred in the embankment. It can be seen in the Figure 8.44 that most of the consolidation occurred in the soft clay layer but the maximum total displacement occurred in the ECS. Figure 8.45 shows the horizontal soil movements occurred in the embankment. Most of the lateral movements occurred at the toe of

the slope and on the right side of the embankment, while at the top of the slope and on the left side only small amount of the movements can be noticed. The vertical soil displacements are presented in Figure 8.46. It is obviously seen that the pattern of color shades from the results of vertical movements in Figure 8.46 is quite similar to the pattern from the results of total movements in Figure 8.44, which means the vertical movement is still a predominant factor in this study.

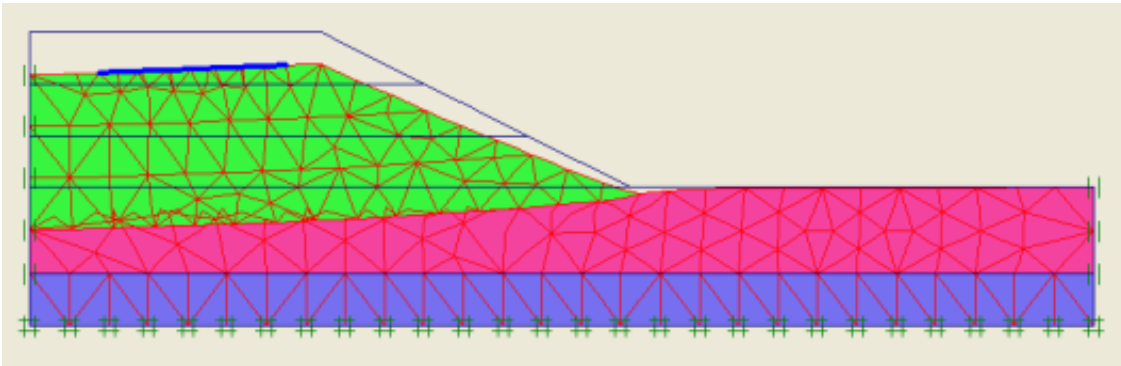


Figure 8.43 Deformed mesh of the test section (displacement scaled up 50 times)

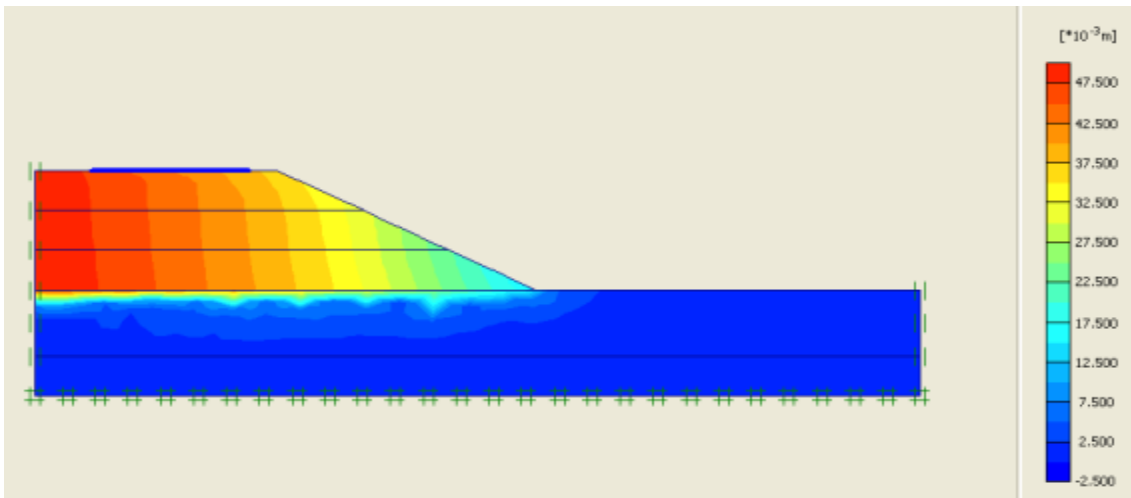


Figure 8.44 Total displacements in the test section

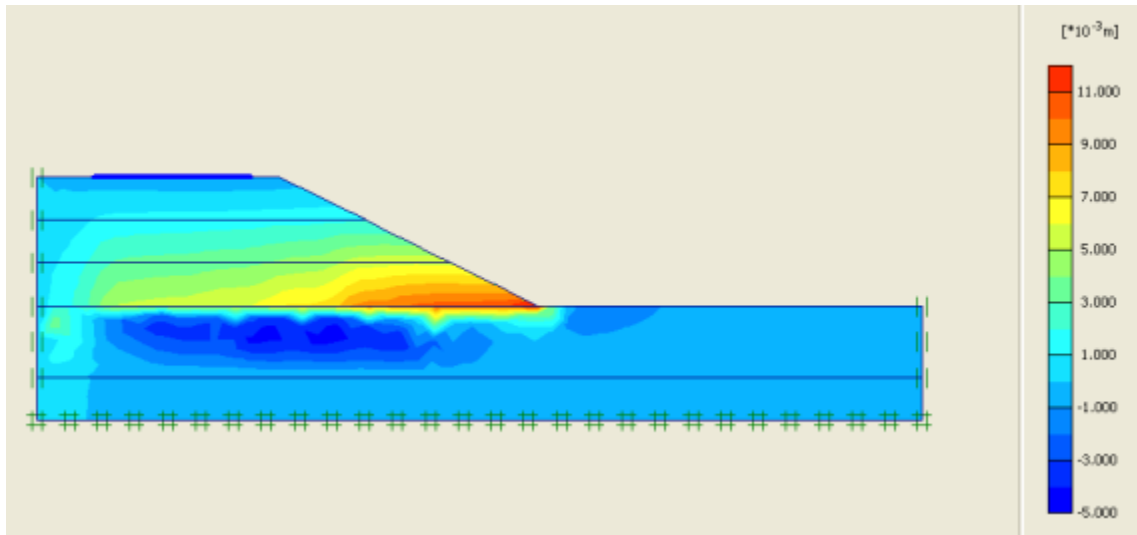


Figure 8.45 Horizontal displacements in the test section

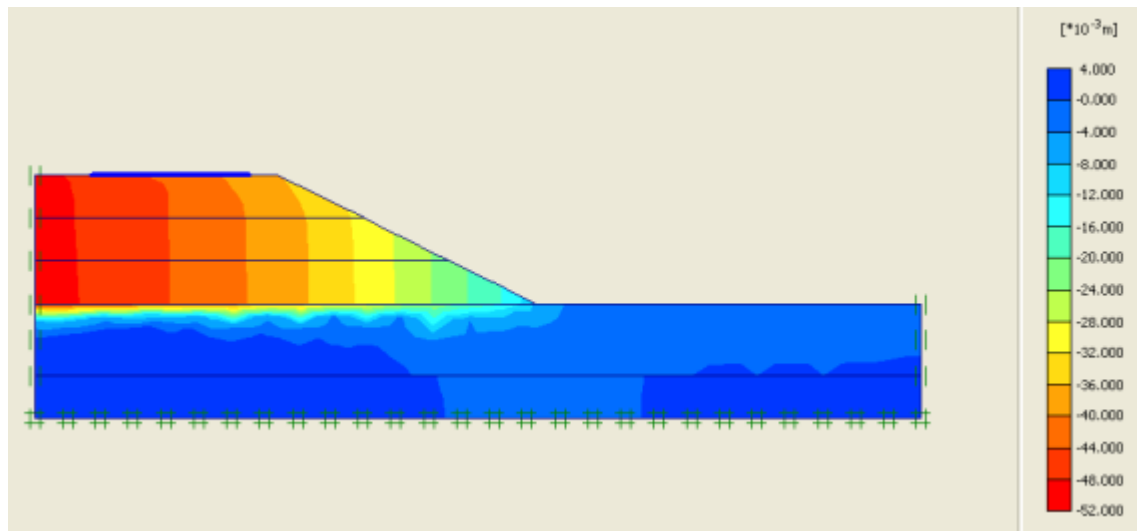


Figure 8.46 Vertical displacements in the test section

8.4.1.6 Model Validation

To validate the parameters used in the model, the results obtained from the above model analysis are used to compare with the monitoring data from the field. The comparisons are performed by using data from elevation surveys to investigate vertical soil displacements. The comparisons are presented in following subsections.

8.4.1.6.1 Comparisons the results of vertical displacements with the elevation surveys

The elevation surveys from Table 7.7 in Chapter 7 were plotted with the results of the numerical analysis as shown in Figure 8.47. It can be seen that the amount of settlements with time from both sources are not indifferent and the prediction showed a good match.

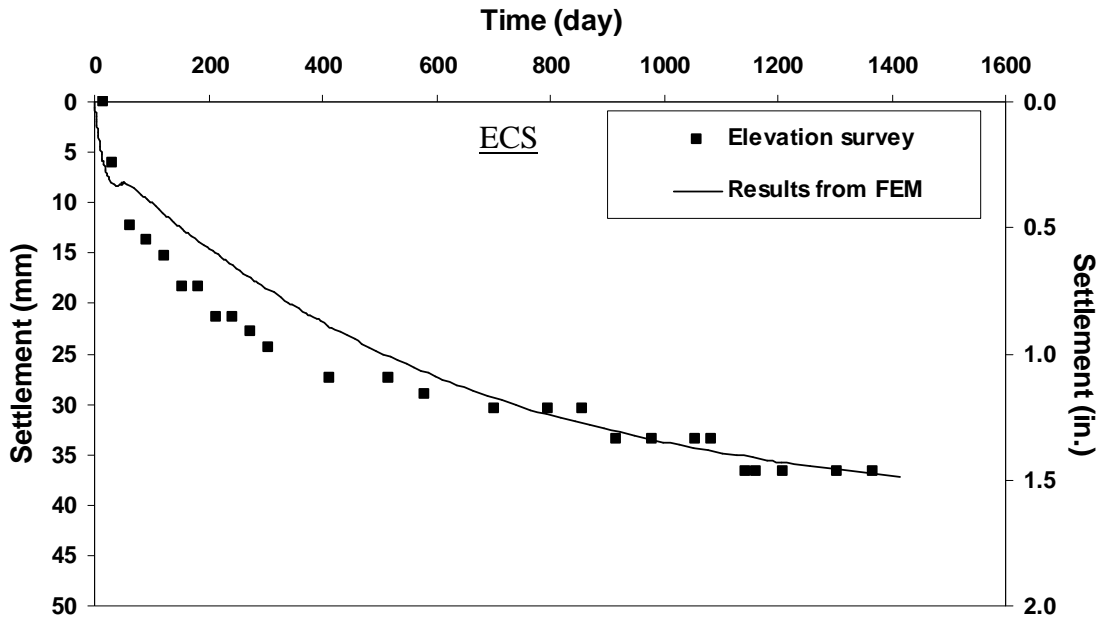


Figure 8.47 Comparison of vertical displacements in a test section between data obtained from elevation surveys and results from numerical analysis

8.4.1.6.2 Comparisons the results of lateral displacements with the data from vertical inclinometer

No data comparison was collected that can be used to perform validation of the lateral soil displacement. From Figure 8.48, it can be noticed that there is no vertical inclinometer casing in the embankment that can provide suitable lateral movement data for model validation. The casings V1 and V2 are located at the locations where the lateral movements can be influenced by different types of embankment fill materials, RAP in a southbound embankment and ECS in a northbound embankment. The casing V3 and V4 were installed very closed to the end of the embankment, whereas a cross-section in the model is ideally a part of a long continuous embankment. Then, the lateral soil movements monitored from casings V3 and V4 could be data influenced by the boundary conditions. The lateral soil movements measured in the vertical

inclinometer casing V1 and V4 are plotted and presented as shown in Figure 8.49 and 8.50, while data from casing V2 are discarded. The reason is the location of the inclinometer casing V2 is too close to the RAP embankment; which the soil movements can be more predominated by RAP than ECS.

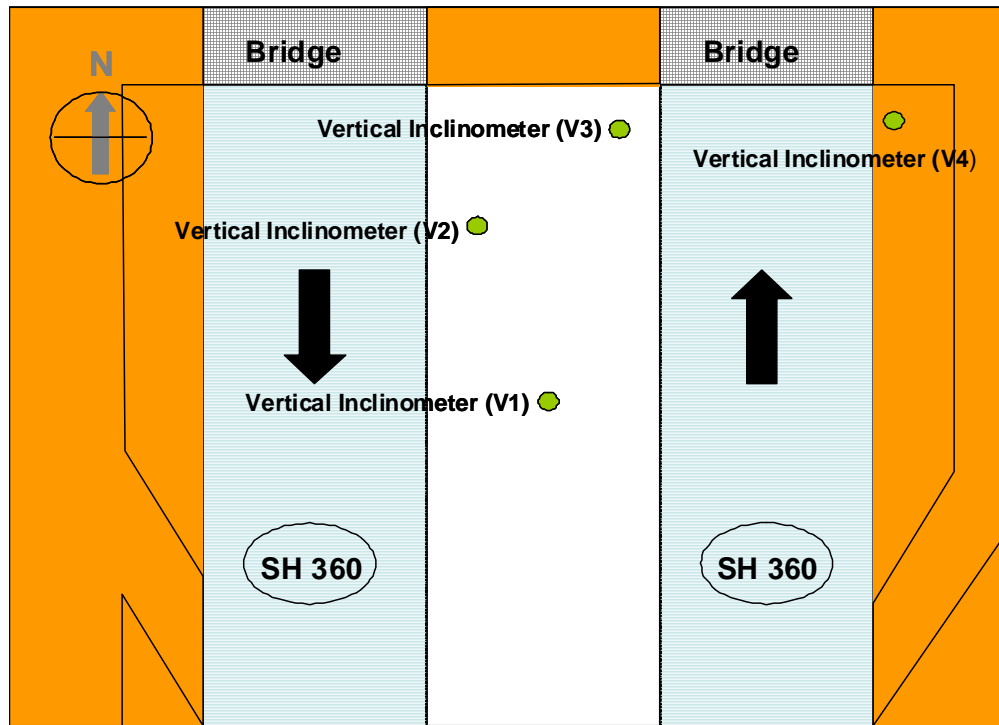
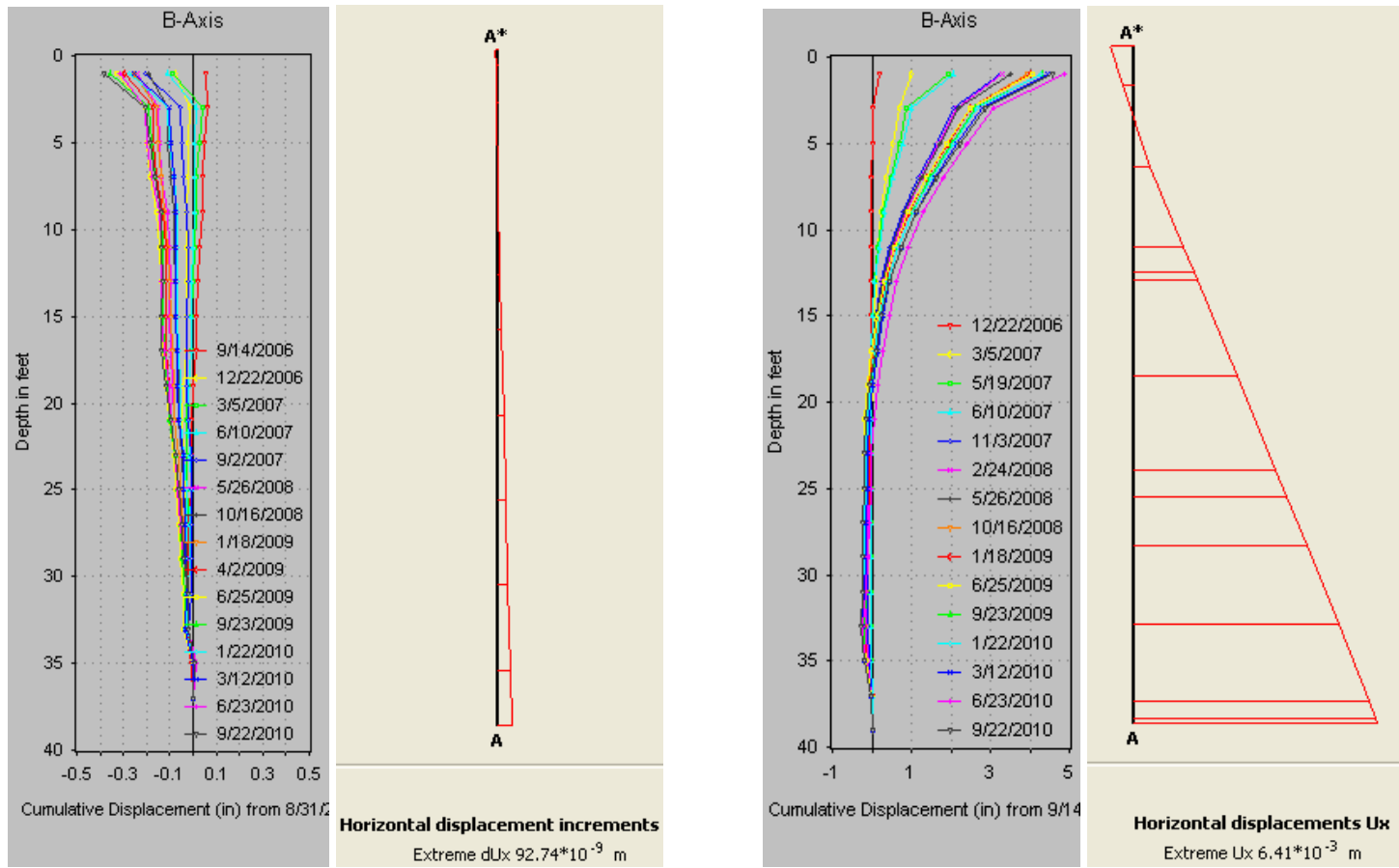


Figure 8.48 Locations of vertical inclinometers installation on ECS embankment, SH 360.

Figure 8.49 (a) and (b) reveals the lateral soil movements in the casing V1 and V4, respectively. In Figure 8.49 (a), only the movements along the embankment cross-section (B-axis) were presented here, since the movement in A-axis cannot be modeled in this analysis. It can be seen in Figure 8.49 (a) that the lateral displacements monitored from the casing V1 move toward the left, while the results from the analysis are extremely small having a displacement pattern different from the monitored data. As already discussed in Chapter 7 that the casing located in the middle of the highway median, the displacements recorded are very small which are close to the results from the numerical analysis. Figure 8.49 (b) shows the lateral soil displacements in a direction of the cross-section of the embankment. It can be seen that the

displacement profile from monitored data has a large displacement at the top and a low value at the bottom of the embankment, which is different from the displacement profile resulting from the numerical analysis. This can be an evidence that apart from the consolidation phenomenon, the lateral movements occurred in the field could come from another reason like soil erosion as suspected in the previous chapter. However, the soil erosion phenomenon is very complicated and not able to be modeled in the Plaxis. It should be noted also that the monitored lateral soil movements from casing V3 are not presented, because mostly the soil movements were influenced from the movement happened around the case V4 and are too complex for the analysis.



(a) (b)
 Figure 8.49 Comparisons of lateral soil movements between monitored data and numerical results in the vertical inclinometers (a) V1 and (b) V4

8.4.2 Control Embankment Section

The control section is an embankment section constructed with local fill and this section was located on the north side of the bridge. The settlement investigations using both elevation surveys in the field and the numerical analysis are performed, which are used further to compare with the values from the ECS embankment test section to evaluate how ECS material can mitigate the settlement problem that can occur in the bridge embankment section. The geometry, boundary conditions and discretization of the control section are the same as the ones used in the ECS test section by replacing the embankment fill material of ECS with sandy clay fill material as shown in Figure 8.50.

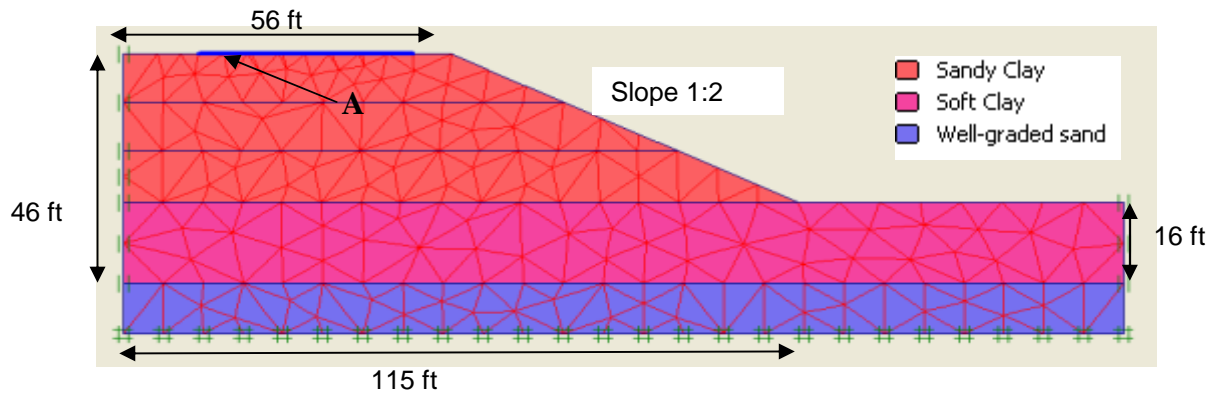


Figure 8.50 Nodes and elements in the control section

8.4.2.1 Settlement analyses

The settlement numerical analyses on the control section at Point A are performed in the same way as was done on the test section. The total embankment of 30 ft (9 m) high was divided into 3 layers with the same duration of the construction phases, load multiplier factor, and traffic load as in the test section analyses. Material properties used in the analyses are given in Table 8.6.

Table 8.6 Properties and model type of the materials used in the control section model analysis

	Unit	Sandy clay	Soft clay	Well-graded Sand
Model type		Soft soil	Soft soil	Mohr-Coulomb
Moist density, γ_m	pcf	92.4	89.3	96.7
Sat. density, γ_s	pcf	17.2	107.4	109.9
Elastic modulus, E_{ref}^{50}	psf	-	-	3.8×10^8
Poisson's Ratio	-	-	-	0.15
Cohesion, c	psf	1.77	0.94	0
Friction Angle, ϕ	°	18	5	33
Permeability, k	ft/min	1×10^{-6}	2×10^{-8}	1.2×10^{-4}
Compression Index, C_c	-	0.12	0.34	-
Recompression Index, C_r	-	.030	0.023	-
Over Consolidation Ratio, OCR	-	3	3	-
Initial void ratio, e_o	-	0.55	0.80	-

8.4.2.2 Results of the model analysis

Figures 8.51 – 8.54 show the results from numerical analysis in the control section. Figure 8.51 presents the deformed mesh of the embankment with a displacement scale enlarged to 20 times. It can be seen that the maximum settlement of the embankment of 0.55 in. (0.14 m) occurred evenly in an area under the embankment crest. The results of the total displacements occurred in the embankment are presented in Figure 8.52. The figure reveals that consolidation mostly occurred in the subgrade layer and that consolidation also resulted in displacements within the embankment. Figures 8.53 and 8.54 show the lateral and vertical soil movements

occurred in the control embankment, respectively. It can be seen that the vertical movement is still a predominant factor in the control embankment section.

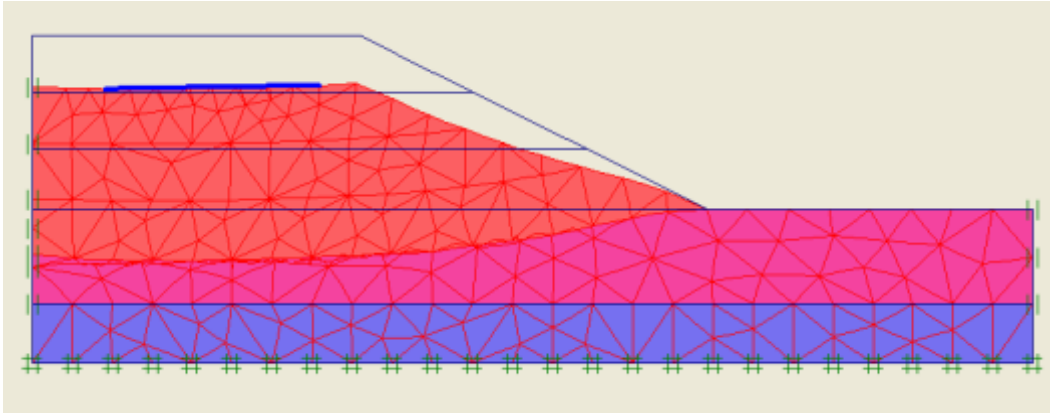


Figure 8.51 Deformed mesh of the control section (displacement scaled up 20 times)

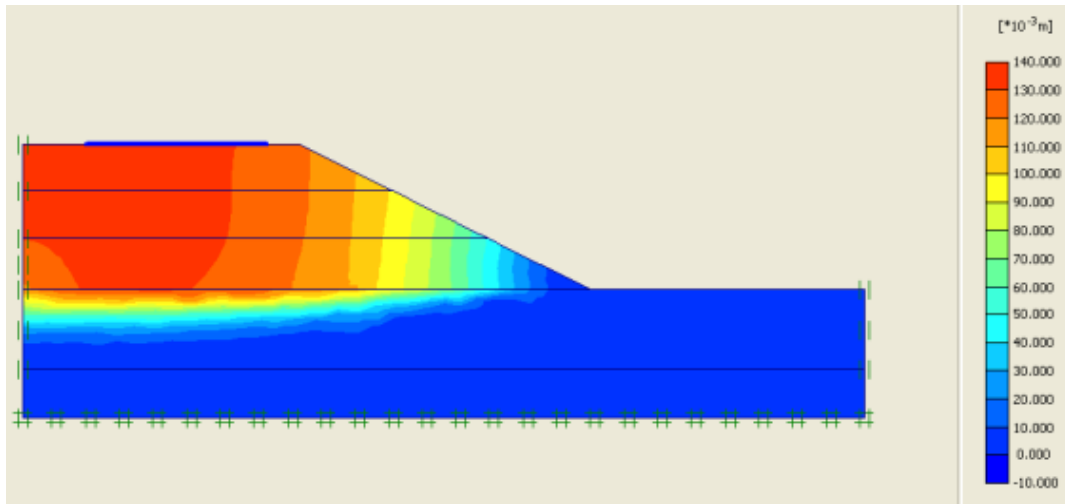


Figure 8.52 Total displacements in the control section

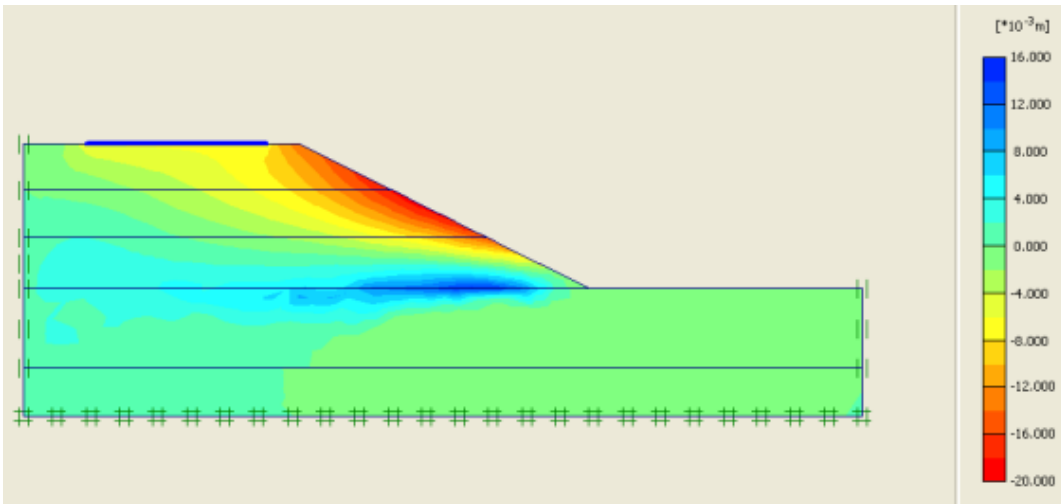


Figure 8.53 Horizontal displacements in the control section

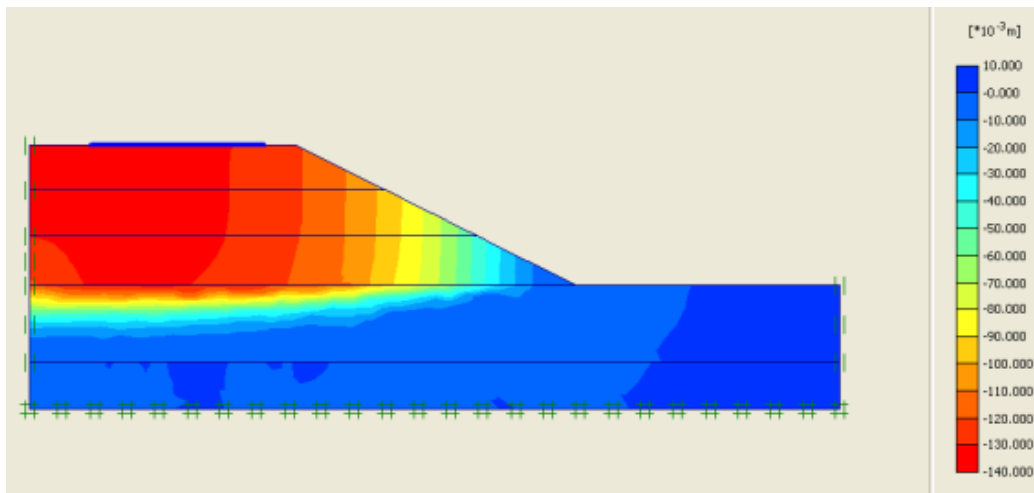


Figure 8.54 Vertical displacements in the control section

8.4.2.3 Validation

To validate the parameters used in the model, the results obtained from the above model analysis are used to compare with the elevation surveys from the field. The elevation surveys from Table 7.8 in Chapter 7 are plotted against the results of the numerical analysis as shown in Figure 8.55. It can be seen that time-settlement curves of both data are in agreement.

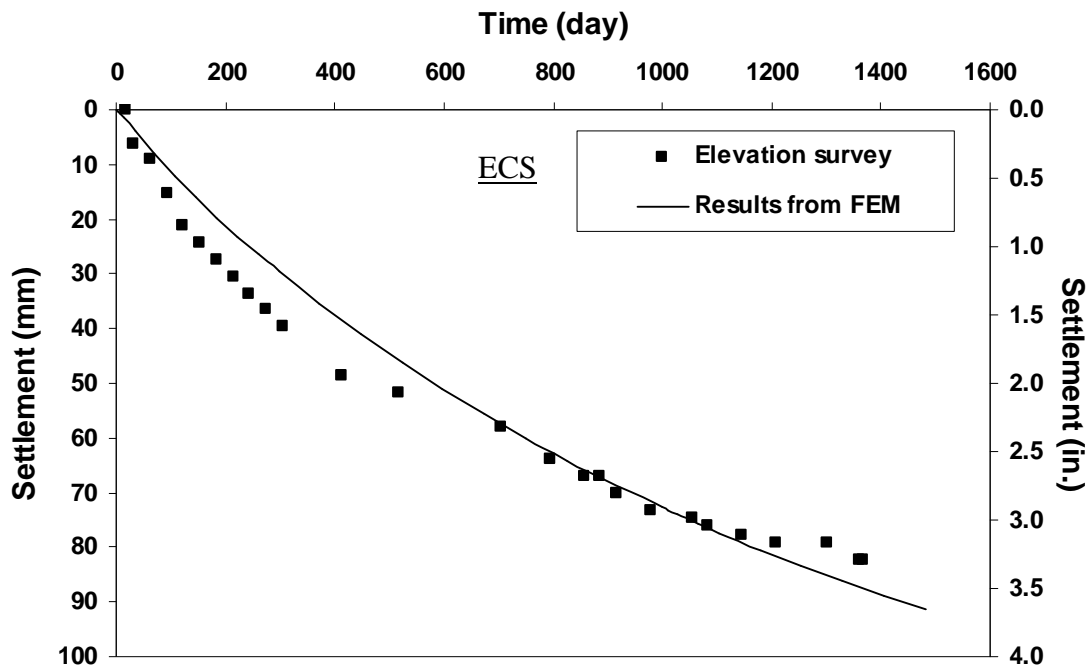


Figure 8.55 Comparison of vertical displacements in a test section between data obtained from elevation surveys and results from numerical analysis

8.4.3 Analysis of Vertical Soil Movements

A hyperbolic method (Lin and Wong, 1999) is used to predict the long term settlement of the test and control sections in this study. According to Eq. (8.4), the elevation survey data from both control and test section are plotted against a function of time-settlement ratio as shown in Figure 8.56.

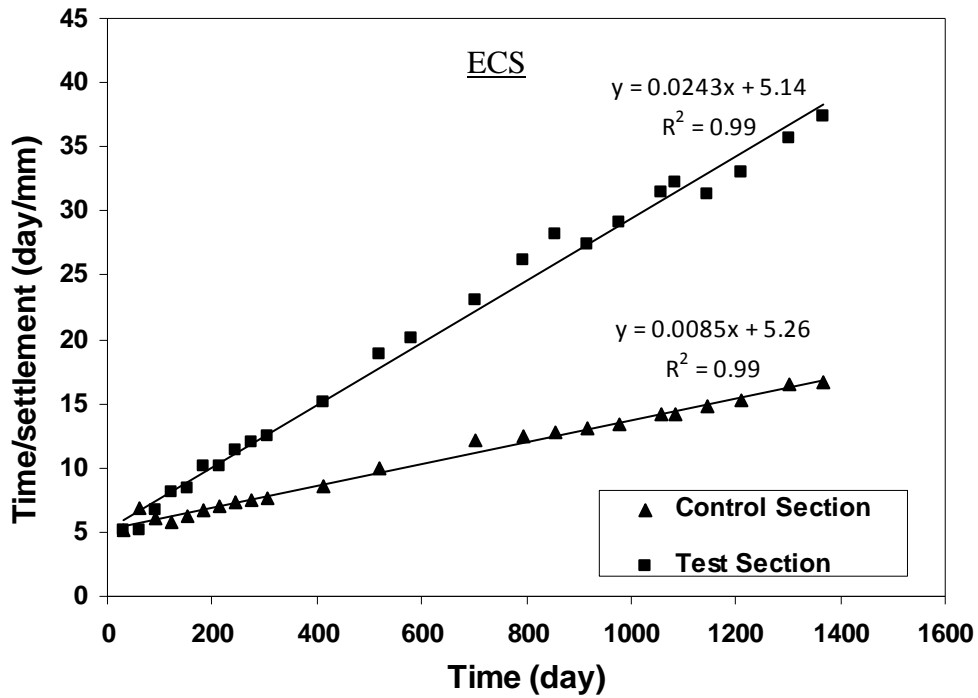


Figure 8.56 Regression equations from hyperbolic model to predict soil settlement values in both test and control sections

With the regression equations obtained in Figure 8.56 and the magnitude of soil settlements at a specific time (t) in the embankments can be obtained as already derived in Eq. (8.5).

Therefore, the soil settlement occurred at time (t) in a test section is equal to:

$$s = \frac{t}{(5.1468 + 0.0243t)} \quad \text{mm} \quad (8.8)$$

and the soil settlement occurred at time (t) in a control section is equal to:

$$s = \frac{t}{(5.2608 + 0.0085t)} \quad \text{mm} \quad (8.9)$$

By solving Eq.(8.8), (8.9) and with the time increment of 20 days, the soil settlement occurred in both embankments at the specific time interval can be plotted against data from elevation surveys and results from the numerical model which are presented in Figures 8.57 and 8.58. From both figures, it is seen that the predicted soil settlements from the hyperbolic

model and the FEM models are in agreement with the measured values from the elevation surveys. That means the numerical model in the FEM and the hyperbolic equation from Eq. (8.8) and (8.9) can be used to predict the settlements occurred in both embankments and the results of the prediction are shown in Table 8.7.

Table 8.7 Settlement predictions from the Hyperbolic and FEM Models for the Test section

Settlements at year (in.)	Elevation surveys*	Hyperbolic model (extrapolated data)				FEM Model			
	4	4	10	20	30	4	10	20	30
Test section	1.44	1.41	1.53	1.58	1.59	1.46	1.62	1.75	1.91
Control section	3.36	3.22	3.94	4.25	4.37	3.50	4.76	5.31	5.35

Note: * - Measured Data

From Figure 8.57, it is clearly seen that the results from extrapolation data and FEM in both of the test and control embankments are in agreement.

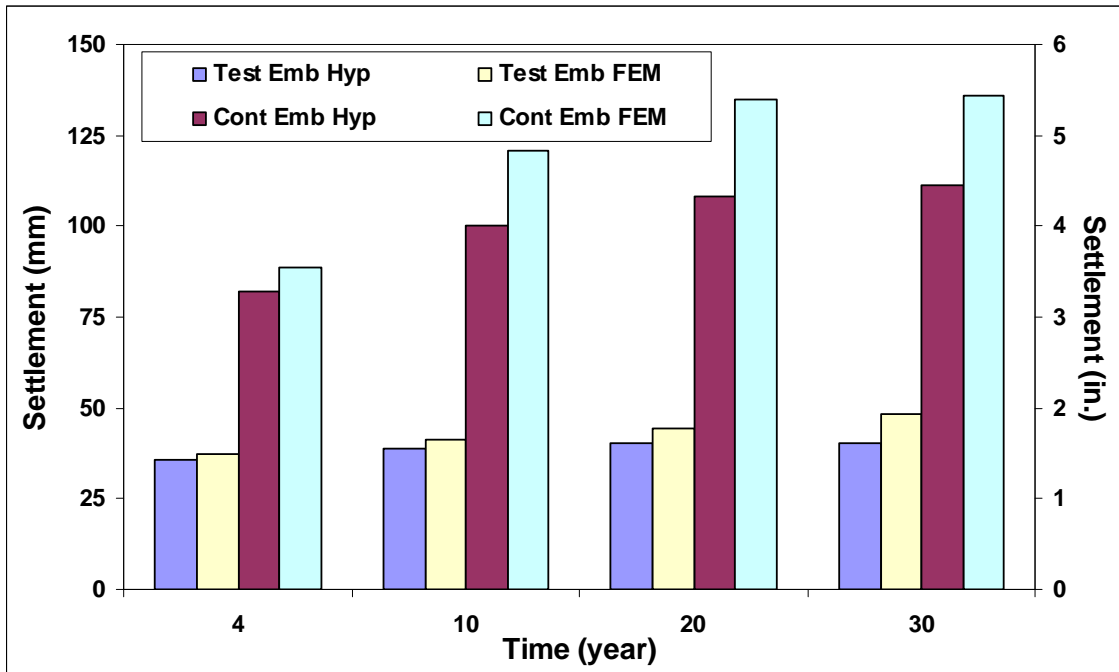


Figure 8.57 Settlement values from data extrapolation and FEM

8.4.4 Prediction of Soil Movements Occurred in an ECS Section with Variations of Embankment Configurations

To investigate the effects of slope and height of the embankment configurations on the settlement, those two parameters are varied for various scenarios in this study.

8.4.4.1 Influence of embankment slope

In order to study the effect of slope on the amount of the settlement occurred in the embankment, as already been performed in section 8.3.5.2 the gradient of the embankment is changed with various V: H ratios, 1:1, 1:2, 1:3, and 1:4, while the height of the embankment is kept constant at 30 ft (9 m). Figure 8.58 shows a monitored point A and the embankment model with a slope of 1:1 (V: H).

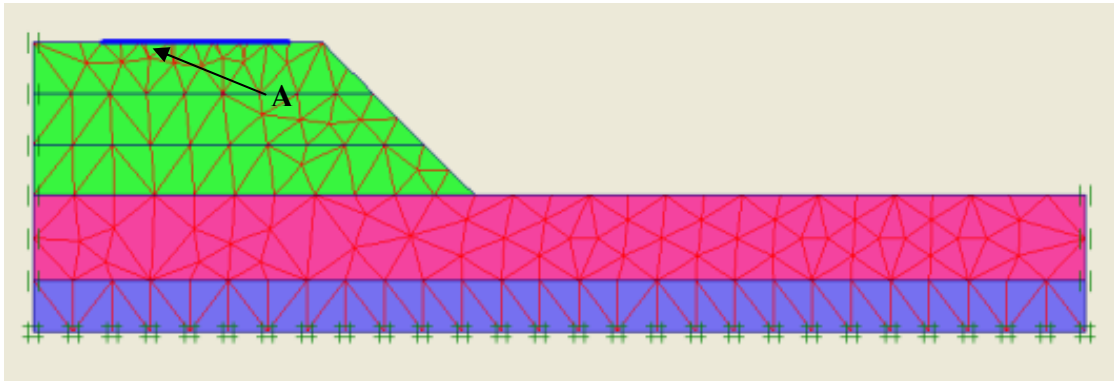


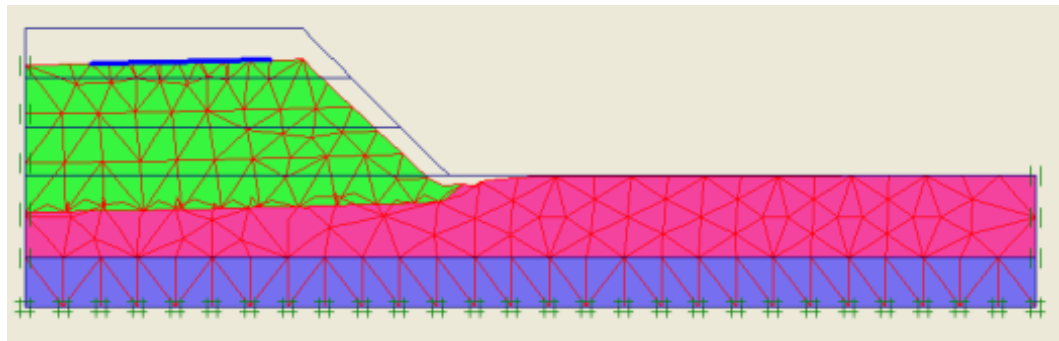
Figure 8.58 Geometry of the test section with a slope (V: H) of 1:1

The results from numerical analysis are shown in Table 8.8. It can be seen that both horizontal and vertical soil displacement values occurred in embankment with the various slopes in this study are not significant different.

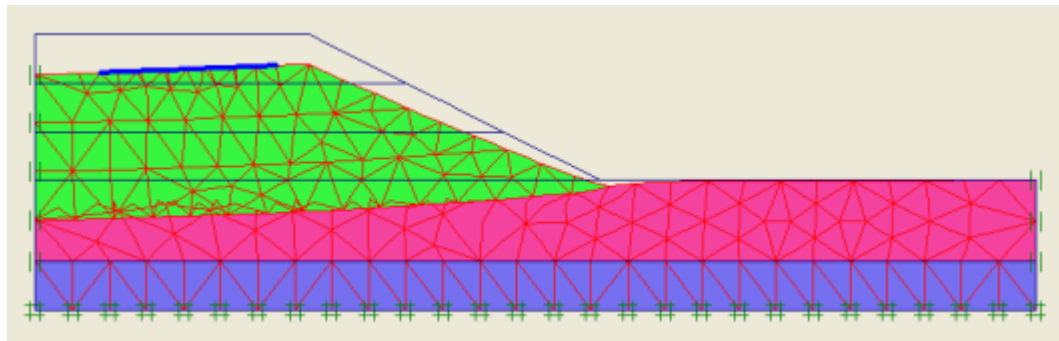
Table 8.8 Maximum soil displacements with various embankment slopes

Slope (V:H)	Vertical displacement		Horizontal displacement	
	in.	mm	in.	mm
1:1	1.73	43.95	0.68	17.23
1:2	1.91	48.63	0.47	11.91
1:3	1.96	49.70	0.38	9.55
1:4	2.16	54.80	0.35	8.80

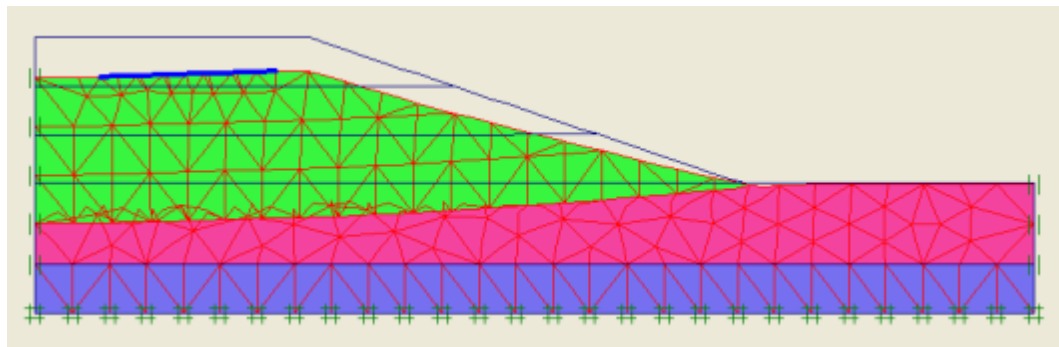
Figure 8.59 shows the deformed mesh of the embankment with a various slope by scaling it up to 50 times. As shown in Figure 8.59, it is clearly seen the weight of the embankment structure can affect the extent consolidated area in the soft clay layer. With the milder slope, the settlement can me found in the wider area. It can be concluded if the slope stability is not problematic; the more settlement can be induced by the wider slope. The gravity load of the embankment is considered as a main factor in this case.



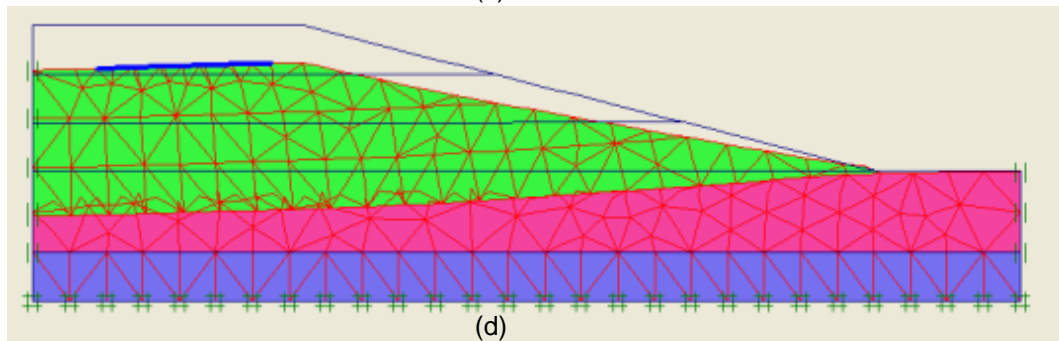
(a)



(b)



(c)



(d)

Figure 8.59 Deformed mesh showing total settlements in the embankments with various slopes V:H; a) 1:1, b) 1:2, c) 1:3, and d) 1:4

8.4.4.2 Influence of embankment height

Another analysis is performed to examine the effect of embankment height on the soil settlement. The heights of the embankment are varied from 20 to 40 ft (6.0 to 12.0 m), while the slope ratio is kept constant at 1:2 (V: H). Figure 8.60 shows point A, which is selected to study in these whole analyses and the embankment model with a height of 20 ft (6.0 m) and slope of 1:2 (V: H). It should be noted that the width of embankment at its base is also varied according to the height of embankment from case to case in order to maintain the slope value at 1 :2.

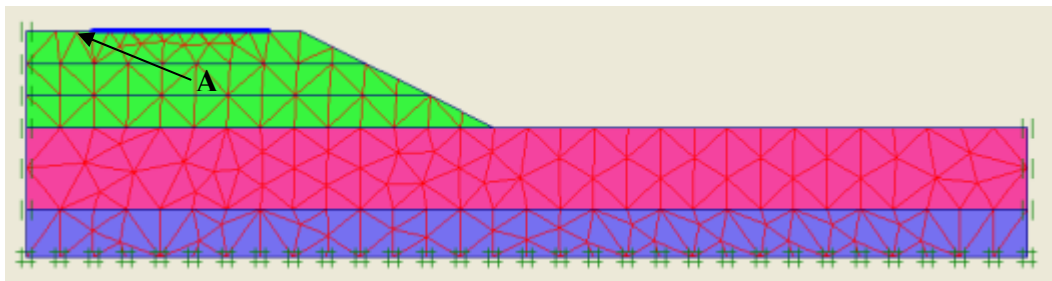


Figure 8.60 Geometry of the test section with a height of 20 ft (6.0 m)

Figure 8.62 shows time-settlement curves from different height of the embankment at Point A in the test section. It can be seen from the figure that the highest settlement value is 2.8 in. (71 mm) when the height of the embankment is 40 ft (12 m), and the lowest value is 0.27 in. (7 mm) when the height is 20 ft (6 m). That means the magnitudes of soil settlements are influenced by the height of the embankment, on the other hand, the gravity load exerted from the embankment.

8.4.4.3 Conclusion from variable studies

It can be concluded that the height of the embankment has a great influence on the amount of settlement in the test section in this study. On the contrary, the slope of the embankment does not affect much on the magnitude of the settlement, but on the coverage of the consolidated area in the soft clay layer as seen in Figure 8.59. This is a reason that the subgrade soil is soft clay; therefore, the behavior of the consolidation in the subgrade depends

on the gravity load and its extent sitting on it. With the more weight increased due to the higher embankment, the more settlement can be expected.

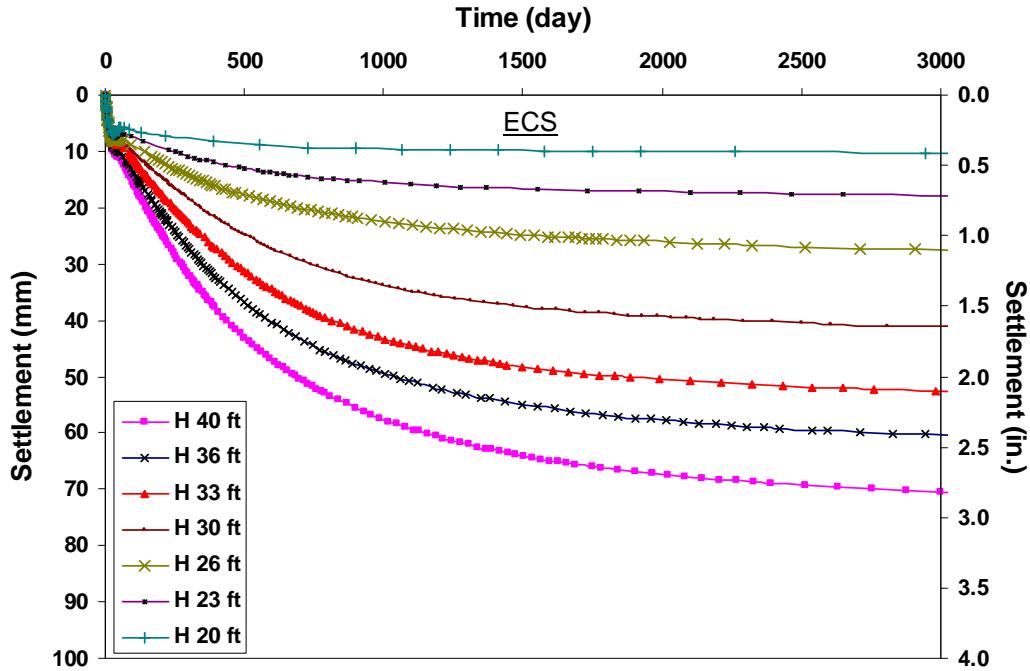


Figure 8.61 Time-settlement in the DSM treated section with various height of embankment

8.4.4.4 Design chart for the embankment filled with ECS

From the variable studies, it is seen that the most influent factor for the settlement control in the embankment constructed with the ECS is the height of the embankment. Therefore, a design chart was established according to the various heights of embankment between 20 - 40 ft (6 – 12 m). According to the following design step-by-step procedures, the ECS embankment design can be demonstrated as showed in Figure 8.62.

1. Establish a tolerate settlement occurred in the embankment.
2. With that allowable settlement value, draw parallel to the x-axis until the settlement value in the long-term is satisfied.
3. From Figure 8.62, it can be seen that if the allowable settlement is 2 in. (50 mm), the height of the embankment should be designed less than 33 ft (10 m).

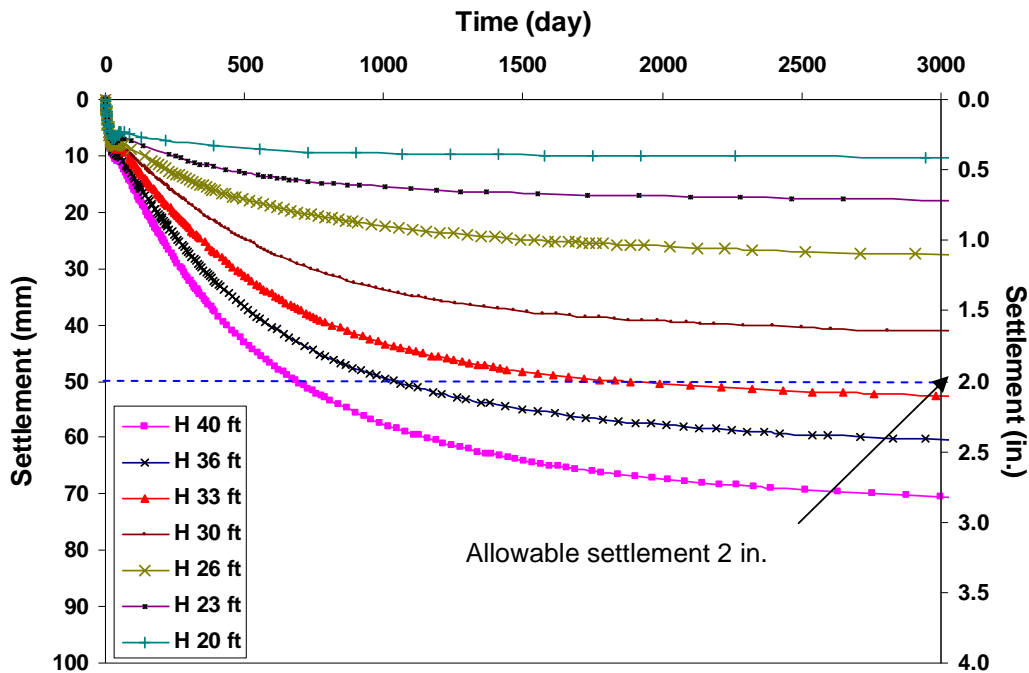


Figure 8.62 Design chart for ECS embankment

8.5 Summary

This chapter presents the details of the numerical analysis. The data from laboratory studies in Chapter 5 and from the site monitored data presented in Chapter 7 are used as input data for the numerical analysis in the FEM model and in the hyperbolic model (Lin and Wong, 1999) to obtain the settlement values occurred in the embankments at various long time periods. In this study, the analyses are performed on two bridge sites, DSM site on I30 and ECS site on SH360, in Arlington, and each bridge site has a control and a test section to compare the effective of each mitigation method i.e. deep soil mixing for foundation soil improvement and light weight fill embankment section.

To perform the analyses, three tasks are attempted on modeling and validation, settlement prediction and comparisons, and modeling with various embankment configurations. For the model validation, the soil parameters and embankment geometry are used as the input parameters in the model. In this task, after the numerical model had been completely executed,

the results from the numerical analyses are compared with the monitored data from the field to validate the model. The second task, settlement prediction, is performed after the model validation in the first task has been satisfied. In this task, the predictions are forecasted to obtain the settlements occurred in longer time durations of 10, 20 and 30 years using hyperbolic model, and the results from the analyses performed on both test and control sections are then compared to evaluate the effective of the embankment constructed with and without mitigation method. The last task is performed to understand how the amount of the settlement occurred in the treated embankment can be affected by various embankment geometries.

For the DSM site, the long-term settlement predictions are performed and the results show that the DSM can be a viable technique to use as a mitigation method for the bump problem. The DSM can lessen the magnitude of the settlements from 9.5 to 1.6 in. (240 to 40 mm) within 2 years and from 10.6 to 2.5 in. (270 to 64 mm) within 10 years. Moreover, other two conclusions can be drawn from the variation of embankment configurations study. First, the area-ratio between DSM and subgrade soil - with the most preferable values between 0.5 and 0.6 - is a major factor in decreasing the amount of settlement occurred in the embankment. Second, without the subgrade improvement technique the weight of the embankment governs the amount of settlements. As being seen from the factor study in the variance of height and slope of the embankment that the higher settlement can be expected from the higher embankment and the size of consolidated area is influenced by the extension of the slope.

For the ECS site, it can be concluded that using lightweight as a backfill material can reduce the settlement occurred in the embankment. Since the gravity load from embankment exerts on the subgrade is a main factor governs the settlement in the ECS site, the embankment constructed with the lightweight ECS has the amount of settlement less than the one constructed with a normal fill; and the higher embankment experiences more settlements than the lower one. However, it should be noted that using the ECS as a backfill material is not a concrete technique to reduce the settlement. Although within 30 years using lightweight fill can reduce the

settlement by 30 %, this method does not impede the consolidation phenomenon. Nevertheless, the settlement in the embankment, which induced by the consolidation, will still exist and remedial techniques are necessary performed in the long-term.

In conclusion, based on the study, it is found out that the DSM technique is considered as an effective method. It can reduce the amount of settlement occurred in the embankment and also impede the consolidation happened in the soft soil layer. Therefore, the settlements occurred in the DSM site are not only small but also will be terminated in a short duration. Another mitigation method in this study is using the lightweight material as an embankment fill. This technique can reduce the settlement in the embankment also. However, according to the previous discussion, the remedial works are still necessary to be employed in this type of embankment for the long-term service.

CHAPTER 9
SUMMARY AND CONCLUSIONS

9.1 General

The differential settlements between bridge approach and bridge deck is termed as “the Bump” and this is considered as one of the main problem that affects the performance of the bridge structures. Many state highway agencies in the United States reported this as one of their major maintenance problem as every year these agencies have been spending over \$100 million on maintenance and repairs to the bridges and highways damaged by this bump problem. In addition, this bump can cause inconvenience to traveling passengers. Recently, there have been several methods utilized to mitigate this settlement problem such as using driven piles, drilled shafts, flowable fill, ECS, DSM columns, geosynthetics, and others. In this research, two treatment methods are considered for the subgrade and embankment fill conditions in north Texas region for potential reduction in overall settlements. These two mitigation methods researched here are the use of DSM columns and ECS. Additionally, another method of using deep foundations with Geopier is also investigated, however with limited focus.

One method to study the effectiveness of mitigation methods in reducing the settlements at the bridge approach was to study and investigate the settlements occurred in bridge embankments in real field conditions. Therefore, three bridge sites in Texas were selected in this research and these include DSM site on IH30 in Arlington, ECS site on SH360 in Arlington and Geopier site on SH6, in Houston. Both field visits were performed to observe soil settlements occurred in the embankments in periodical basis, every fortnight for DSM and ECS sites and every six months for Geopier site. In general, each bridge site has the test (treated) and control

(untreated) sections. The settlement data observed from both sections were then compared to evaluate the efficiencies of each mitigation method in decreasing the amount of settlement.

The data collected in the field are used not only for the mitigation settlement efficiency evaluation, but also for a settlement analysis study. Two numerical models using FEM and a hyperbolic model for time scale extension are used in this research. For the FEM, the data collected from the field instrumentation were employed to validate the model with the results from the FEM. The hyperbolic model formulated by Lin and Wong (1999) used the observed field data to establish the time-settlement equation for each embankment. Once validations are done, the models are used for further modeling for hypothetical embankment sections. After the FEM model validation, the model was used to predict the settlement occurred in the embankments in the long-term in 10, 20 and 30 years.

Both test and control sections are simulated in the FEM model with the embankment geometry and surcharge loading from traffic with different DSM and ECS values and these results are used to develop design methods for DSM and ECS fill material selection.

9.2 Summary and Conclusions

The major objective of the research is to address the effectiveness of each mitigation method in reducing the settlement occurred in the embankment. The following conclusions are obtained for each method considered in the research.

Efficacy of DSM columns in reducing settlements in the embankment

I. Field Instrumentation and Monitoring Studies

- a) The monitored data from the horizontal inclinometer show that the DSM method was successful in mitigating the settlement underneath the approach slab induced from the traffic load. The settlement occurred under an approach slab section (0.1 in., or 2.5 mm) was lower than the values under a pavement (0.5 in., or 12.7 mm) and slope fill (0.75 in., or 19.0 mm).

- b) Vertical soil movements monitored from extensometers reveal that the settlements values in embankment at the depth of 10, 20 and 40 ft were equal to 0.20, 0.13 and 0.05 in. (5.1, 3.3, 1.3 mm.), respectively. These results show that the monitored settlement values are very small at different depths throughout the embankment; the DSM is an effective method to reduce the settlements. The same trend was also shown in the results of Sondex; sensor rings moved within very small range (+/- 0.15 in., or 3.8 mm)
- c) Data from elevation surveys show the amount of the settlements occurred in the control section was more than the same in the test section. The reduction in the surface movement in the DSM treated embankment was attributed to the enhancement of subgrade foundation achieved through the DSM technique. This can indicate the effectiveness of the DSM in improving the performance of the embankments in undergoing less settlement in this study.
- d) The lateral movements monitored in both DSM test and control sections are very low. With the variations of the casing profiles of a small movement less than 0.1 in., it indicates that the lateral movements are not critical in the assessment of deep soil treatment methods in mitigating approach slab settlements

II. Numerical analysis studies, results and comparison studies with field data

- a) The analytical predictions of soil movements in the DSM treated section are in a good agreement with the field observations data monitored from all instruments including horizontal inclinometer, total station, rod extensometer and sondex devices. Also, hyperbolic model is used to take the initial settlements and then extend to interpret the long term settlements. Overall, these analyses indicate that the accuracy of the model not only for calculating the settlement in the present conditions, but also for predicting the settlement over a long-term time frame.

- b) When comparing the settlement values between the treated and untreated sections from the model analysis, it reveals that the DSM columns could reduce the settlement happened in the test section from 9.4 in. (240 mm) to 1.6 in. (40 mm) in 2 years and from 10.9 in. (277 mm) to 2.6 in. (66 mm) for the long-term duration.
- c) Analyses are attempted using 1) DSM area ratios, 2) embankment heights, and 3) slopes. The results from this study reveal that the most effective method in reducing the embankment settlement is by using a suitable area-ratio, which has a value between 0.5-0.6. Lowering the embankment height is also another effective method as it reduces gravity loads exerting on the subgrade. Hence lesser settlement due to consolidation of the soft clay layer has occurred. Therefore, by lowering the height of embankment, this approach slab can also experience less embankment settlement. However, with traffic weight related variables may increase the settlements as stress transfer in the subsoils will be high and hence this approach is sometimes not possible to implement.

Efficacy of ECS in reducing settlements in the embankment

III. Field Instrumentation and Monitoring Studies

- a) By comparing the settlement values from elevation surveys in both test and control sections, it can be seen that the ECS embankment experienced the settlement only 1.44 in. (36 mm), while the control embankment has experienced a total settlement of 3.36 in. (85 mm) already. This means the lightweight fill material such as ECS, can be used to mitigate the settlement at the bridge approach.
- b) A wide opening between a highway pavement and its shoulder could be seen during the site visits. The opening on the highway allowed more precipitation flowing into the embankment and this could induce erosion, which made the settlement problem become more severe.

- c) The granular material with no cohesion between the particles, like ECS, could be easily washed away by the water intrusion, especially in the open area like the outer slope of the embankment. Consequently, that area will have lesser soil mass and lower density than other locations. This occurrence could be observed during the site visits that the approach slab was moved toward the outer slope, where has a lower soil density. In addition, the data monitored at the vertical inclinometer (V4) reveals a good concurrence. Therefore, for the embankment constructed with a granular material effective drainage and erosion control methods should be also provided.

IV. Numerical analysis studies, results and comparison studies with field data

- a) The results from vertical soil settlement analysis from the numerical modeling in the ECS test and the control sections are in accord with the elevation surveys data performed in both sections. These signify that the models for both sections are accurate enough to estimate soil settlements in the future.
- b) It is noted that the results of lateral soil displacements from the numerical studies differ from monitored data collected from the vertical inclinometers. This is a result as there is no vertical inclinometer installed at locations suitable for the data comparison. The vertical inclinometers installed in the inner side of the embankment yield lateral soil displacement data influenced by two embankments constructed with different fill materials, ECS and RAP. As the data from the inclinometers in the outer slope cannot be used for the data comparison, since the inclinometer was installed at the end of the embankment. This situation is totally different from a simulated cross-section in the model, which is a part of continuous embankment.
- c) From the numerical analyses, the results show that the embankment constructed with the ECS will have a long-term settlement in 30 years of 1.89 in. (48 mm), while

the embankment constructed with the local fill will have a settlement of 5.4 in. (136 mm) in the same time interval.

- d) It should be noted that although using the lightweight fill material, like ECS, to construct an embankment can lessen the amount of the settlement to one-third compared with the values predicted in the normal fill embankment in this study, this technique does not impede the consolidation phenomenon occurred in the clay layer. It can be seen from the analysis results that the settlements in the test section are still increasing from 1.61, 1.77 to 1.93 in. (41, 45 to 48 mm) at the year 10, 20 and 30, respectively. Therefore, remedial works are still necessary to be performed in this type of embankment throughout its long-term service.

9.3 Limitation and Recommendation

- a) The settlement comparison in the DSM site is not satisfied, since the control section is not a real representative of the untreated section. Consequently, the monitored settlement values are less than what they were expected.
- b) The Plaxis, a Finite Element Program used in the numerical analysis in this study, still has its limitation in modeling soil erosion behavior. Therefore, this complicate phenomenon could not be simulated in the ECS site, and the results from the numerical analysis were not actually matched with the data from the field, especially with the monitored lateral soil displacement data.

REFERENCES

- [1] Abendroth, R. E., Greimann, L.F. and LaViolette, M. D. (2007). "An Integral Abutment Bridge With Precast Concrete Piles." *Final Rep., IHRB Project TR-438, CTRE Project No. 99-48*, IOWA Department of Transportation, Center for Transportation Research and Education Report, Ames, Iowa.
- [2] Aboshi, H. and Suematsu, N. (1985), "Sand Compaction Pile Method: State-of-the-Art Paper." *Proc. of 3rd International Geotechnical seminar on Soil Improvement Methods*, Nanyang Technological University, Singapore.
- [3] Abu al-Eis, K. and LaBarca, I. K. (2007). "Evaluation of the URETEK Method of Pavement Lifting." *Rep. No. WI-02-07*, Wisconsin Department of Transportation, Division of Transportation Systems Development, Madison, Wisconsin.
- [4] Abu-Hejleh, N., Hanneman, D., White, D. J. and Ksouri, I. (2006). "Flowfill and MSE Bridge Approaches: Performance, Cost and Recommendations for Improvements." *Report No. CDOT-DTD-R-2006-2*. Colorado Department of Transportation, Denver
- [5] Abu-Hejleh, N., Wang, T. and Zornberg, J.G. (2000). "Performance of Geosynthetic-Reinforced Walls Supporting Bridge and Approaching Roadway Structures." *ASCE Geotechnical Special Publication No. 103, Advances in Transportation and Geoenvironmental Systems Using Geosynthetics (2000)* 218–243.
- [6] Abu-Hejleh, N., Zornberg, J.G., Wang, T. and Watcharamonthein, J. (2003). "Design Assessment of Founders-Meadows GRS Abutment Structure." *Proc., 82nd Annual TRB Meeting*.
- [7] Albajar, L., Gascón, C., Hernando, A. and Pacheco, J. (2005). "Transiciones de Obra de Paso-Terraplén. Aproximación al Estado del Arte y Experiencias Españolas." Asociación Técnica de Carreteras, Ministerio de Fomento.
- [8] American Association of State Highway and Transportation Official AASHTO. (2004). *LRFD Bridge Design Specification, 3rd edition, with 2006 interim revisions*, Washington D.C.
- [9] Amini, F. (2004). "Dynamic cone penetrometer in quality control of compaction, state-of-the-art report." *Proc., Geotrans 2004 – Geotechnical Engineering for Transportation Projects*, Geotechnica; Special Publications No. 126, Yegian and Kavazanjian, eds., ASCE, Los Angeles, Ca., 1023-1031.
- [10] Ampadu, S. and Arthur, T. (2006). "The dynamic cone penetrometer in compaction verification on a model road pavement." *Geotech Test. J.*, ASTM, 29(1), 70-79.
- [11] Arasteh, M. (2007). "Innovations in compaction control and testing." Presented at 2007 Construction Conference. Bismarck, North Dakota.

- [12] Ardani, A. (1987) "Bridge Approach Settlement." *Report No. CDOT-DTP-R-87-06*, Colorado Department of Highways, Denver, Co.
- [13] Arockiasamy, M., Arockiasamy, Butrieng, N. and Sivakumar, M. (2004). "State-of-the-Art of Integral Abutment Bridges: Design and Practice." *Journal of Bridge Engineering*, ASCE, September/October, 2004, 497-506.
- [14] Arsoy, S., Barker, R. M. and Duncan, J. M. (1999). "The Behavior of Integral Abutment Bridges." *Rep. No. VTRC 00-CR3*, Virginia Transportation Research Council, Charlottesville, VA.
- [15] Arsoy, S., Duncan, J. M. and Barker, R.M. (2002). Performance of Piles Supporting Integral Bridges. *Transportation Research Record 1808*, Washington, D.C.
- [16] Atkinson, M.S. and Eldred, P. (1981). "Consolidation of soil using vertical drains" *Geotechnique*, 31(1), 33-43.
- [17] Bakeer, M., Shutt, M., Zhong, J., Das, S. and Morvant, M. (2005). Performance of Pile-Supported Bridge Approach Slabs." *Journal of Bridge Engineering*, ASCE.
- [18] Barksdale, R.D., and Bachus, R.C. (1983) "Design and Construction of Stone Columns, Vol. 1" *Rep. No. FHWA/RD-83/026*, Federal Highway Administration, Washington, D.C.
- [19] Barron, R. A. (1948) "Consolidation of Fine-Grained Soils by Drain Wells", *Transactions of ASCE No. 2346*, pp. 718-754.
- [20] Barron, R. F., Wright, J., Kramer, C., Andrew, W. H, Fung, H. and Liu, C. (2006), "Cement Deep Soil Mixing Remediation of Sunset North Basin Dam" *Dam Safety 2006*, Association of Dam Safety Officials.
- [21] Bathe, K.-J. (2003). *Finite Element Procedures*, Prentice-Hall of India, New Delhi
- [22] Baumann, V. and Bauer, G.E.A. (1974). "The Performance of Foundations on Various Soils Stabilized by the Vibro-Compaction Method." *Canadian Geotechnical Journal*, 509-530.
- [23] Bergado, D.T, and Patawaran, M.A.B. (2000). "Recent developments of ground improvement with pvd on soft Bangkok clay." *Proc. Intl. seminar on Geotechnics in Kochi 2000*, Kochi, Japan, October, 2000.
- [24] Bergado, D.T., Anderson, T.R, Miura, N, and Balasubramaniam, A.S. (1996). "Soft Ground Improvement in lowland and other environments." ASCE, New York.
- [25] Bergado, D.T., Miura, N., gh, N. And Panichayatum, B. (1988). "Improvement of Soft Bangkok Clay using Vertical Band Drains Based on Full Scale Test." *Proc. of the International Conference on Engineering Problems of Regional Soils*, Beijing, China, 379-384.
- [26] Bergado, D.T., Singh, N., Sim, S.H., Panichayatum, B., Sampaco, C.L. and Balasubramaniam, A.S. (1990) "Improvement of Soft Bangkok Clay Using Vertical Drains Compacted with Granular Piles." *Geotextiles and Geomembranes*, 9, 203-231.

- [27] Bowders, J., Loehr, E., Luna, R. and Petry, T.M. (2002). "Determination and Prioritization of MoDOT Geotechnical Related Problems with Emphasis on Effectiveness of Designs for Bridge Approach Slabs and Pavement Edge Drains." *Project Rep. No. R199-029*, Missouri Department of Transportation, Jefferson.
- [28] Bowles, J. E. (1988). *Foundation Analysis and Design*, McGraw-Hill, New York.
- [29] Bozozuk, M. (1978) "Bridge Foundations Move." *Transportation Research Record 678: Tolerable Movements of Bridge Foundations, Sand Drains, K-Test, Slopes, and Culverts*, Transportation Research Board, National Research Council, Washington, D.C. 17–21.
- [30] Brewer, W.E. (1992). "The Design and Construction of Small Span Bridges and Culvert Using Controlled Low Strength Material (CLSM)." *FHWA/OH-93/014*, Ohio Department of Transportation, Columbus, 129.
- [31] Brewer, W. B., Hayes, C. J., and Sawyer, S. (1994). "URETEK Construction Report," *Construction Report*, Report Number OK 94(03), Oklahoma Department of Transportation.
- [32] Briaud, J. L., James, R. W., and Hoffman, S. B. (1997) NCHRP synthesis 234: Settlement of Bridge Approaches (the bump at the end of the bridge), Transportation Research Board, National Research Council, Washington, D.C. pp.75.
- [33] Bridge Design Manual. Texas Department of Transportation, December 2001.
- [34] Brown, D.A., Steve, D.D., Thompson, W.R., and Lazarte, C. A. (2007) "Design and Construction of Continuous Flight Auger (CFA) Piles", *Geotechnical Engineering Circular No. 8*, Federal Highway Administration, Washington, D. C.
- [35] Bruce, D. (2001). "An Introduction to the Deep Mixing Methods as Used in Geotechnical Applications. Volume III. The Verification and Properties of Treated Ground." Report No. FHWA-RD-99-167, US Department of Transportation, Federal Highway Administration, 2001.
- [36] Bugrov, A.K. (1975). "The finite element method in consolidation analyses of water-saturated soils", *Power Technology and Engineering (Formerly Hydrotechnical Construction)*, Vol. 9, No. 7, 661-668.
- [37] Burde, H.J. (2004). "FE in Geotechnical Engineering", Stichting Postcademish Onderwijs Civile Techniek en Bouwtechniek, Noordwijkerhout, The Netherlands, January, 2004.
- [38] Burdette, E.G., S.C. Howard, J.B. Tidwell, E.P. Wasserman, E.E. Ingram, J.H. Deatherage, and D.W. Goodpasture. 2004. Lateral Load Tests on Prestressed Concrete Piles Supporting Integral Abutments. *PCI Journal*, 49(5), 70–77.
- [39] Burke, M.P. (1987). "Bridge Approach Pavements, Integral Bridges, and Cycle-Control Joints." *Transportation Research Record 1113*, TRB, National Research Council, Washington D.C., 54-65.
- [40] Burke, M.P. (1993). Integral bridges: attributes and limitations. *Transportation Research Record 1393* p. 1-8. Transportation Research Board, 75th Annual Meeting.

- [41] Burke, G. (2001) "Current Methods of Sampling and Testing of Soil Cement and Their Limitations." Proceedings of International Workshop on Deep Mixing Technology, Vol. 2, National Deep Mixing Program, Oakland, CA. 2001.
- [42] Bush, D.I., Jenner, C.G., and Bassett, R.H., 1990. The design and construction of geocell foundation mattress supporting embankments over soft ground. *Geotextiles and Geomembranes*, 9: 83-98.
- [43] Buss, W.E. (1989). "Iowa Flowable Mortar Saves Bridges and Culverts." *Transportation Research Record* 1234, TRB, National Research Council, Washington, DC, pp. 30-34.
- [44] Byle, M. J. (1997). "Limited Mobility Displacement Grouting - When "Compaction Grout" is Not Compaction Grout." Grouting: Compaction, Remediation, Testing, Proceedings of GeoLogan Geolnstitute Conference, Geotechnical Special Publication No. 66, Logan, Utah, ASCE, p. 32-43.
- [45] Byle, M. J. (2000). "An Approach to the Design of LMD Grouting." *Geotechnical Special Publication 104*, Advances in Grouting and Ground Modification, Proceedings of Sessions of Geo-Denver 2000, Wallace Baker Memorial Symposium, ASCE, Denver, Colorado, 94-110.
- [46] Cai, C. S., Voyiadjis, G. Z. and Xiaomin, S. (2005). "Determination of Interaction between Bridges Concrete Approach Slab and Embankment Settlement." Department of Civil Engineering, Louisiana State University, Baton Rouge, La.
- [47] Chini, S. A., Wolde-Tinsae, A. M., and Aggour, M. S. (1992). "Drainage and Backfill Provisions for Approaches to Bridges." University of Maryland, College Park.
- [48] Cooper, M.R. and Rose, A.N. (1999). "Stone column support for an embankment on deep alluvial soils." *Proc of the Institution of Civil Engineers*, Geotechnical Engineering, 137(1),15-25.
- [49] Cotton, D. M., Kilian, A. P., and Allen, T. (1987). "Westbound Embankment Preload on Rainier Avenue, Seattle, Washington." *Transportation Research Record No. 1119*, Transportation Research Board, Washington D.C., 61-75.
- [50] Cowland. J.W., and Wong, S.C.K. (1993). "Performance of a road embankment on soft clay supported on a geocell mattress foundation." *Geotextiles and Geomembranes*, 12, 687-705.
- [51] Das, S. C., Bakeer, R., Zhong, J., and Schutt, M. (1990). "Assessment of mitigation embankment settlement with pile supported approach slabs." Louisiana Transportation and Research Center, Baton Rouge, La.
- [52] DeMerchant, M., R. and Valsangkar, A., J. (2002). "Plate load tests on geogrid-reinforced expanded shale lightweight aggregate." *Geotextiles and Geomembranes No. 20*, 173–190
- [53] DiMillio, A.F. (1982). "Performance of Highway Bridge Abutments Supported by Spread Footings on Compacted Fill." *Final Rep. No. FHWA/RD-81/184*, Federal Highway Administration, Washington, D.C.
- [54] Du, L. (2008). Personal communication, Texas Department of Transportation.

- [55] Du, L., Arellano, M., K. J. Folliard, Nazarian, S. and Trejp D. (2006). "Rapid-Setting CLSM for Bridge Approach Repair: A Case Study". *ACI Material Journal*/ September-October 2006, pp. 312-318.
- [56] Dumas, C., Munsukhani, S., Porbaha, A., Short, D.R., Cannon, R.R., McLain, W.K., Putcha, S., Macnub, A., Lwin, M.M., Pelnik III, T.W., Brown, D.A. and Christopher, R.B. (2003). "Innovative Technology for Accelerated Construction of Bridge and Embankment Foundations in Europe", *FHWA, Rep. No. PL-03-014*.
- [57] Dunn, K. H. Anderson, G.H. Rodes, T.H., and Zieher, J.J. (1983). "Performance Evaluation of Bridge Approaches." Wisconsin Department of Transportation.
- [58] Dupont, B. and Allen, D. (2002). "Movements and Settlements of Highway Bridge Approches." *Rep. No. KTC-02-18/SPR-220-00-1F*, Kentucky Transportation Center Report, Lexington, KY.
- [59] EBA Engineering, Inc. (1992). *Final Report: Summary results obtained from the auger cast piles investigation. Study DTFH 692-Q-00062*. FHWA, U.S. Department of Transportation.
- [60] Edgar, T. V., Puckett, J. A., and D'Spain, R. B. (1989). "Effect of Geotextile on Lateral Pressure and Deformation in Highway Embankments." *Geotextiles and Geomembranes*, 8(4), 275-306.
- [61] Elias, V., Christopher, B. R., and Berg, R.R. (2001). "Mechanically Stabilized Earth Walls and Reinforced Soil Slopes Design and Construction Guidelines." FHWA NHI-00- 043.
- [62] Expanded Shale, Clay and Slate (ESCS) (2004). "Light weight aggregate for geotechnical applications." Information Sheet 6001 – www.escci.org.
- [63] Federal Highway Administration (2000). "Priority, Market-Ready Technologies and Innovations", *Rep. No. FHWA-HRT-04-053*.
- [64] Fox, N.S. and Cowell, M.J. (1998). *Geopier Foundation and Soil Reinforcement Manual*, Geopier Foundation Company, Inc., Scottsdale, AZ.
- [65] Gabr, M., Hopkins, K., Coonse, J, and Hearne, T. (2000). "DCP criteria for performance evaluation of pavement layers." *J. Perf. Of Constr. Facil.*, ASCE, 14(4), 141-148.
- [66] Gallivan, L. (2008). "An Intelligent Compaction Era has Arrived." *Rep. No. FHWA-HRT-08-012*, Focus, USDOT.
- [67] Girton, D. D., Hawkinson, T.R. and Greimann, L.F. (1991). "Validation of design recommendations for integral-abutment piles." *Journal of Structural Engineering*, ASCE, 117(7), 2117-2134.
- [68] Goughnour, R. R. and Bayuk, A.A. (1979). "A Field Study of Long-term Settlement of Loads Supported by Stone Column in Soft Ground." *Proc of International Conference on Soil Reinforcement: Reinforced Earth and Other Techniques*, Vol. 1, Paris, 279-286.
- [69] Greimann, L. F. and Wolde-Tinsae, A. M. (1988). "Design model for piles in jointless bridges." *Journal of Structural Engineering*, ASCE, 114(6),1354-1371.

- [70] Greimann, L. F., Abendroth, R.E., Johnson, D.E. and Ebner, P.B. (1987). "Pile Design and Tests for Integral Abutment Bridges." *Final Rep. Iowa DOT Project HR 273, ERI Project 1780, ISU-ERI-Ames-88060*, Ames, Iowa.
- [71] Greimann, L. F., Yang, P-S. and Wolde-Tinsae, A. M. (1983). "Skewed Bridges with Integral Abutments." *Transportation Research Record 903: Bridges and Culverts*, Transportation Research Board, National Research Council, Washington, D.C., 64-72.
- [72] Greimann, L. F., Yang, P-S. and Wolde-Tinsae, A. M. (1986). "Nonlinear analysis of integral abutment bridges." *Journal of Structural Engineering*, ASCE, 112(10), 2263-2280.
- [73] Grover, R. A. (1978). "Movement of Bridge Abutments and Settlements of Approach Pavements in Ohio." *Transportation Research Record 678*, Washington, D.C.
- [74] Ha, H., Seo, J., and Briaud, J-L. (2002). "Investigation of Settlement at Bridge Approach Slab Expansion Joint: Survey and Site Investigations." *Rep. No. FHWA/TX-03/4147-1*, Texas Transportation Institute, Texas A&M University, College Station, TX.
- [75] Hansbo, S. (1979) "Consolidation of Clay by Bandshaped Prefabricated Drains." *Ground Engineering*, 12(5), 16-25.
- [76] Hansbo, S. (1997) "Aspects of Vertical Drain Design: Darcian or Non-Darcian Flow." *Geotechnique*, 47(5), 983-992.
- [77] Hansbo, S. (1997) "Practical Aspects of Vertical Drain Design." *Proceedings of 14th International Conference on Soil Mechanics and Foundation Engineering*, Vol. 3, Hamburg.
- [78] Hansbo, S. (2001) "Consolidation Equation Valid for both Darcian or Non-Darcian Flow", *Geotechnique*, 51(1), 51-54.
- [79] Hartlen, J. (1985). "Pressure Berms, Soil Replacement and Lightweight Fills." *Soil Improvement Methods, Proceedings of the Third International Geotechnical Seminar*, Nanyang Technological Institute, Singapore, 101-111.
- [80] Hausmann, M. R. (1990). "Engineering Principles of Ground Modification", McGraw-Hill Publishing Company, New York.
- [81] Holm, T., A., and Valsangkar, A., J. (1993). "Lightweight aggregate soil mechanics: properties and applications." *Transportation Research Record*, No. 1422 , 7-13.
- [82] Holm, T. A., and Ooi, O. S. (2003). "Moisture dynamics in lightweight aggregate and concrete." *6th International Conference on the Durability of Concrete*, Thessaloniki, Greece.
- [83] Holtz, R.D. and Kovacs, W.D. (1981). "An Introduction to Geotechnical Engineering." Prentice Hall Inc., Englewoods Cliffs, New Jersey, 733.
- [84] Hopkins, T.C. (1969). "Settlement of Highway Bridge Approaches and Embankment Foundations." *Rep. No. KYHPR-64-17; HPR-1(4)*, Kentucky Transportation Center, Lexington, Kentucky.

- [85] Hopkins, T. C. (1973). "Settlement of Highway Bridge Approaches and Embankment Foundations." *Rep. No. KYHPR-64-17; HPR-1(8)*, Kentucky Transportation Center, Lexington, Kentucky, 40.
- [86] Hopkins, T.C. (1985). "Long-Term Movements of Highway Bridge Approach Embankments and Pavements". University of Kentucky, Transportation Research Program.
- [87] Hopkins, T.C. and Deen, R.C. (1970). "The Bump at the End of the Bridge." *Highway Research Record No. 302*, Highway Research Board, National Research Council, Washington, D.C., 72-75.
- [88] Hoppe, E. J. and Gomez, J. P. (1996). "Field study of an integral backwall bridge." *Rep. No. VTRC 97-R7*, Virginia Transportation Research Council, Charlottesville, VA.
- [89] Hoppe, E.J. (1999). "Guidelines for the Use, Design, and Construction of Bridge Approach Slabs." *Rep. No. VTRC 00-R4*, Virginia Transportation Research Council, Charlottesville, VA.
- [90] Horvath, J. (2000). "Integral Abutment Bridges: Problem and Innovative Solutions Using EPS Geofoam and other Geosynthetics." *Research Report No. CE/GE-00-2*, Manhattan College, Bronx, New York.
- [91] Horvath, J. S. (1991). "Using Geosynthetics to Reduce Surcharge-Induced Stresses on Rigid Earth Retaining Structures." *Transportation Research Record 1330*, 47-53.
- [92] Horvath, J. S. (2005). "Integral-Abutment Bridges: Geotechnical Problems and Solutions Using Geosynthetics and Ground Improvement." *IAJB 2005 - The 2005 FHWA Conference on Integral Abutment and Jointless Bridges*. 16-18 March, Baltimore, Maryland, USA.
- [93] Hsi, J. and Martin, J. (2005). "Soft Ground Treatment and Performance, Yelgun to Chinderah Freeway, New South Wales, Australia." *In Ground Improvement-Case Histories*, Elsevier Geo-Engineering Book Series, Volume 3, 563-599.
- [94] Hsi, J. P. (2007). "Managing Difficult Ground-Case Studies." *Proceedings of First Sri Lankan Geotechnical Society International Conference on soil and Rock Engineering*, Colombo.
- [95] Hsi, J. P. (2008). "Bridge Approach Embankments Supported on Concrete Injected Columns." *Proceedings of The Challenge of Sustainability in the Geoenvironment*, ASCE, Geocongress 08, New Orleans, Louisiana.
- [96] HVJ Associates (2003). Report of Geotechnical Investigation Reconstruction and Widening of US-90A at SH-6, Segment 3, Houston, Texas.
- [97] Indraratna, B., Balasubramaniam, A. S. and Ratnayake, P. (1994). "Performance of Embankment Stabilized with Vertical drains on Soft Clay." *Journal of Geotechnical Engineering*, ASCE, 120(2), 257-273.
- [98] James, R.W., Zhang, H. and Zollinger, D.G. (1991). "Observations of severe abutment backwall damage." *Transportation Research Record 1319*, Transportation Research Board, 55-61.

- [99] Jamiolkowski, M., Lancellota, R. and Wolski, W. (1983). "Precompression and speeding up consolidation." *Proceedings, Eight European Conference on Soil Mechanics and Foundation Engineering*, Vol 3, Helsinki.
- [100] Japan Railway (JR) Technical Research Institute (1998). "Manual on Design and Construction of Geosynthetic-Reinforced Soil Retaining Wall."
- [101] Jayawickrama, P., Nash, P., Leaverton, M. and Mishra, D. (2005). "Water Intrusion in Base/Subgrade Materials at Bridge Ends." *TxDOT Report, FHWA/TX-06/0-5096-1*, Texas Tech University, Lubbock, Texas.
- [102] Jenner, C.G., Basset, R.H., and Bush, D.I. (1988). "The use of slip line fields to assess the improvement in bearing capacity of soft ground given by cellular foundation mattress installed at the base of an embankment." *In Proceedings of the International Geotechnical Symposium on Theory and Practice of Earth Reinforcement*, Balkema, Rotterdam, 209-214.
- [103] Kamel, M.R., Benak, J.V., Tadros, M.K. and Jamshidi, M. (1996). "Prestressed Concrete Piles in Jointless Bridges." *PCI Journal*, 41(2), 56–67.
- [104] Kramer, S. L. and Sajer, P. (1991) "Bridge Approach Slab Effectiveness." *Final Report*, Washington State Department of Transportation, Olympia, Washington.
- [105] Krishnaswamy, N.R., Rajagopal, K., and Madhavi Latha, G. (2000). "Model studies on geocell supported embankments constructed over soft clay foundation." *Geotechnical Testing Journal*, ASTM, 23: 45-54.
- [106] Kristiansen. H. and Davies, M. (2004). "Ground improvement using rapid impact compaction." *Proceedings of 13th World Conference on Earthquake Engineering*, Vancouver, B.C, pp 1-10.
- [107] Kunin, J. and Alampalli, S. (2000). "Integral Abutment Bridges: Current Practice in United States and Canada." *ASCE Journal of Performance of Constructed Facilities*, 14(3), 104-111.
- [108] Laguros, J. G., Zaman, M. M., and Mahmood, I. U. (1990). "Evaluation of Causes of Excessive Settlements of Pavements Behind Bridge Abutments and their Remedies; Phase II. (Executive Summary)." *Rep. No. FHWA/OK 89 (07)*, Oklahoma Department of Transportation.
- [109] Lawton, E.C., and Fox, N.S. (1994). "Settlement of Structures Supported on Marginal or Inadequate Soils Stiffened with Short Aggregate Piers." *ASCE GSP No. 40*, Vertical and Horizontal Deformations of Foundations and Embankments, ASCE, Vol. 2, 962-974.
- [110] Lawton, E. C., Fox, N. S. and Handy, R. L. (1994). "Control of Settlement and Uplift of Structures Using Short Aggregate Piers." *Proceedings, IN-SITU Deep Soil Improvements*.
- [111] Lawton, E., and Merry, S. (2000). "Performance of Geopier Supported Foundations During Simulated Seismic Tests on Northbound Interstate 15 Bridge Over South Temple, Salk Lake City, Utah." *Final Reprt No. UUCVEEN 00-03*. University of Utah.

- [112] Lawver, A., French, C., and Shield, C. K. (2000). "Field Performance of an Integral Abutment Bridge." *Transportation Research Record: Journal of the Transportation Research Board*, 1740, 108-111.
- [113] Lenke, L. R. (2006). "Settlement Issues-Bridge Approach Slabs." *Rep. No. NM04MNT-02*, New Mexico Department of Transportation.
- [114] Lien, B. H. and Fox, N. S. (2001) "Case Histories of Geopier® Soil Reinforcement for Transportation Applications." Proc. of Asian Institute of Technology Conference, Bangkok, Thailand.
- [115] Lin, Q.L., Wong, I.H. (1999). "Use of Deep Cement Mixing to Reduce Settlements at Bridge Approaches." *Journal of Geotechnical and Geoenvironmental Engineering*, ASCE, Vol. 125(4),309.
- [116] Liu, H.L., Ng, C.W.W., and Fei, K. (2007). "Performance of a Geogrid-Reinforced and Pile-Supported Highway Embankment over Soft Clay: Case Study." *Journal of Geotechnical and Geoenvironmental Engineering*, ASCE, 133(12),1483-1493.
- [117] Long, J.H., Olson, S.M. and Stark, T.D. (1998). "Differential Movement at Embankment/Bridge Structure Interface in Illinois." *Transportation Research Record No. 1633*, Transportation Research Board, Washington, D.C., 53-60.
- [118] Lukas, R.G. (1986) "Dynamic Compaction for Highway Construction, Vol. 1, Design and construction Guidelines." *Rep. No. FHWA/RD-86/133*, Federal Highway Administration, National Technical Information Service, Washington, D.C.
- [119] Lukas, R.G. (1995) "Dynamic Compaction, Geotechnical Engineering Circular No. 1" *Rep. No. FHWA-SA-95-037*, Federal Highway Administration, Washington, D.C.
- [120] Luna R., Jonathan L. R., and Andrew, J. W. (2004). "Evaluation of Bridge Approach Slabs, Performance and Design." *Rep. No. RDT 04-010*, Department of Civil, Architectural and Environmental Engineering, University of Missouri, Rolla.
- [121] Maddison, J. D., Jones, D. B., Bell, A. L., and Jenner, C. G. (1996). "Design and performance of an embankment supported using low strength geogrids and vibro concrete columns." *Geosynthetics: Applications, design and construction*, De Groot, Den Hoedt, and Termaat, eds., Balkema, Rotterdam, The Netherlands, 325–332.
- [122] Magnan, J. (1994). "Methods to reduce the settlement of embankments on soft clay: A review." *Proc., Vertical-Horizontal Deformations of Foundations and Embankments*, ASCE, New York, 77–91.
- [123] Mahmood, I. U. (1990). "Evaluation of causes of bridge approach settlement and development of settlement prediction models." PhD Thesis, University of Oklahoma, Norman, Okla.
- [124] McKenna, J.M., Eyre, W.A., and Wolstenholme, D. R. (1975). "Performance of an Embankment Supported by Stone Columns in Soft Ground." *Geotechnique*, 25(1), 51-59.
- [125] McVay, M., Armaghani, B. and Casper, R. (1994). "Design and construction of auger-cast piles in Florida." *Transportation Research Record*, 1447, 10-18.

- [126] Mekkawy, M., White, D.J., Souleiman, M.T. and Sritharan, S. (2005). "Simple Design Alternatives to Improve Drainage and Reduce Erosion at Bridge Abutments." *Proceedings of the 2005 Mid-Continent Transportation Research Symposium*, Ames, Iowa.
- [127] Michell, J. K., and Huber, T.R (1985) "Performance of a Stone Column Foundation." *Journal of Geotechnical Engineering*, ASCE, 111(2), 205-223.
- [128] Miller, E. A., and Roycroft, G. A., (2004). "Compaction Grouting Test Program for Liquefaction Control." *Journal of Geotechnical and Geoenvironmental Engineering*, ASCE, 355-361.
- [129] Mimura, C.S., Kimura, S.A. (1995). "A light-weight solution." *Proceedings Geosynthetics '95*, Nashville, Tennessee, Vol. 1, 39-51.
- [130] Minks, A.G., Wissmann, K.J., Caskey, J.M., and Pando, M.A. (2001). "Distribution of Stresses and Settlements below Floor Slabs Supported by Rammed Aggregate Piers." *Proceedings of 54th Canadian Geotechnical Conference*, Calgary, Alberta, Canada, 16-19.
- [131] Monley, GJ., and Wu, J. T. (1993). Tensile Reinforced Effects on Bridge Approach Settlement. *Journal of Geotechnical Engineering*, 119(4), 749-763.
- [132] Moore, W. (2006). "Intelligent compaction: Outsmarting Soil and Asphalt." www.constructionequipment.com/article/CA6321917.html.
- [133] Munoz, A. and Mattox, M. (1977) "Vibroreplacement and Reinforced Earth Unite to Strengthen a Weak Foundation." *Civil Engineering*, ASCE, 58-62.
- [134] Narsavage, P. (2007). "Downdrag in Foundation Design." Ohio Department of Transportation. www.odotnet.net/geotechnical/Web_Links/Docs/2007_Consult_Workshop/Downdrag.ppt.
- [135] Nassif, H. (2002). "Finite Element Modeling of Bridge Approach and Transition Slabs." *Rep. No. FHWA-NJ-2002-007*, Department of Civil and Environmental Engineering, Center for Advanced Infrastructure & Transportation (CAIT), Rutgers, New Jersey.
- [136] Neely, W. J. (1991). "Bearing capacity of auger-cast piles in sand". *Journal of Geotechnical Engineering*, 117(2), 331-345.
- [137] Nicholson D.P. and Jardine R.J. (1982). "Performance of vertical drains at Queenborough bypass." *Vertical Drains*, the Institution of Civil Engineers: London, 67-90.
- [138] O'Neill, M. W. (1994). "Review of augered pile practice outside the United States". *Transportation Research Record*, 1447, 3-9.
- [139] ODOT. (2005). "Bridge Foundation Design Practices and Procedures." Bridge Engineering Section, Oregon Department of Transportation, 20.
- [140] Opland, W. H., and Barnhart, V. T. (1995). "Evaluation of The URETEK Method for Pavement Undersealing." *Research Rep. No. R-1340*, Michigan Department of Transportation in Cooperation with the U.S. Department of Transportation.
- [141] PCI. (2001). "The State of the Art of Precast/Prestressed Integral Bridges." Precast/Prestressed Concrete Institute, Chicago, Illinois.

- [142] Pierce, C. E., Baus, R. L., Harries, K. A. and Yang, W. (2001) "Investigation into Improvement of Bridge Approaches in South Carolina", *Summary Report, Rep. No. FHWA-SC-01-02*, South Carolina Department of Transportation.
- [143] Porbaha, A. (1998). "State of the Art in Deep Mixing Technology, Part I: Basic Concepts and Overview of Technology." *Ground Improvement*, 2(2), 81-92.
- [144] Porbaha, A. (2000). "State of the Art in Deep Mixing Technology: Design Considerations." *Ground Improvement*, 4(3), 111-125.
- [145] Porbaha, A. and Roblee, C. (2001). "Challenges for Implementation of Deep Mixing in the USA." *Proceedings of International Workshop on Deep Mixing Technology*, National Deep Mixing Program, Oakland, CA., 2 volumes.
- [146] Rahman, F., Hossain, M. and Romanoschi, S. (2007). "Intelligent Compaction Control of Highway Embankments Soil." *86th Annual Meeting of the Transportation Research Board*, Washington, D.C., 2007.
- [147] Rathmayer, H. (1996). "Deep Mixing Methods for Soft Subsoil Improvement in the Nordic Countries." *Proceedings of IS-Tokyo '96*, The 2nd International Conference on Ground Improvement Geosystems, 14-17 May 1996, Tokyo, 869-878.
- [148] RECON (2007). DSM Work Plan Report for Project: STP 2007 (165) MM IH 30 Tarrant County, Houston Texas
- [149] Report on Texas Bridges (2006). Prepared by the Bridge Division of the Texas Department of Transportation, Austin, Texas.
- [150] Rixner, J.J., Kraemer, S.R., and Smith, A.D. (1986). "Prefabricated Vertical Drains, Vol. 1." *Rep. No. FHWA-RD-86/168*, Federal Highway Administration, Washington, D.C.
- [151] Rowe, R.K., Gnanendran, C.T., Landva, A.O. and Valsangkar, A.J. (1995). "Construction and performance of a full-scale geotextile reinforced test embankment." *Canadian Geotechnical Journal*, 32(3), 512-534.
- [152] Saride, S, Sirigiripet, S.K, Puppala, A. J, Williammee, R. (2008). "Performance of Expanded Clay Shale (ECS) as an Embankment Backfill." In the Proceedings of International Conference on 'The Challenges of Sustainability in the Geoenvironment', American Society of Civil Engineers, Geocongress- 2008. March 9-12, New Orleans, Louisiana, USA.
- [153] Schaefer, V.R, Koch, J.C. (1992). "Void Development under Bridge Approaches," *Rep. No. SD90-03*, South Dakota Department of Transportation.
- [154] Seo, J. (2003). "The Bump at the End of the Bridge: An Investigation." Dissertation submitted in partial fulfillment of the requirements for the degree of the Doctor of Philosophy, Texas, A&M University, College Station, Texas.
- [155] Seo, J., Ha, H. S., and Briaud, J.L. (2002). "Investigation of Settlement at Bridge Approach Slab Expansion Joint: Numerical Simulation and Model Tests." *Rep. No. FHWA/TX-03/4147-2*, Texas Transportation Institute, Texas A&M University, College Station, Texas.

- [156] Serridge, C.J. and Synac, O. (2007). "Ground Improvement Solutions for Motorway Widening Schemes and New Highway Embankment Construction Over Soft Ground." *Ground Improvement Journal*, 11(4), 219-228.
- [157] Shen, S.-L., Hong, Z.-S., and Xu, Y.-S. (2007). "Reducing Differential Settlements of Approach Embankments." *Proc. of Institute of Civil Engineers, Geotechnical Engineering*, Issue GE4, 215-226.
- [158] Siemeier, J.A., Young, D. and Beberg, D. (2000). "Comparison of the dynamic cone penetrometer with other tests during subgrade and granular base characterization in Minnesota." *Nondestructive Testing of Pavements and Backcalculation of Moduli: Third Volume*, ASTM STP 1375, Tayabji and Lukanen, eds., ASTM, West Conshohocken, Pa., 175-188.
- [159] Sluz, A., Sussmann, T. R., and Samavedam, G. (2003). "Railroad Embankment Stabilization Demonstration for High-Speed Rail Corridors." *Grouting and Ground Treatment* (GSP No. 120). 3rd International Specialty Conference on Grouting and Ground Treatment. February 10–12, New Orleans, Louisiana, USA.
- [160] Smadi, O. (2001). "The strength of flowable mortar." http://www.ctre.iastate.edu/PUBS/tech_news/2001/julaug/flowable_mortar.pdf
- [161] Snethen, D. R. and Benson, J. M. (1998). "Construction of CLSM Approach Embankment to Minimize the Bump at the End of the Bridge." *The Design and Application of Controlled Low-Strength Materials (Flowable Fill)*, ASTM STP 1331.
- [162] Soltesz, S. (2002). "Injected Polyurethane Slab Jacking." *Final Report*, Rep. No. FHWA-OR-RD-02-19, Oregon Department of Transportation Research Group.
- [163] Stark, T. D., Olson, S. M., and Long, J. H. (1995). "Differential Movement at the Embankment/Structure Interface Mitigation and Rehabilitation." *Rep. No. IABH1, FY 93*, Illinois Department of Transportation, Springfield, Illinois.
- [164] Stewart, C. F. (1985). "Highway Structure Approaches." California Department of Transportation, Sacramento, CA.
- [165] Stoll, R.D. and Holm, T.A. (1985). "Expanded shale lightweight fill: geotechnical properties." *Journal of Geotechnical Engineering*, ASCE 111 (GT8), 1023–1027.
- [166] Strauss, J., Dahnke, D. and Nonamaker, F.(2004) "Compaction Grouting to Mitigate Settlement Beneath Approach Fills, California State Route 73 at Laguna Canyon Road", *Geotechnical Engineering for Transportation Project*, ASCE, 1876-1883.
- [167] Tadros, M.K., and Benak, J.V. (1989). "Bridge Abutment and Approach Slab Settlement (Phase I Final Report), University of Nebraska, Lincoln.
- [168] Terzaghi, K. (1943) "Theoretical Soil Mechanics." John Wiley and Sons, New York.
- [169] Timmerman, D.H. (1976). "An Evaluation of Bridge Approach Design and Construction Techniques." *Final Report*, Rep. No. OHIODOT-03-77, Ohio Department of Transportation.

- [170] Transportation Research Board. (2008). "Intelligent Soil Compaction Systems." *Rep. No. NCHRP 21-09*. Washington, D.C.
- [171] Unified Facilities Criteria (UFC). (2004). "Pavement Design For Roads, Streets, Walk, and Open Storage Area." *Rep. No. UFC 3-250-01FA*, US Army Corps of Engineers.
- [172] Vipulanandan, C., Kim, M.G., and O'Neill, M.W. (2004). "Axial Performance of Continuous Flight Auger Piles for Bearing", *Project Report No. 7-3940-2*, Texas Department of Transportation, Austin, Texas.
- [173] Wahls, H. E. (1990). *NCHRP Synthesis of Highway Practice No. 159: Design and Construction of Bridge Approaches*. Transportation Research Board, National Research Council, Washington, D.C.
- [174] Walkinshaw, J. L. (1978). "Survey of Bridge Movements in the Western United States." *Transportation Research Record 678: Tolerable Movements of Bridge Foundations, Sand Drains, K-Test, Slopes, and Culverts*, Transportation Research Board, National Research Council, Washington, D.C., 6–12.
- [175] White, D. J. and Suleiman, M.T. (2004). "Design of Short Aggregate Piers to Support Highway Embankments." 83rd Annual Meeting Transportation Research Board, Washington, D.C.
- [176] White, D., Mohamed, M., Sritharan, S. and Suleiman, M. (2007). "Underlying" Causes for Settlement of Bridge Approach Pavement Systems." *Journal of Performance of Constructed Facilities*, ASCE, 273-282.
- [177] White, D., Sritharan, S., Suleiman, M., Mohamed M. and Sudhar, C. (2005). "Identification of the Best Practices for Design, Construction, and Repair of Bridge Approaches." *CTRE. Project 02-118*, Iowa State University. Ames, Iowa.
- [178] White, D.J., Wissman, K., Barnes, A.G. and Gaul, A.J. (2002). "Embankment Support: A Comparison of Stone Column and Rammed Aggregate Pier Soil Reinforcement." *Proc. 81st Annual TRB Meeting*, Washington, D. C.
- [179] Williammee, R. (2008) Personal communication, Fort Worth District Materials Engineer, Texas Department of Transportation.
- [180] Wissmann, K. J. and Fox, N.S. (2000). "Design and analysis of Short Aggregate Piers to reinforce soils." *Proceedings, Geotechnical Colloquium, Technical University Darmstadt, Fermany, March 25, 2000*.
- [181] Wolde-Tinsae, A.M, Aggour, S.M. and Chini, S.A. (1987). "Structural and Soil Provisions for Approaches to Bridges." *Interim Report AW087-321-046*, Maryland Department of Transportation.
- [182] Won, M. S. and Kim, Y. S. (2007). "Internal Deformation Behavior of Geosynthetic-reinforced Soil Walls." *Geotextiles and Geomembranes*, 25(1), 10-22.
- [183] Wong, H. K. W, and Small, J. C. (1994). "Effect of Orientation of Bridge Slabs on Pavement Deformation." *Journal of Transportation Engineering*, 120(4), 590-602.

- [184] Wu, J.T.H., Lee, K.Z.Z., Helwany, B. S. and Ketchart, K. (2006). "Design and Construction Guidelines for Geosynthetic-Reinforced Soil Bridge Abutments with a Flexible Facing." *Proc. NCHRP Report 556*. Transportation Research Board, Washington DC.
- [185] Wu, J.T.H., Lee, K.Z.Z. and Ketchart, K. (2003). "A Review of Case Histories on GRS Bridge-Supporting Structures with Flexible Facing." *Proc. 82nd Annual TRB Meeting*.
- [186] Zelada, G. A., and Stephenson, R. W. (2000). "An Evaluation of Auger Cast-in-Place Pile Design Methodologies for Compression Loading." *Proc. of Int. Conf. on New Technological and Design Developments in Deep Foundations*, Geo-Denver 2000, ASCE, August 5-8, 2000, Denver.

BIOGRAPHICAL INFORMATION

Ekarut Archeewa was born in June 13, 1971 in Ubol Ratchathani province, Thailand. He finished his high school from Triam Udom Suksa in 1990, and received his bachelor degree in Civil Engineering from Chulalongkorn University, the best and most selective university in Thailand in 1993. After his graduation, he started working as a transport engineer at Asian Engineering Consultant (AEC) Company for one year. Thereafter, he has been working for the government since 1995. Ekarut is a well-round knowledge engineer. During the first ten years in Department of Public Works, Ministry of Interior, he was assigned to be a project engineer responsible for water supply projects for municipalities and villages in Thailand. His tasks involved from topography survey, project feasibility study and preliminary evaluation, structural design for water supply facilities, pipe network design and the construction monitoring. With his excellent working performance and academic background, he was among a very few engineers achieved a Professional Engineering license (Thailand) within the first three years after graduation. He got a scholarship from the German government to have a professional training in Germany in 1999, and from the Netherlands to study his Master of Science in Hydraulic Engineering and River Basin Development in 2003. In 2005, he was relocated to Department of Water Resources, Ministry of Natural Resources and assigned as a project engineer responsible for water resource projects, including project feasibility study, irrigation network for Khong-Chi-Mun river basin design, and flood prevention in the northern area of Thailand study.

In August 2008, Ekarut pursued a Ph.D. program in civil engineering at the University of Texas at Arlington (UTA). He completed Doctor of Philosophy in Civil Engineering with the minor field of geotechnical in December 2010. Under the supervision of Dr. Anand J Puppala, Ekarut Archeewa has four papers already published.